

Synthesis of Four Diastereomeric Linoleic Triols and Development of a Large Scale Convergent
Approach to Apoptolidinone C

By

Robert Woods Davis

Dissertation

Submitted to the Faculty of the

Graduate School of Vanderbilt University

In partial fulfillment of the requirements

for the degree of

DOCTOR OF PHILOSOPHY

In

Chemistry

May 31, 2018

Nashville, Tennessee

Approved:

Gary A. Sulikowski, Ph.D.

Brain O. Bachmann, Ph.D.

Steven D. Townsend, Ph.D.

Joshua P. Fessel, M.D., Ph.D.

For Chelsea

“Startups are business experiments performed with other people’s money”

-Antonio Garcia Martinez

ACKNOWLEDGEMENTS

I came to graduate school a wide-eyed biology major in search of a true education in organic synthesis. Although I didn't understand what that meant at the time, I can look back now and say with absolute confidence that I was provided every opportunity to learn I could've asked for. I am truly grateful to my advisor, Dr. Gary Sulikowski, for providing me this. He always pushed me to be a better chemist and I feel the training environment he fostered allowed me to grow leaps and bounds from where I was at the outset of my career. His work ethic and enthusiasm for chemistry set a good example for the group to follow, and despite his busy schedule he carves out time to discuss projects on an individual basis every week. Chemistry can be very frustrating and is inherently difficult, but I have learned that continual and consistent effort allows us to break through plateaus and advance projects. I know I will take the lessons learned with me the rest of my life, and I am truly grateful for the opportunities provided to me by Gary.

I am grateful to my committee members Dr. Brian Bachmann, Dr. Steven Townsend, and Dr. Joshua Fessel. You have all welcomed me into your office (announced or unannounced) and been nothing but supportive and helpful through all of our interactions. Brian has always kept the big picture in focus for me, and even let me run around his lab trying to learn the chemical biology side of things. Steve is always there to provide advice and help me keep things in perspective, which I frequently need. Josh has always welcomed me and guided me through the biology of my projects, letting me pick his brain about random epidemiological intrigues and provided a great perspective on graduate school and life.

A special thanks to Dr. Alan Brash. Although not an official committee member, as a collaborator, Alan is inspirational. He is a rigorous scientist and has taken many hours of his life

to teach me biological and pharmacological methods. I very much appreciate his efforts in my education.

I would never have applied to graduate school were it not for Dr. Kevin Minbiole, who instilled a passion for basic science in me as a young student. After taking several classes with Kevin as an undergraduate, he took me into his group my junior year and let me explore several areas of research interest. Following graduation, Kevin moved to Villanova, and I followed for a Master's degree where I discovered a great desire to pursue organic synthesis. A common pattern among my advisors, Kevin's work ethic and enthusiasm are infectious and I am forever grateful for all he has done for me. He is a terrific advisor, mentor and friend.

Besides having great mentorship at the faculty level, I have been very very fortunate to find incredible mentors at the undergraduate and graduate level. For starters, Georgia Stoyanov and Devon Flaherty in particular got my training started as an undergraduate at James Madison University. At Villanova University I received a considerably high amount of mentorship and overall help from Dr. Tom Umile. I very much owe Dr. Tom, he is an amazingly patient man. At Vanderbilt, the list is seemingly endless. Dr. Brendan Dutter, Dr. Marta Wenzler, and Dr. Bobby Boer took me under their wing despite being busy graduate students and set me on a proper path. I must thank all Sulikowski lab members past and present, Dr. Susan Ramos-Hunter, Jason Hudlicky, Chris Fullenkamp, Jenny Benoy, Zach Austin, Quinn Bumpers, Alex Allweil, Jade Williams, Cal Larson and Danielle Penk for the great conversations revolving around chemistry. You all also kept me sane and made coming into lab fun.

Dr. Jonathon Hempel, Dr. Plamen Christov, Dr. Kwangho Kim, and Dr. Ian Romaine have always been more than willing to help and teach me when I asked. In addition, Dr. Carmelo Rizzo, Dr. Francesca Gruppi, Dr. Chanchal K. Malik, Dr. Arnie R. de Leon and Ms. Tracy Johnson-

Salyard allowed me to learn and grow significantly my first summer in Nashville and were always supportive and understanding as I transitioned to synthetic chemistry. David Earl went out of his way to teach me and make sure I understood many biological techniques, and in addition is a great friend.

As far as graduate student mentors go, Dr. Katherine Chong was the best. She always helped me when I needed it and made me figure things out on my own when it was appropriate. She was tough and held me to high expectations, always setting an example of near perfection for me to strive towards. I owe a great deal to her, from the coffee sessions where she listened, to all the advice she gave, to the effort she put into my success. She was a great mentor and will always be a great friend.

I have been very fortunate to work with many smart and talented (much more so than myself) undergraduate, rotation, REU, and summer students. Emily Janeira, I look forward to asking you for a job one day. Jake Black, you already gave me one.

I have met some incredible people I have the privilege of calling friends in Nashville. You have all always understood when I couldn't be there and been very supportive of me in my pursuits. I feel very lucky to know you all. Ella, Logan, Justin, Sarrah, Kellie, Melo, Ashton, and the whole Station 40 crew, you are all the best. Within the department Thomas Struble has been an amazing friend, roommate and dog trainer. Wouldn't have made it without you. Wes Bauer, Evan Gizzie, Matt Knowe, Bandrew, Berk, Mike Turo, Jade Bing, and Mike Danneman, when I look back on graduate school I will always think of all the fun times we had. And a shout out to Ms. Carol Simpson for always brightening my day.

Keeping in touch with my friends from high school and college has provided me with many great laughs, and they always directly or indirectly remind me who I am, where I come from, where

I'm headed, and why. Keeping things in perspective has been very important for me, and I'm thankful for the great conversations I've been able to have with Robert, Tyler, Trevor, Patrick, Patrick and Daniel in particular.

It goes without saying, I wouldn't be here without my family. My parents are model people. They work hard and always do the right thing. They treat others with respect and are kind, warm, loving people. I know they are always a phone call away. They encourage me to stick things out when I want to quit but support me in any decision I make. I am truly blessed. In addition, I have acquired a new set of parents who took me in right away as a member of their family. My parents and my in-laws have always kept me grounded and on the right track.

This document is dedicated to my wife, Chelsea, for one reason. It would not exist without her. The past seven years have been...a lot, to say the least. We went through all of it together and if she was not by my side, I know I wouldn't have made it. She was always understanding and always supportive. I can't imagine life without her.

TABLE OF CONTENTS

	Page
DEDICATION.....	ii
ACKNOWLEDGMENTS.....	iv
LIST OF FIGURES.....	ix
LIST OF SCHEMES.....	xiii
LIST OF ABBREVIATIONS.....	xvi
Chapter	
I. SYNTHESIS OF FOUR ISOMERIC LINOLEIC TRIOL.....	1
The role of linoleic acid in the mammalian epidermal water barrier.....	1
Synthesis of key building blocks.....	9
Total Synthesis of Linoleic Triols.....	18
References.....	27
Experimental Methods.....	30
Appendix A1: Spectra Relevant to Chapter 1.....	45
II. DEVELOPMENT OF A LARGE SCALE CONVERGENT APPROACH TO APOPTOLIDINONE C.....	100
Apoptolidin: Isolation, Structure, and Biological Activity.....	100
Chemical Synthesis of Apoptolidins.....	105
Progress Toward Apoptolidinone C.....	120
References.....	127
Experimental Methods.....	130
Appendix A2: Spectra Relevant to Chapter 2.....	138

LIST OF FIGURES

Figure	Page
1.1 Essential fatty acids, arachidonic acid and linoleic acid.....	1
1.2 Structures of linoleic acid-rich ceramides.....	2
1.3 Representation of relationship of corneocytes, cornified envelope, corneocyte lipid envelope and lipid lamellae.....	3
1.4 Covalent bond between very long chain fatty acid of the epidermal sphingoside and the cornified lipid envelope, forming the mammalian epidermal water barrier.....	4
1.5 Conversion of linoleate-rich ceramide to covalently-bound ceramide, through previously unknown enzymatic means.....	5
1.6 Linoleate-containing ceramide, a substrate for oxidation and conversion of linoleatae moiety to the 9 <i>R</i> -hydroperoxide derivative via 12 <i>R</i> -LOX.....	6
1.7 Conversion of the 9 <i>R</i> -hydroperoxy linoleic acid metabolite to the 9 <i>R</i> ,10 <i>R</i> 13 <i>R</i> -epoxyalcohol by eLOX3.....	6
1.8 Conversion of the 9 <i>R</i> ,10 <i>R</i> 13 <i>R</i> -epoxyalcohol of linoleic acid to the 9 <i>R</i> ,10 <i>R</i> 13 <i>R</i> -trihydroxy linoleic acid.....	7
1.9 Oxidation of linoleate-rich ceramides by 12 <i>R</i> -LOX, eLOX3, EH3, leading to an intact epidermal water barrier.....	7
1.10 Eight possible linoleatae-trihydroxy isomers produced via epoxyalcohol opening.....	8
1.11 Chemical shifts of 1.53 , 1.58 , 1.59 and $\Delta^{S,R}\delta$ of 1.58 and 1.59	26
A1.1 400 MHz ¹ H-NMR and 100 MHz ¹³ C-NMR spectrum of 1.15 in CDCl ₃	46
A1.2 100 MHz DEPT 135 NMR spectrum of 1.15 in CDCl ₃	47
A1.3 400 MHz ¹ H-NMR and 100 MHz ¹³ C-NMR spectrum of 1.16 in CDCl ₃	48
A1.4 100 MHz DEPT 135 NMR spectrum of 1.16 in CDCl ₃	49
A1.5 400 MHz ¹ H-NMR and 100 MHz ¹³ C-NMR spectrum of 1.17 in CDCl ₃	50
A1.6 100 MHz DEPT 135 NMR spectrum of 1.17 in CDCl ₃	51

A1.7	400 MHz ^1H -NMR and 100 MHz ^{13}C -NMR spectrum of 1.19 in CDCl_3	52
A1.8	100 MHz DEPT 135 NMR spectrum of 1.19 in CDCl_3	53
A1.9	400 MHz ^1H -NMR and 100 MHz ^{13}C -NMR spectrum of 1.11 in CDCl_3	54
A1.10	100 MHz DEPT 135 NMR spectrum of 1.11 in CDCl_3	55
A1.11	400 MHz ^1H -NMR and 100 MHz ^{13}C -NMR spectrum of 1.33 in CDCl_3	56
A1.12	100 MHz DEPT 135 NMR spectrum of 1.33 in CDCl_3	57
A1.13	400 MHz ^1H -NMR and 100 MHz ^{13}C -NMR spectrum of 1.34 in CDCl_3	58
A1.14	100 MHz DEPT 135 NMR spectrum of 1.34 in CDCl_3	59
A1.15	400 MHz ^1H -NMR and 100 MHz ^{13}C -NMR spectrum of 1.35 in CDCl_3	60
A1.16	100 MHz DEPT 135 NMR spectrum of 1.35 in CDCl_3	61
A1.17	400 MHz ^1H -NMR and 100 MHz ^{13}C -NMR spectrum of S2 in CDCl_3	62
A1.18	100 MHz DEPT 135 NMR spectrum of S2 in CDCl_3	63
A1.19	400 MHz ^1H -NMR and 100 MHz ^{13}C -NMR spectrum of 1.9 in CDCl_3	64
A1.20	100 MHz DEPT 135 NMR spectrum of 1.9 in CDCl_3	65
A1.21	400 MHz ^1H -NMR and 100 MHz ^{13}C -NMR spectrum of 1.38 in CDCl_3	66
A1.22	100 MHz DEPT 135 NMR spectrum of 1.38 in CDCl_3	67
A1.23	400 MHz ^1H -NMR and 100 MHz ^{13}C -NMR spectrum of 1.39 in CDCl_3	68
A1.24	100 MHz DEPT 135 NMR spectrum of 1.39 in CDCl_3	69
A1.25	400 MHz ^1H -NMR spectrum of 1.42 in CDCl_3	70
A1.26	400 MHz ^1H -NMR and 100 MHz ^{13}C -NMR spectrum of 1.43 in CDCl_3	71
A1.27	100 MHz DEPT 135 NMR spectrum of 1.43 in CDCl_3	72
A1.28	400 MHz ^1H -NMR and 100 MHz ^{13}C -NMR spectrum of 1.45 in CDCl_3	73
A1.29	100 MHz DEPT 135 NMR spectrum of 1.45 in CDCl_3	74

A1.30	400 MHz ¹ H-NMR and 100 MHz ¹³ C-NMR spectrum of 1.44 in CDCl ₃	75
A1.31	100 MHz DEPT 135 NMR spectrum of 1.44 in CDCl ₃	76
A1.32	400 MHz ¹ H-NMR and 100 MHz ¹³ C-NMR spectrum of 1.47 in CDCl ₃	77
A1.33	100 MHz DEPT 135 NMR spectrum of 1.47 in CDCl ₃	78
A1.34	400 MHz ¹ H-NMR and 100 MHz ¹³ C-NMR spectrum of 1.46 in CDCl ₃	79
A1.35	100 MHz DEPT 135 NMR spectrum of 1.46 in CDCl ₃	80
A1.36	400 MHz ¹ H-NMR and 100 MHz ¹³ C-NMR spectrum of 1.1 in MeOD.....	81
A1.37	400 MHz ¹ H-NMR and 100 MHz ¹³ C-NMR spectrum of 1.48 in CDCl ₃	82
A1.38	100 MHz DEPT 135 NMR spectrum of 1.48 in CDCl ₃	83
A1.39	400 MHz ¹ H-NMR and 100 MHz ¹³ C-NMR spectrum of 1.49 in CDCl ₃	84
A1.40	100 MHz DEPT 135 NMR spectrum of 1.49 in CDCl ₃	85
A1.41	400 MHz ¹ H-NMR spectrum of 1.50 in CDCl ₃	86
A1.42	400 MHz ¹ H-NMR and 100 MHz ¹³ C-NMR spectrum of 1.51 in CDCl ₃	87
A1.43	100 MHz DEPT 135 NMR spectrum of 1.51 in CDCl ₃	88
A1.44	400 MHz ¹ H-NMR and 100 MHz ¹³ C-NMR spectrum of 1.53 in CDCl ₃	89
A1.45	100 MHz DEPT 135 NMR spectrum of 1.53 in CDCl ₃	90
A1.46	400 MHz ¹ H-NMR and 100 MHz ¹³ C-NMR spectrum of 1.52 in CDCl ₃	91
A1.47	100 MHz DEPT 135 NMR spectrum of 1.52 in CDCl ₃	92
A1.48	400 MHz ¹ H-NMR and 100 MHz ¹³ C-NMR spectrum of 1.55 in CDCl ₃	93
A1.49	100 MHz DEPT 135 NMR spectrum of 1.54 in CDCl ₃	94
A1.50	400 MHz ¹ H-NMR and 100 MHz ¹³ C-NMR spectrum of 1.54 in CDCl ₃	95
A1.51	100 MHz DEPT 135 NMR spectrum of 1.54 in CDCl ₃	96
A1.52	400 MHz ¹ H-NMR and 100 MHz ¹³ C-NMR spectrum of 1.2 in MeOD.....	97

A1.53	400 MHz ¹ H-NMR spectrum of 1.58 and 1.59 in CDCl ₃	98
A1.53	400 MHz ¹ H-NMR spectrum of 1.62 and 1.63 in CDCl ₃	99
2.1	Structure of the <i>Nocardiosis sp.</i> FU40 metabolite Apoptolidin A.....	98
2.2	Structures of apoptolidin's A-H.....	99
2.3	EC ₅₀ of four apoptolidin glycovariants against H292 cells.....	100
2.4	Fluorescent Cy3-tagged apoptolidin A and H and Cy3-bicyclononyne.....	101
A2.1	400 MHz ¹ H-NMR and 100 MHz ¹³ C-NMR spectrum of S3 in CDCl ₃	139
A2.2	400 MHz ¹ H-NMR and 100 MHz ¹³ C-NMR spectrum of S4 in CDCl ₃	140
A2.3	400 MHz ¹ H-NMR and 100 MHz ¹³ C-NMR spectrum of 2.4 in CDCl ₃	141
A2.4	400 MHz ¹ H-NMR and 100 MHz ¹³ C-NMR spectrum of S5 in CDCl ₃	142
A2.5	400 MHz ¹ H-NMR and 100 MHz ¹³ C-NMR spectrum of 2.61 in CDCl ₃	143
A2.6	400 MHz ¹ H-NMR and 100 MHz ¹³ C-NMR spectrum of S6 in CDCl ₃	144
A2.7	400 MHz ¹ H-NMR and 100 MHz ¹³ C-NMR spectrum of 2.62 in CDCl ₃	145
A2.8	400 MHz ¹ H-NMR and 100 MHz ¹³ C-NMR spectrum of 2.6 in CDCl ₃	146
A2.9	400 MHz ¹ H-NMR and 100 MHz ¹³ C-NMR spectrum of S7 in CDCl ₃	147
A2.10	400 MHz ¹ H-NMR and 100 MHz ¹³ C-NMR spectrum of 2.64 in CDCl ₃	148
A2.11	400 MHz ¹ H-NMR and 100 MHz ¹³ C-NMR spectrum of 2.35 in CDCl ₃	149
A2.12	400 MHz ¹ H-NMR and 100 MHz ¹³ C-NMR spectrum of 2.71 in CDCl ₃	150
A2.13	400 MHz ¹ H-NMR and 100 MHz ¹³ C-NMR spectrum of 2.74 in CDCl ₃	151
A2.14	400 MHz ¹ H-NMR and 100 MHz ¹³ C-NMR spectrum of S8 in CDCl ₃	152
A2.15	400 MHz ¹ H-NMR and 100 MHz ¹³ C-NMR spectrum of 2.75 in CDCl ₃	153

LIST OF SCHEMES

Scheme	Page
1.1	General synthetic strategy toward lipid mediators.....9
1.2	Synthesis of alkyne 1.11 from L-tartaric acid.....10
1.3	Alkynyl displacement reported by Sakai.....11
1.4	Synthesis of substrates as potential alternatives to triflate 1.1811
1.5	Select examples of displacement conditions with bromide 1.2012
1.6	Select examples of displacement conditions and substrates.....13
1.7	Formation of 1.27 through anion stabilization and proposed alternative nucleophiles... 14
1.8	Synthesis of alkyne 1.10 from 2-deoxy-L-ribose.....15
1.9	Strategy toward triols 1.1 and 1.3 , from 1.9 , 1.13 and 1.3215
1.10	Synthesis of alkyne 1.9 from D-tartaric acid.....16
1.11	Retrosynthetic strategy toward triols 1.2 and 1.4 , from 1.10 , 1.13 and 1.3216
1.12	Synthesis of vinyl iodide 1.32 and phosphonate side chain 1.1317
1.13	Successful sonogashira coupling of 1.9 and 1.32 , followed by failed hydrogenation of the enyne moiety.....18
1.14	Attempted hydrogenations of enyne 1.3819
1.15	Successful hydrogenation of enyne 1.40 and 1.38 using Borohydride-Nickel(II)-complex.....19
1.16	Oxidation and Horner-Wadsworth-Emmons reaction to afford enone 1.43 , followed by Luche reduction of enone 1.43 , yielding epimeric alcohols 1.44 and 1.4520
1.17	Acetal de-protection affording trihydroxy linoleate esters 1.46 and 1.47 followed by hydrolysis of 1.47 to yield acid 1.121
1.18	Sonogashira coupling of 1.10 and 1.32 , followed by hydrogenation to afford alcohol 1.49 , oxidation and Horner-Wadsworth-Emmons reaction, followed by Luche reduction of enone 1.51 yielding epimeric alcohols 1.52 and 1.5322

1.19	Acetal de-protection affording trihydroxy linoleate esters 1.54 and 1.55 , followed by hydrolysis of 1.54 to yield acid 1.2	23
1.20	Synthesis of Mosher esters 1.56-1.63	24
1.21	Model conformation for Mosher ester analysis.....	25
2.1	Koert's retrosynthetic strategy toward Apoptolidinone A.....	105
2.2	Synthesis of weinreb amide 2.7	106
2.3	Synthesis of the Southern hemisphere of apoptolidinone A.....	107
2.4	Synthesis of the Northern hemisphere.....	108
2.5	Completion of apoptolidinone A.....	109
2.6	Crimmin's approach to apoptolidinone A.....	109
2.7	Synthesis of aldehyde 2.26 via Crimmin's aldol technology.....	110
2.8	Crimmin's aldol to afford the non-Evan's <i>syn</i> adduct 2.27	110
2.9	Synthesis of cross metathesis precursor, diene 2.30	111
2.10	Cross metathesis to yield the seco-acid precursor 2.31	111
2.11	The Nelson group's strategy toward apoptolidinone C.....	112
2.12	Enantioselective catalysis employed in Nelson's synthesis of apoptolidinone C.....	113
2.13	Synthesis of the key fragments dibromide 2.32 and vinyl boronate 2.34	114
2.14	Synthesis of trienoate 2.41 via iterative cross-couplings.....	114
2.15	Sulikowski's approach to apoptildinone A.....	115
2.16	Synthesis of vinyl stannane 2.48	116
2.17	Synthesis of key aldehyde 2.49	116
2.18	Synthesis of the western hemisphere through Suzuki coupling.....	117
2.19	Synthesis of late-stage intermediate 2.53 via aldol.....	118

2.20	Completion of the total synthesis of apoptolidinone A.....	119
2.21	Our original synthetic strategy to apoptolidinone C.....	120
2.22	Synthesis of aldehyde 2.62	121
2.23	Synthesis of key fragment methyl ketone 2.35	122
2.24	Aldol reactions between auxiliary 2.65 and aldehydes 2.66-2.68	122
2.25	Revised synthetic strategy toward apoptoldinone C.....	123
2.26	Synthesis of key fragment 2.71 from acrolein.....	123
2.27	Failed selective hydrostannylation of alkyne 2.72	124
2.28	Current strategy toward apoptolidinone C.....	124
2.29	Synthesis of key fragment 2.78	125
2.30	Proposed completion of apoptolidinone C.....	126

LIST OF ABBREVIATIONS

2,2-DMP	2,2-dimethoxypropane
9 <i>R</i> -HPODE	9 <i>R</i> -hydroperoxide
12 <i>R</i> -LOX	12 <i>R</i> -lipoxygenase
Ac	acetyl
AcOH	acetic acid
Ag ₂ O	silver oxide
AIBN	azobisisobutyronitrile
Bcl-2	B-cell lymphoma 2
Bn	benzyl
br	broad
°C	degrees Celsius
CBS	Corey-Bakshi-Shibata catalyst
CH ₂ Cl ₂	dichloromethane
Cy3	Cyanine 3
d	doublet
δ	chemical shift in ppm
DiBAIH	diisobutylaluminum hydride
DIEA	diisopropylethylamine
DMAP	4-dimethylaminopyridine
DMF	dimethylformamide
DMP	Dess-Martin periodinane
DMPU	1,3-Dimethyl-3,4,5,6-tetrahydro-2(1H)-pyrimidinone
DMSO	dimethylsulfoxide
E1A	Adenovirus early region A1
EC ₅₀	half maximal effective concentration
EDA	ethylene diamine
EFA	essential fatty acid
EH3	epoxide hydrolase 3
eLOX3	epidermal lipoxygenase 3

eq	equivalents
Et ₂ O	diethyl ether
Et ₃ N	triethylamine
EtOH	ethanol
EtOAc	ethyl acetate
g	gram
h	hour
HKD ₂	hemiketal D ₂
HKE ₂	hemiketal E ₂
HMPA	hexamethylphosphoramide
HRMS	high-resolution mass spectrum
HWE	Horner-Wadsworth-Emmons
Hz	Hertz
IBX	2-iodoxybenzoic acid
ImH	imidazole
<i>J</i>	coupling constant
LDA	lithium diisopropylamine
LiAlH	lithium aluminum hydride
LiBr	lithium bromide
LYas	mouse B lymphoma cells
M	molar
m	multiplet or milli
Me	methyl
MeCN	acetonitrile
MeI	methyl iodide
MeOH	methanol
μ	micro
min	minutes
mol	mole
MsCl	methanesulfonyl chloride

MTPA	α -methoxy- α -trifluoromethylphenylacetic acid
N	normal concentration
NaH	sodium hydride
NaHMDS	sodium bis(trimethylsilyl)amide
<i>n</i> -BuLi	<i>n</i> -butyllithium
NMP	<i>N</i> -methyl-2-pyrrolidinone
NMR	nuclear magnetic resonance
OAc	acetoxy
PCC	pyridinium chlorochromate
PPh ₃	triphenylphosphine
Ph	phenyl
PMB	<i>para</i> -methoxybenzyl
ppm	parts per million
PPTS	pyridinium <i>p</i> -toluenesulfonate
<i>p</i> -TSA	<i>para</i> -toluenesulfonic acid
q	quartet
rt	room temperature
s	singlet
sEH	soluble epoxide hydrolase
t	triplet
TBAF	tetra- <i>n</i> -butylammonium fluoride
TBDPS	<i>tert</i> -butyldiphenylsilyl
TBDPSCl	<i>tert</i> -butyldiphenylsilyl chloride
TBS	<i>tert</i> -butyldimethylsilyl
TBSCl	<i>tert</i> -butyldimethylsilyl chloride
TES	triethylsilyl
TESCl	triethylsilyl chloride
TFA	trifluoroacetic acid
Tf ₂ O	trifluoromethanesulfonic anhydride
THF	tetrahydrofuran
TMS	trimethylsilyl

TMSCHN ₂	trimethylsilyl diazomethane
TMSCl	trimethylsilyl chloride
TsCl	tosyl chloride
VLFA	very long chain fatty acid

CHAPTER I

SYNTHESIS OF FOUR ISOMERIC LINOLEIC TRIOLS

The role of linoleic acid in the mammalian epidermal water barrier

It has been observed since 1929 that certain polyunsaturated fatty acids are required in the diet¹ (Figure 1.1). These essential fatty acids (EFA) form a diverse array of bioactive lipid mediators that act on a large number of selective receptors in nearly every tissue and cell in the body.² In this way, EFA signaling influences nearly every process in human physiology. It is therefore of no surprise that excessive actions of EFA derived mediators are implicated in heart disease, cancer proliferation, mental health disorders, and numerous other diseases, including EFA deficiency and ichthyosis.²

The hallmark sign of EFA deficiency, scaly skin, is associated with epidermal water loss due to failure to form a functional epidermal water barrier.³ This phenotype is also observed as a result of the human genetic disorders of ichthyosis, a disease characterized by “dry, thickened, and scaly skin”.³ In rats with EFA-deficiency, one common observation is increased water consumption due to trans-epidermal water loss.³

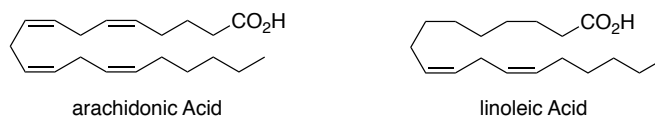


Figure 1.1 Essential fatty acids, arachidonic acid and linoleic acid

Reintroduction of linoleic acid into the diet of EFA-deficient rats results in increased growth in size due to the effect of linoleate restoring the epidermal water barrier.¹ Interestingly, all members of the linoleic acid family show restoration of the epidermal water barrier and increased growth of

these rats. Introduction of arachidonic acid to the diet of EFA-deficient rats showed restoration of the epidermal water barrier and even greater growth in size than linoleate. These results led some to infer that arachidonic acid was *the* essential fatty acid, and that linoleic acid (18 carbons) serves as a precursor for arachidonate (20 carbons). This hypothesis was turned on its head when linoleic acid-rich lipids such as linoleate glucosylceramide, linoleate ceramide, and linoleate very long chain fatty acid were identified in human, rat and pig epidermal tissue¹ (Figure 1.2).

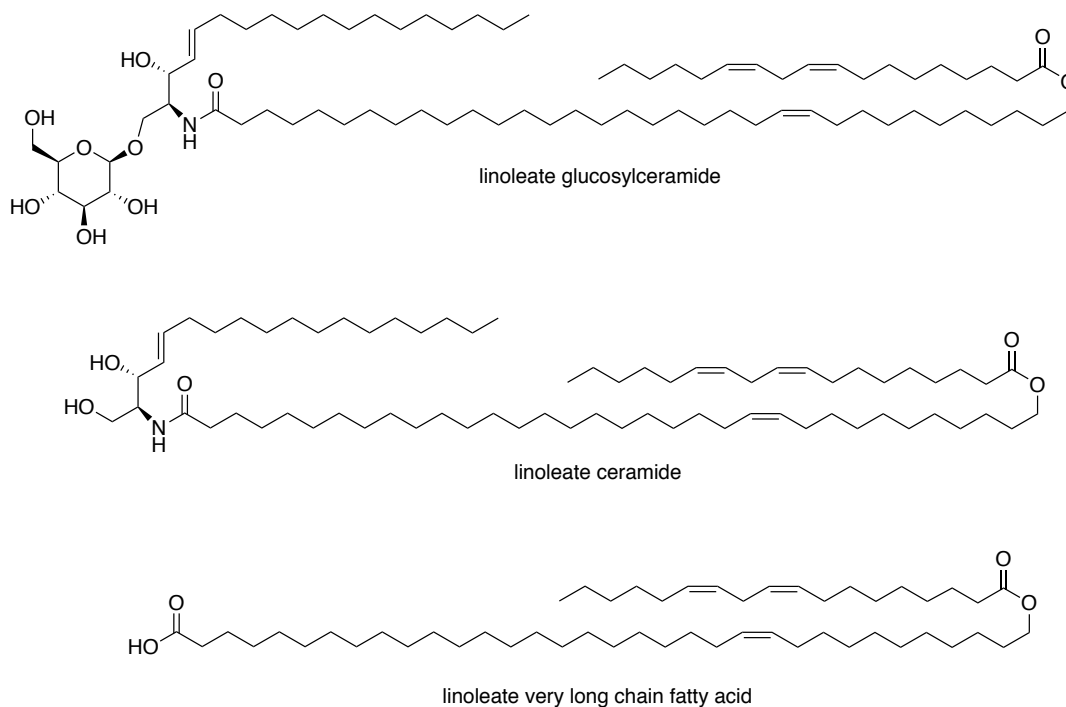


Figure 1.2 Structures of linoleic acid-rich ceramides.

In fact, arachidonic acid was almost completely absent from the outer epidermal tissue. While it was unclear whether these lipids serve as structural components of the intact water barrier or whether the oxidation of the linoleic moiety was essential, these lipid bodies were known to be important in formation of the epidermal water barrier. The final thread of evidence came in 1986, when Hansen showed that while arachidonate restored the epidermal barrier in EFA-deficient rats,

only linoleate was found in the epidermal ceramides, suggesting a conversion of arachidonate to linoleate.¹ With linoleic acid being recognized as *the* essential fatty acid in barrier formation, attention turned to investigating the structural role of the linoleate-rich epidermal ceramides.^{3,4,5}

In order to understand the role of linoleate-rich ceramides, an understanding of how the mammalian epidermal water barrier forms is necessary, starting with defining corneocyte structure. Corneocytes are dead flat cells that make up the outer epidermis in mammalian skin.^{4,5} Each corneocyte is surrounded by a layer of polymerized protein, called the corneocyte envelope (Figure 1.3). The ω -hydroxyl-very long chain fatty acids (VLFA) of epidermal ceramides are covalently bound to these polymerized cross-linked proteins, constituting the corneocyte lipid envelope (Figure 1.4). It is this covalent linkage between lipids and the underlying protein that creates a waterproof barrier in the outer epidermis.^{4,5}

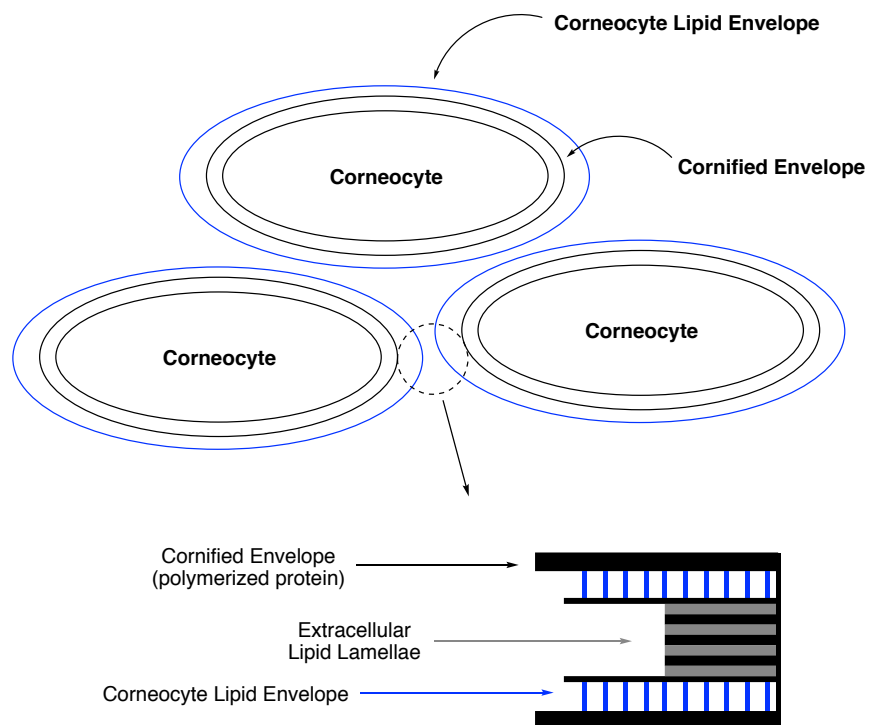


Figure 1.3 Representation of relationship of corneocytes, cornified envelope, corneocyte lipid envelope and lipid lamellae

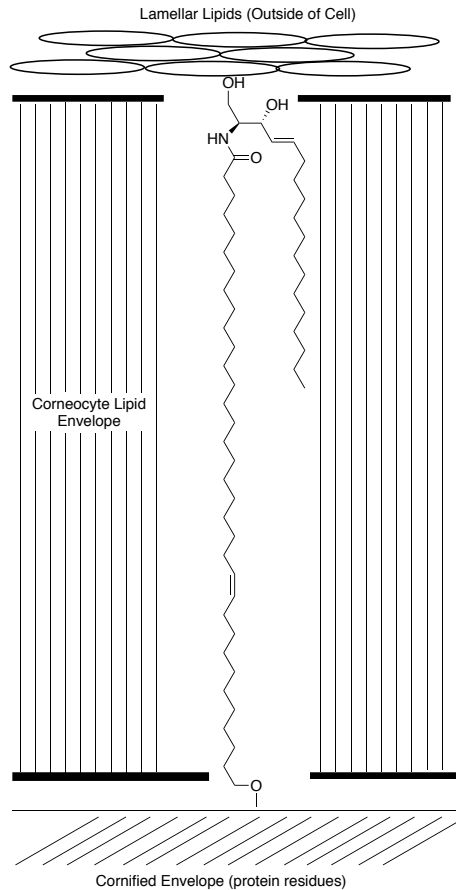


Figure 1.4 Covalent bond between very long chain fatty acid of the epidermal sphingoside and the cornified lipid envelope, forming the mammalian epidermal water barrier

The absence of this linkage leads to trans-epidermal water loss and the symptoms of congenital ichthyosis. While many genes must work in concert to establish the mammalian epidermal water barrier, a single mutation in one leads to ichthyosis (Figure 1.5). One such gene product, 12*R*-lipoxygenase (12*R*-LOX) is essential.⁶ Mutation or deletion of 12*R*-LOX shows a remarkable reduction in covalent linkage of ω -hydroxyl-VLFA ceramides to the corneocyte envelope. Additionally, absence or mutation of epidermal lipoxygenase 3 (eLOX3), leads to ~50% reduction in covalent linkage between the two.⁶ While the importance of 12*R*-LOX, eLOX3, and linoleic acid is irrefutable, their mechanism and roles were unknown until recently.

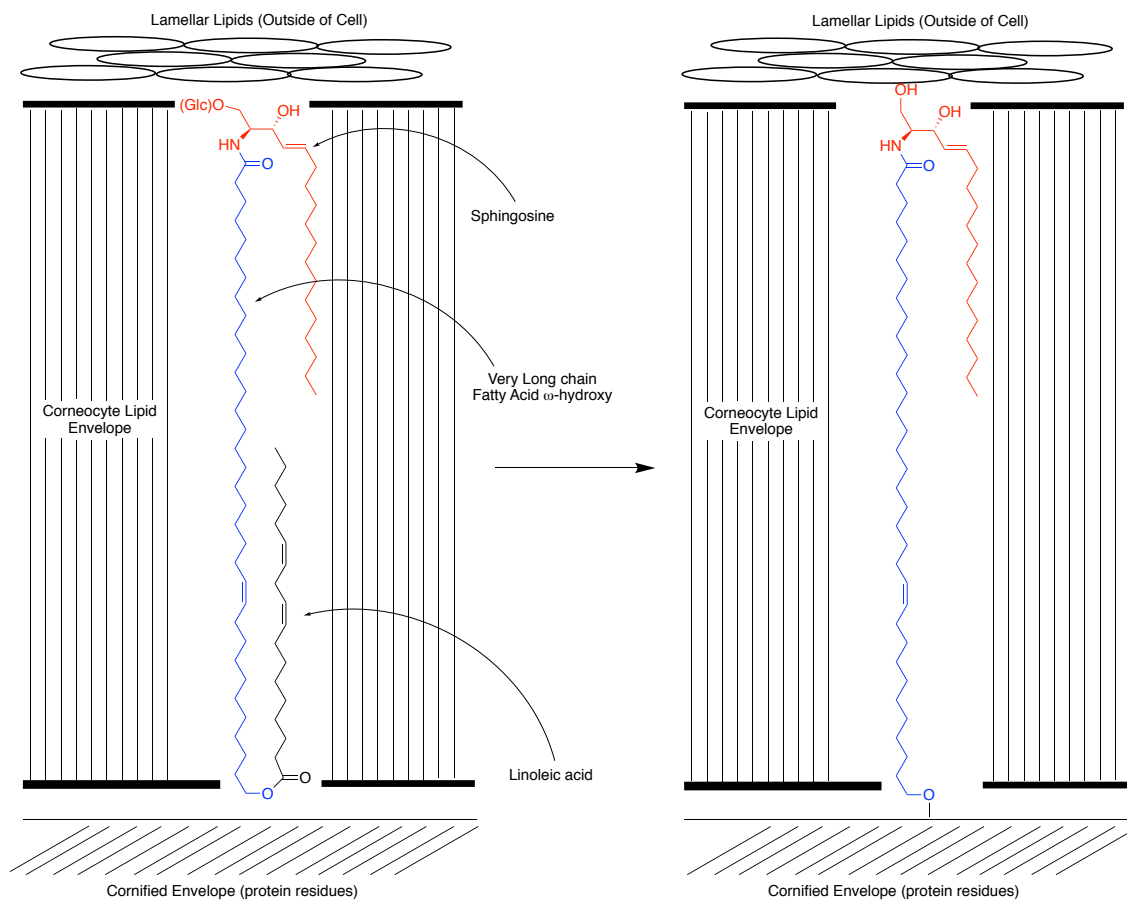


Figure 1.5 Conversion of linoleate-rich ceramide to covalently-bound ceramide, through previously unknown enzymatic means

In 2011, the Brash group reported that the linoleic moiety of the epidermal ceramides is selectively oxidized by 12R-LOX, yielding the 9R-hydroperoxide (9R-HPODE) derivative (Figure 1.6).^{3,6}

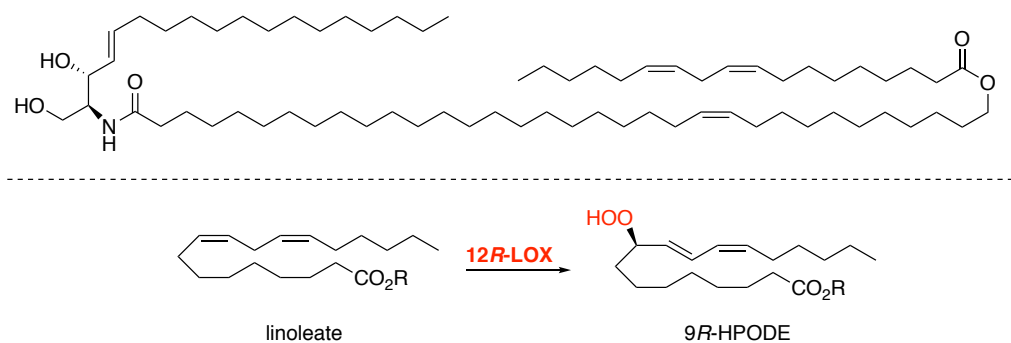


Figure 1.6 Linoleate-containing ceramide, a substrate for oxidation and conversion of linoleate moiety to the 9*R*-hydroperoxide derivative via 12*R*-LOX

eLOX3 in turn catalyzes the conversion of 9*R*-HPODE specifically to the 9*R*,10*R*-epoxy-13*R*-hydroxy-epoxyalcohol derivative (Figure 1.7). These oxidative events were shown to be necessary for formation of the epidermal water barrier, as absence of LOX metabolites were correlated with failure to form the cornified lipid envelope.^{3,6}

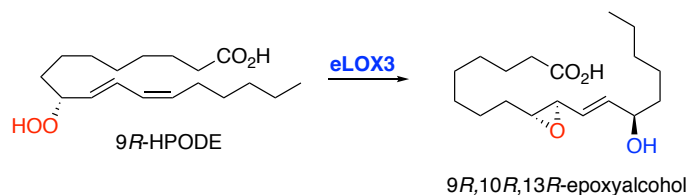


Figure 1.7 Conversion of the 9*R*-hydroperoxy linoleic acid metabolite to the 9*R*,10*R*,13*R*-epoxyalcohol by eLOX3

Recently, the selective hydrolytic opening of the epoxide moiety of this epoxyalcohol was shown to afford the trihydroxy derivative. This transformation, catalyzed by epoxide hydrolase 3 (EH3) or soluble epoxide hydrolase (sEH) was shown to be essential for barrier formation as well (Figure 1.8).⁷

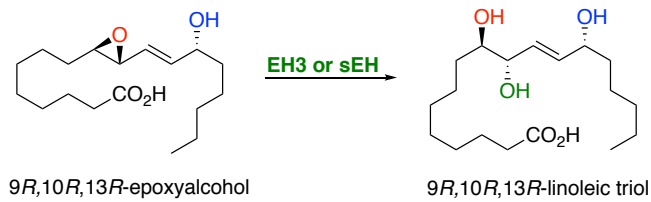


Figure 1.8 Conversion of the $9R,10R,13R$ -epoxyalcohol of linoleic acid to the $9R,10R,13R$ -trihydroxy linoleic acid

At this point, the oxidized linoleate triol moiety is hydrolyzed, allowing the ω -hydroxyl-VLFA to covalently bind the cornified envelope and create an intact barrier (Figure 1.9).^{4,5} These findings shine light on an important physiological process. It is the formation of the epidermal water barrier that allows life on dry land to exist, and for practical purposes this work has huge implications in understanding atopic dermatitis, a condition of large clinical importance.⁸

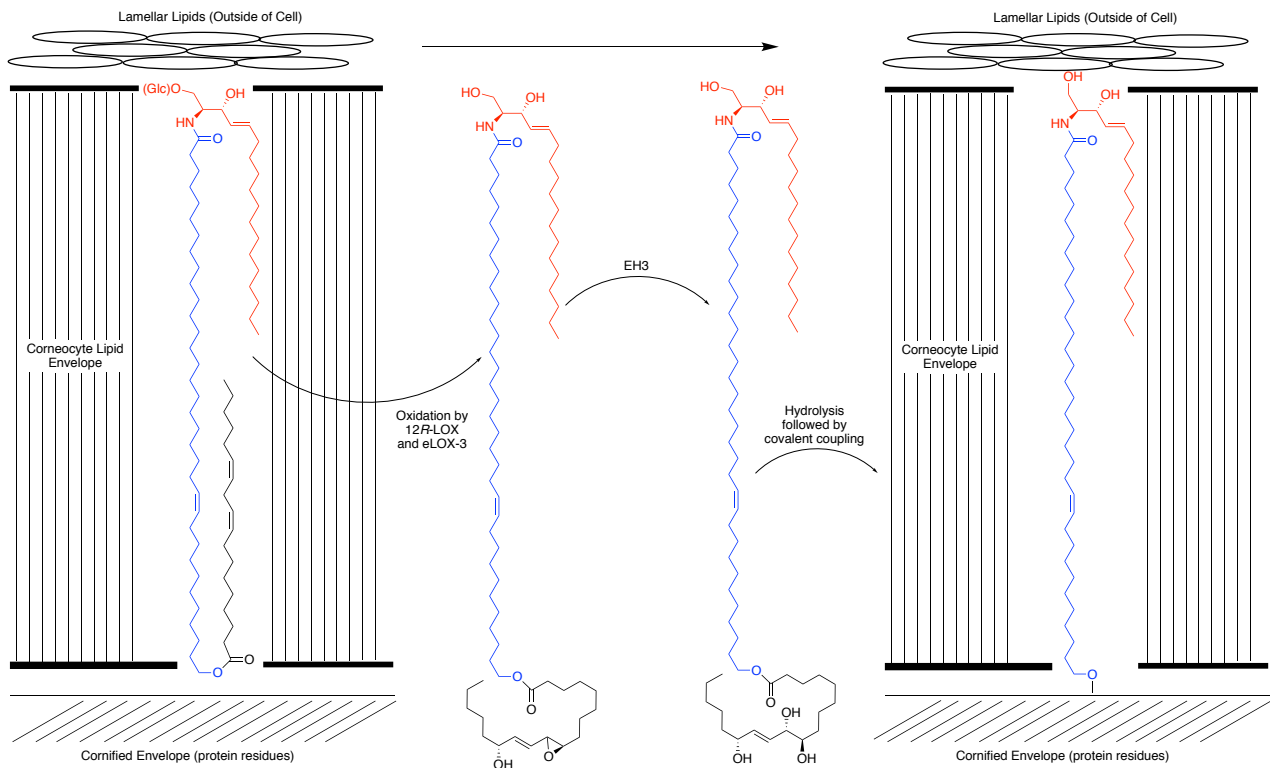


Figure 1.9 Oxidation of linoleate-rich ceramides by 12R-LOX, eLOX-3, and EH3, leading to an intact epidermal water barrier

While much has been learned, gaps in our understanding of this process remain. First, many isomers can and are produced via this oxidative pathway, albeit, some in minor amounts. Epoxyalcohols of varying stereochemistry at the 9,10 and 13 position can be opened to form either the 9,10,13-trihydroxy linoleic acids (1.1-1.4) or the 9,12,13-trihydroxy linoleic acids (1.5-1.8) (Figure 1.10). Analysis of these isomers is critical for furthering our understanding of barrier formation. This is complicated by the difficulty in identifying and quantifying the linoleate triols produced in this process, as isomers possess nearly identical chromatographic and spectroscopic properties. While several synthetic routes to access the 9,12,13-trihydroxy series have been developed⁸⁻¹⁴, the 9,10,13-trihydroxy series has yet to be synthesized. Further study will be greatly advanced with the aide of isomerically pure synthetic standards. With this, and the importance of other lipid mediators in mind, we sought a common synthetic strategy to allow access to lipid mediators of interest, including the linoleic triols described.

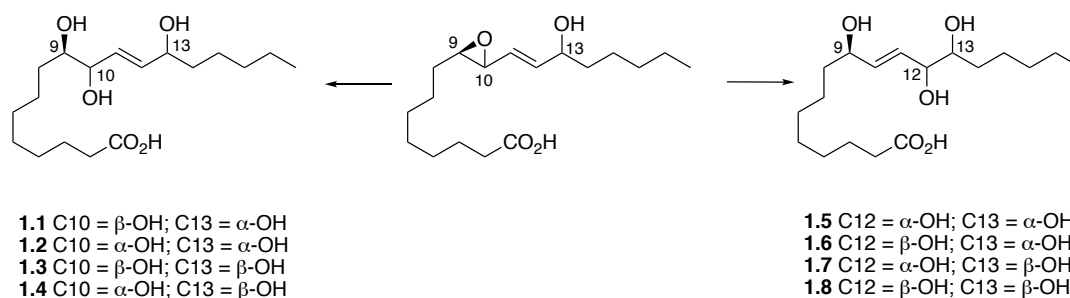
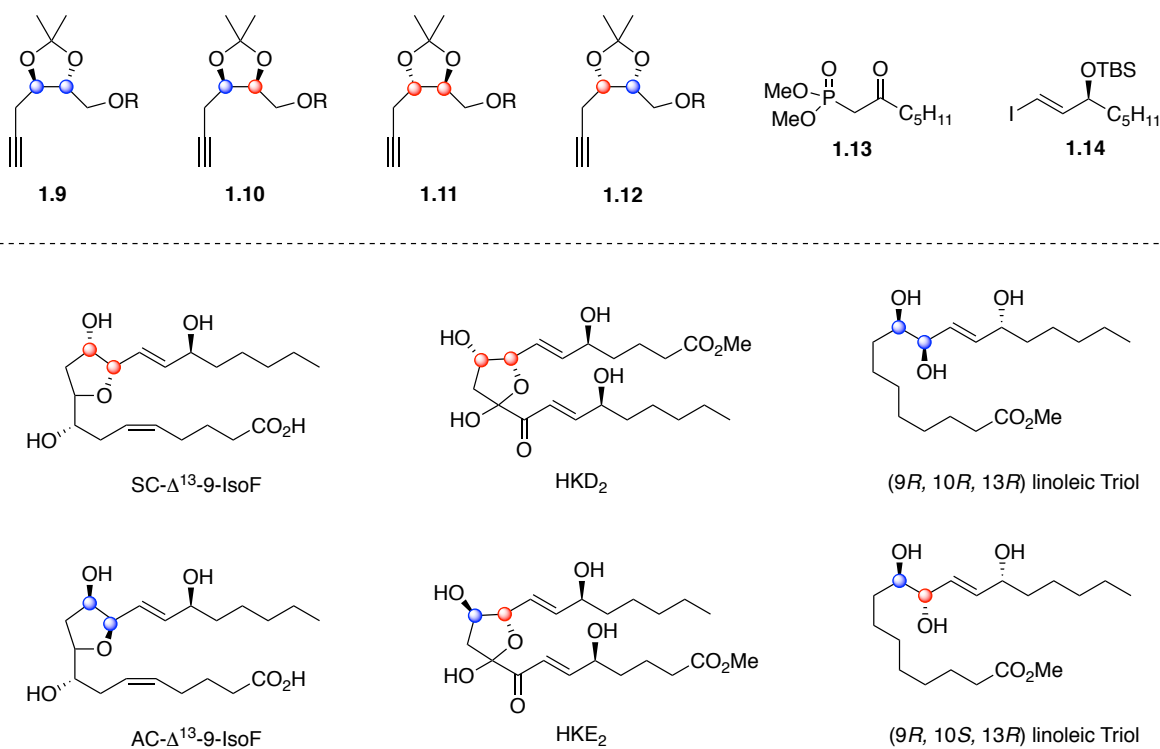


Figure 1.10 Eight possible linoleate-trihydroxy isomers produced via epoxyalcohol opening

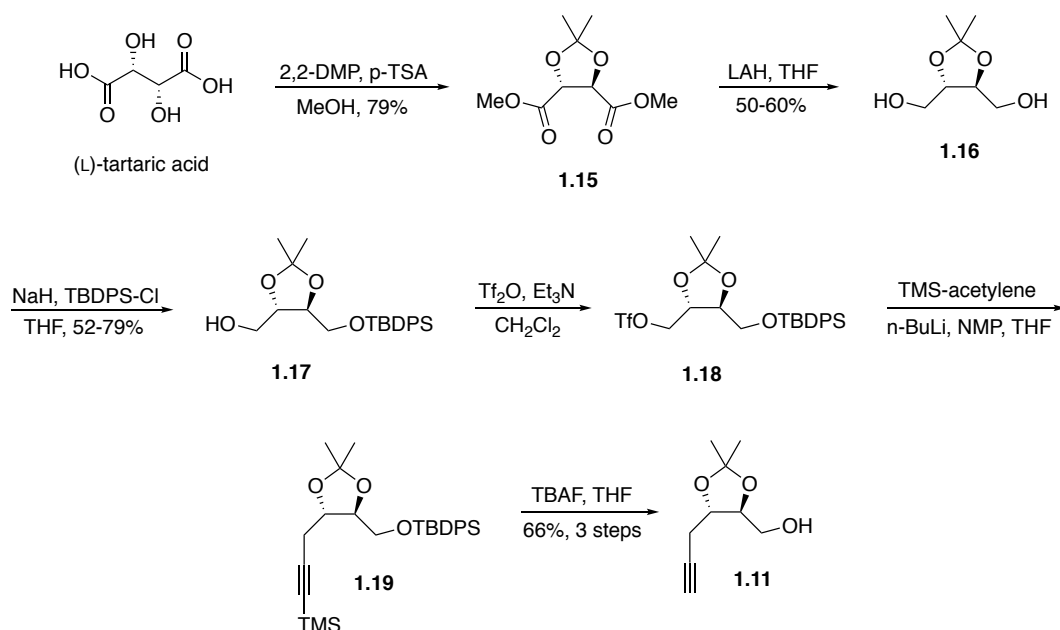
Synthesis of Key Building Blocks

Our lab is interested in the chemical synthesis of a variety of lipid metabolites, due to their interesting structural motifs and to be defined biological profiles. When looking at this diverse subset of natural products, a few common structural themes arise. The prevalence of 1,2-diols of varying stereochemistry appears frequently, and an allylic alcohol with a pentyl-chain is a common motif. We hypothesize the use of isomeric alkynes **1.9-1.12** and building blocks **1.13** and **1.14** can be used as common intermediates toward a wide array of lipid mediators, including linoleic triols, hemiketals, and isofurans (Scheme 1.1). Our synthetic strategy toward the diastereomeric linoleic triols benefits from insights gained during our synthetic studies directed towards hemiketal D₂, hemiketal E₂, and the isofurans, thus these will be briefly discussed.



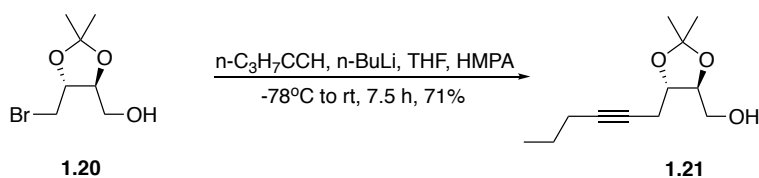
Scheme 1.1 General synthetic strategy toward lipid mediators

Our synthetic strategy directed towards hemiketal **D₂** starts from alkyne **1.11**, which is synthesized from the L-tartaric acid (Scheme 1.2). A one-pot acetal protection and Fischer esterification affords **1.15** in good yields and subsequent treatment with lithium aluminum hydride affords the desired diol **1.16**.¹⁵ Mono-protection of diol **1.16** with *tert*-butyldiphenylchlorosilane yields alcohol **1.17** in 79% yield.^{15,16} Conversion of the alcohol to the corresponding triflate **1.18** followed by displacement with lithium trimethylsilyl acetylide then affords the alkyne **1.19**.¹⁶ Removal of the TBDPS protecting group with tetrabutylammonium fluoride affords the alkynyl building block **1.11** in 66% yield over 3 steps.¹⁶



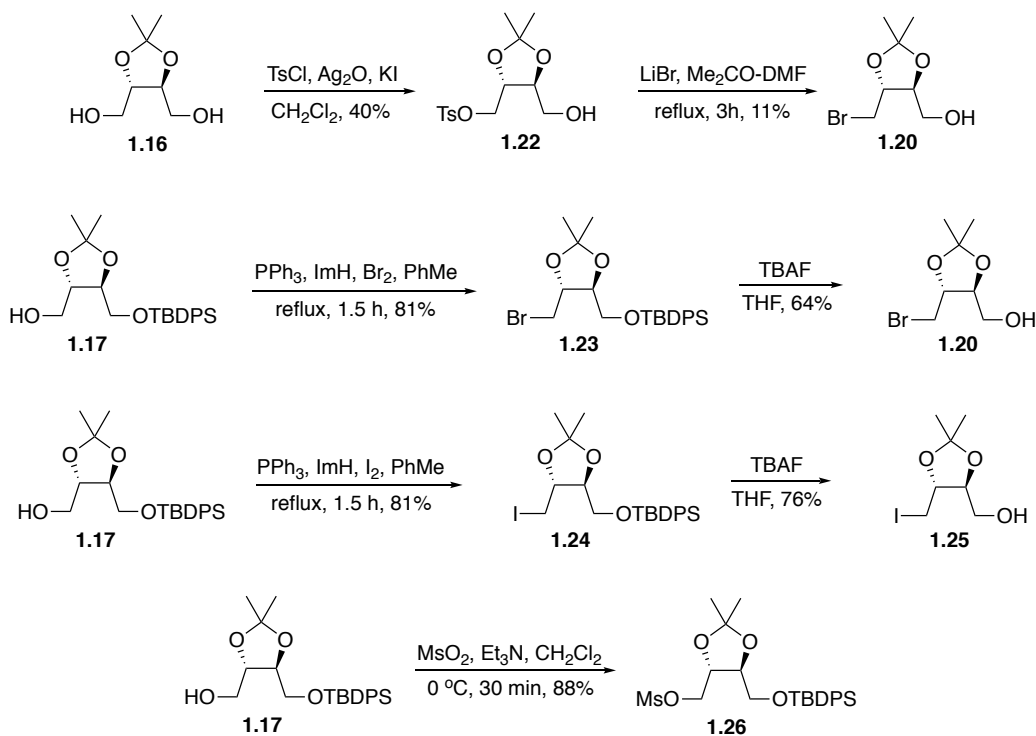
Scheme 1.2 Synthesis of alkyne **1.11** from L-tartaric acid

While developing this route, we observed triflate **1.18** to be moderately stable in solution and minimally stable to silica gel chromatography. Inspired by a report from Sakai and co-workers (Scheme 1.3), we considered an alkyl halide or tosylate as alternative substrates that would be significantly more stable and potentially avoid the use of a TBDPS protecting group.¹⁷ With this intent, we investigated a variety of leaving groups (Scheme 1.4) as potential alternatives to the unstable triflate **1.18**.



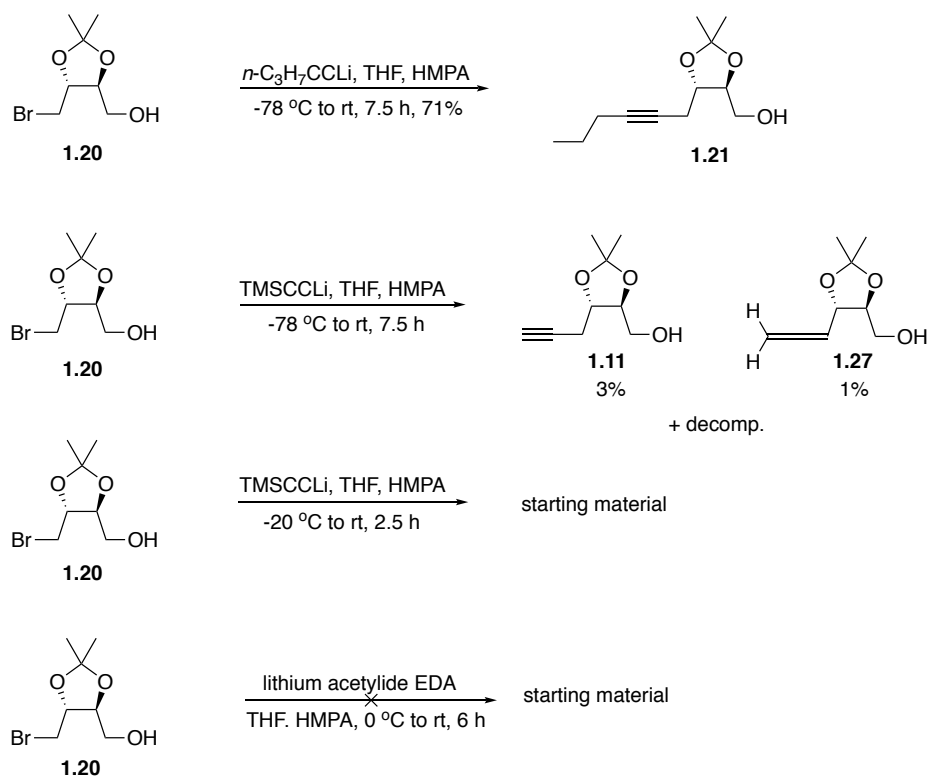
Scheme 1.3 Alkynyl displacement reported by Sakai

Diol **1.16** was mono-protected with *p*-toluenesulfonyl chloride, yielding a potential substrate for displacement (**1.22**), and could be converted to the bromide **1.20** via Finkelstein conditions (Scheme 1.4).¹⁷ This method proved low yielding, and alternative strategies were explored. Starting from alcohol **1.17**, Appel conditions afforded the bromide or iodide **1.23** and **1.24**, respectively, which were investigated as potential substrates.¹⁸ De-protection of **1.23** or **1.24** with TBAF afforded the corresponding alcohols **1.20** and **1.25**, offering two more potential substrates for the desired displacement. Conversion of the alcohol **1.27** to the mesylate **1.26** proceeded in 88% yield (Scheme 1.4).¹⁹



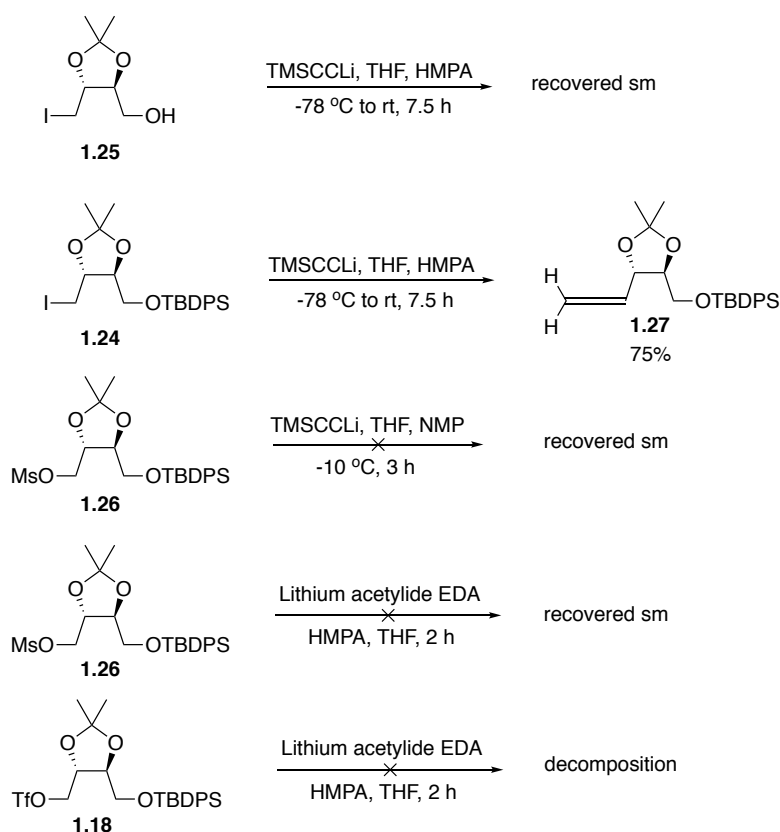
Scheme 1.4 Synthesis of substrates as potential alternatives to triflate **1.18**

We were very encouraged when, in our hands, the displacement reported by Sakai and co-workers was reproduced in almost identical yields (ca. 70%), and we found the bromide starting material **1.20** to be bench stable (Scheme 1.5).¹⁶ Using the conditions from Sakai, we attempted displacement of the bromide with the preferred trimethylsilyl acetylide in place of 1-pentyne. To our dismay, only trace amounts of the desired product **1.11**, and allene **1.27** were isolated from the reaction. We reasoned that the excessive equivalents of n-butyllithium were leading to decomposition, however, despite many attempts to optimize the reaction conditions, we could not encourage displacement without excess n-butyllithium. A variety of conditions utilizing lithium acetylide ethylene diamine complex were examined²⁰, but only starting material was recovered from these attempts (Scheme 1.5).



Scheme 1.5 Select examples of displacement conditions with bromide **1.20**

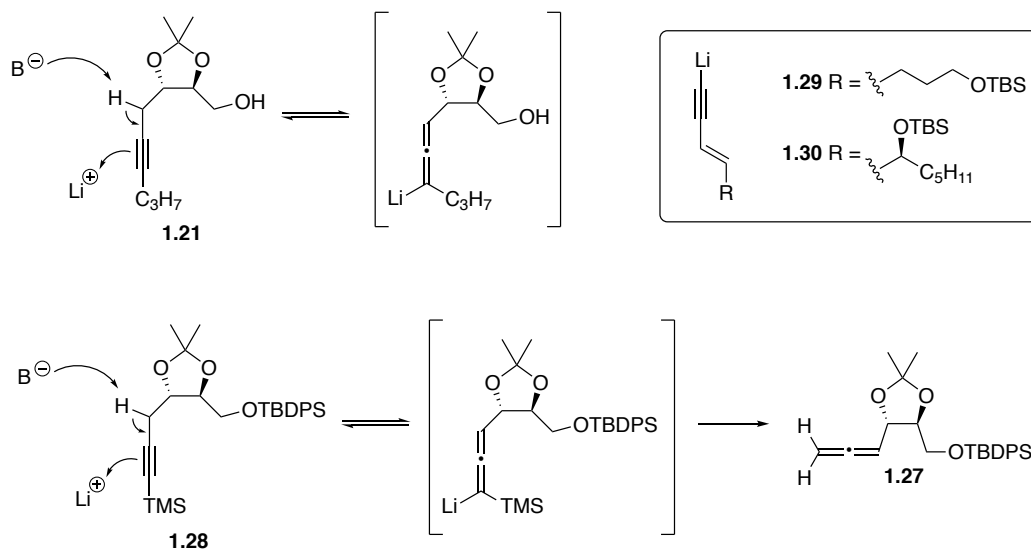
Undeterred, we turned our attention to other leaving groups. Using a variety of conditions, we saw either recovery of starting material or complete decomposition in the case of tosylate **1.22**, iodide **1.25**, or mesylate **1.26** (Scheme 1.6). It should be mentioned that treatment of triflate **1.18** with lithium acetylide-EDA complex led to decomposition only. To our surprise, treatment of iodide **1.24** under Sakai's conditions, with trimethylsilyl acetylide, afforded allene **1.27** in 75% yield with no observed decomposition.



Scheme 1.6 Select examples of displacement conditions and substrates

Allene formation is only observed under conditions of excessive *n*-butyllithium and trimethylsilyl acetylide. Under analogous conditions utilizing the lithiate of pentyne, no allene formation is observed. The *d*-orbitals of silicon presumably provides greater stabilization of the intermediate lithiate anion than the alkyl chain of **1.21** (Scheme 1.7). To suppress undesired allene formation but take advantage of halide stability, future work could investigate the lithiate addition of enyne nucleophiles. For example, **1.29** could be employed to install the α -side chain

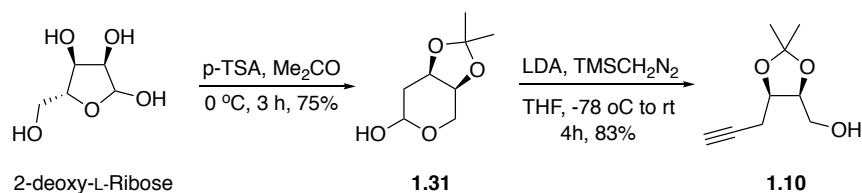
of the linoleic triols **1.1-1.4** in a more convergent approach, or **1.30** could be used to install the ω -side chain of HKE₂ (Scheme 1.7).



Scheme 1.7 Formation of **1.27** through anion stabilization and proposed alternative nucleophiles

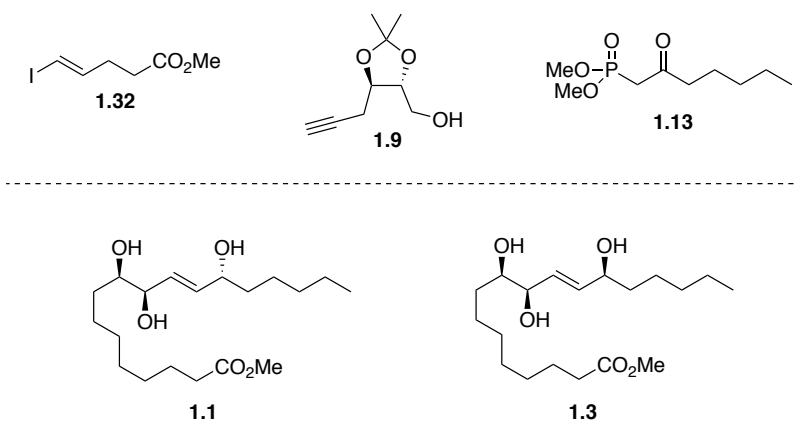
While interesting, these results were not followed up, due to the need for high concentrations of HMPA and a large excess of n-butyllithium (Scheme 1.6). After an exhaustive screen of conditions, leaving groups, and nucleophiles, our original conditions to convert triflate **1.18** to alkyne **1.19** using THF and NMP as the solvent system at -20 °C were found to be the highest yielding, and to date this reaction has been run on as many as 20 grams of material.

Efforts towards hemiketal E₂ required an efficient synthesis of cis-acetonide alkyne **1.10**. Starting from commercially available 2-deoxy-L-ribose, acetal protection followed by Colvin rearrangement afforded the desired alkyne in good yields and only two synthetic steps (Scheme 1.9).²³ This chemistry has been demonstrated on a 20 gram scale in regards to the acetal protection and a 5 gram scale in regards to the Colvin rearrangement.



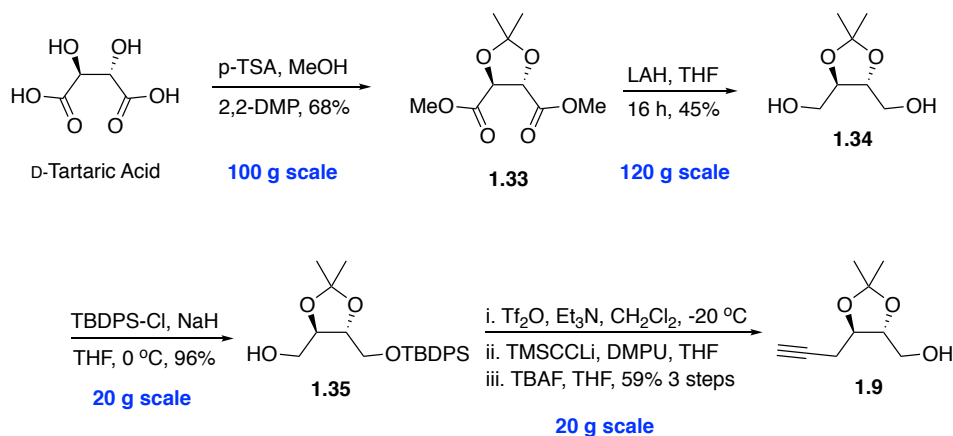
Scheme 1.8 Synthesis of alkyne **1.10** from 2-deoxy-L-ribose

With these robust routes to isomeric alkynes **1.11** and **1.10** in place, we turned our attention to the total synthesis of the epimeric linoleic triols **1.1-1.4** (Scheme 1.10). The synthesis of triols **1.1** and **1.3** started from alkyne **1.9**, which was synthesized from D-tartaric acid (Scheme 1.10).^{15,16}



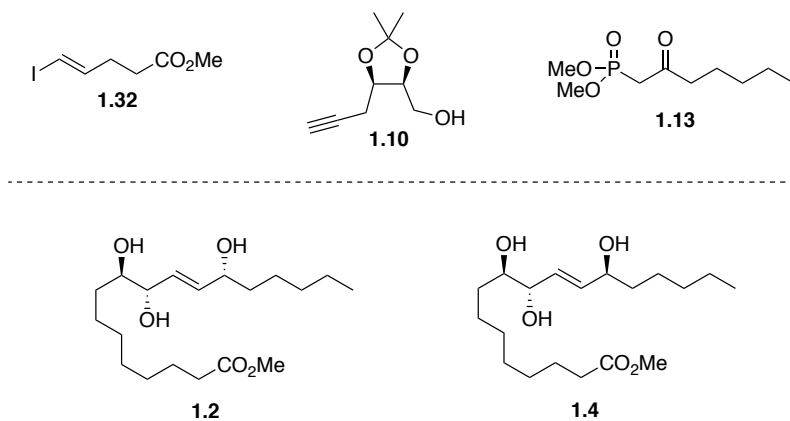
Scheme 1.9 Strategy toward triols **1.1** and **1.3**, from **1.9**, **1.13** and **1.32**

Conversion to the corresponding methyl ester **1.33** has been performed starting from 100 grams of D-tartaric acid, and reduction of ester **1.33** has been demonstrated on as much as 120 grams of material. Mono-protection and the triflation-displacement-de-protection sequence all proceeded as expected (Scheme 1.11). We have found two ways to successfully handle the unstable triflate intermediate. The crude reaction mixture can be quickly filtered through a plug of silica to afford crude triflate, which must be used immediately in the next reaction. If the triflate must be stored, it must be concentrated from benzene three times and stored under vacuum over P₂O₅ until further use.



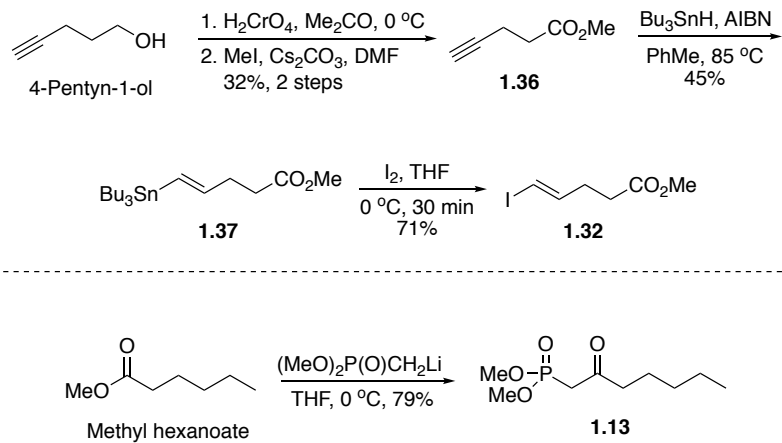
Scheme 1.10 Synthesis of alkyne **1.9** from D-tartaric acid

Triols **1.2** and **1.4** were synthesized starting from 2-deoxy-L-ribose derived alkyne **1.10**, using the same vinyl iodide **1.32** and phosphonate building block **1.13** as triols **1.1** and **1.3** (Scheme 1.12).



Scheme 1.11 Strategy toward triols **1.2** and **1.4**, from **1.10**, **1.13** and **1.32**

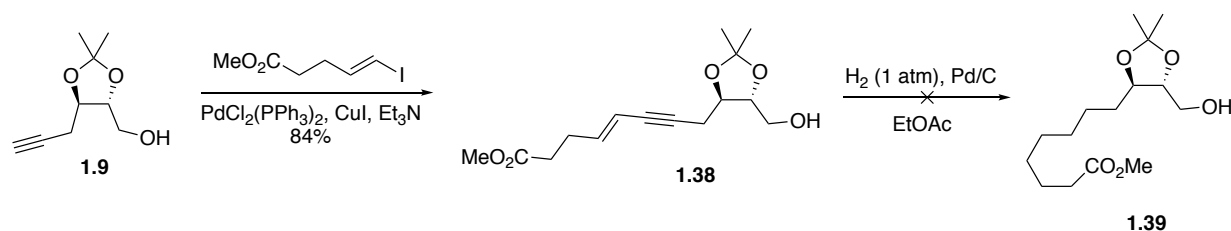
Our necessary phosphonate **1.13** was synthesized in one step via Claisen condensation of dimethyl methylphosphonate and methyl hexanoate in 79% yield (Scheme 1.13).²⁴ Synthesis of vinyl iodide **1.32** began from pentynol. Reaction with Jones's reagent afforded the carboxylic acid²⁵, which was immediately treated with Cs_2CO_3 and MeI to afford the methyl ester **1.36**²⁶ in a 32% yield over 2 steps. Radical-mediated hydrostannylation^{27,28} followed by tin-iodine exchange yielded the known vinyl iodide **1.32**²⁹ (Scheme 1.13).



Scheme 1.12 Synthesis of vinyl iodide **1.32** and phosphonate side chain **1.13**

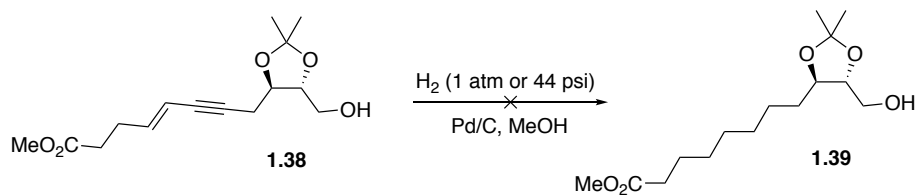
Total Synthesis of Linoleic Triols

With our key building blocks in hand, alkyne **1.9** and vinyl iodide **1.32** were subjected to Sonogashira conditions to afford the desired enyne **1.38** in 84% yield (Scheme 1.13). We then sought to reduce the enyne moiety to the corresponding alkane **1.39**. Attempted enyne reduction using palladium on carbon under 1 atm of hydrogen and ethyl acetate as the solvent produced no reaction.



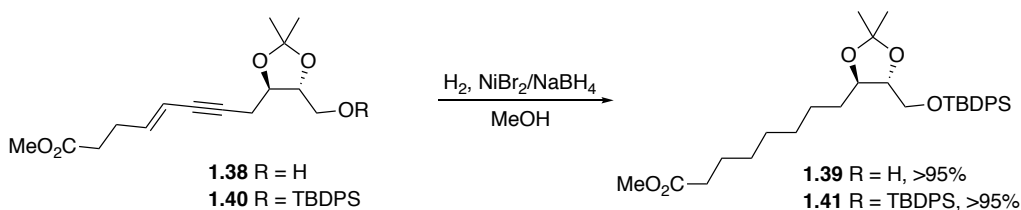
Scheme 1.13 Successful sonogashira coupling of **1.9** and **1.32**, followed by failed hydrogenation of the enyne moiety

When subjected to hydrogenation conditions in methanol, an inseparable mixture of semi-reduced alkene products was obtained (Scheme 1.15). In an attempt to optimize these more promising conditions, the hydrogenation was attempted at 44 psi of hydrogen. These harsher conditions led to acetal deprotection and afforded, again, an inseparable mixture of semi-reduced alkene products (Scheme 1.15).



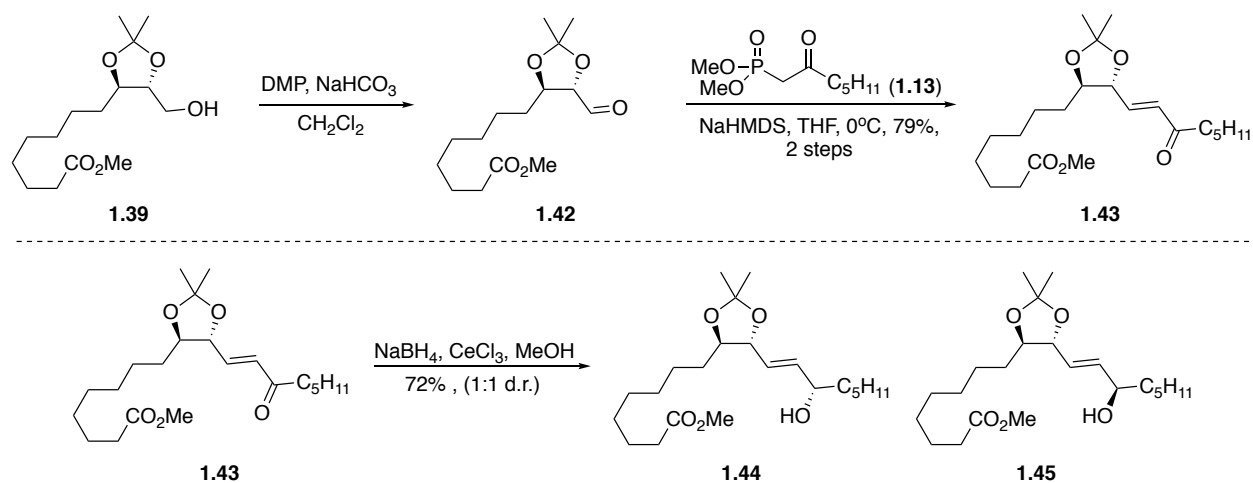
Scheme 1.14 Attempted hydrogenations of enyne **1.38**

Reduction conditions reported by Jiang and co-workers utilizing a $\text{NiCl}_2/\text{NaBH}_4$ complex as the hydrogen transfer reagent proceeded to cleanly reduce the enyne without acetal deprotection.³⁰ Using NiBr_2 in place of NiCl_2 we successfully reduced enyne **1.40** to alkane **1.41** in >95% yield (Scheme 1.16). In hopes of developing a route free from silyl-protecting groups, we attempted these conditions to reduce enyne **1.38** to alcohol **1.39**. Using this substrate, semi-reduction to an inseparable mixture of alkenes was observed. This problem was solved by simply changing the order of addition to the reaction mixture. We found addition of NaBH_4 to pre-complexed NiBr_2 and alcohol **1.38** resulted in complete, quantitative conversion of enyne **1.38** to alcohol **1.39** (Scheme 1.16).



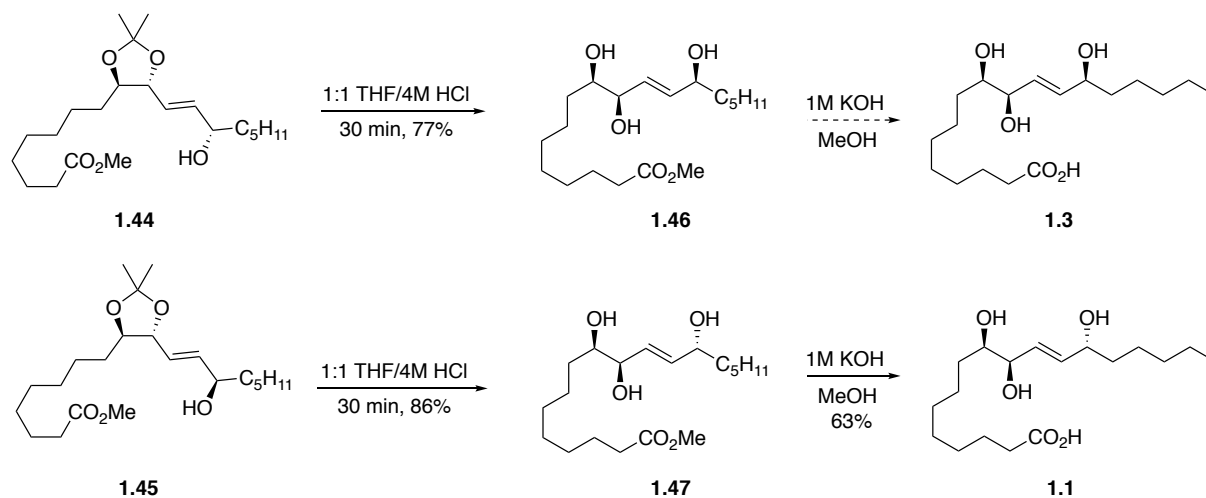
Scheme 1.15 Successful hydrogenation of enyne **1.40** and **1.38** using Borohydride-Nickel(II)-complex

Next, oxidation of alcohol **1.39** with Dess-Martin periodinane afforded the corresponding aldehyde that was directly subjected to Horner-Wadsworth-Emmons conditions to afford the desired enone **1.43** in 79% yield over two steps (Scheme 1.17). Reduction of the enone under Luche conditions yielded the epimeric alcohols **1.44** and **1.45** as a 1:1 mixture of isomers, which were separable by flash column chromatography (Scheme 1.18). The stereochemistry of the epimers was assigned using Mosher ester analysis, which will be discussed following the results of our synthetic efforts.



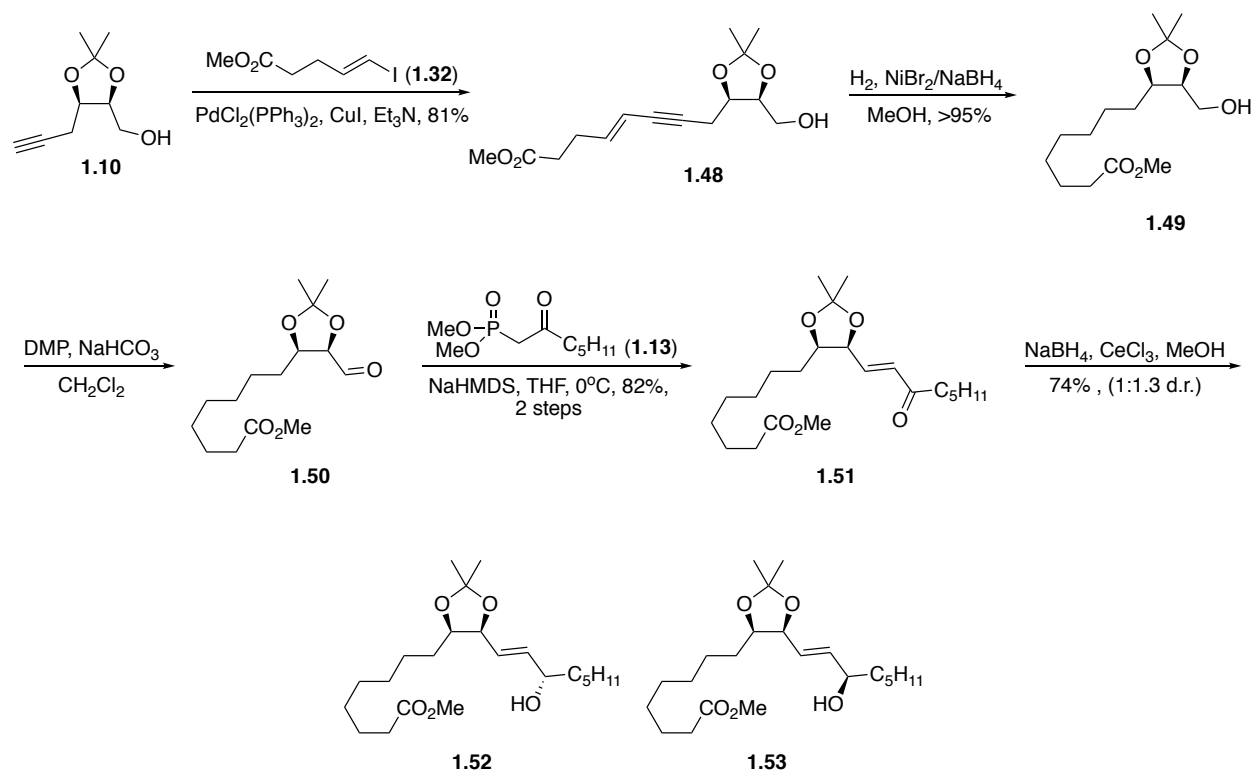
Scheme 1.16 Oxidation and Horner-Wadsworth-Emmons reaction to afford enone **1.43**, followed by Luche reduction of enone **1.43**, yielding epimeric alcohols **1.44** and **1.45**

Acetal de-protection under standard conditions gives the desired triols **1.46** and **1.47** in good yields and only 30 minute reaction times (Scheme 1.19). The resultant methyl ester **1.47** was hydrolyzed and used as a standard for the study of epoxide hydrolase activity in forming the epidermal water barrier.⁷



Scheme 1.17 Acetal de-protection affording trihydroxy linoleate esters **1.46** and **1.47**, followed by hydrolysis of **1.47** to yield acid **1.1**

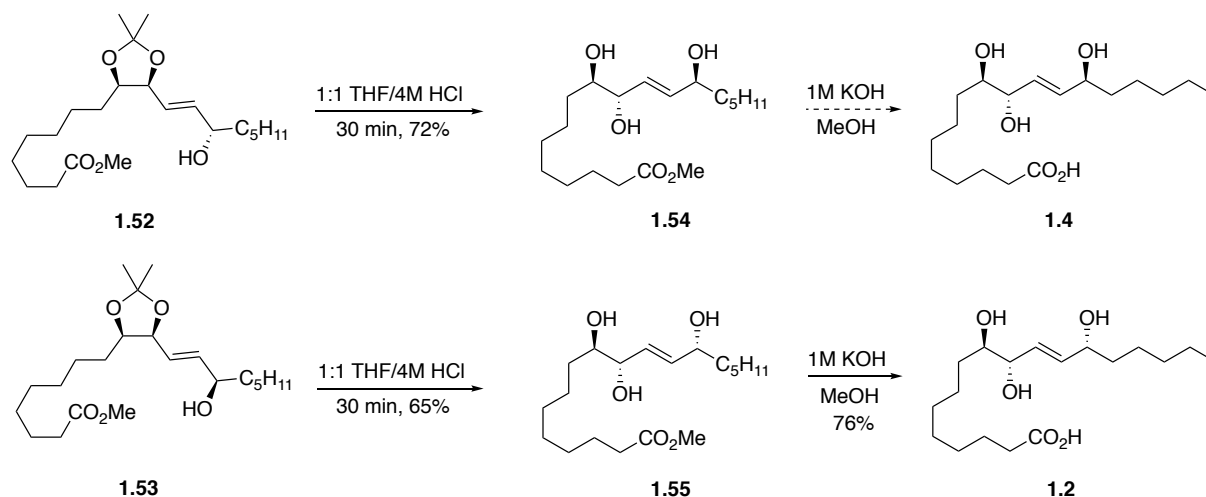
Turning our attention to triols **1.2** and **1.4**, Sonogashira coupling of alkyne **1.10** and vinyl iodide **1.32** gave the desired enyne **1.48** in 81% yield. Using our optimized conditions, enyne **1.48** was reduced to alcohol **1.49** in quantitative yield (Scheme 1.20).³⁰



Scheme 1.18 Sonogashira coupling of **1.10** and **1.32**, followed by hydrogenation to afford alcohol **1.49** and oxidation and Horner-Wadsworth-Emmons reaction to afford enone **1.51**, followed by Luche reduction of enone **1.51** yielding epimeric alcohols **1.52** and **1.53**

Oxidation and subsequent Horner-Wadsworth-Emmons reaction gave the enone **1.51** in 82% yield over two steps (Scheme 1.21). Reduction of enone **1.51** using Luche conditions gave a 1:1.3 ratio of isomers **1.52** and **1.53** (Scheme 1.22) and the stereochemistry of each epimer was assigned using Mosher ester analysis.

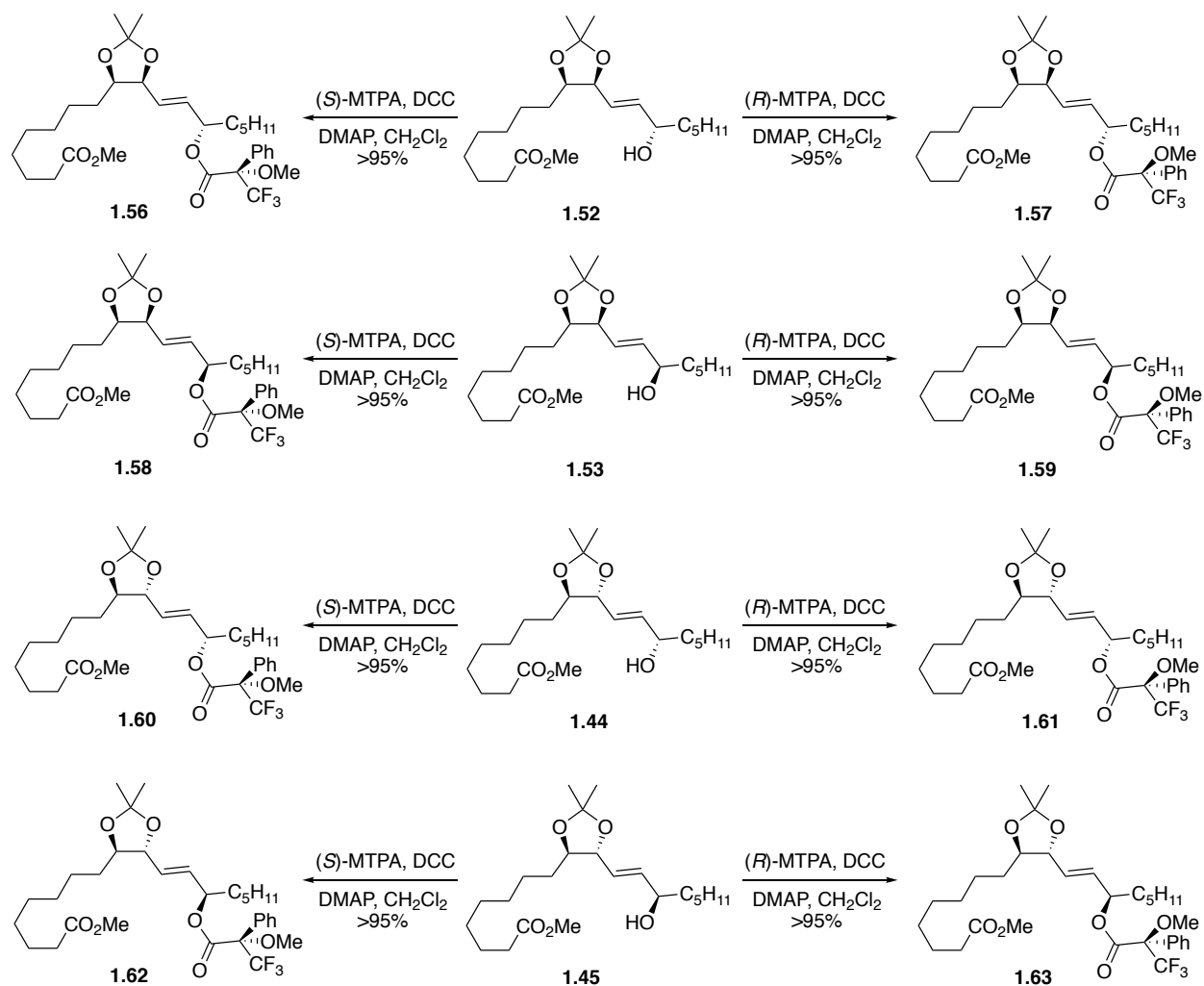
Luche conditions should afford a mixture of isomers, which were separated, and carried forward. Acetal de-protection proceeded as expected, affording the desired triol methyl esters in good yields (Scheme 1.23). Ester **1.55** was hydrolyzed to acid **1.2** and, along with **1.1**, used as standard to study the epoxide hydrolase activity discussed earlier.⁷



Scheme 1.19 Acetal de-protection affording trihydroxy linoleate esters **1.54** and **1.55**, followed by hydrolysis of **1.55** to yield acid **1.2**

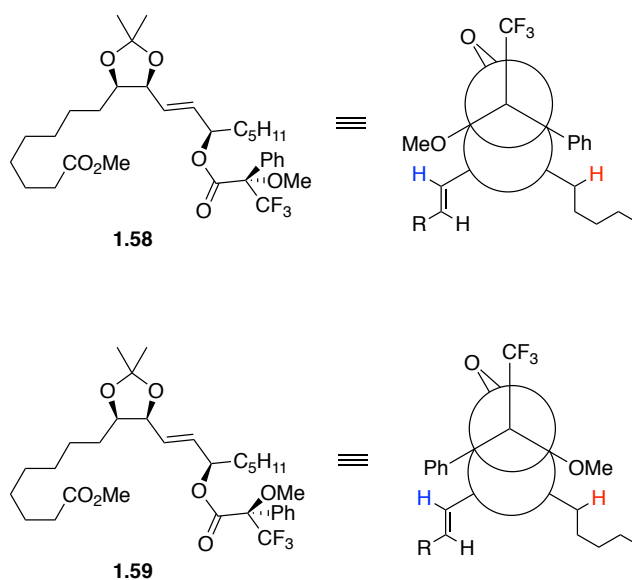
Determination of Stereochemistry

Among the many methods used to determine absolute stereochemistry of non-racemic molecules, Mosher ester analysis is the most common.³¹ The alcohol of unknown stereochemistry is esterified with a chiral carboxylic acid of known stereochemistry, MTPA being the most common. The first step of the analysis is coupling of the alcohol to both enantiomers of Mosher's acid (MTPA).³¹ To determine absolute configuration, alcohols **1.44**, **1.45**, **1.52**, and **1.53** were each esterified with both (*R*)-MTPA and (*S*)-MTPA to afford Mosher esters **1.56-1.63** (Scheme 1.20). To demonstrate the analysis, alcohol **1.53** will be used as an example.



Scheme 1.20 Synthesis of Mosher esters **1.56-1.63**

The Mosher ester method relies on the empirical conformation of each diastereomer (**1.58** and **1.59**) in the *s-trans* configuration with the trifluoromethyl, secondary alcohol and carbonyl groups all syn-coplanar to one another (Scheme 1.21).



Scheme 1.21 Model conformation for Mosher ester analysis

^1H NMR spectroscopy is then used and the spectra of both the (*R*) and (*S*)-MTPA diastereomers (**1.58** and **1.59**) are analyzed. The phenyl ring of the MTPA is known to shield the protons residing above and below it through anisotropy. The consequence of this shielding effect is a large difference in the chemical shift between the (*S*) and (*R*) diastereomers. These shifts are recorded in a table and the change in shift between (*S*) and (*R*) diastereomers ($\Delta^{S,R}\delta$) is recorded. In this case, we can determine the configuration of the secondary alcohol moiety of **1.53** to be (*R*). The anisotropic effect of the phenyl ring has shielded the alkenyl proton, moving its shift further upfield. Through conformational analysis this means the alkenyl proton is below the phenyl ring of the (*R*)-Mosher ester, which is only possible (in this case) if the secondary alcohol is of the (*R*) configuration.

1.53 δ (ppm)	1.58 δ (ppm)	1.59 δ (ppm)	$\Delta^{S,R} \delta$ (ppm)
5.84	5.79	5.78	0.01
5.64	5.75	5.60	0.15
	5.48	5.47	0.01
4.13	4.13	4.13	0
3.97	3.96	3.94	0.02
3.65	3.64	3.64	0
2.28	2.30	2.30	0

Figure 1.11 Chemical shifts of **1.53**, **1.58**, and **1.59** and $\Delta^{S,R} \delta$ of **1.58** and **1.59**

References

1. Hansen, H. S., The essential nature of linoleic acid in mammals *Trends Biochem Sci* **1986**, 11, 263-265.
2. Lands, B., Consequences of essential fatty acids *Nutrients* **2012**, 4, 1338-1357.
3. Zheng, Y., Yin, H., Boeglin, W. E., Elias, P. M., Crumrine, D., Beier, D. R., Brash, A. R., Lipoxygenases mediate the effect of essential fatty acid in skin barrier formation: A proposed role in releasing omega-hydroxyceramide for construction of the corneocyte lipid envelope *J. Biol. Chem.* **2011**, 286, 24046-24056.
4. Furstenberger, G., Kreig, P., The role of lipoxygenases in epidermis *Biochim. Biophys. Acta* **2014**, 1841, 390-400
5. Munoz-Garcia, A., Thomas, C. P., Keeney, D. S., Zheng, Y., Brash, A. R., The importance of the lipoxygenase-hexoxilin pathway in the mammalian epidermal barrier *Biochim. Biophys. Acta* **2014**, 1841, 401-408.
6. Chiba, T., Thomas, C. P., Calcutt, M. W., Boeglin, W. E., O'Donnell, V. B., Brash, A. R., The precise structures and stereochemistry of trihydroxy-linoleates esterified in human and porcine epidermis and their significance in skin barrier function: Implication of an epoxide hydrolase in the transformation of linoleate *J. Biol. Chem.* **2016**, 291, 14540-14554.
7. Yamanashi, H., Boeglin, W. E., Morisseau, C., Davis, R. W., Sulikowski, G. A., Hammock, B. D., Brash, A. R. Catalytic activities of mammalian epoxide hydrolases with *cis* and *trans* fatty acid epoxides relevant to skin barrier formation *J. Lipid Res.* **2018**, 59, 684-695.
8. Kuwahara, S., Miura, A. A concise synthesis of pinellic acid using a cross-metathesis approach *Tetrahedron* **2009**, 65, 3364-3368.
9. Chattopadhyay, S., Mahato, S., Sharma, A. A chemoenzymatic asymmetric synthesis of (9*S*,12*S*,13*S*)-pinellic acids *Tetrahedron Lett.* **2009**, 50, 4986-4988.
10. Sabitha, G., Bhikshapathi, M., Reddy, E. V., Yadav, J. S. Synthesis of (-)-pinellic acid and its (9*R*,12*S*,13*S*)-diastereomer *Helv. Chim. Acta* **2009**, 92, 2052-2057.
11. Prasad, K. R., Swin, B. Stereoselective total synthesis of (+)-pinellic acid from L-(+)-tartaric acid *Tetrahedron: Asymmetry* **2008**, 19, 1134-1138.
12. Naidu, S. V., Kumar, P. Enantioselective synthesis of (-)-pinellic acid *Tetrahedron Lett.* **2007**, 48, 2279-2282.
13. Sabitha, G., Reddy, E. V., Bhikshapathi, M., Yadav, J. S. Total synthesis of (9*S*,12*R*,13*S*)-pinellic acid *Tetrahedron Lett.* **2007**, 48, 313-315.

14. Sunazuka, T., Shirahata, T., Yoshida, K., Yamamoto, D., Harigaya, Y., Nagai, T., Kiyohara, H., Yamada, H., Kuwajima, I., Omura, S. Total synthesis of pinellic acid, a potent oral adjuvant for nasal influenza vaccine. Determination of the relative and absolute configuration *Tetrahedron Lett.* **2002**, 43, 1265-1268.
15. Mash E. A., Nelson K. A., Van Deusen S., Hemperly S. B., 1,4-di-*O*-alkyl threitols from tartaric acid: 1,4-di-*O*-benzyl-L-threitol *Org. Synth.* **1993**, 8, 155.
16. Mukai C., Kim J. S., Uchiyama M., Sakamoto S., Hanaoka M., Stereoselective construction of optically active bicyclo[3.3.0]octenone derivatives based on the Pauson-Khand reaction *J. Chem. Soc. Perkin Trans 1* **1998**, 2903-2915.
17. Suemune, H., Harabe, T., Sakai, K., Syntheses of unsaturated trihydroxy C-18 fatty acids isolated from rice plants suffering from rice blast disease *Chem. Pharm. Bull.* **1988**, 36, 3632-3637.
18. Davies, S. G., Foster, E. M., Frost, A. B., Lee, J. A., Roberts, P. M., Thomson, J. E., On the origins of diastereoselectivity in the conjugate additions of the antipodes of lithium *N*-benzyl-(*N*- α -methylbenzyl)amide to enantiopure *cis*- and *trans*-dioxolane containing α,β -unsaturated esters *Org. Biomol. Chem.* **2012**, 10, 6186-6200.
19. Bailey, S. J., Wales, S. M., Willis, A. C., Keller, P. A., Ring-opening and –expansion of 2,2'-biaziridine: Access to diverse enantiopure linear and bicyclic vicinal diamines *Org. Lett.* **2014**, 16, 4344-4347.
20. Bjorkling, F., Norin T., Unelius, R., Synthesis of 8*Z*, 10*z*-dodecadienyl acetate using a general method applicable to *Z,Z*-1,3-dienes *Synth. Commun.* **2006**, 6, 463-472.
21. Cohen, N., Banner, B. L., Laurenzano, A. J., Carozza, L., 2,3-*O*-isopropylidene-D-erythronolactone [Furo[3,4-*d*]-1,3-dioxol-4(3*aH*)-one, dihydro-2,2-dimethyl-(3*aR-cis*)-] *Org. Synth.* **1985**, 63, 127.
22. Awasaguchi, K., Miyazawa, M., Uoya, I., Inoue, K., Nakamura, K., Yokoyama, H., Kakuda, H., Hirai, Y., Synthesis of spiro C-aryl glycoriboside via Pd(II)-catalyzed spirocyclization *Synlett* **2010**, 16, 2392-2396.
23. McDonald, F. E., Hurtak, J. A., Synthesis of the ABC substructure of brevenal by sequential *exo*-mode oxacyclizations of acyclic polyene precursors *Org. Lett.* **2017**, 19, 6036-6039.
24. Hayashi, K., Tanimoto, H., Zhang, H., Morimoto, T., Nishiyama, Y., Kakiuchi, K., Efficient synthesis of α,β -Unsaturated alkylimines performed with allyl cations and azides: Application to the synthesis of an ant venom alkaloid *Org. Lett.* **2012**, 14, 5728-5731.
25. Tung, C. L., Wong, C. T. T., Fung, E. Y. M., Li, X., Traceless and chemoselective amine bioconjugation via phthalimidine formation in native protein modification *Org. Lett.* **2016**, 18, 2600-2603.

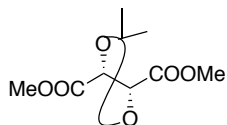
26. Hwang, S. H., Wagner, K., Xu, J., Yang, J., Li, X., Cao, Z., Morisseau, C., Lee, K. S. S., Hammock, B. D., Chemical synthesis and biological evaluation of ω -hydroxy polyunsaturated fatty acids *Bioorganic Med. Chem. Lett* **2017**, 27, 620-625.
27. White, J. D., Jensen, M. S., Cyclopropane-containing eicosanoids of marine origin. biomimetic synthesis of constanolactones A and B from the alga *Constantinea simplex* *J. Am. Chem. Soc.* **1995**, 117, 6224-6233.
28. Beachard, A., Phillips, V. A., Lloyd, M. D., Threadgill, M. D., Synthesis of 2-(4-carboxybutenyl)- and 2-(4-carboxybutynyl)-cyclopentene- 1-carboximides *Tetrahedron* **2009**, 65, 8176-8184.
29. Pang, J., Lee, D., Studies on the total synthesis of amphidinolide O. A stereoselective synthesis of C12-C17 Fragment *Bull. Korean Chem. Soc.* **2002**, 23, 1173-1176.
30. Yin, B., Cai, C., Lai, J., Zhang, Z., Huang, L., Xu, L., Jiang, H., Sodium borohydride-nickel chloride-methanol catalytic system for regioselective reduction of electron-rich conjugated dienes and reductive cleavage of allyl esters involving π -allylnickel intermediates *Adv. Synth. Catal.* **2011**, 353, 3319-3324.
31. Hoye, T. R., Jeffrey, C. S., Shao, F., Mosher ester analysis for the determination of absolute configuration of stereogenic (chiral) carbinol carbons *Nat. Protoc.* **2007**, 2, 2451-2458.

Experimental Methods

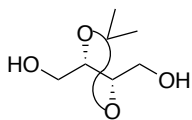
General Procedure: All reactions sensitive to air or moisture were conducted in flame-dried or oven dried glassware under an atmosphere of argon. Reaction temperatures were controlled using a thermocouple thermometer and analog hotplate stirrer. Reactions were conducted at room temperature (rt, approximately 23 °C) unless otherwise noted. Flash column chromatography was conducted using silica gel 230-400 mesh. Analytical thin-layer chromatography (TLC) was performed on E. Merck silica gel 60 F254 plates and visualized using UV, *p*-anisaldehyde stain, and potassium permanganate stain. Yields were reported as isolated, spectroscopically pure compounds.

Materials: Solvents were obtained from either an MBraun MB-SPS solvent system or freshly distilled. THF was distilled from sodium/benzophenone. MeOH was dried over magnesium and stored over molecular sieves. CH₂Cl₂ and N-methylpyrrolidinone were dried over CaH₂, distilled, and stored over molecular sieves. Et₃N and diisopropylethylamine were dried over CaH₂, distilled, and stored over KOH pellets. Oxalyl chloride was distilled fresh, prior to use. All starting materials and reagents were used as received unless noted otherwise. The molarity of *n*-butyllithium solutions was determined by titration using diphenylacetic acid as an indicator (average of three determinations).

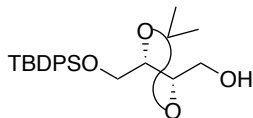
Instrumentation: ¹H NMR spectra were recorded on Bruker 400, 500, or 600 MHz spectrometers and are reported relative to deuterated solvent signals. Data for ¹H NMR spectra are reported as follows: chemical shift (δ ppm), multiplicity (s = singlet, d = doublet, t = triplet, q = quartet, p = pentet, m = multiplet, br = broad, app = apparent), coupling constants (Hz), and integration. ¹³C NMR spectra were recorded on Bruker 100, 125, or 150 MHz spectrometers and are reported relative to deuterated solvent signals. Mass spectra were recorded on a Waters Synpat G2S HDMS spectrometer.



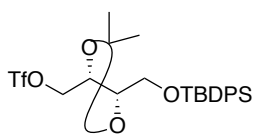
1.15: To a suspension of L-Tartaric acid (25 g, 168 mmol) and methanol (10 mL) was added 2,2-dimethoxypropane (47.5 mL) and p-TSA (100 mg, cat.). The reaction was heated to 70°C and stirred at this temperature until a dark red color was obtained (~1 h). Additional 2,2-dimethoxypropane (25 mL) and cyclohexane (113 mL) were added. The flask was fitted with a Vigreux column and shortpath distillation head. The mixture was heated and the acetone-cyclohexane and methanol-cyclohexane azeotropes were slowly removed over a 6 hour period (~150 mL). The mixture was cooled to room temperature and potassium carbonate (250 mg) was added. The reaction was stirred until the dark red color abated. Volatiles were removed *in vacuo* and the product was purified by vacuum distillation (0.5 mmHg, 94-110°C) to yield **1.15** (32.6 g, 89%) as a clear yellow oil. $[\alpha]_D^{20}$ -49.2 (CHCl₃, *c* 1.0); ¹H NMR (400 MHz, CDCl₃) δ : 4.81 (s, 2H), 3.83 (s, 6H), 1.49 (s, 6H); ¹³C NMR (CDCl₃, 100 MHz): δ : 169.7, 113.5, 76.7, 52.45, 26.0. *m/z* calcd. for C₉H₁₄O₆ [M+Na]⁺ 241.0681 found 241.0777. Identical in all respects to published data¹



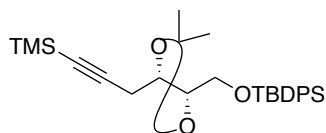
1.16: A suspension of LAH (5.84 g, 154 mmol) in diethyl ether (98 mL) was refluxed for 30 min. The suspension was then allowed to cool to room temperature and a solution of **1.15** (20.0 g, 91.7 mmol) in diethyl ether (49 mL) was added dropwise over 1 h. The suspension was brought to reflux and allowed to stir for 3 h. The reaction was cooled to 0 °C and quenched carefully with H₂O (5.84 mL), 4 N NaOH (5.84 mL), then H₂O (18.2 mL) and stirred until the grey color of LAH was no longer present. The mixture was filtered and the filter cake was washed with diethyl ether. The combined organic extract was dried (MgSO₄), filtered, and concentrated *in vacuo*. The product was purified by vacuum distillation (81-94 °C, 0.01 mm) to afford of **1.16** (10.3 g, 70%) as a pale yellow oil. $[\alpha]_D^{20}$ -2.4 (CHCl₃, *c* 1.0); ¹H NMR (CDCl₃, 400 MHz): δ : 4.02 (m, 2H), 3.76 (m, 4H), 1.96 (br. s, 2H), 1.44 (s, 6H); ¹³C NMR (CDCl₃, 400 MHz): δ : 109.6, 78.2, 62.3, 27.4. *m/z* calcd. for C₇H₁₄O₄ [M+H]⁺ 163.0970 found 163.0795. Identical in all respects to published data



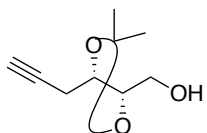
1.17: To a suspension of NaH (60%, 4.4 g, 110 mmol) in THF (363 mL) at 0 °C was added a solution of **1.16** (10.0 g, 61.7 mmol) in THF (36.3 mL) via dropwise addition. The resulting suspension was allowed to stir at that temperature for 1 h, then a solution of TBDPSCl (16.0 mL, 61.7 mmol) in THF (36.3 mL) was added dropwise and the reaction was warmed to room temperature and allowed to stir for 2 h. The resulting suspension was carefully quenched with H₂O and extracted with Et₂O (3 x 50 mL). The combined organic extracts were washed with H₂O (50 mL) and brine (50 mL), dried (MgSO₄), filtered, and concentrated *in vacuo*. The residue was purified by flash column chromatography (4:1 hexanes/ethyl acetate) to afford **1.17** (18.8 g, 75%) as a pale yellow oil. $[\alpha]_D^{20}$ -0.71 (CHCl₃, *c* 1.4); ¹H NMR (400 MHz, CDCl₃) δ: 7.68-7.65 (m, 4H), 7.46-7.37 (m, 6H), 4.09-4.05 (m, 1H), 4.00-3.94 (m, 1H), 3.84-3.79 (m, 2H), 3.76-3.72 (m, 1H), 3.69-3.63 (m, 1H), 2.06 (br, 1H), 1.41 (s, 3H), 1.39 (s, 3H), 1.06 (s, 9H); ¹³C NMR (100 MHz, CDCl₃) δ: 136.0, 133.3, 130.2, 128.7, 128.1, 109.5, 79.9, 77.9, 64.5, 62.9, 27.4, 27.3, 27.2, 19.5. *m/z* calcd. for C₂₃H₃₂O₄Si [M+Na]⁺ 423.1959 found 423.2069. Identical in all respects to published data



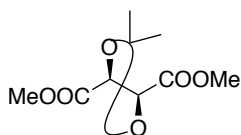
1.18: To a solution of alcohol **1.17** (20.0 g, 49.9 mmol) and Et₃N (20.9 mL, 150 mmol) in CH₂Cl₂ (832 mL) at -20 °C was added trifluoromethanesulfonic anhydride (12.6 mL, 74.9 mmol) dropwise. The reaction was stirred for 30 min at -20°C, and quenched with sat. aq. NaHCO₃ (500 mL). The layers were separated and the organic layer was washed with water (500 mL), and brine (500 mL). The organic layer was dried (MgSO₄), filtered, and concentrated *in vacuo*. The resulting residue was filtered through a short pad of silica gel (10:1 Hex/EtOAc). The triflate was used immediately in the next reaction.



1.19: To a solution of (trimethylsilyl)acetylene (5.97 g, 60.8 mmol) in THF (350 mL) stirring at -20 °C was added n-BuLi (2.0 M in hexanes, 25.3 mL) dropwise. The reaction was stirred at -20°C for 30 min. A solution of the crude triflate **1.18** (ca. 13 g, 25 mmol) in THF (150 mL) and NMP (100 mL) was added. The reaction mixture was stirred at -20 °C for 1 h, quenched with sat. aq. NH₄Cl (500 mL) and extracted with EtOAc (3 x 500 mL). The combined organic extracts were washed with water (500 mL) and brine (500 mL), dried (MgSO₄), filtered, and concentrated *in vacuo*. The residue **1.19** was filtered through a short pad of silica gel (10:1 Hex/EtOAc). The filtrate was concentrated *in vacuo* and used immediately in the next reaction. $[\alpha]_D^{20}$ -5.1 (CHCl₃, *c* 2.3); ¹H NMR (400 MHz, CDCl₃) δ : 7.68 (m, 4H), 7.41 (m, 6H), 4.06 (m, 2H), 3.83 (d, 2H), 1.43 (s, 3H), 1.40 (s, 3H), 1.07 (s, 9H), 0.12 (s, 6H). ¹³C NMR (100 MHz, CDCl₃) δ : 135.5, 133.2, 133.1, 129.6, 127.6, 108.9, 102.0, 87.0, 79.8, 75.5, 63.9, 27.1, 27.0, 26.7, 23.9, 19.2, -0.08. *m/z* calcd. for C₂₈H₄₀O₃Si₂ [M+Na]⁺ 503.2406 found 503.2571

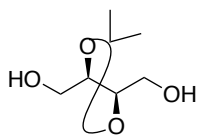


1.11: To a solution of **1.19** (300 mg, 0.62 mmol) in THF (6 mL) at rt was added a solution of TBAF (1M in THF, 1.4 mL). Let stir at rt for 1 h. The reaction was diluted with EtOAc (5 mL) and washed with brine (3 mL). The layers were separated and the aqueous layer was extracted with EtOAc (3 x 10 mL). The combined organic extracts were dried (MgSO₄), filtered, and concentrated *in vacuo*. The residue was purified by flash column chromatography (4:1 Hex/EtOAc) to afford **1.11** (69 mg, 66% over 3 steps) as a clear oil. $[\alpha]_D^{20}$ 2.8 (CHCl₃, *c* 1); ¹H NMR (400 MHz, CDCl₃) δ : 4.03 (m, 1H), 3.99 (m, 1H), 3.94 (m, 1H), 3.86 (m, 1H), 2.59 (m, 2H), 2.04 (s, 1H), 2.04 (br s, 1H), 1.42 (s, 3H), 1.41 (s, 3H); ¹³C NMR (CDCl₃, 100 MHz): δ : 109.1, 80.9, 79.3, 74.3, 70.8, 62.1, 27.0, 22.7. *m/z* calcd. for C₉H₁₄O₃ [M+H]⁺ 170.0942 found 170.9641. Identical in all respects to published data



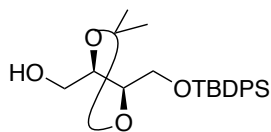
1.33: To a suspension of D-Tartaric acid (25 g, 168 mmol) and methanol (10 mL) was added 2,2-dimethoxypropane (47.5 mL) and p-TSA (100 mg, cat.). The reaction was heated to 70°C and stirred at this temperature until a dark red color was obtained (~1 h). Additional 2,2-dimethoxypropane (25 mL) and cyclohexane (113

mL) were added. The flask was fitted with a Vigreux column and shortpath distillation head. The mixture was heated and the acetone-cyclohexane and methanol-cyclohexane azeotropes were slowly removed over a 6 hour period (150 mL). The mixture was cooled to room temperature and potassium carbonate (250 mg) was added. The reaction was stirred until the dark red color abated. Volatiles were removed *in vacuo* and the product was purified by vacuum distillation (0.5 mmHg, 94-110°C) to yield **1.33** (29.8 g, 81%) as a clear oil. $[\alpha]_D^{20}$ 49.0 (CHCl₃, *c* 1.0); ¹H NMR (400 MHz, CDCl₃) δ : 4.81 (s, 2H), 3.83 (s, 6H), 1.49 (s, 6H); ¹³C NMR (CDCl₃, 100 MHz): δ : 169.75, 113.49, 76.68, 52.42, 25.98. *m/z* calcd. for C₉H₁₄O₆ [M+Na]⁺ 241.0681 found 241.0768. Identical in all respects to published data



1.34: To a suspension of LAH (8.87 g, 138 mmol) in THF (135 mL) at 0°C was added a solution of **1.33** (30 g, 138 mmol) in THF (66 mL) via dropwise addition. The mixture was allowed to warm to rt and stirred for 16 h. The suspension was

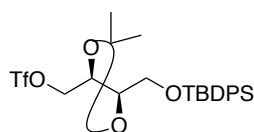
cautiously quenched by dropwise addition of water (120 mL), and the reaction was allowed to stir until the grey color of unquenched LAH was no longer present. The mixture was then filtered through a pad of celite (100 g) and the filtrate was concentrated *in vacuo*. The residue was purified by vacuum distillation (0.5 mmHg at 120-124°C) to afford **1.34** (10 g, 45% yield) as a clear viscous oil. $[\alpha]_D^{20}$ 1.96 (CHCl₃, *c* 1.08); ¹H NMR (400 MHz, CDCl₃) δ : 4.02 (t, 2H), 3.80 (dd, 2H), 3.71 (dd, 2H) 1.43 (s, 6H); ¹³C NMR (CDCl₃, 100 MHz): δ : 109.2, 77.76, 61.86, 26.97. *m/z* calcd. for C₇H₁₄O₄ [M+H]⁺ 163.0970 found 163.0875. Identical in all respects to published data



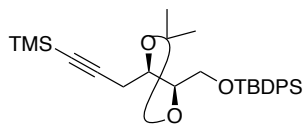
1.35: To a suspension of NaH (4.42 g, 111 mmol, 60% dispersion) in THF (350 mL) at 0°C was added a **1.34** (10 g, 61.6 mmol) dropwise over 30 min. After complete addition the reaction was allowed to stir for 30 min.

A solution of TBDPS-Cl (17 g, 61.6 mmol) in THF (25 mL) was added dropwise and the reaction was allowed to stir for 16 h. The reaction was cautiously quenched by addition of water (400 mL). The aqueous layer was extracted with Et₂O (3 x 300 mL). The combined organic extracts were dried (MgSO₄), filtered, and concentrated *in vacuo*. The residue was purified by flash column chromatography (4:1 hexanes/ethyl acetate) to afford **1.35** (23.8 g, >95%) as a colorless oil. $[\alpha]_D^{20}$

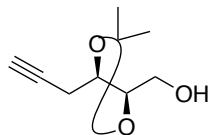
0.69 (CHCl₃, *c* 1.6); ¹H NMR (400 MHz, CDCl₃) δ: 7.68-7.65 (m, 4H), 7.46-7.37 (m, 6H), 4.09-4.05 (m, 1H), 4.00-3.94 (m, 1H), 3.84-3.79 (m, 2H), 3.76-3.72 (m, 1H), 3.69-3.63 (m, 1H), 2.06 (br, 1H), 1.41 (s, 3H), 1.39 (s, 3H), 1.06 (s, 9H); ¹³C NMR (400 MHz, CDCl₃) δ: 136.0, 133.3, 130.2, 128.7, 128.1, 109.5, 79.9, 77.9, 64.5, 62.9, 27.4, 27.3, 27.2, 19.5. *m/z* calcd. for C₂₃H₃₂O₄Si [M+Na]⁺ 423.1959 found 423.2066. Identical in all respects to published data



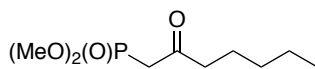
S1: To a solution of alcohol **1.35** (10 g, 25 mmol) and Et₃N (10.5 mL, 75 mmol) in CH₂Cl₂ (100 mL) at -20 °C was added trifluoromethanesulfonic anhydride (6.25 mL, 37.5 mmol) via dropwise addition. The reaction was stirred for 30 min at -20°C, washed with sat. aq. NaHCO₃ (100 mL), water (100 mL), and brine (100 mL). The organic layer was dried (MgSO₄), filtered, and concentrated *in vacuo*. The resulting residue was filtered through a short pad of silica gel (10:1 Hex/EtOAc) and the unstable triflate was used immediately in the next reaction.



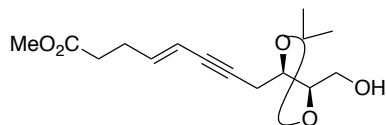
S2: To a solution of (trimethylsilyl)acetylene (5.97 g, 60.8 mmol) in THF (350 mL) stirring at -20 °C was added *n*-BuLi (2.0 M in hexanes, 25.3 mL) via dropwise addition. The reaction was stirred at -20°C for 30 min. A solution of the crude triflate **S1** (ca. 13 g, 25 mmol) in THF (150 mL) and NMP (100 mL) was added. The reaction mixture was stirred at -20 °C for 1 h, quenched with sat. aq. NH₄Cl (500 mL) and extracted with EtOAc (3 x 500 mL). The combined organic extracts were washed with water (500 mL) and brine (500 mL), dried (MgSO₄), filtered, and concentrated *in vacuo*. The residue was purified by flash column chromatography (10:1 Hex/EtOAc) to afford **S2** (8.8 g, 74%) as a clear oil. [α]_D²⁰ 2.8 (CHCl₃, *c* 1); ¹H NMR (400 MHz, CDCl₃) δ: 7.67 (m, 4H), 7.37 (m, 6H), 4.04 (m, 2H), 3.82 (d, 2H), 2.62 (dd, 2H), 1.42 (s, 3H), 1.39 (s, 3H), 1.05 (s, 9H), 0.11 (s, 9H); ¹³C NMR (CDCl₃, 100 MHz): δ: 135.6, 133.2, 129.6, 127.6, 108.9, 102.0, 87.0, 79.9, 75.5, 63.9, 27.1, 27.1, 26.8, 23.9, 19.2, -0.08. *m/z* calcd. for C₂₈H₄₀O₃Si₂ [M+Na]⁺ 503.2406 found 503.2570



1.9: To a solution of **S2** (300 mg, 0.62 mmol) in THF (6 mL) at rt was added a solution of TBAF (1M in THF, 1.4 mL). Let stir at rt for 1 h. Diluted with EtOAc (5 mL) and washed with brine (3 mL). The layers were separated and the aqueous layer was extracted with EtOAc (3 x 10 mL). The combined organic extracts were dried (MgSO₄), filtered, and concentrated *in vacuo*. The residue was purified by flash column chromatography (4:1 Hex/EtOAc) to afford **1.9** (62 mg, 59% over 3 steps) as a clear oil. $[\alpha]_D^{20}$ -2.8 (CHCl₃, *c* 1); ¹H NMR (400 MHz, CDCl₃) δ : 4.03 (m, 1H), 3.99 (m, 1H), 3.94 (m, 1H), 3.86 (m, 1H), 2.59 (m, 2H), 2.04 (s, 1H), 2.04 (br s, 1H), 1.42 (s, 3H), 1.41 (s, 3H); ¹³C NMR (CDCl₃, 100 MHz): δ : 109.1, 80.9, 79.3, 74.3, 70.8, 62.1, 27.0, 22.7. *m/z* calcd. for C₉H₁₄O₃ [M+Na]⁺ 202.0833 found 202.0862

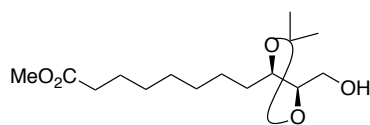


1.13: To a solution of phosphonate (10.3 g, 83 mmol) in freshly distilled THF (50 mL) at -78°C was added n-butyllithium (35 mL, 2.5 M in hexanes) dropwise and the reaction was stirred for 30 min. Methyl hexanoate (6 g, 46 mmol) was added dropwise over 20 min and the reaction was allowed to warm to room temperature overnight. The reaction was quenched with sat. aq. NH₄Cl (15 mL) and diluted with ethyl acetate (40 mL). The layers were separated and the aqueous layer was extracted with ethyl acetate (3 x 40 mL). The combined organic extracts were washed with brine (40 mL), dried (MgSO₄), filtered, and concentrated *in vacuo*. The residue was purified by column chromatography (2:1 to 1:2 hexanes/ethyl acetate gradient) to afford **1.13** (7.66 g, 76%) as a colorless oil. ¹H NMR (400 MHz, CDCl₃): δ : 3.81 (s, 3H), 3.78 (s, 3H), 3.12 (d, 2H), 2.61 (t, 2H), 1.60 (t, 2H), 1.29 (m, 4H), 0.91 (t, 3H). ¹³C NMR (100 MHz, CDCl₃): δ : 201.9, 52.9, 43.9, 41.8, 40.5, 30.9, 22.9, 22.3, 13.7. Identical in all respects to published data

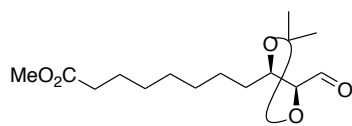


1.38: To a solution of **1.32** (459 mg, 1.91 mmol) in Et₃N (20 mL) at room temperature was added copper (I) iodide (109 mg, 0.57 mmol) and bis(triphenylphosphine)palladium(II) dichloride (134 mg, 0.19 mmol). The resulting mixture was degassed. To this mixture was added **1.9** (780.4 mg, 1.91 mmol) as a solution in Et₃N (4.5 mL). The reaction mixture was stirred at room temperature for 16 h, then concentrated *in vacuo*. The resulting residue was dissolved in EtOAc (70 mL),

washed with water (1 x 15 mL) and NH₄Cl (2 x 15 mL). The organic extract was dried (MgSO₄) and concentrated in vacuo. The residue was purified by flash column chromatography (Hexanes to 9:1 Hexanes/Ethyl acetate gradient) to afford **1.38** (819 mg, 82%) as a light yellow oil: $[\alpha]_D^{20}$ -0.04 (CHCl₃, *c* 1); ¹H NMR (400 MHz, CDCl₃) δ 7.71 (t, *J* = 1.5 Hz, 4H), 7.40 (m, 6H), 6.01 (m, 1H), 5.47 (d, *J* = 15.7 Hz, 1H), 4.13 (m, 1H), 3.95 (m, 1H), 3.83 (m, 2H), 3.68 (s, 3H), 2.66 (m, 2H), 2.41 (m, 4H), 1.44 (s, 3H), 1.42 (s, 3H), 1.07 (s, 9H); ¹³C NMR (100 MHz, CDCl₃) δ 173.3, 141.5, 135.9, 133.5, 130.0, 128.0, 111.2, 109.4, 84.9, 81.0, 80.7, 76.2, 64.0, 51.9, 33.4, 28.4, 27.5, 27.4, 27.1, 24.1, 19.5. *m/z* calcd. for C₁₅H₂₂O₅ [M+Na]⁺ 305.1358 found 305.1477

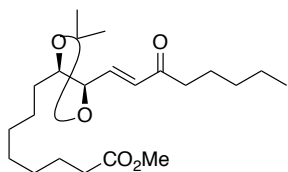


1.39: To a suspension **1.38** (300 mg, 1.06 mmol) and Nickel (II) bromide (24 mg, 0.11 mmol) in MeOH (18 mL) at 0 °C was added sodium borohydride (281 mg, 7.44 mmol). The resulting black suspension was stirred at 0 °C for 10 min, then the flask was evacuated and purged with hydrogen gas. The reaction was allowed to warm to room temperature and stir 16 h. The reaction mixture was filtered through a plug of celite and washed with MeOH (3 x 5 mL). The combined filtrate and washings were concentrated in vacuo. The resulting residue was dissolved in EtOAc (70 mL), washed with water (15 mL), dried (MgSO₄), filtered and concentrated *in vacuo* to afford **AA-42** (291 mg, >95%) of as a colorless oil, which was used without further purification: $[\alpha]_D^{20}$ -0.02 (CHCl₃, *c* 0.42); ¹H NMR (400 MHz, CDCl₃) δ 7.69 (m, 4H), 7.41 (m, 6H), 3.95 (m, 1H), 3.76 (m, 2H), 3.73 (m, 1H), 3.68 (s, 3H), 2.31 (t, *J* = 7.4 Hz, 2H), 1.63 (m, 2H), 1.56 (m, 2H), 1.41 (s, 3H), 1.38 (s, 3H), 1.32 (m, 8H), 1.07 (s, 9H); ¹³C NMR (100 MHz, CDCl₃) δ 174.5, 135.9, 133.5, 133.4, 129.97, 129.94, 127.9, 108.6, 81.3, 78.8, 64.4, 51.7, 34.3, 33.6, 29.8, 29.4, 29.3, 27.7, 27.2, 27.0, 26.3, 25.2, 19.5. *m/z* calcd. for C₁₅H₂₈O₅ [M+Na]⁺ 311.1827 found 311.1934

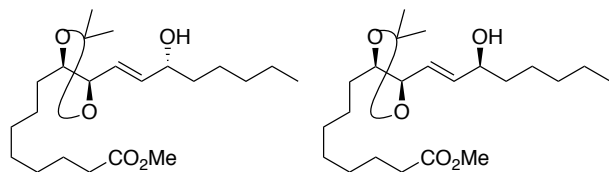


1.42: To a solution of **1.39** (106 mg, 0.37 mmol) in dichloromethane (10 mL) at room temperature were sequentially added NaHCO₃ (27 mg, 0.32 mmol) and Dess-Martin Periodinane (235 mg, 0.56 mmol). The resulting reaction mixture was stirred at room temperature for 1.5 h and quenched with 25% Na₂S₂O₃ (8 mL) and NaHCO₃ (8 mL). The organic layer was separated, dried (MgSO₄), and concentrated *in vacuo*. The residue was filtered through a plug of silica gel (hexanes to 3:2

hexanes/ethyl acetate gradient) to afford **1.40** (69 mg, 65%) as a colorless oil. The unstable aldehyde was used without further purification: $^1\text{H NMR}$ (400 MHz, CDCl_3) δ 9.73 (d, $J = 2.4$ Hz, 1H), 4.04 (m, 1H), 3.93 (dd, $J = 2.4, 7.6$ Hz, H), 3.68 (s, 3H), 2.31 (t, $J = 7.5$ Hz, 2H), 1.66 (m, 4H), 1.49 (s, 3H), 1.43 (s, 3H), 1.32 (m, 8H).



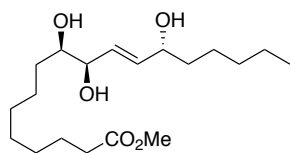
1.43: To a solution of **1.13** (66 mg, 0.30 mmol) in THF (1 mL) at 0 °C was added sodium bis(trimethylsilyl)amide (1 M solution in THF, 240 μL , 0.24 mmol) dropwise. After stirring at 0 °C for 5 min, the ice bath was removed and the reaction was allowed to warm to room temperature and stirred for an additional 30 min. White solid was formed during this period. The reaction mixture was cooled to 0 °C and a solution of **1.40** (68 mg, 0.24 mmol) in THF (2.5 mL) was added. The reaction was stirred at 0 °C for 30 min and quenched with water (5 mL). The aqueous layer was extracted with EtOAc (2 x 10 mL). The combined organic extracts were dried (MgSO_4), filtered, and concentrated *in vacuo*. The residue was purified by flash column chromatography (hexanes to 17:3 hexanes/ethyl acetate gradient) to afford **1.43** (75 mg, 82%) as a colorless oil: $[\alpha]_D^{20}$ 0.04 (CHCl_3 , c 1.0); $^1\text{H NMR}$ (400 MHz, CDCl_3) δ 6.71 (dd, $J = 5.8, 15.8$ Hz, 1H), 6.38 (dd, $J = 1.2, 15.8$ Hz, 1H), 4.15 (m, 1H), 3.73 (m, 1H), 3.68 (s, 3H), 2.57 (t, $J = 7.4$ Hz, 2H), 2.31 (t, $J = 7.4$ Hz, 2H), 1.63 (m, 6H), 1.45 (s, 3H), 1.43 (s, 3H), 1.32 (m, 12H), 0.90 (t, $J = 6.8$ Hz, 3H); $^{13}\text{C NMR}$ (100 MHz, CDCl_3) δ 200.5, 174.5, 141.8, 130.7, 109.6, 81.0, 80.8, 51.7, 41.2, 34.3, 32.3, 31.7, 29.7, 29.33, 29.2, 27.5, 27.0, 26.2, 25.1, 24.0, 22.7, 14.2. m/z calcd. for $\text{C}_{22}\text{H}_{38}\text{O}_5$ $[\text{M}+\text{Na}]^+$ 405.2609 found 405.2792



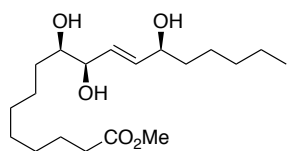
1.44 and 1.45: To a solution of **1.43** (120 mg, 0.31 mmol) and $\text{CeCl}_3 \cdot 7\text{H}_2\text{O}$ (140 mg, 0.38 mmol) in methanol (3.1 mL) stirring at 0 °C was added NaBH_4 (12 mg, 0.31 mmol). The reaction was stirred at 0 °C for 1 h, then rt for 3 h. The solvent was removed *in vacuo* and the crude residue was purified by flash chromatography (4:1 hexanes/ethyl acetate) to afford **1.45** (59 mg, 50%, $r_f = 0.11$) and **1.44** (60 mg, 50%, $r_f = 0.10$) as clear oils.

1.45: $[\alpha]_D^{20}$ -1.37 (CHCl₃, *c* 0.58); ¹H NMR (400 MHz, CDCl₃) δ : 5.84 (m, 1H), 5.65 (m, 1H), 4.12 (m, 1H), 3.98 (t, 1H), 3.65 (s, 3H), 3.64 (m, 1H), 2.28 (t, 2H), 1.59 (m, 2H), 1.46 (s, 6H), 1.34 (m, 4H), 1.28 (m, 14H), 0.87 (t, 3H). ¹³C NMR (100 MHz, CDCl₃) δ 137.9, 127.2, 108.3, 81.7, 80.7, 71.8, 51.3, 37.0, 33.9, 31.7, 31.6, 29.3, 28.9, 27.2, 26.8, 25.9, 25.0, 24.8, 22.4, 13.9. *m/z* calcd. for C₂₂H₄₂O₅ [M+Na]⁺ 407.2766 found 407.2922

1.44: $[\alpha]_D^{20}$ 4.2 (CHCl₃, *c* 0.33); ¹H NMR (400 MHz, CDCl₃) δ : 5.84 (m, 1H), 5.65 (m, 1H), 4.12 (m, 1H), 3.97 (t, 1H), 3.65 (s, 3H), 3.64 (m, 1H), 2.28 (t, 2H), 1.50 (m, 2H), 1.44 (s, 6H), 1.39 (m, 4H), 1.29 (m, 14H), 0.87 (t, 3H). ¹³C NMR (100 MHz, CDCl₃) δ 174.1, 137.9, 127.5, 108.3, 81.7, 80.6, 72.1, 51.3, 36.9, 33.9, 31.7, 31.6, 29.6, 29.4, 29.0, 28.9, 27.2, 26.8, 25.9, 25.0, 24.8, 22.5, 13.9. *m/z* calcd. for C₂₂H₄₂O₅ [M+Na]⁺ 407.2766 found 407.292.

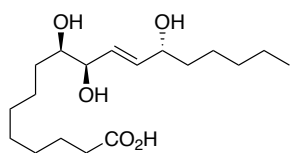


1.47: To a solution of **1.45** (16 mg, 0.04 mmol) in THF (1 mL) was added 4M HCl (1 mL). The reaction was stirred for 30 min and extracted with EtOAc (3 x 5 mL). The combined organic extracts were washed with Brine, dried (MgSO₄), filtered, and concentrated *in vacuo*. The residue was purified by flash chromatography (3:7 hexanes/ EtOAc) to afford **1.47** (12 mg, 86%) as a clear oil: $[\alpha]_D^{20}$ 0.84 (CHCl₃, *c* 0.33); ¹H NMR (400 MHz, CDCl₃) δ : 5.85 (dd, 1H, *J* = 8, 8 Hz), 5.72 (dd, 1H, *J* = 8, 8 Hz), 4.13 (m, 1H), 3.93 (t, 1H), 3.65 (s, 3H), 3.45 (m, 1H), 2.29 (t, 2H), 1.60 (m, 2H), 1.51 (m, 4H), 1.30 (m, 14H), 0.88 (t, 3H); ¹³C NMR (CDCl₃, 100 MHz): δ : 136.4, 129.4, 75.3, 74.50, 71.9, 51.4, 37.1, 33.9, 32.8, 31.6, 29.2, 29.0, 28.9, 25.4, 24.9, 24.8, 22.5, 13.9. *m/z* calcd. for C₁₉H₃₆O₅ [M+Na]⁺ 367.2453 found 367.2598



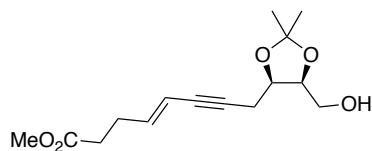
1.46: To a solution of **1.44** (15 mg, 0.04 mmol) in THF (1 mL) was added 4M HCl (1 mL). The reaction was stirred for 30 min and extracted with EtOAc (3 x 5 mL). The combined organic extracts were washed with Brine, dried (MgSO₄), filtered, and concentrated *in vacuo*. The residue was purified by flash chromatography (3:7 hexanes/ EtOAc) to afford **1.46** (10 mg, 77%) as a clear oil: $[\alpha]_D^{20}$ 0.67

(CHCl₃, *c* 0.42); ¹H NMR (400 MHz, CDCl₃) δ: 5.85 (dd, 1H, *J* = 8, 8 Hz), 5.72 (dd, 1H, *J* = 8, 8 Hz), 4.14 (m, 1H), 3.92 (t, 1H), 3.66 (s, 3H), 3.45 (m, 1H), 2.29 (t, 2H), 1.55 (m, 2H), 1.51 (m, 4H), 1.30 (m, 14H), 0.88 (t, 3H); ¹³C NMR (CDCl₃, 100 MHz): δ: 174.2, 136.5, 129.7, 75.4, 74.4, 72.2, 51.4, 37.2, 33.9, 32.9, 31.6, 29.6, 29.3, 29.2, 28.9, 25.4, 25.0, 24.8, 22.5, 13.9. *m/z* calcd. for C₁₉H₃₆O₅ [M+Na]⁺ 367.2453 found 367.2598



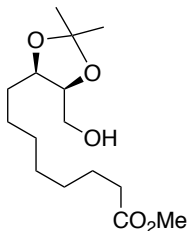
1.1: To a solution of **1.47** (1 mg, 0.002 mmol) in MeOH (1 mL) was added 1 M KOH (1 mL). After 30 min the reaction was deemed complete by RP-HPLC. A solution of 1 M aq. KH₂PO₄ (0.5 mL) and 1 M HCl (0.9 mL) was added. The aqueous layer was extracted with EtOAc (3 x 1 mL).

The combined organic extracts were washed with brine (1 mL) dried (MgSO₄), filtered, and concentrated *in vacuo* to afford **1.1** (0.7 mg, 63%) ¹H NMR (400 MHz, CD₃OD): δ = 5.59 (m, 2H), 3.95 (m, 1H), 3.80 (m, 1H), 3.31 (m, 1H), 2.17 (t, 2H), 1.50 (m, 2H), 1.43 (m, 4H), 1.24 (m, 14H), 0.82 (t, 3H). ¹³C NMR (100 MHz, CD₃OD): δ = 176.21, 135.08, 129.55, 75.05, 74.29, 71.58, 36.86, 33.48, 32.05, 31.52, 29.15, 28.89, 28.72, 25.35, 24.75, 24.60, 22.23, 12.90.

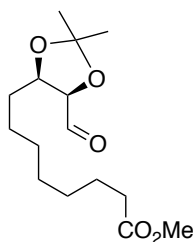


1.48: A suspension of **1.32** (50mg, 0.21 mmol), CuI (10mg, 0.05 mmol) and PdCl₂(PPh₃)₂ (12mg, 0.018 mmol) in triethylamine (2mL, 0.1 M) was thoroughly degassed. A solution of **1.10** (30mg, 0.18 mmol) in triethylamine (0.5mL, 0.35 M) was added dropwise

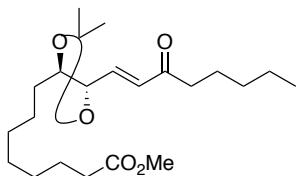
and the reaction was stirred for 16 h. The volatiles were removed *in vacuo* and the residue was dissolved in ethyl acetate (10 mL), washed with water (5 mL), and sat. aq. NH₄Cl (5 mL). The organic layer was dried (MgSO₄), filtered, and concentrated *in vacuo*. The crude residue was purified by flash column chromatography (hexanes to 3:2 hexanes/ethyl acetate gradient) to afford **1.48** (25 mg, 52% yield) as a clear oil. [α]_D²⁰ -24.2 (*c* 1.0, CHCl₃); ¹H NMR (400 MHz, CDCl₃): δ = 6.11 (m, 1H), 5.53 (d, 1H), 4.38 (m, 2H), 3.86 (m, 2H), 3.69 (s, 3H), 2.70 (m, 2H), 2.42 (m, 4H), 1.49 (s, 3H), 1.39 (s, 1H); ¹³C NMR (100 MHz, CDCl₃): δ = 172.8, 141.7, 110.5, 108.5, 84.3, 80.6, 77.54, 75.2, 61.1, 51.5, 33.0, 27.9, 27.7, 25.2, 20.7. *m/z* calcd. for C₁₅H₂₂O₅ [M+Na]⁺ 305.1358 found 305.1477



1.49: To a suspension of NiBr (cat.) and **1.48** (25mg, 0.09 mmol) in MeOH (3 mL) at 0°C was added NaBH₄ (12mg, 0.32 mmol). The reaction was stirred for 10 min at 0°C and a black color was observed. The reaction vessel was evacuated, placed under an atmosphere of hydrogen gas (1 atm), and allowed to warm to rt and stir overnight. The reaction was filtered through celite and a plug of silica and washed with ethyl acetate. The filtrate was concentrated *in vacuo* to afford **1.49** (25 mg, >95%) as a clear oil. $[\alpha]_D^{20}$ -13.2 (*c* 1.0, CHCl₃); ¹H NMR (400 MHz, CDCl₃): δ = 4.13 (m, 2H), 3.65 (s, 3H), 3.59 (m, 2H), 2.30 (t, 2H), 1.60 (m, 2H), 1.45 (s, 3H), 1.36 (s, 3H), 1.30 (m, 10H); ¹³C NMR (100 MHz, CDCl₃): δ = 174.1, 107.9, 77.8, 61.7, 51.3, 33.9, 29.6, 29.3, 29.0, 28.9, 28.7, 28.2, 26.5, 25.4, 24.8. *m/z* calcd. for C₁₅H₂₈O₅ [M+Na]⁺ 311.1827 found 311.1973

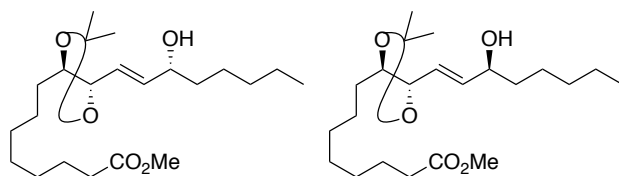


1.50: To a solution of compound **1.49** (105 mg, 0.36 mmol) in dichloromethane (10 mL) at room temperature were sequentially added NaHCO₃ (26 mg, 0.31 mmol) and Dess-Martin Periodinane (233 mg, 0.55 mmol). The resulting reaction mixture was stirred at room temperature for 1.5 h and quenched with 25% Na₂S₂O₃ (8 mL) and NaHCO₃ (8 mL). The organic layer was separated, dried (MgSO₄) and concentrated *in vacuo*. The resulting residue was dissolved in hexane and filtered through a celite plug which was washed with hexane. The combined filtrate and washings were concentrated to afford **1.50** (95 mg of crude aldehyde) as a light yellow oil which was used without further purification: ¹H NMR (400 MHz, CDCl₃) δ 9.64 (d, *J* = 3.4 Hz, 1H), 4.33 (m, 1H), 4.25 (dd, *J* = 3.5, 7.1 Hz, 1H), 3.68 (s, 3H), 2.31 (t, *J* = 7.5 Hz, 2H), 1.64 (m, 2H), 1.62 (s, 3H), 1.51 (m, 2H), 1.42 (s, 3H), 1.31 (m, 8H).



1.51: To a solution of **1.13** (106 mg, 0.47 mmol) in THF (2 mL) at 0 °C was added sodium bis(trimethylsilyl)amide (1 M solution in THF, 400 μL, 0.40 mmol) dropwise. After stirring at 0 °C for 5 min, the ice bath was removed and the reaction was allowed to warm to room temperature and stirred for an additional 30 min. White solid was formed during this period. The the reaction mixture was cooled to 0 °C and the crude **1.50** was added as a solution in THF (5 mL).

The reaction was stirred at 0 °C for 30 min and quenched with water (10 mL). The aqueous layer was extracted with EtOAc (2 x 15 mL). The combined organic layers were dried (MgSO₄) and concentrated *in vacuo*. The residue was purified by flash column chromatography (hexanes to 17:3 hexanes/ethyl acetate gradient) to afford **1.51** (105 mg, 72% over two steps) as a colorless oil: $[\alpha]_D^{20}$ -0.8 (*c* 1.0, CHCl₃); ¹H NMR (400 MHz, CDCl₃) δ 6.68 (dd, *J* = 6.3, 15.8 Hz, 1H), 6.32 (dd, *J* = 1.2, 15.8 Hz, 1H), 4.65 (m, 1H), 4.24 (m, 1H), 3.67 (s, 3H), 2.56 (t, *J* = 7.4 Hz, 2H), 2.30 (t, *J* = 7.4 Hz, 2H), 1.63 (m, 4H), 1.53 (s, 3H), 1.46 (m, 2H), 1.31 (m, 12H), 0.90 (t, *J* = 6.8 Hz, 3H); ¹³C NMR (100 MHz, CDCl₃) δ 200.4, 174.5, 141.4, 131.1, 109.1, 78.6, 77.9, 51.7, 41.1, 34.3, 31.7, 30.8, 29.5, 29.34, 29.25, 28.3, 26.5, 25.8, 25.1, 24.1, 22.7, 14.2. *m/z* calcd. for C₂₂H₃₈O₅ [M+Na]⁺ 405.2609 found 405.2779

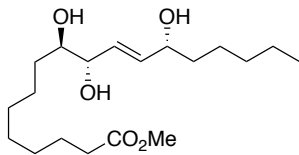


1.52 and 1.53: To a solution of **1.51** (10 mg, 0.026 mmol) and CeCl₃·7H₂O (11 mg, 0.031 mmol) in methanol (0.2 mL) stirring at 0 °C was added NaBH₄ (1 mg, 0.026 mmol). The

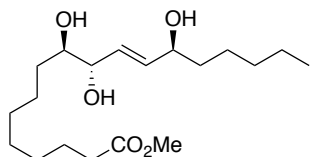
reaction was stirred at 0 °C for 1 h, then rt for 3 h. The solvent was removed *in vacuo* and the crude residue was purified by flash chromatography (4:1 hexanes/ethyl acetate) to afford **1.53** (4 mg, 40%, *r_f* = 0.11) and **1.52** (4 mg, 40%, *r_f* = 0.10) as clear oils.

1.53: $[\alpha]_D^{20}$ -1.92 (CHCl₃, *c* 0.42); ¹H NMR (400 MHz, CDCl₃) δ: 5.70 (m, 2H), 4.48 (m, 1H), 4.11 (m, 2H), 3.64 (s, 3H), 2.28 (t, 2H), 1.59 (m, 2H), 1.46 (s, 6H), 1.34 (m, 4H), 1.28 (m, 14H), 0.87 (t, 3H). ¹³C NMR (100 MHz, CDCl₃) δ 174.1, 137.1, 126.9, 108.0, 78.9, 78.2, 72.3, 51.3, 36.9, 33.9, 31.6, 30.3, 29.6, 29.3, 29.0, 28.9, 28.2, 26.0, 25.5, 25.0, 24.8, 22.5, 13.9. *m/z* calcd. for C₂₂H₄₀O₅ [M+Na]⁺ 407.2766 found 407.2922

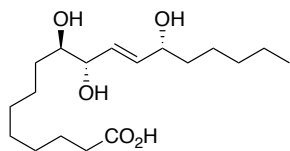
1.52: $[\alpha]_D^{20}$ 1.30 (CHCl₃, *c* 0.92); ¹H NMR (400 MHz, CDCl₃) δ: 5.65 (m, 2H), 4.49 (m, 1H), 4.12 (m, 2H), 3.65 (s, 3H), 2.28 (t, 2H), 1.60 (m, 2H), 1.46 (s, 6H), 1.34 (m, 4H), 1.28 (m, 14H), 0.87 (t, 3H). ¹³C NMR (100 MHz, CDCl₃) δ 174.1, 137.2, 126.3, 107.9, 78.8, 78.2, 71.9, 51.3, 37.0, 33.9, 31.6, 30.3, 29.3, 29.0, 28.9, 28.2, 26.0, 25.5, 24.9, 24.8, 22.5, 13.9. *m/z* calcd. for C₂₂H₄₀O₅ [M+Na]⁺ 407.2766 found 407.2922



1.55: To a solution of **1.53** (13 mg, 0.034 mmol) in THF (1 mL) was added 4M HCl (1 mL). The reaction was stirred for 30 min and extracted with EtOAc (3 x 3 mL). The combined organic extracts were washed with Brine (5 mL), dried (MgSO₄), filtered, and concentrated *in vacuo*. The residue was purified by flash chromatography (3:7 hexanes/ EtOAc) to afford **1.55** (7 mg, 65%) as a clear oil: $[\alpha]_D^{20}$ 3.2 (CHCl₃, *c* 0.25); ¹H NMR (400 MHz, CDCl₃) δ 5.76 (m, 2H), 4.13-4.08 (m, 2H), 3.65 (s, 4H), 2.29 (t, 2H), 1.60 (m, 2H), 1.51 (m, 4H), 1.30 (m, 14H), 0.88 (t, 3H). ¹³C NMR (100 MHz, CDCl₃) δ 174.3, 136.9, 128.2, 75.2, 74.1, 72.4, 51.4, 37.2, 34.0, 32.1, 31.7, 29.7, 29.3, 29.1, 29.0, 25.7, 25.1, 24.8, 22.6, 14.0. *m/z* calcd. for C₁₉H₃₆O₅ [M+Na]⁺ 367.2453 found 367.2598



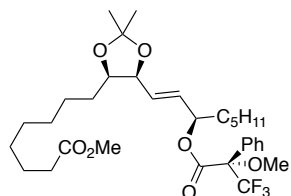
1.54: To a solution of **1.52** (13 mg, 0.034 mmol) in THF (1 mL) was added 4M HCl (1 mL). The reaction was stirred for 30 min and extracted with EtOAc (3 x 3 mL). The combined organic extracts were washed with Brine (5 mL), dried (MgSO₄), filtered, and concentrated *in vacuo*. The residue was purified by flash chromatography (3:7 hexanes/ EtOAc) to afford **1.54** (8 mg, 72%) as a clear oil: $[\alpha]_D^{20}$ 10.2 (CHCl₃, *c* 0.33); ¹H NMR (400 MHz, CDCl₃) δ 5.78 (m, 2H), 4.12-4.09 (m, 2H), 3.66 (s, 4H), 2.29 (t, 2H), 1.60 (m, 2H), 1.55 (m, 4H), 1.30 (m, 14H), 0.88 (t, 3H). ¹³C NMR (100 MHz, CDCl₃) δ 174.3, 136.7, 127.9, 75.1, 74.1, 72.1, 51.4, 37.2, 34.0, 32.0, 31.7, 29.7, 29.3, 29.0, 28.9, 25.6, 25.0, 24.8, 22.6, 14.0. *m/z* calcd. for C₁₉H₃₆O₅ [M+Na]⁺ 367.2453 found 367.2598



1.2: To a solution of **1.55** (1 mg, 0.002 mmol) in MeOH (1 mL) was added 1 M KOH (1 mL). After 30 min the reaction was deemed complete by RP-HPLC. A solution of 1 M aq. KH₂PO₄ (0.5 mL) and 1 M HCl (0.9 mL) was added. The aqueous layer was extracted with EtOAc (3 x 1 mL). The combined organic extracts were washed with brine (1 mL) dried (MgSO₄), filtered, and concentrated *in vacuo* to afford **1.2** (0.8 mg, 76%). ¹H NMR (400 MHz, CD₃OD): δ = 5.60 (m,

2H), 3.96 (m, 1H), 3.84 (m, 1H), 3.40 (m, 1H), 2.17 (t, 2H), 1.50 (m, 2H), 1.43 (m, 4H), 1.24 (m, 14H), 0.81 (t, 3H).

Representative experimental for Mosher ester Analysis



1.58: To a solution of **1.53** (1 mg, 0.002 mmol) in CH₂Cl₂ (0.35 mL) was (*S*)-MTPA (1.5 mg, 0.007 mmol), DCC (1.3 mg, 0.007 mmol), and DMAP (1 mg, 0.007 mmol). The reaction was stirred 24 h. The solvent was removed *in vacuo* and the crude residue was purified by flash chromatography (40:1 hexanes/ethyl acetate) to afford **1.58** (1 mg, >95%) as a clear oil. ¹H NMR (400 MHz, CDCl₃): δ = 7.54 (m, 2H), 7.39 (m, 3H), 5.79 (m, 1H), 5.75 (m, 1H), 4.48 (m, 2H) 4.13 (m, 2H), 3.96 (m, 1H), 3.64 (s, 3H), 2.30 (t, 2H), 1.54 (m, 12H). In an entirely analogous fashion, **1.59** was prepared. ¹H NMR (400 MHz, CDCl₃): δ = 7.54 (m, 2H), 7.39 (m, 3H), 5.78 (m, 1H), 5.60 (m, 1H), 4.48 (m, 2H), 4.13 (m, 2H), 3.94 (m, 1H), 3.64 (s, 3H), 2.30 (t, 2H), 1.53 (m, 12H).

Appendix A1:

Spectra Relevant to Chapter I

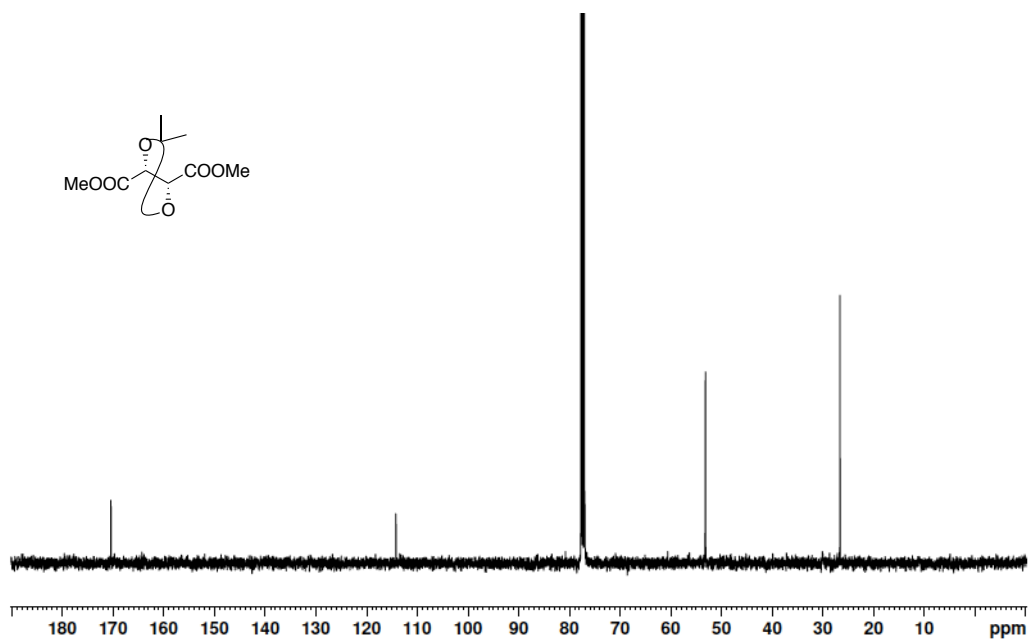
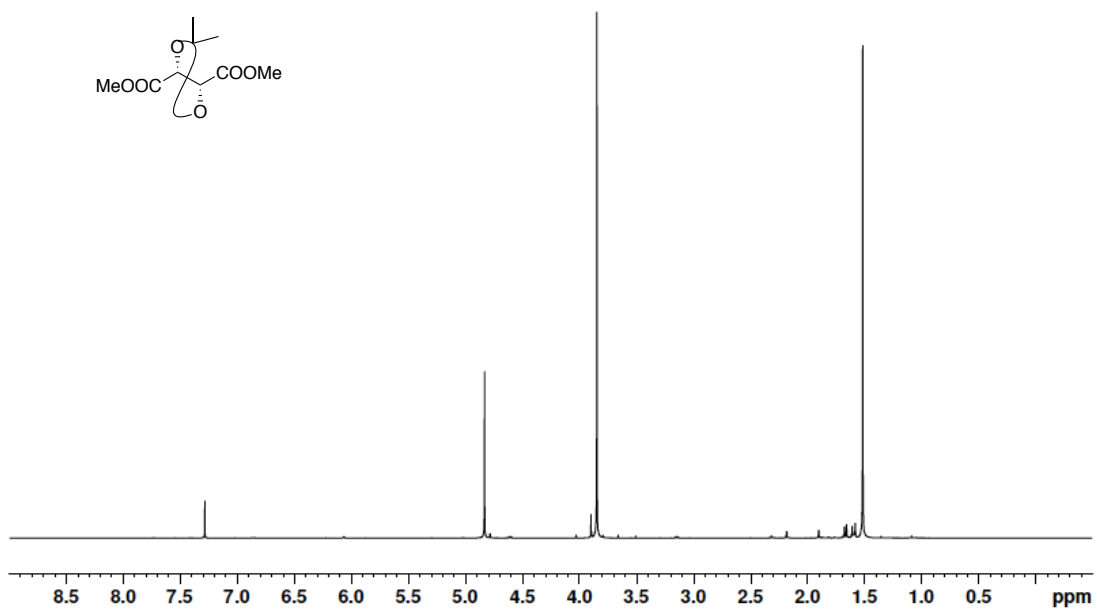


Figure A1.1 400 MHz ^1H -NMR and 100 MHz ^{13}C -NMR spectrum of **1.15** in CDCl_3

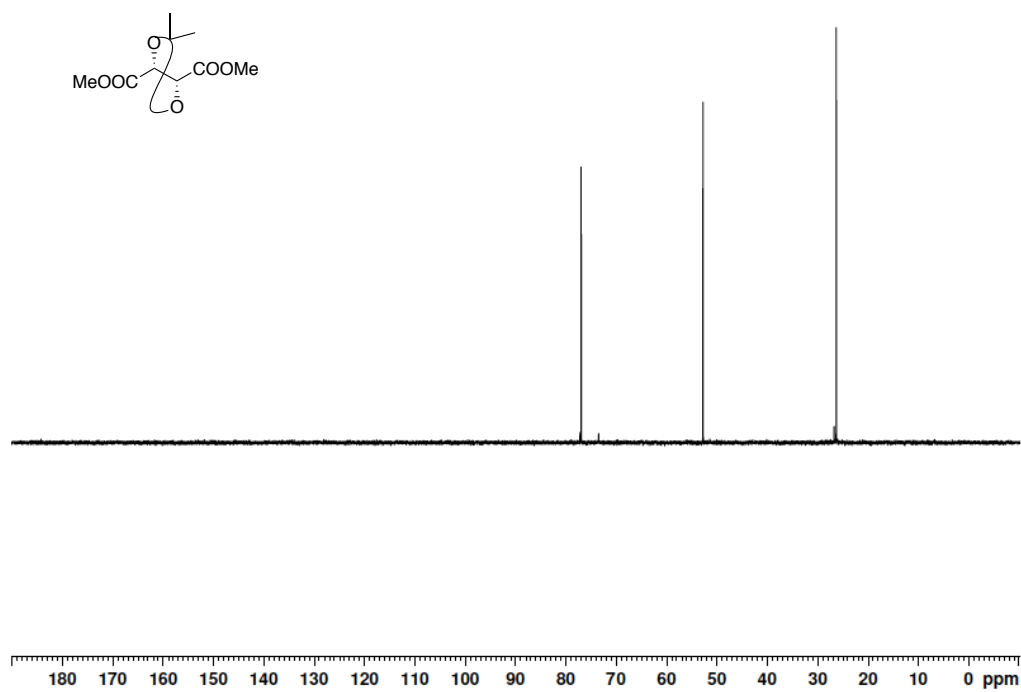


Figure A1.2 100 MHz DEPT 135 NMR spectrum of **1.15** in CDCl_3

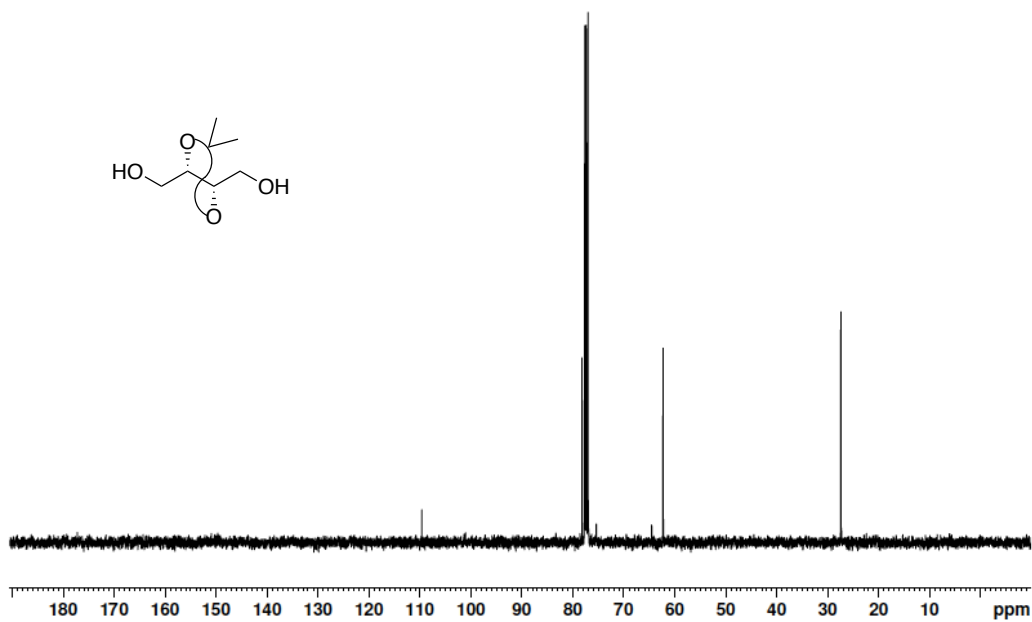
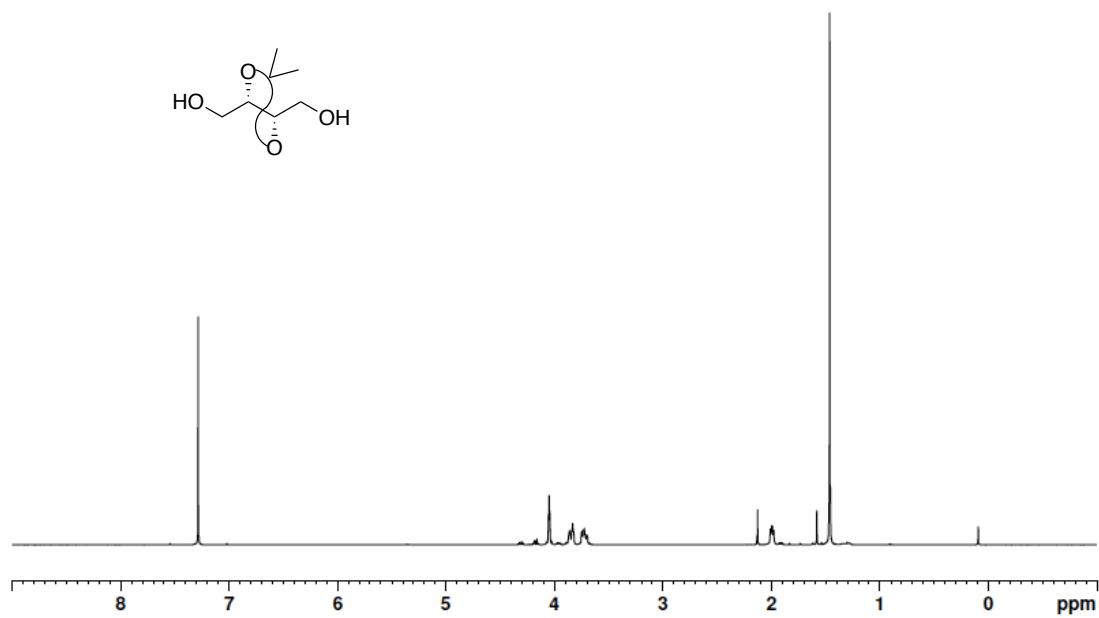


Figure A1.3 400 MHz ¹H-NMR and 100 MHz ¹³C-NMR spectrum of **1.16** in CDCl₃

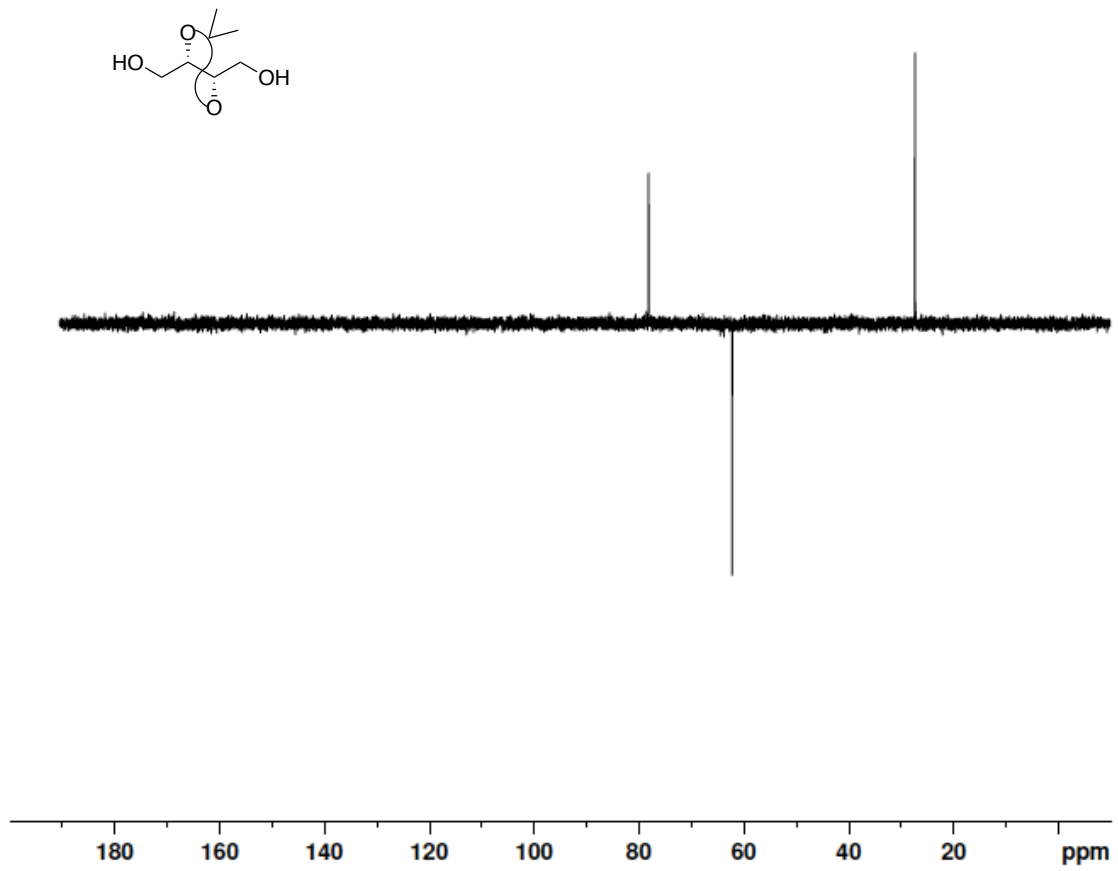


Figure A1.4 100 MHz DEPT 135 NMR spectrum of **1.16** in CDCl₃

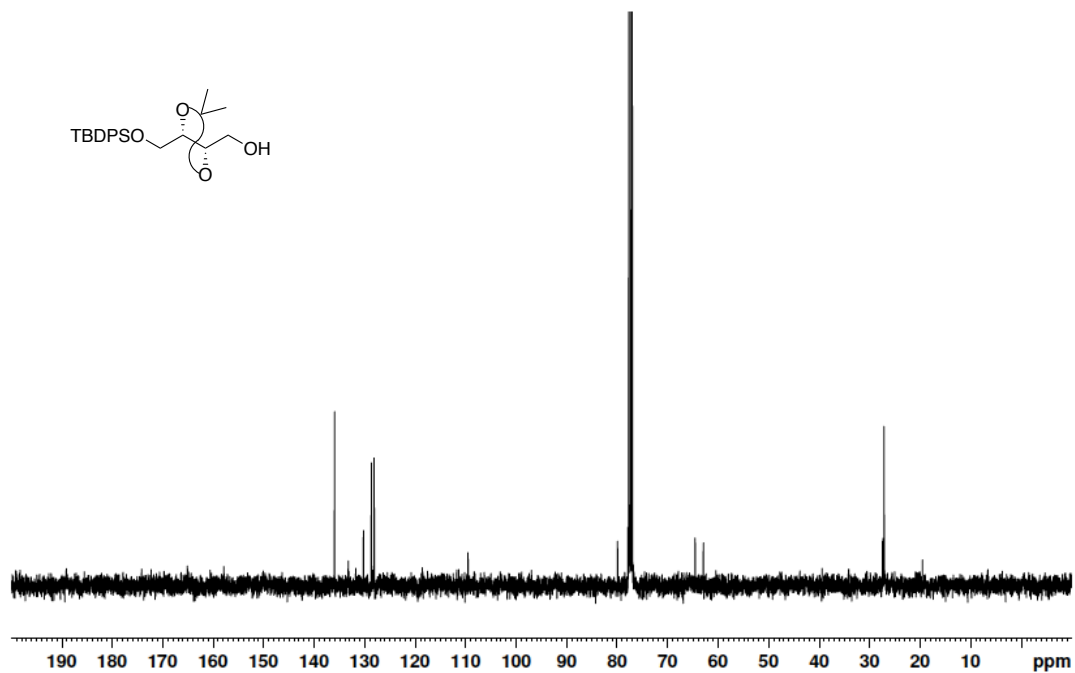
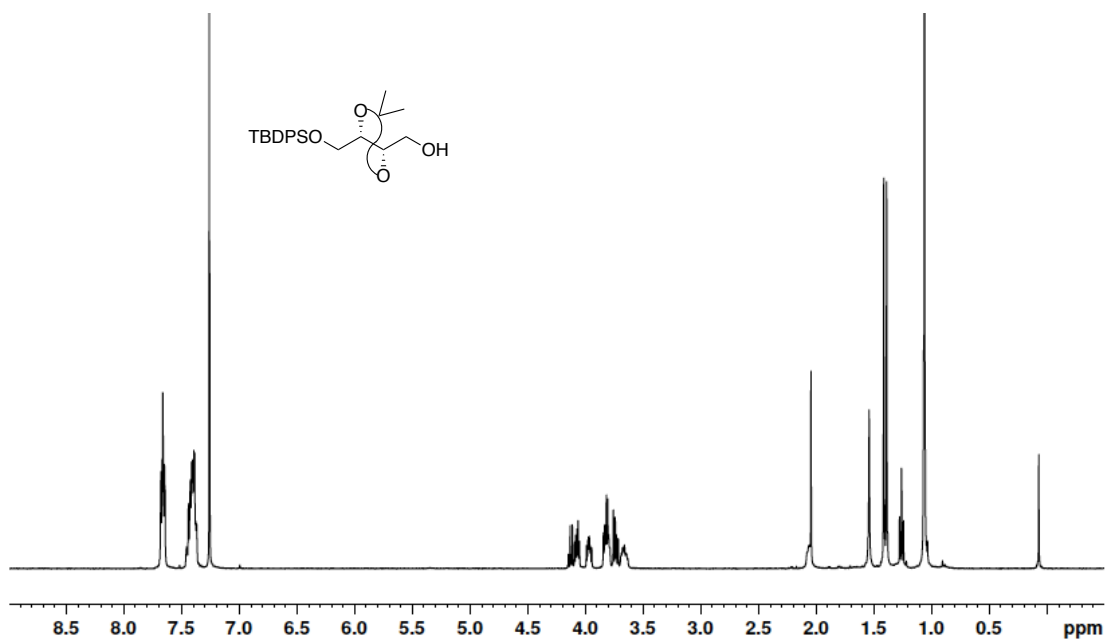


Figure A1.5 400 MHz $^1\text{H-NMR}$ and 100 MHz $^{13}\text{C-NMR}$ spectrum of **1.17** in CDCl_3 .

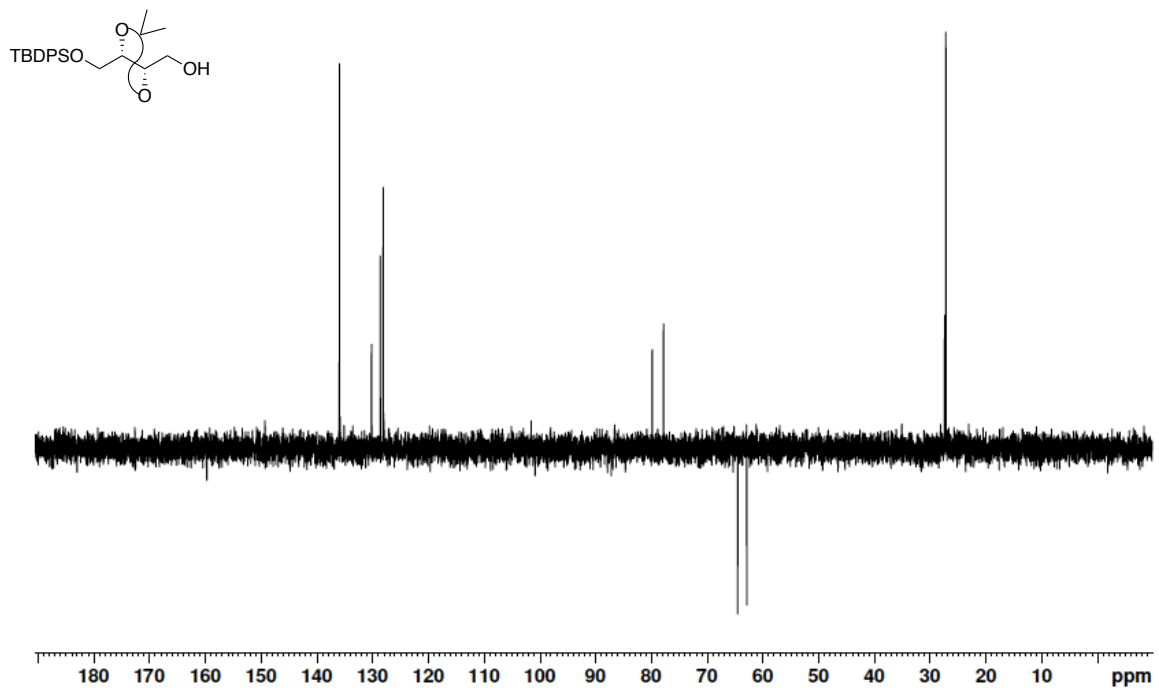


Figure A1.6 100 MHz DEPT 135 NMR spectrum of **1.17** in CDCl_3

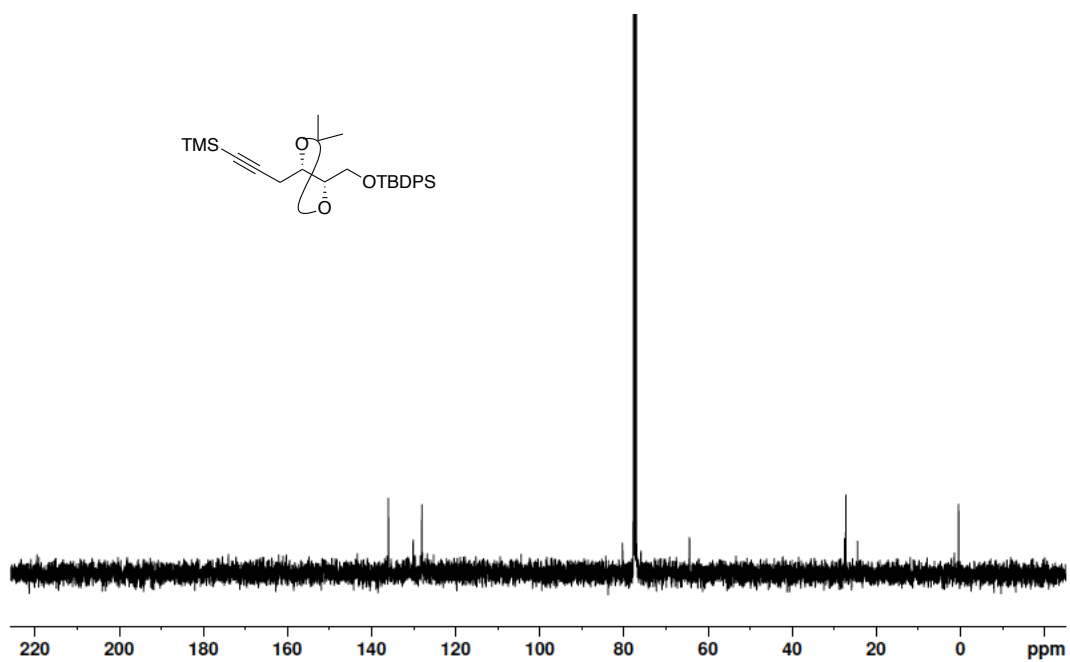
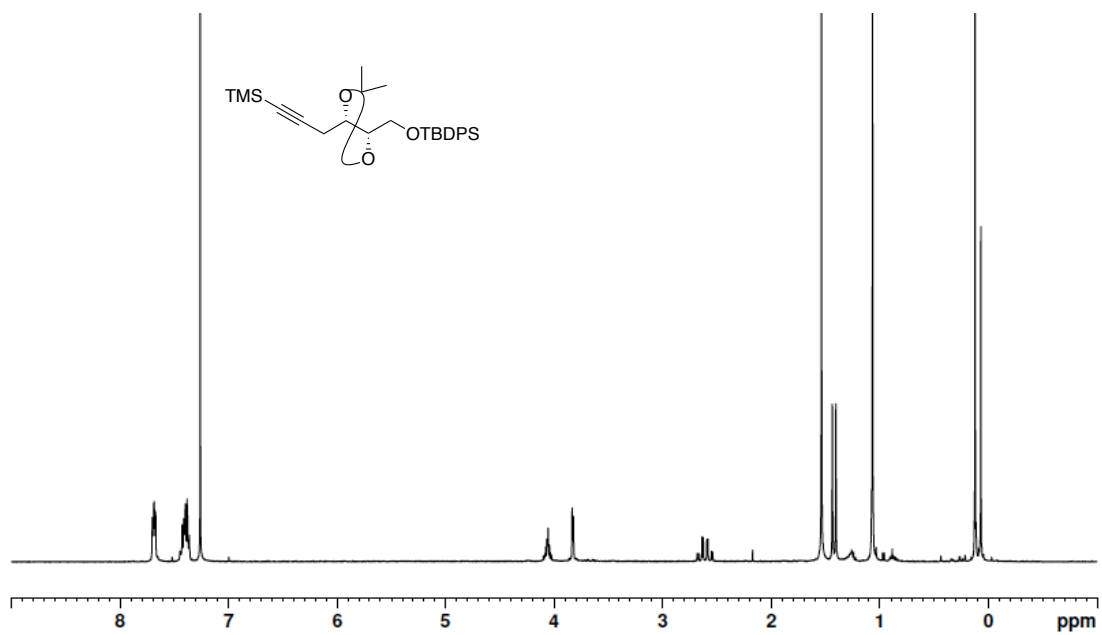


Figure A1.7 400 MHz $^1\text{H-NMR}$ and 100 MHz $^{13}\text{C-NMR}$ spectrum of **1.19** in CDCl_3

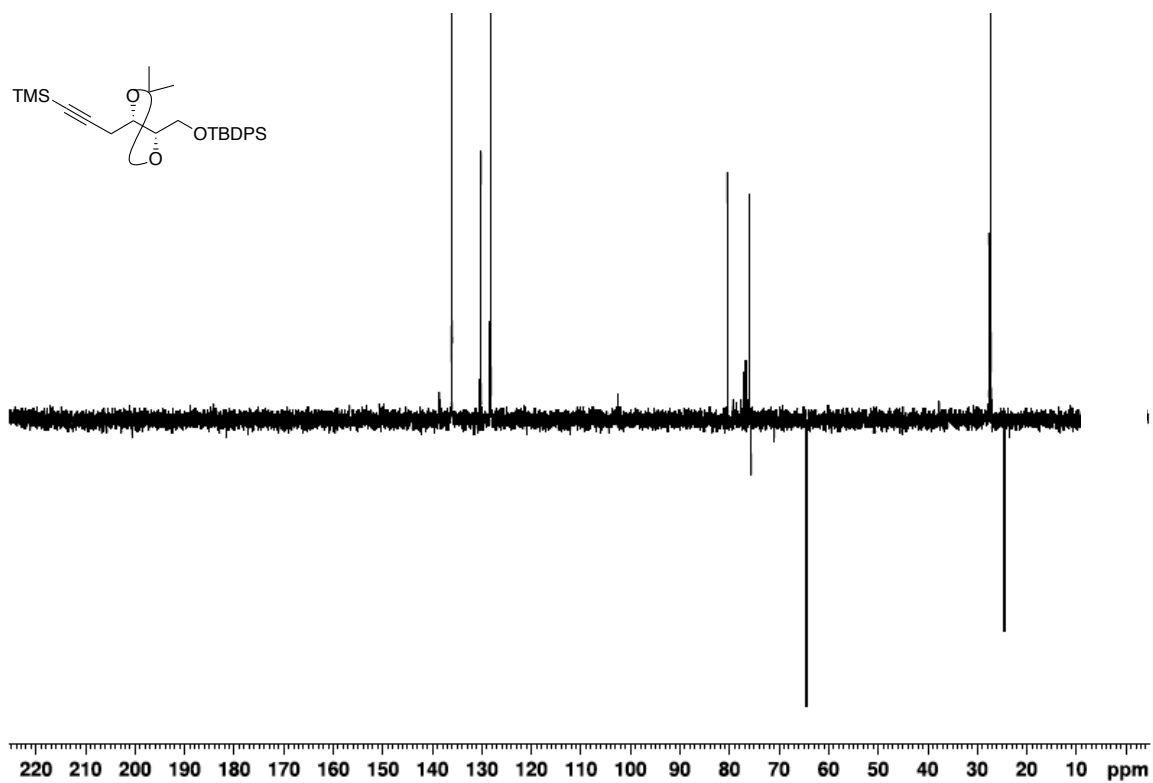


Figure A1.8 100 MHz DEPT 135 NMR spectrum of **1.19** in CDCl₃

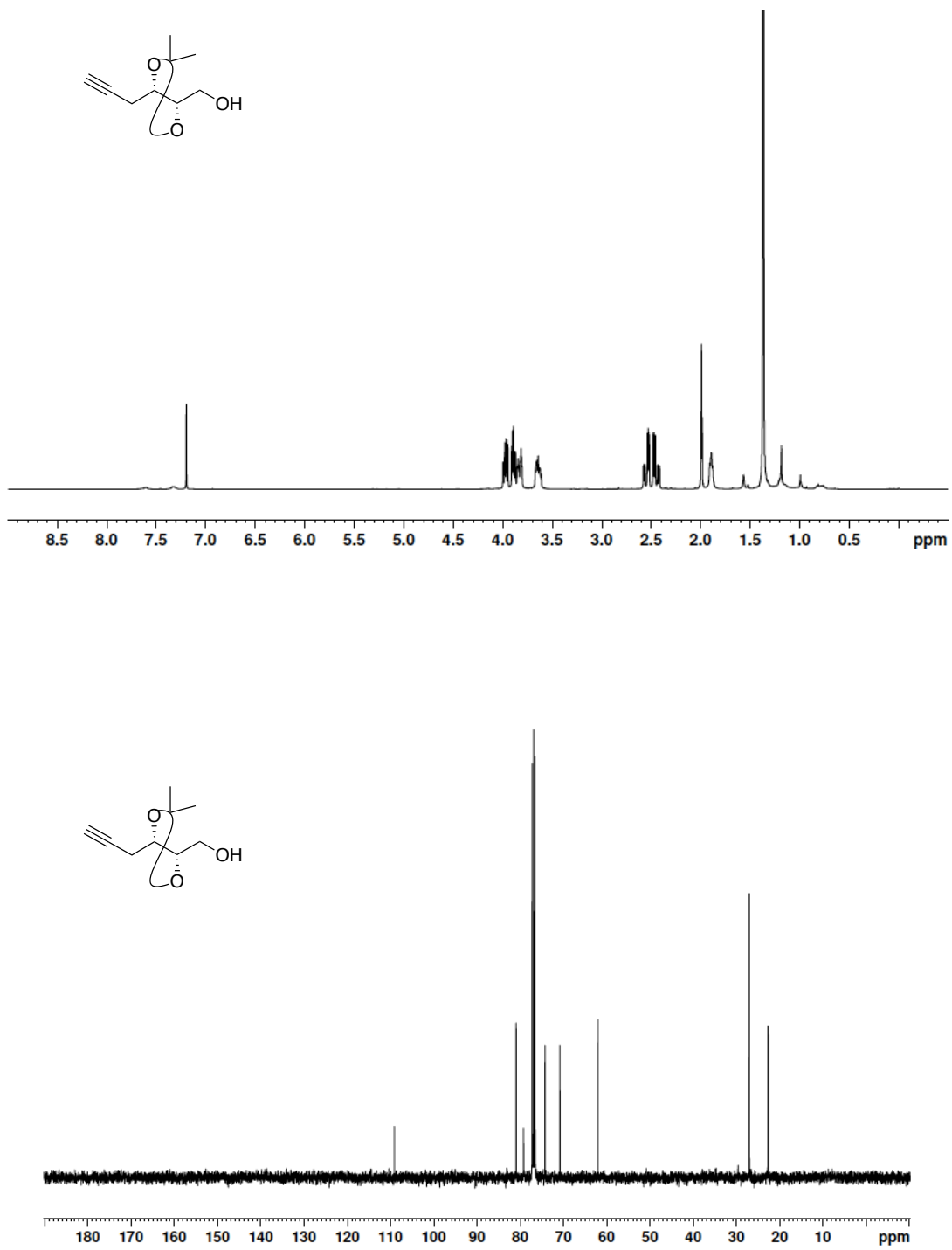


Figure A1.9 400 MHz ¹H-NMR and 100 MHz ¹³C-NMR spectrum of **1.11** in CDCl₃

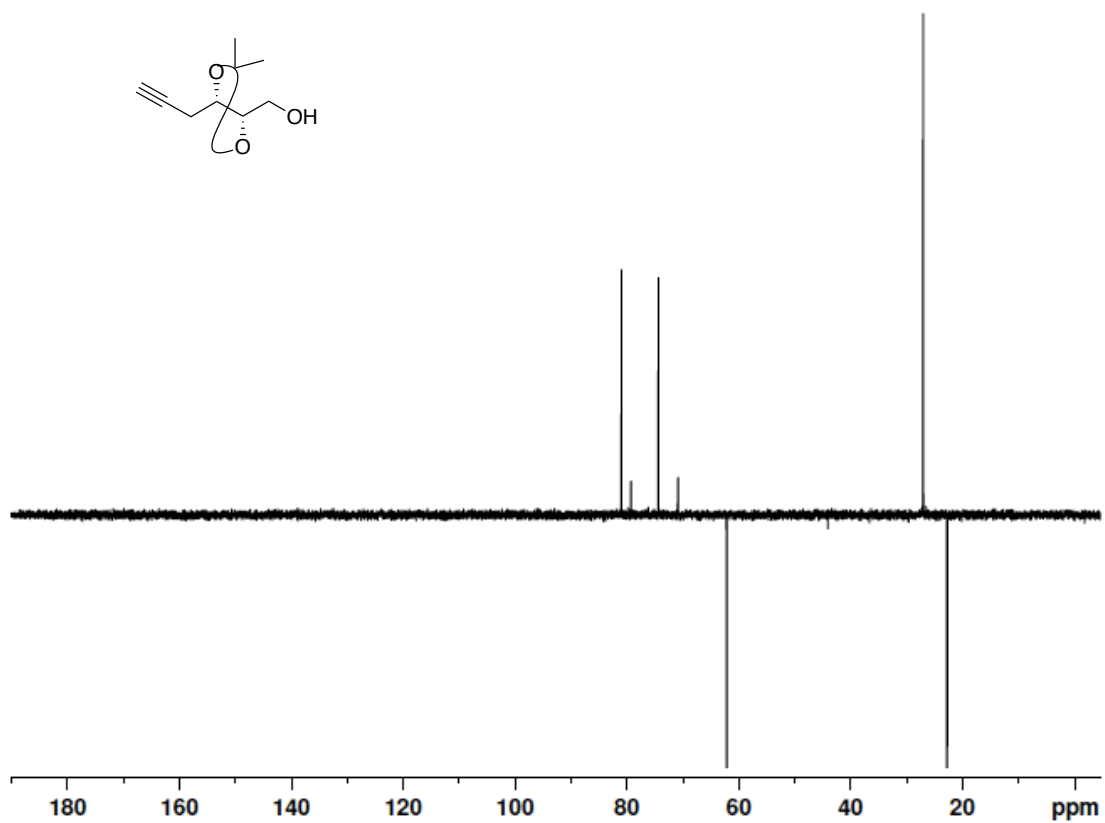


Figure A1.10 100 MHz DEPT 135 NMR spectrum of **1.11** in CDCl_3

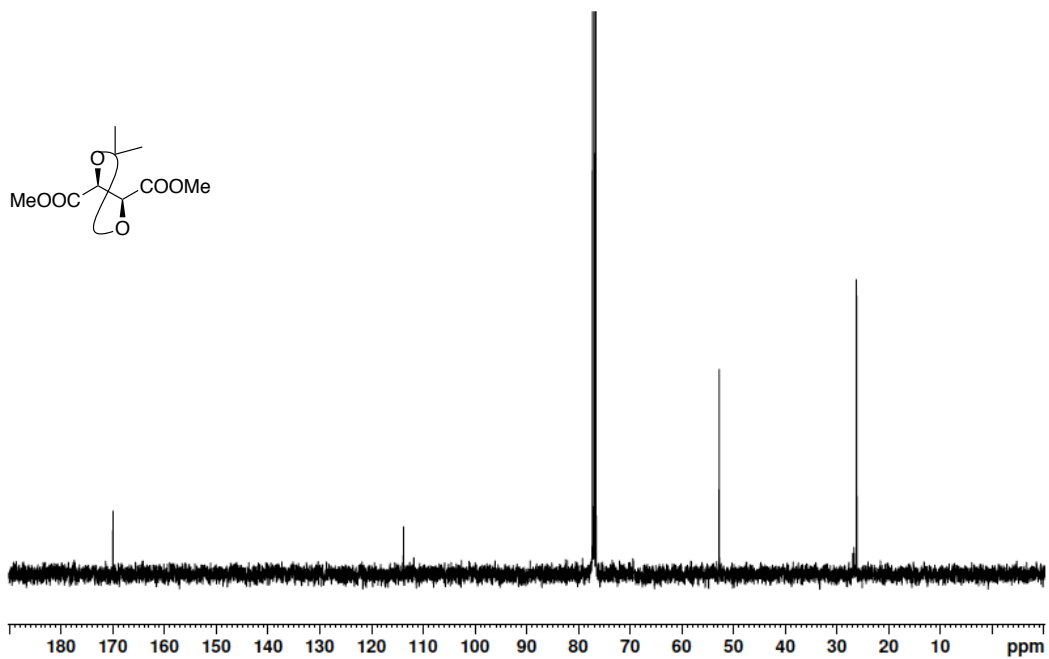
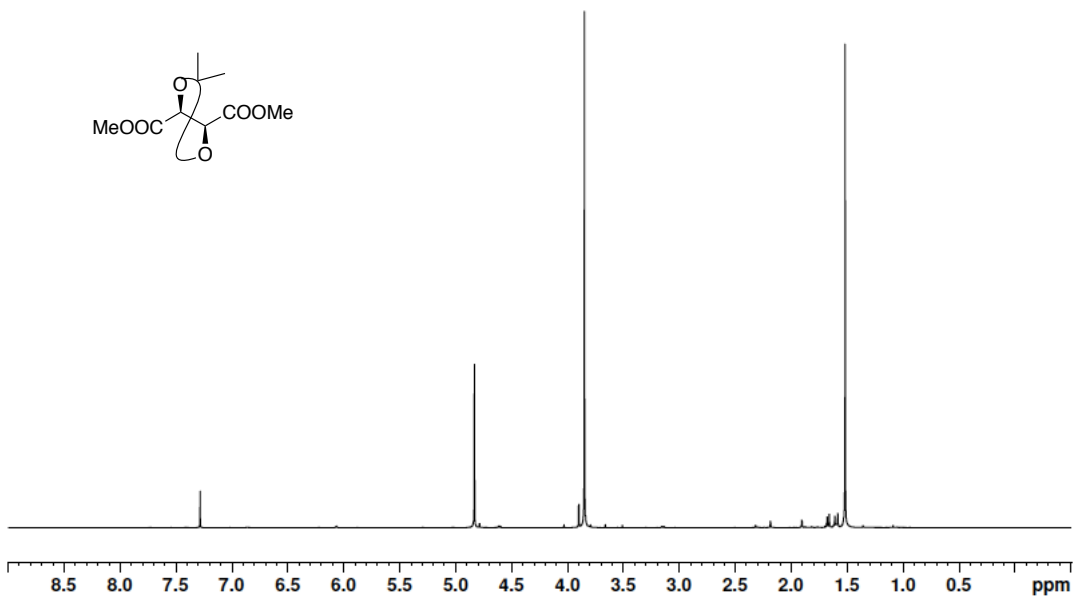


Figure A1.11 400 MHz $^1\text{H-NMR}$ and 100 MHz $^{13}\text{C-NMR}$ spectrum of **1.33** in CDCl_3

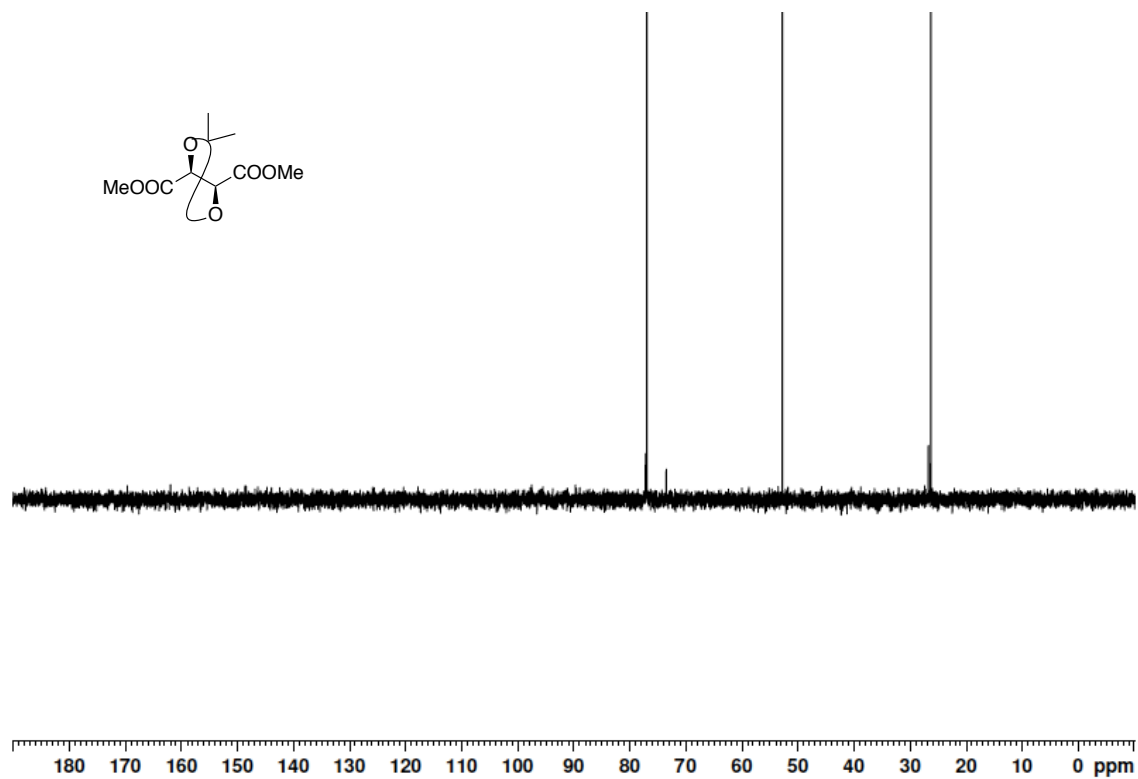


Figure A1.12 100 MHz DEPT 135 NMR spectrum of **1.33** in CDCl₃

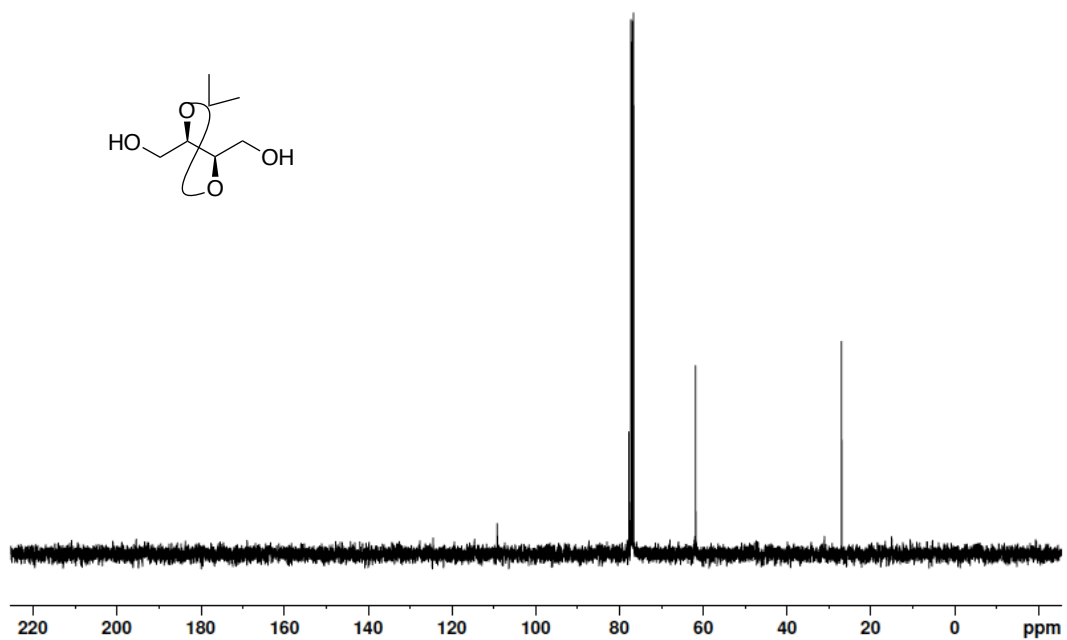
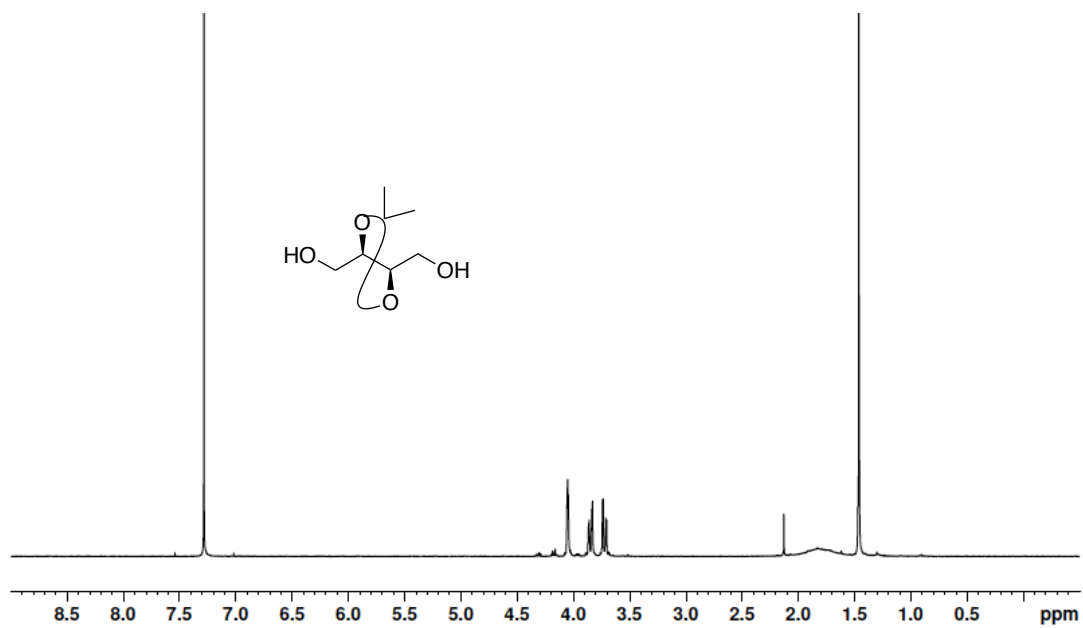


Figure A1.13 400 MHz $^1\text{H-NMR}$ and 100 MHz $^{13}\text{C-NMR}$ spectrum of **1.34** in CDCl_3

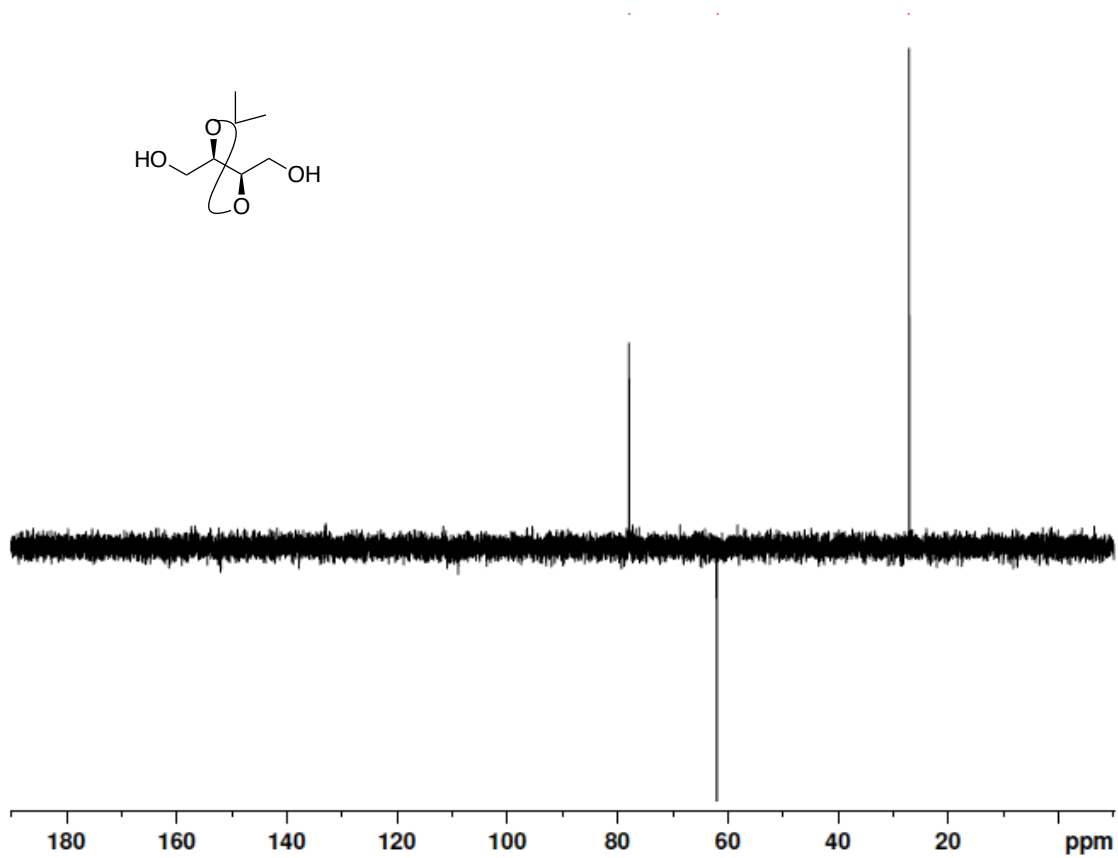


Figure A1.14 100 MHz DEPT 135 NMR spectrum of **1.34** in CDCl₃

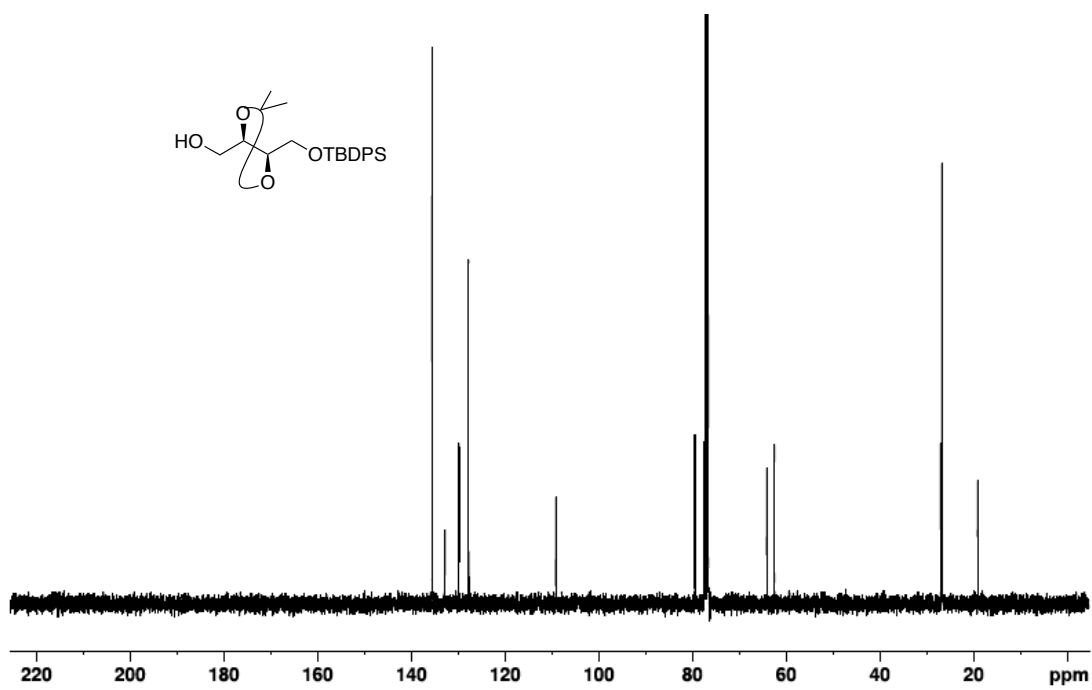
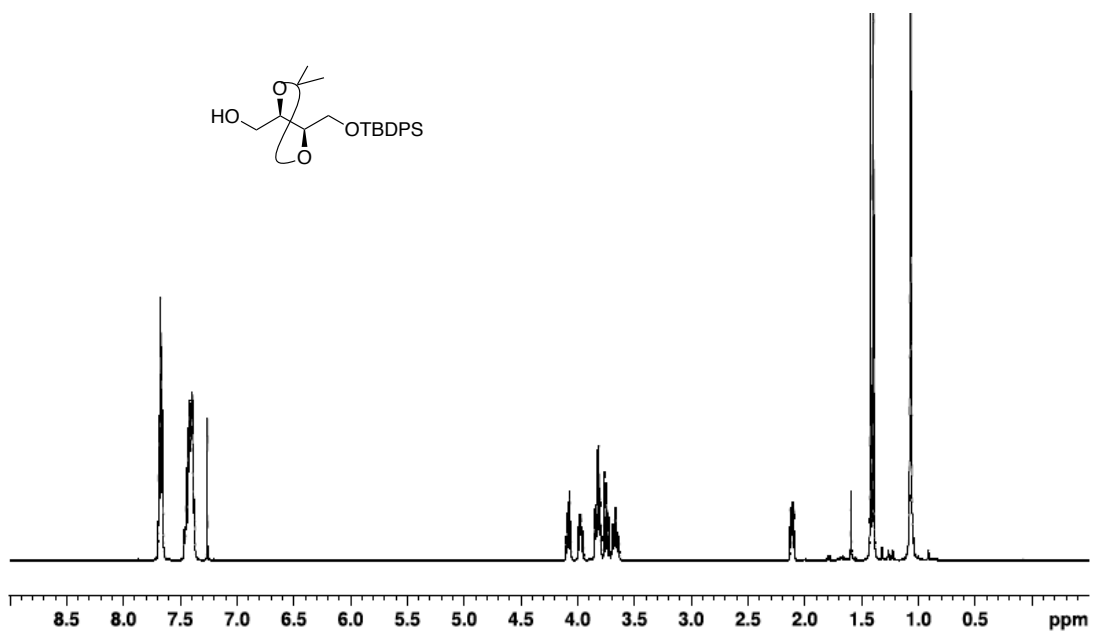


Figure A1.15 400 MHz $^1\text{H-NMR}$ and 100 MHz $^{13}\text{C-NMR}$ spectrum of **1.35** in CDCl_3

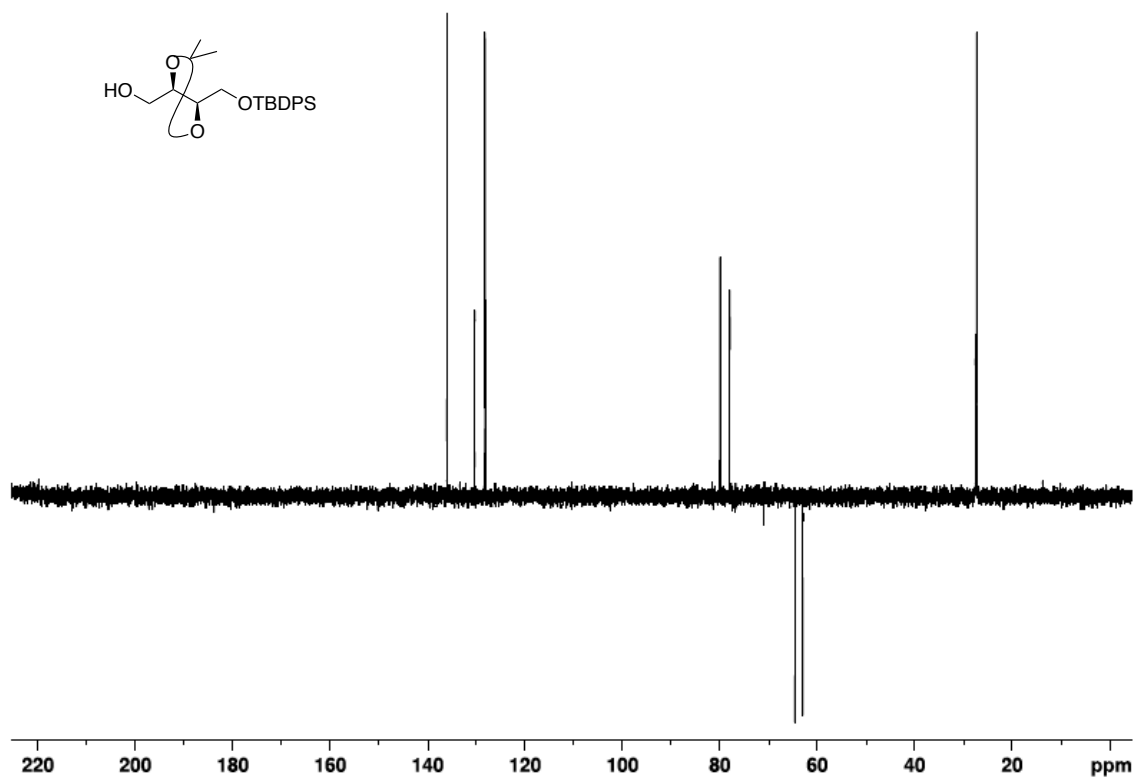


Figure A1.16 100 MHz DEPT 135 NMR spectrum of **1.35** in CDCl_3

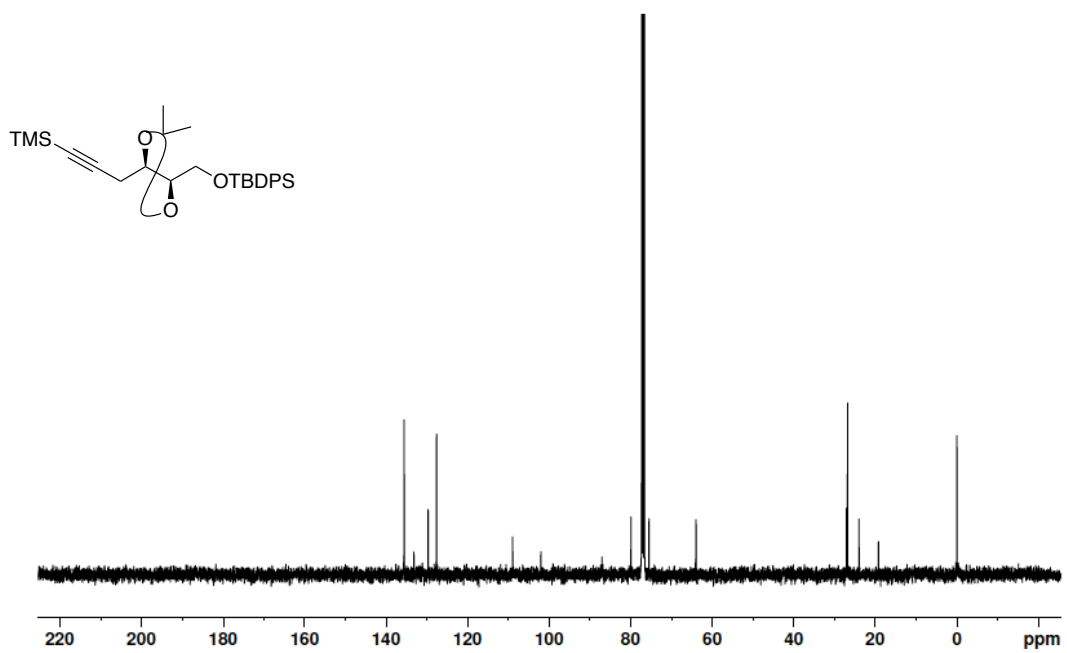
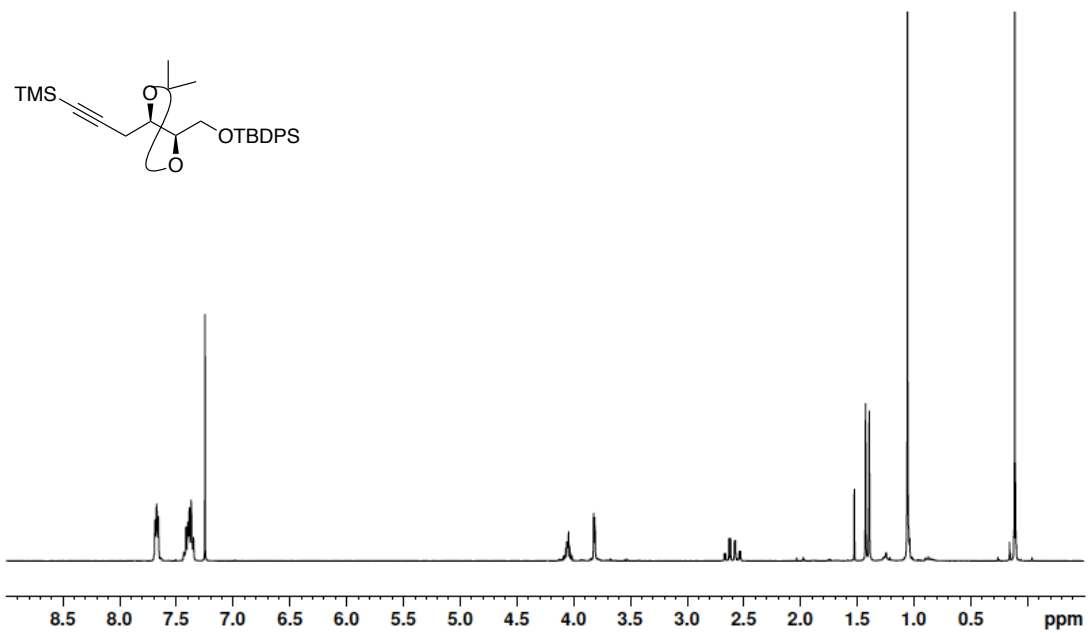


Figure A1.17 400 MHz ¹H-NMR and 100 MHz ¹³C-NMR spectrum of S2 in CDCl₃

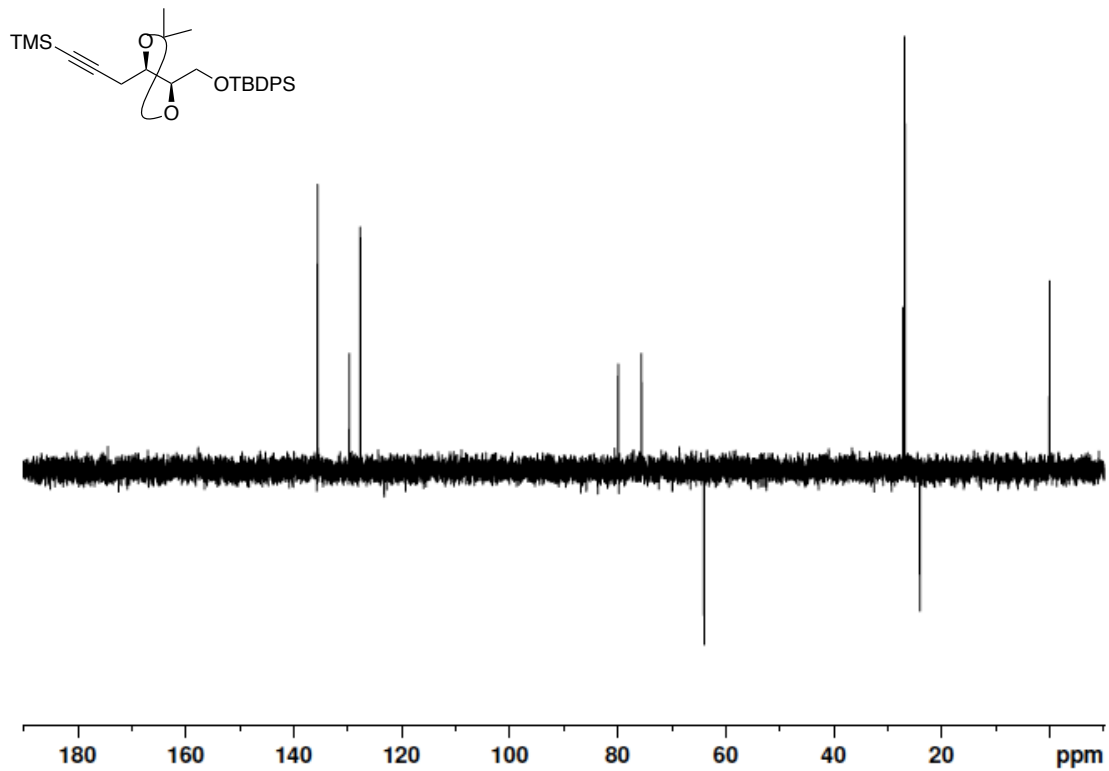


Figure A1.18 100 MHz DEPT 135 NMR spectrum of **S2** in CDCl₃

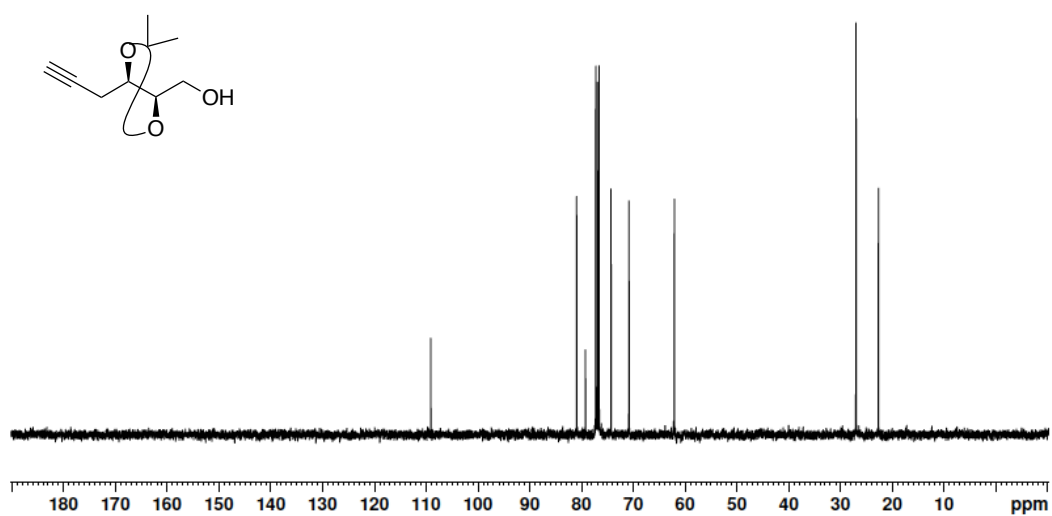
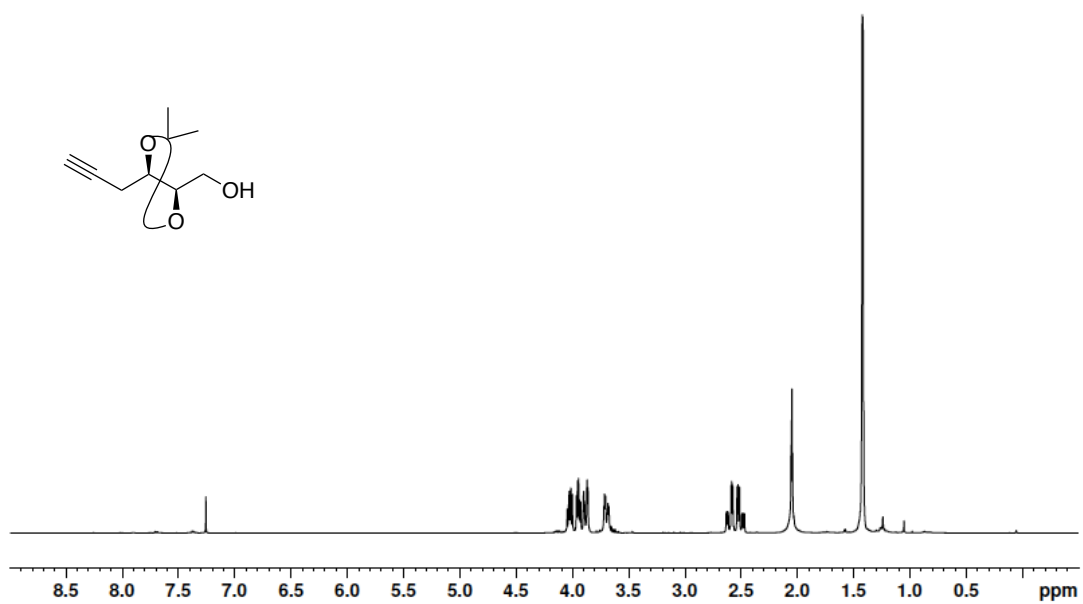


Figure A1.19 400 MHz ¹H-NMR and 100 MHz ¹³C-NMR spectrum of **1.9** in CDCl₃

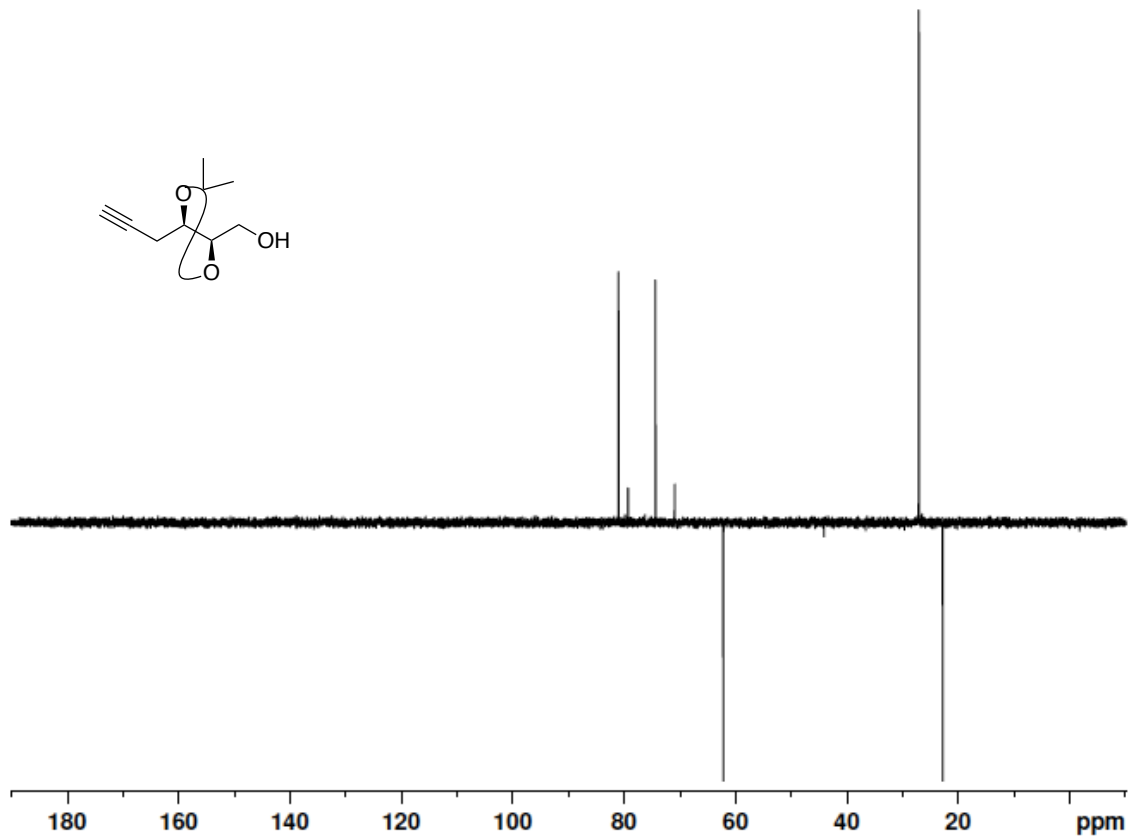


Figure A1.20 100 MHz DEPT 135 NMR spectrum of **1.9** in CDCl₃

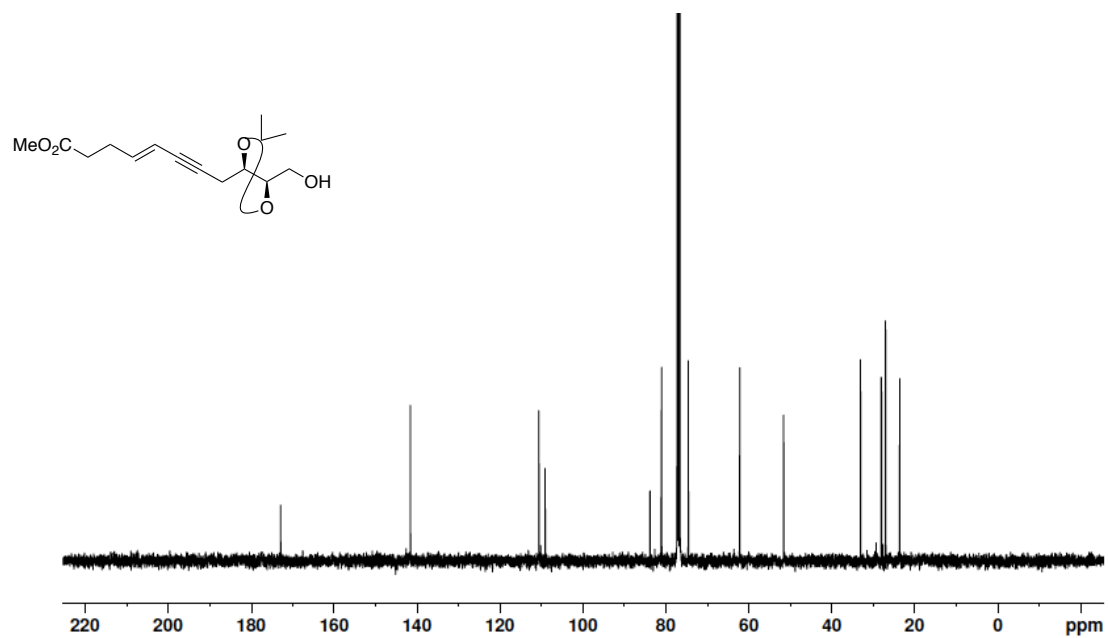
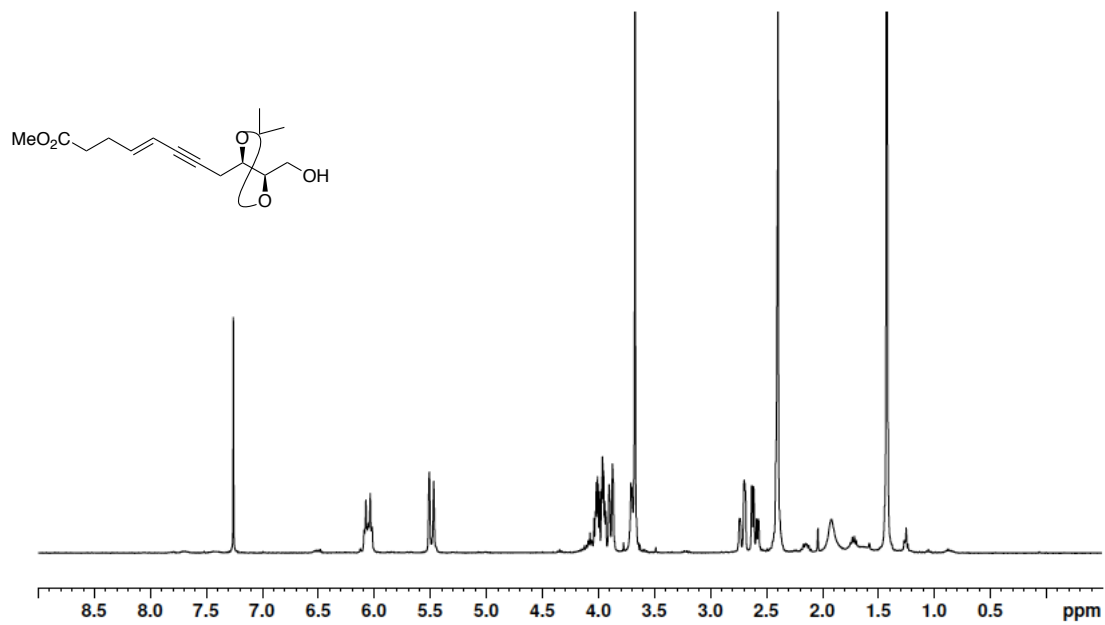


Figure A1.21 400 MHz $^1\text{H-NMR}$ and 100 MHz $^{13}\text{C-NMR}$ spectrum of **1.38** in CDCl_3

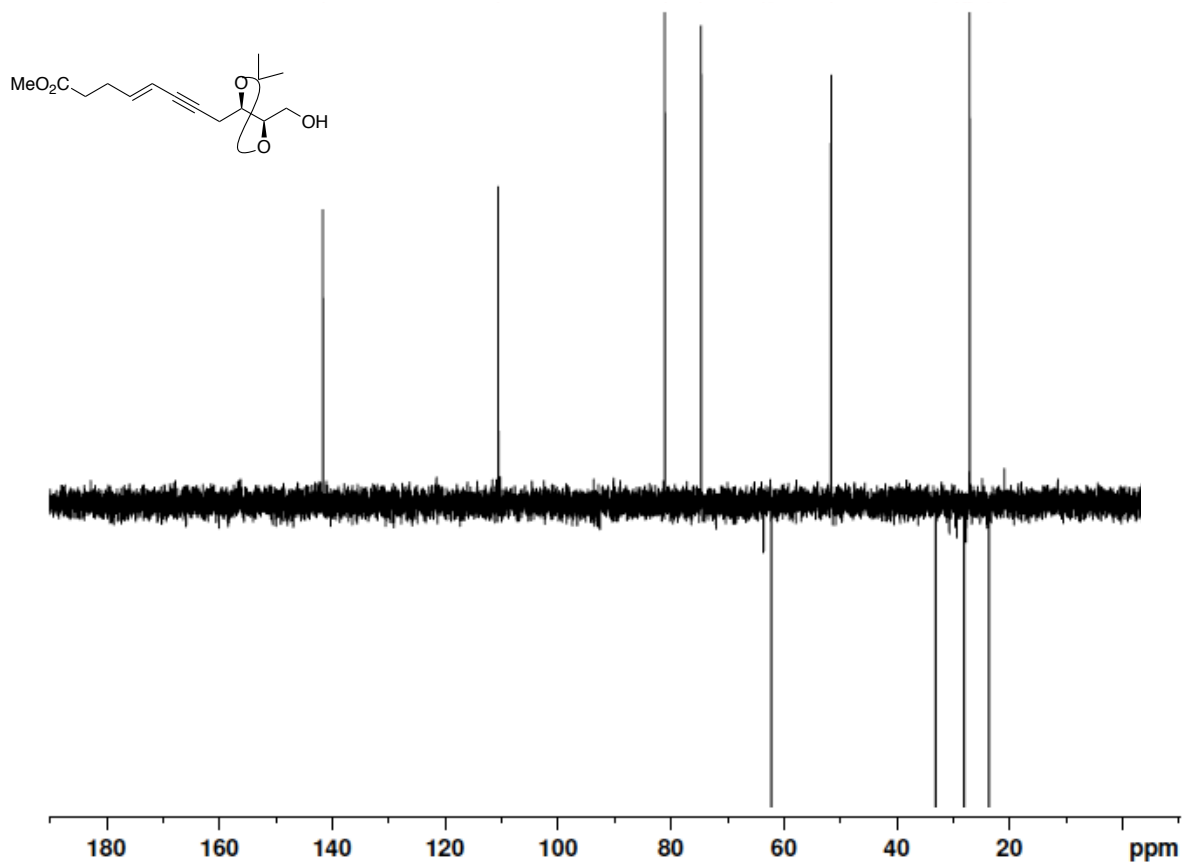


Figure A1.22 100 MHz DEPT 135 NMR spectrum of **1.38** in CDCl₃

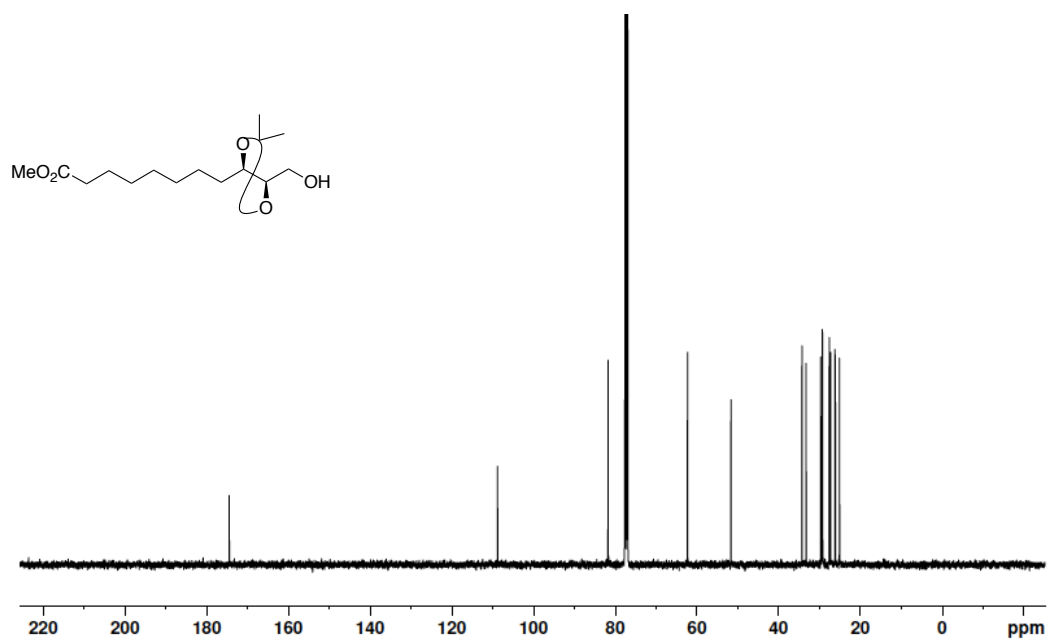
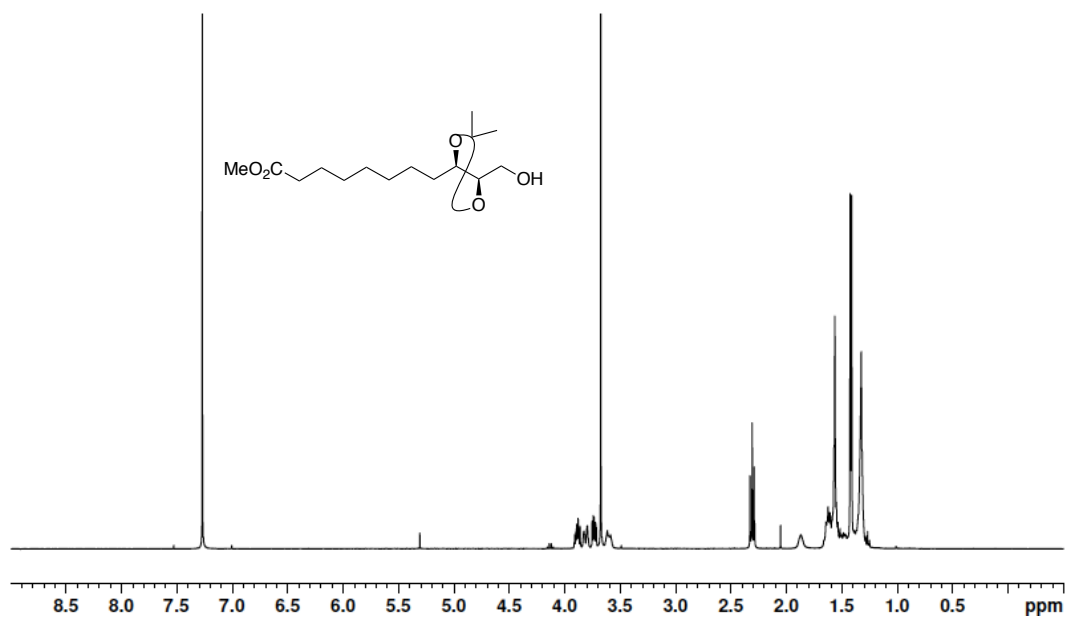


Figure A1.23 400 MHz ¹H-NMR and 100 MHz ¹³C-NMR spectrum of **1.39** in CDCl₃

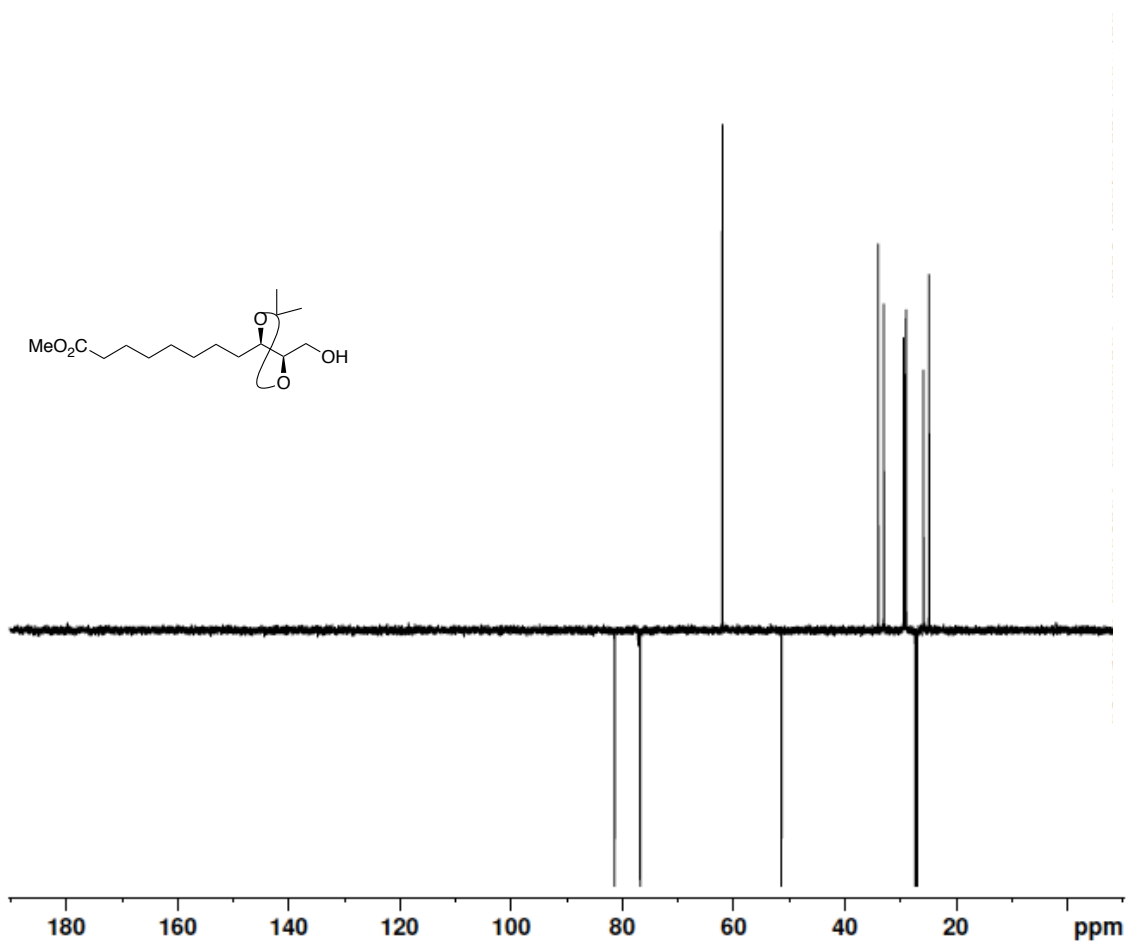


Figure A1.24 100 MHz DEPT 135 NMR spectrum of **1.39** in CDCl₃

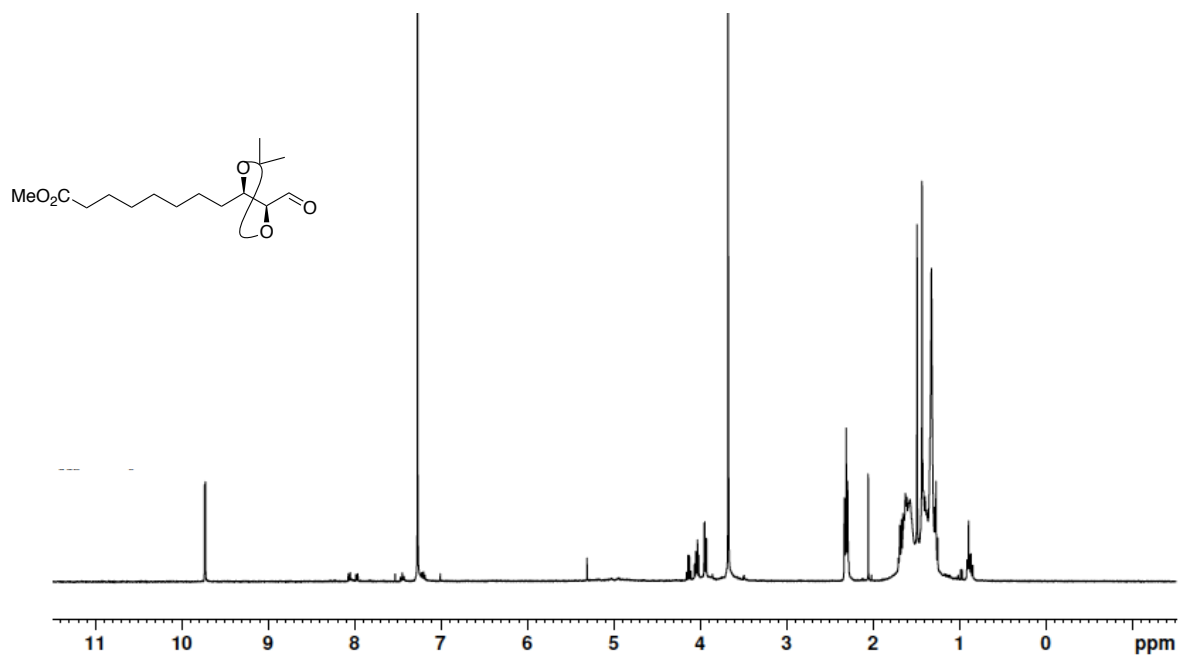


Figure A1.25 400 MHz $^1\text{H-NMR}$ spectrum of **1.42** in CDCl_3

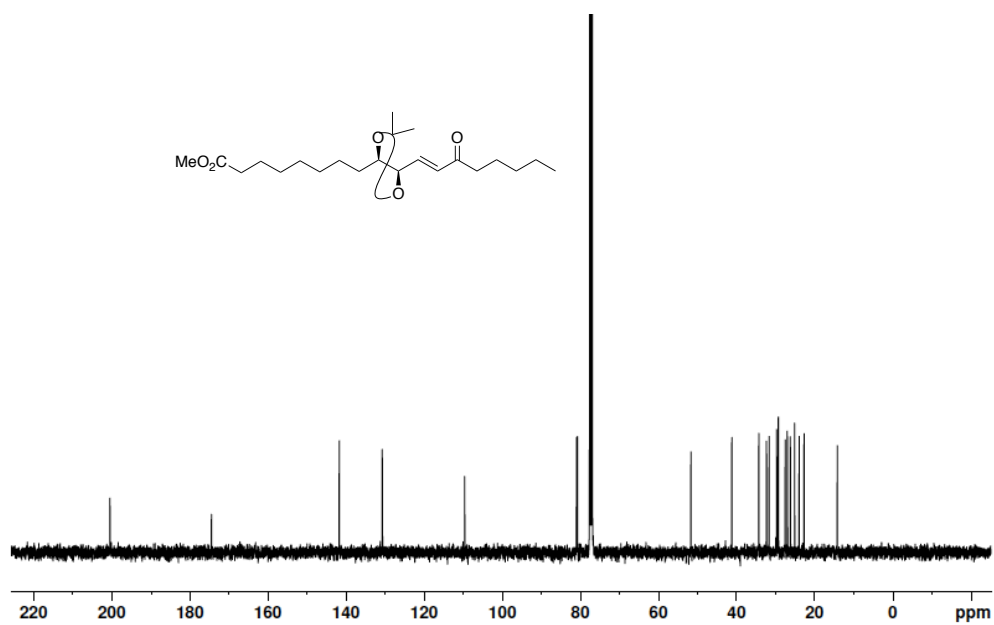
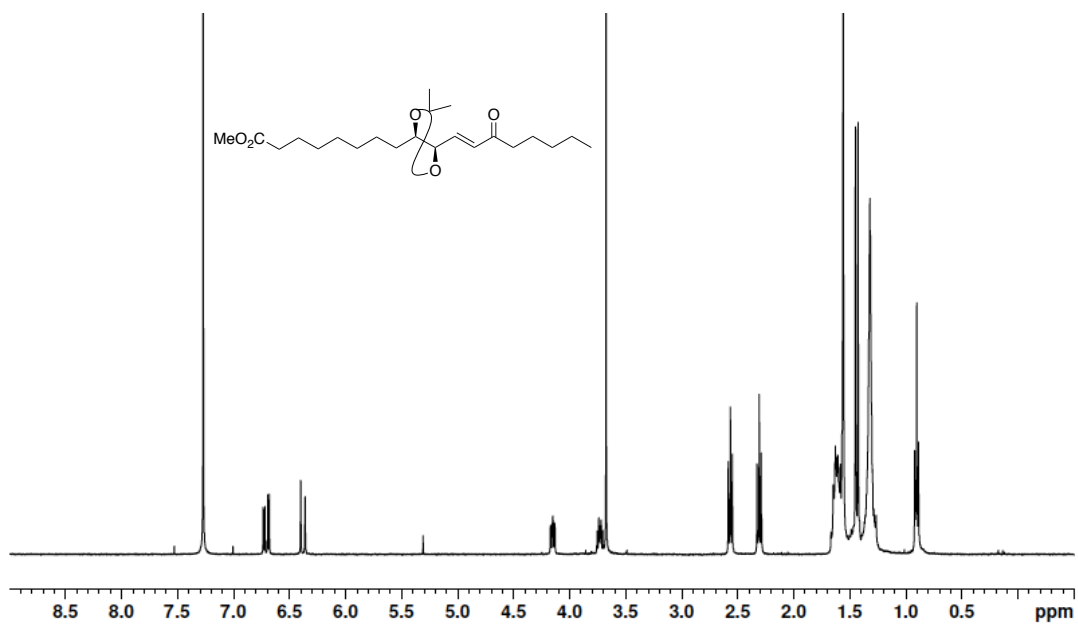


Figure A1.26 400 MHz ¹H-NMR and 100 MHz ¹³C-NMR spectrum of **1.43** in CDCl₃

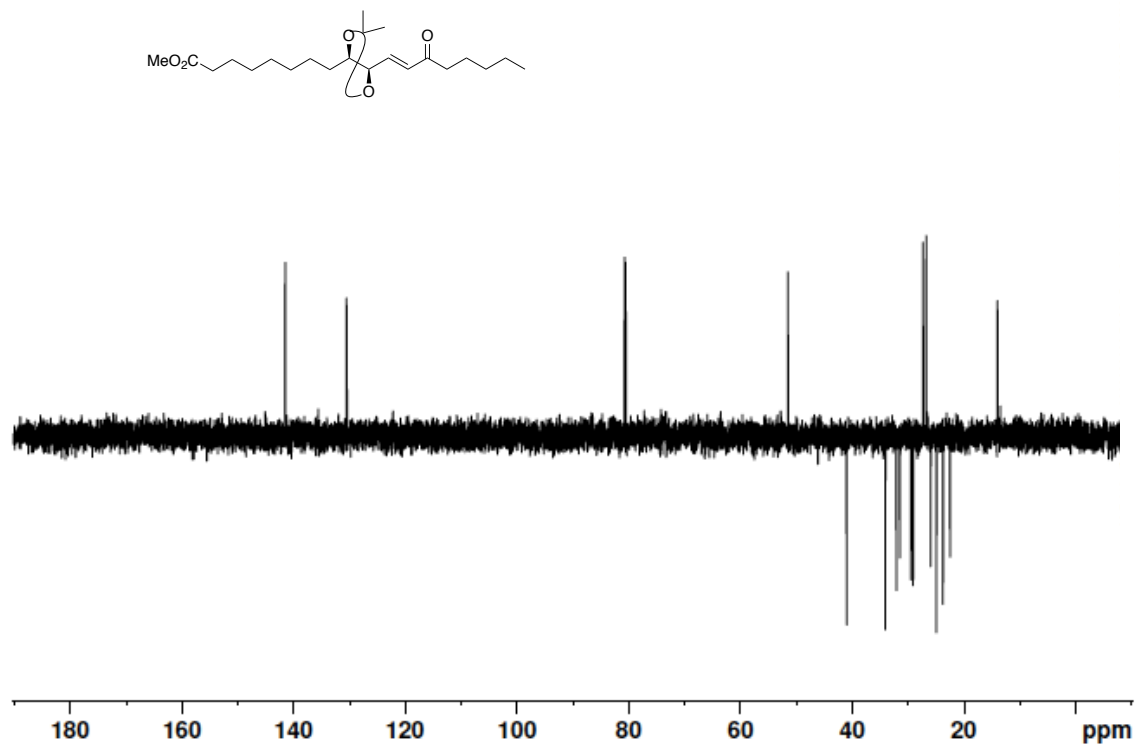


Figure A1.27 100 MHz DEPT 135 NMR spectrum of **1.43** in CDCl_3

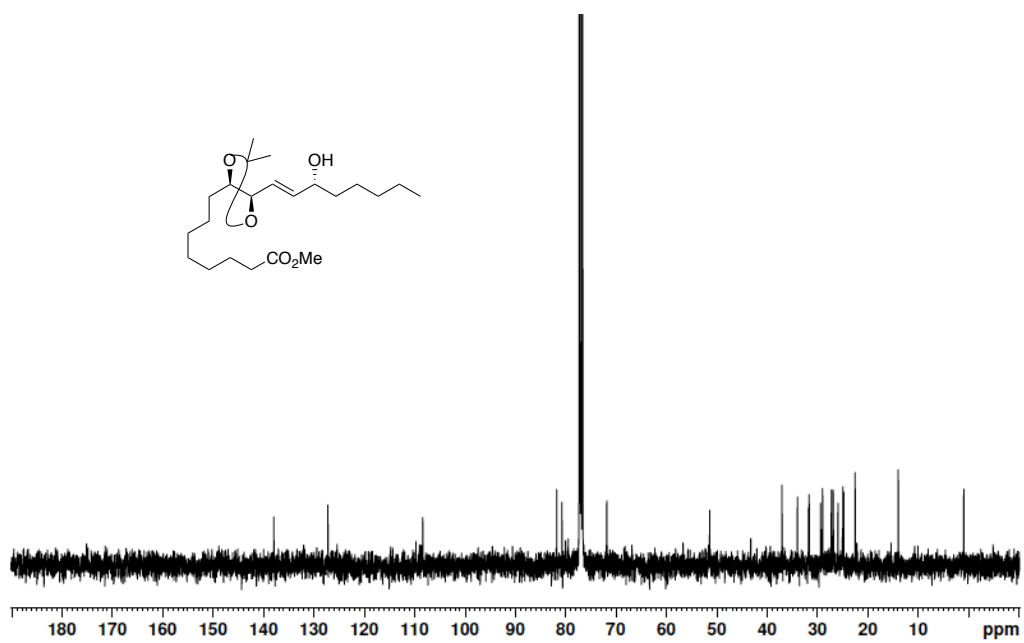
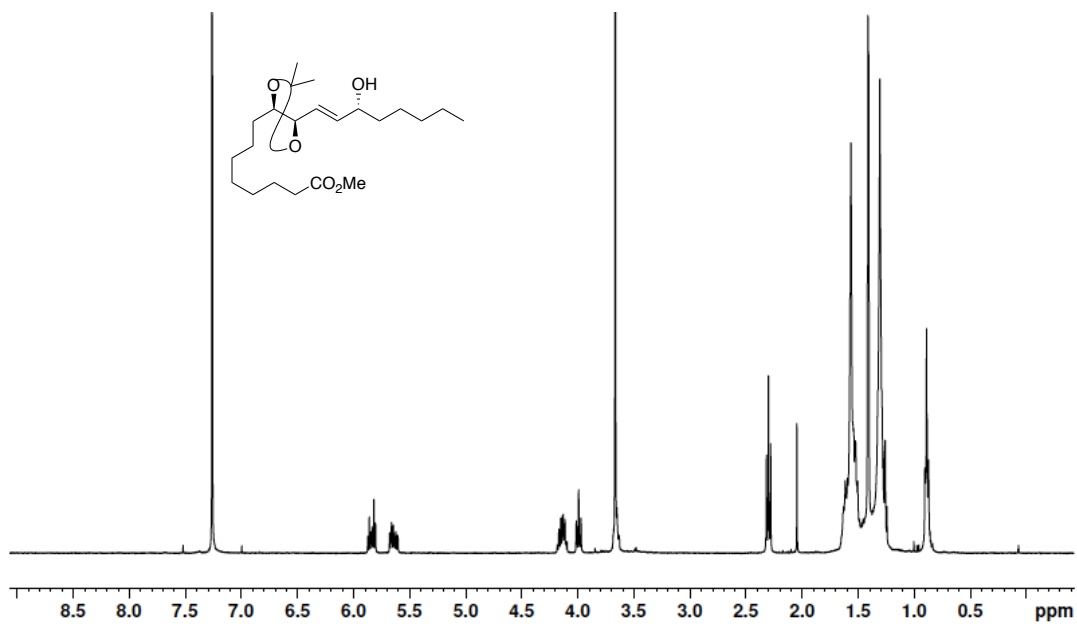


Figure A1.28 400 MHz $^1\text{H-NMR}$ and 100 MHz $^{13}\text{C-NMR}$ spectrum of **1.45** in CDCl_3

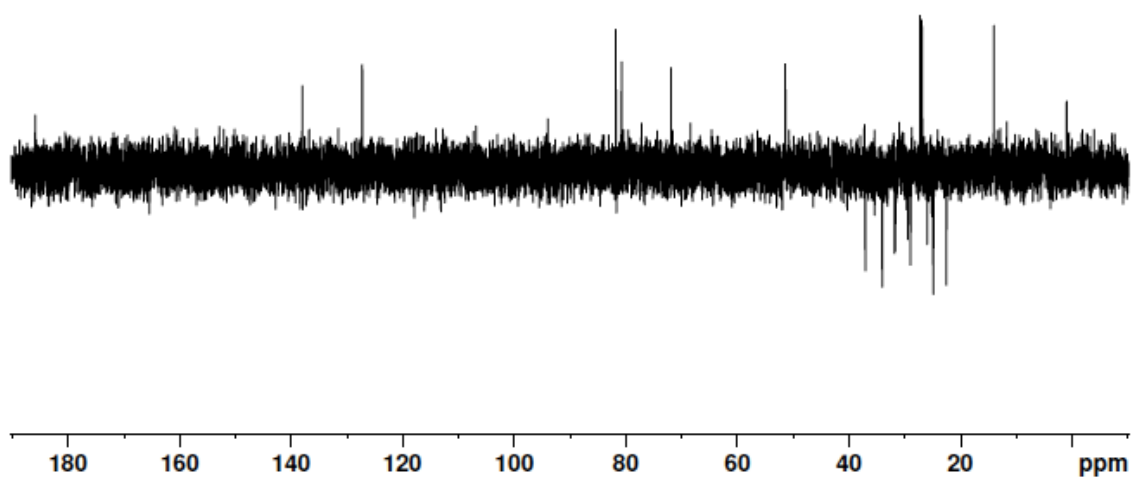
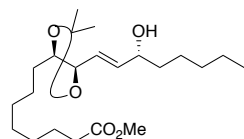


Figure A1.29 100 MHz DEPT 135 NMR spectrum of **1.45** in CDCl_3

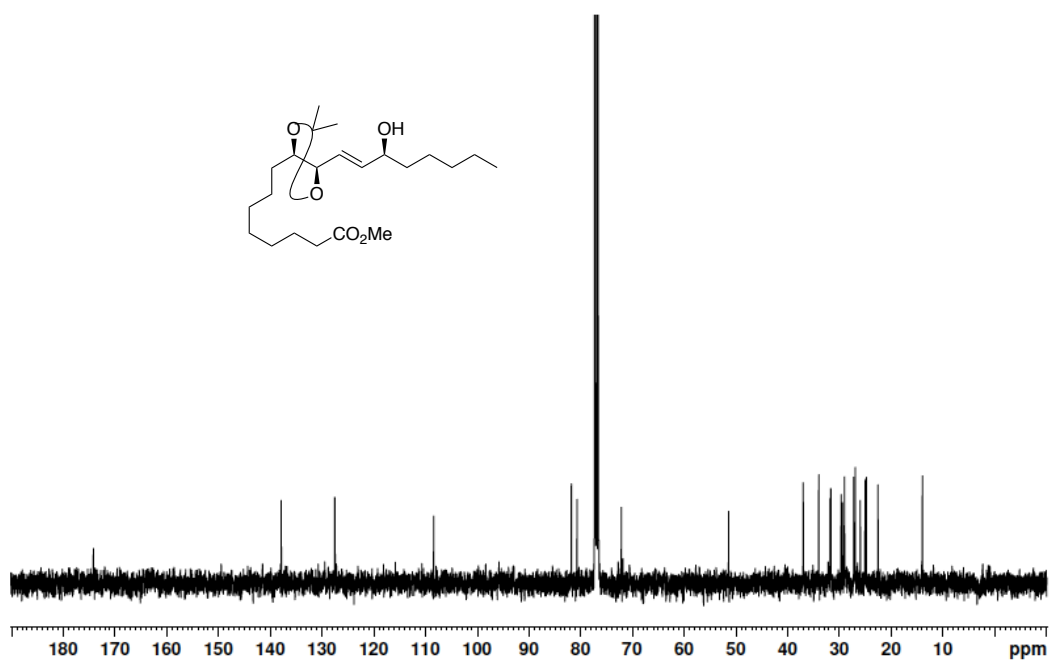
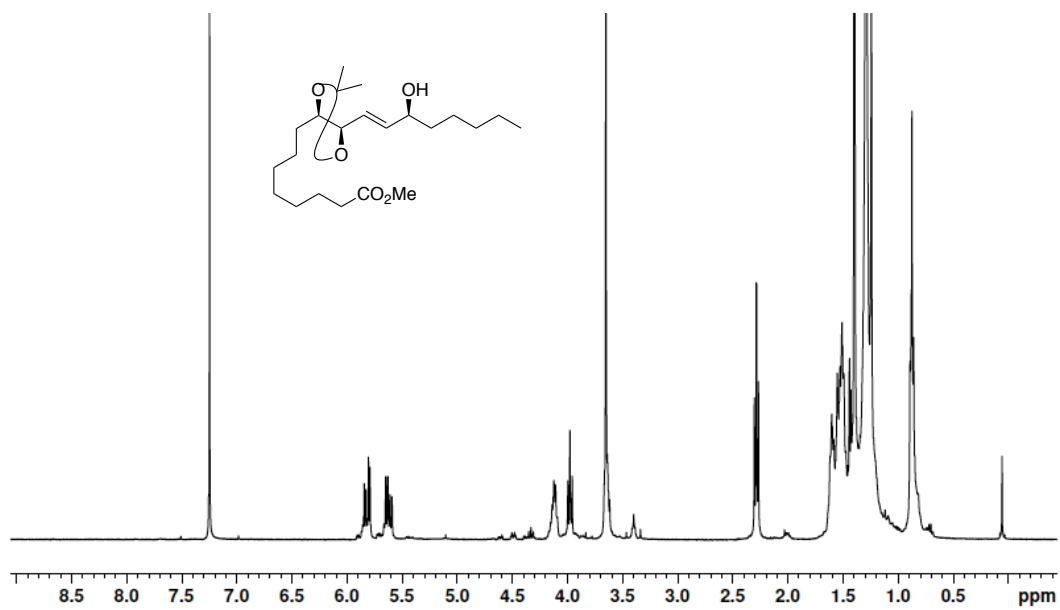


Figure A1.30 400 MHz $^1\text{H-NMR}$ and 100 MHz $^{13}\text{C-NMR}$ spectrum of **1.44** in CDCl_3

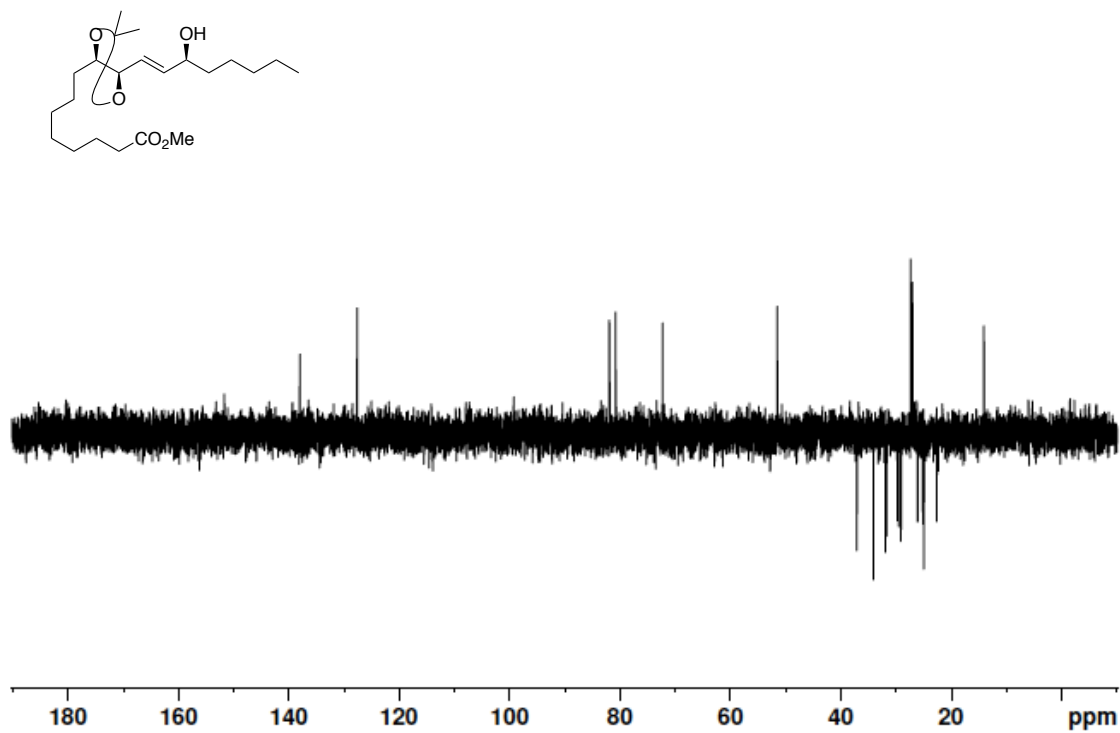


Figure A1.31 100 MHz DEPT 135 NMR spectrum of **1.44** in CDCl₃

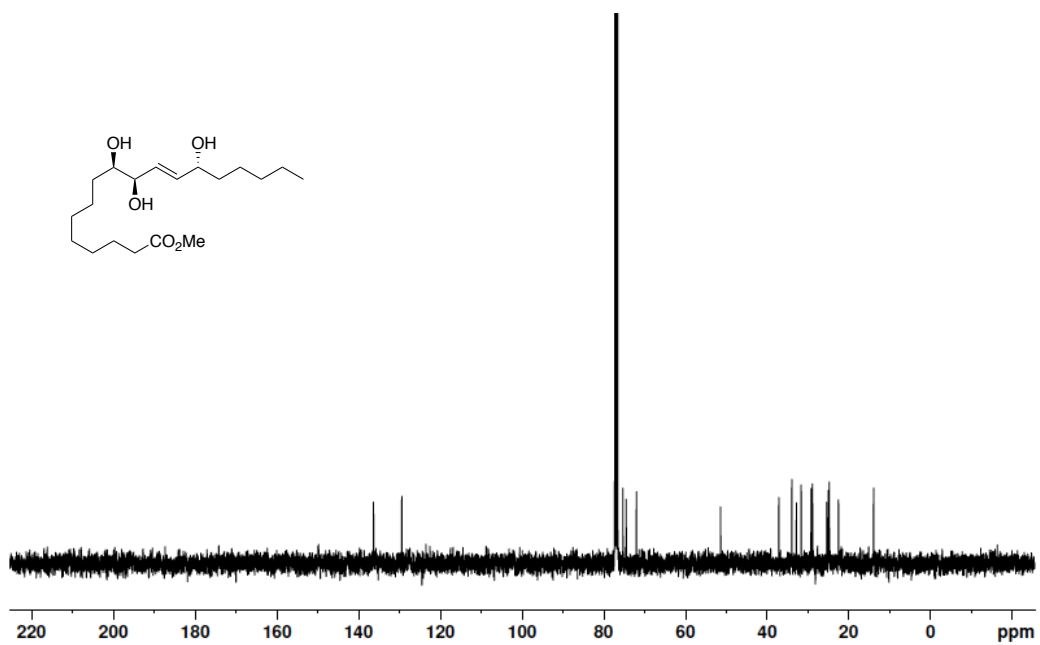
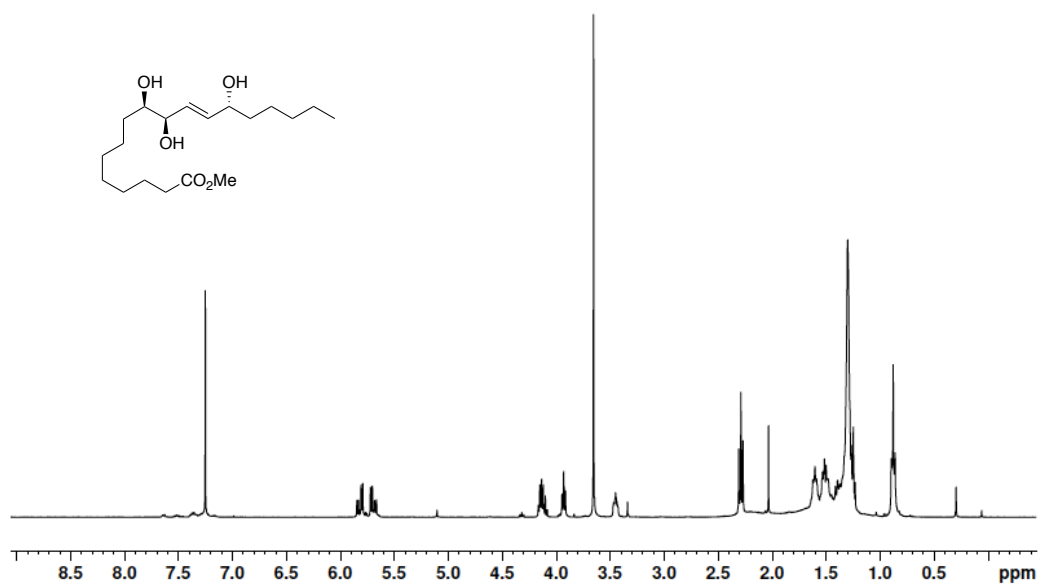


Figure A1.32 400 MHz $^1\text{H-NMR}$ and 100 MHz $^{13}\text{C-NMR}$ spectrum of **1.47** in CDCl_3

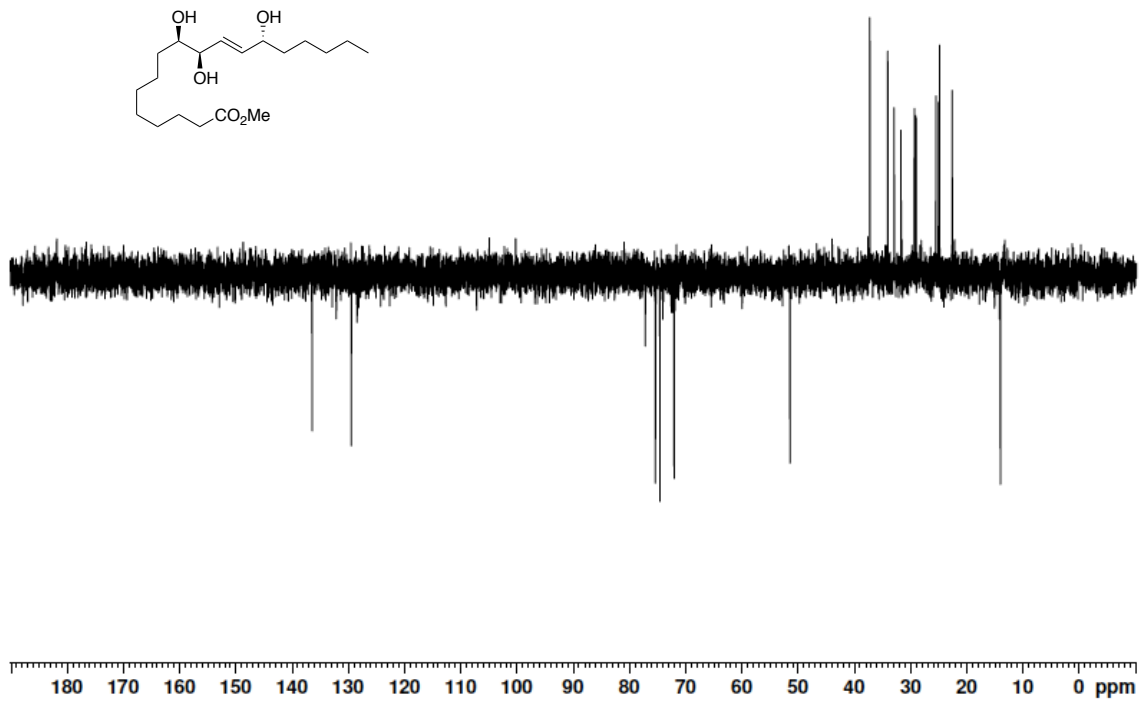


Figure A1.33 100 MHz DEPT 135 NMR spectrum of **1.47** in CDCl_3

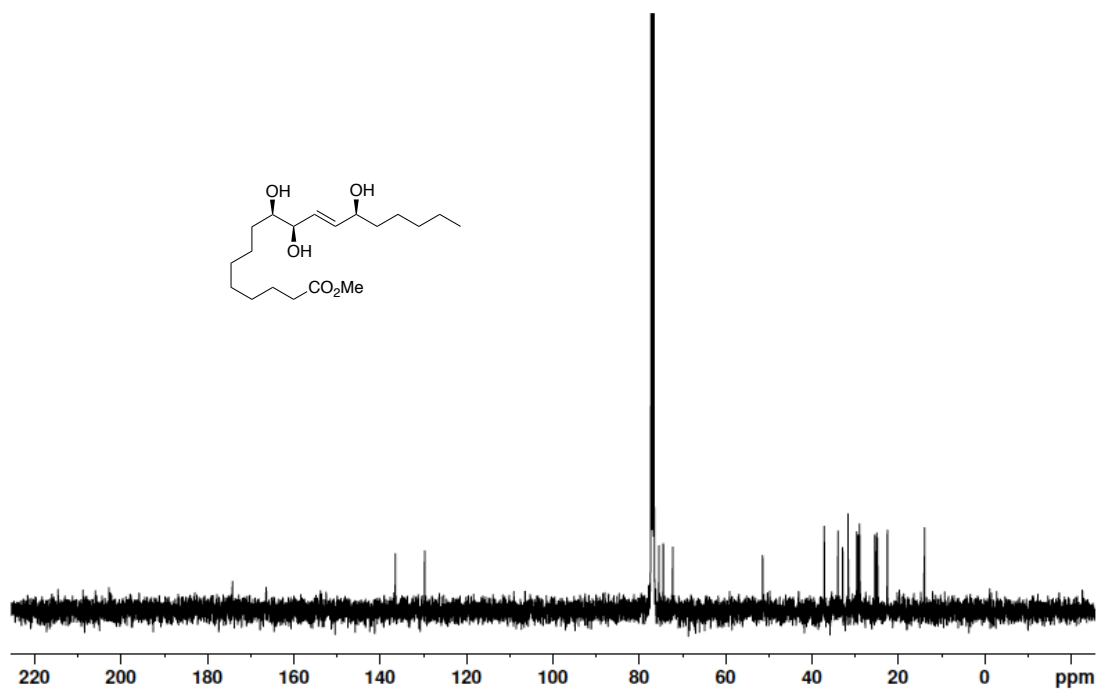
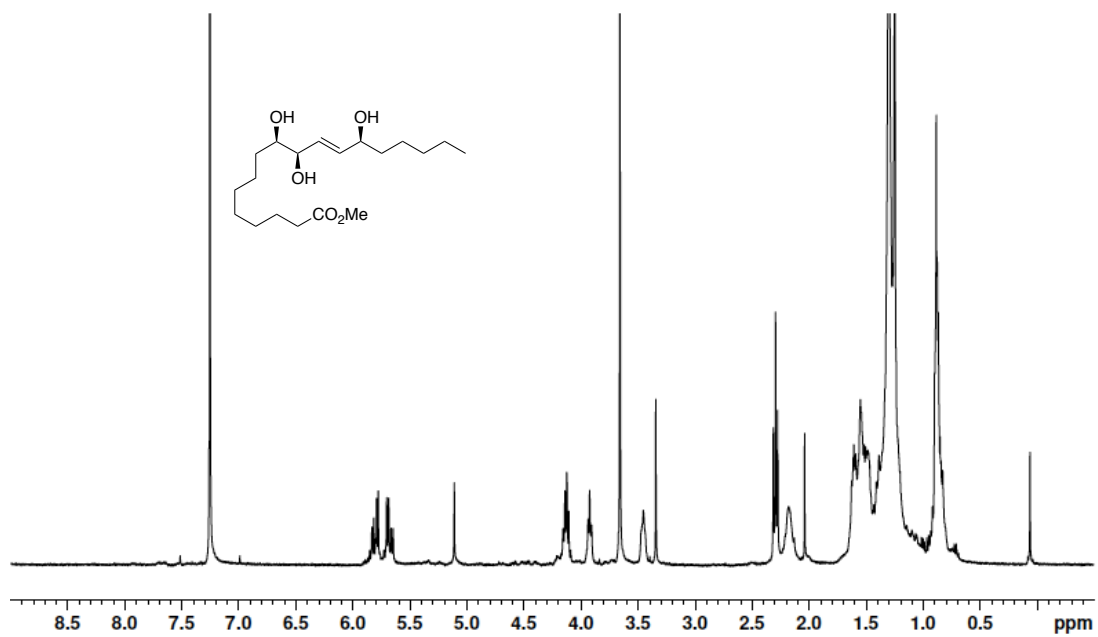


Figure A1.34 400 MHz $^1\text{H-NMR}$ and 100 MHz $^{13}\text{C-NMR}$ spectrum of **1.46** in CDCl_3

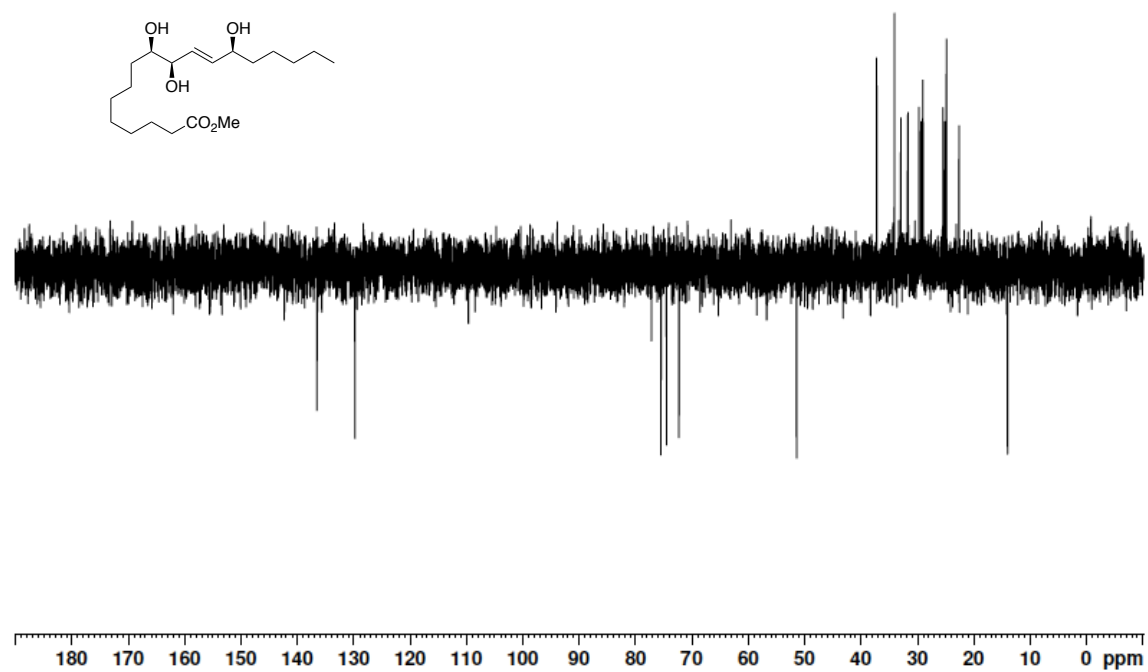


Figure A1.35 100 MHz DEPT 135 NMR spectrum of **1.46** in CDCl_3

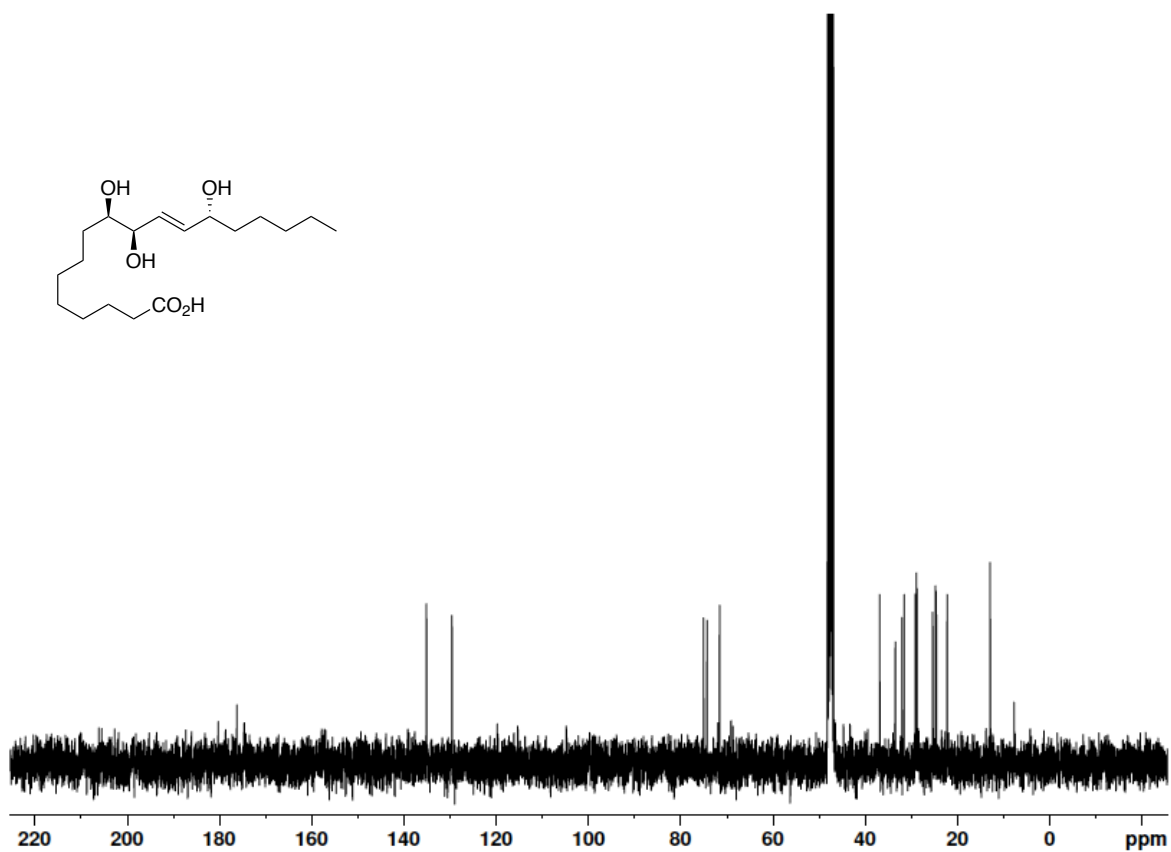
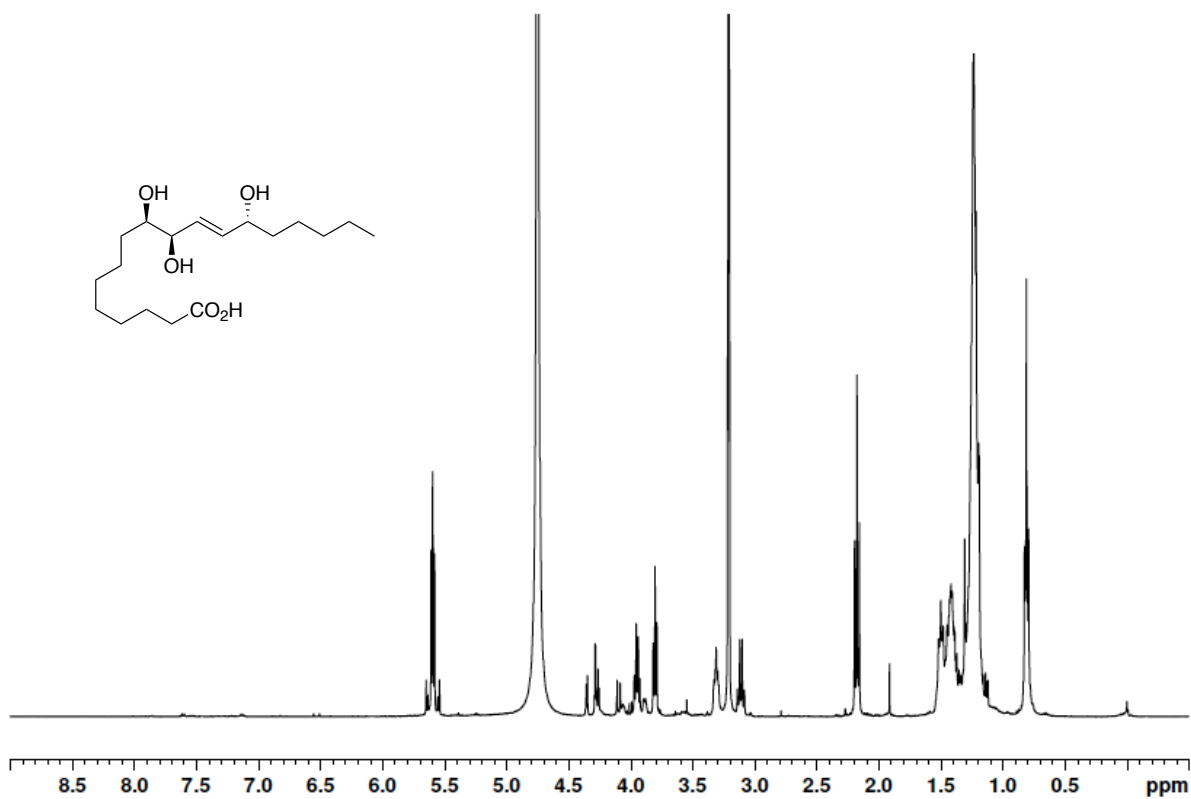


Figure A1.36 400 MHz $^1\text{H-NMR}$ and 100 MHz $^{13}\text{C-NMR}$ spectrum of **1.1** in MeOD

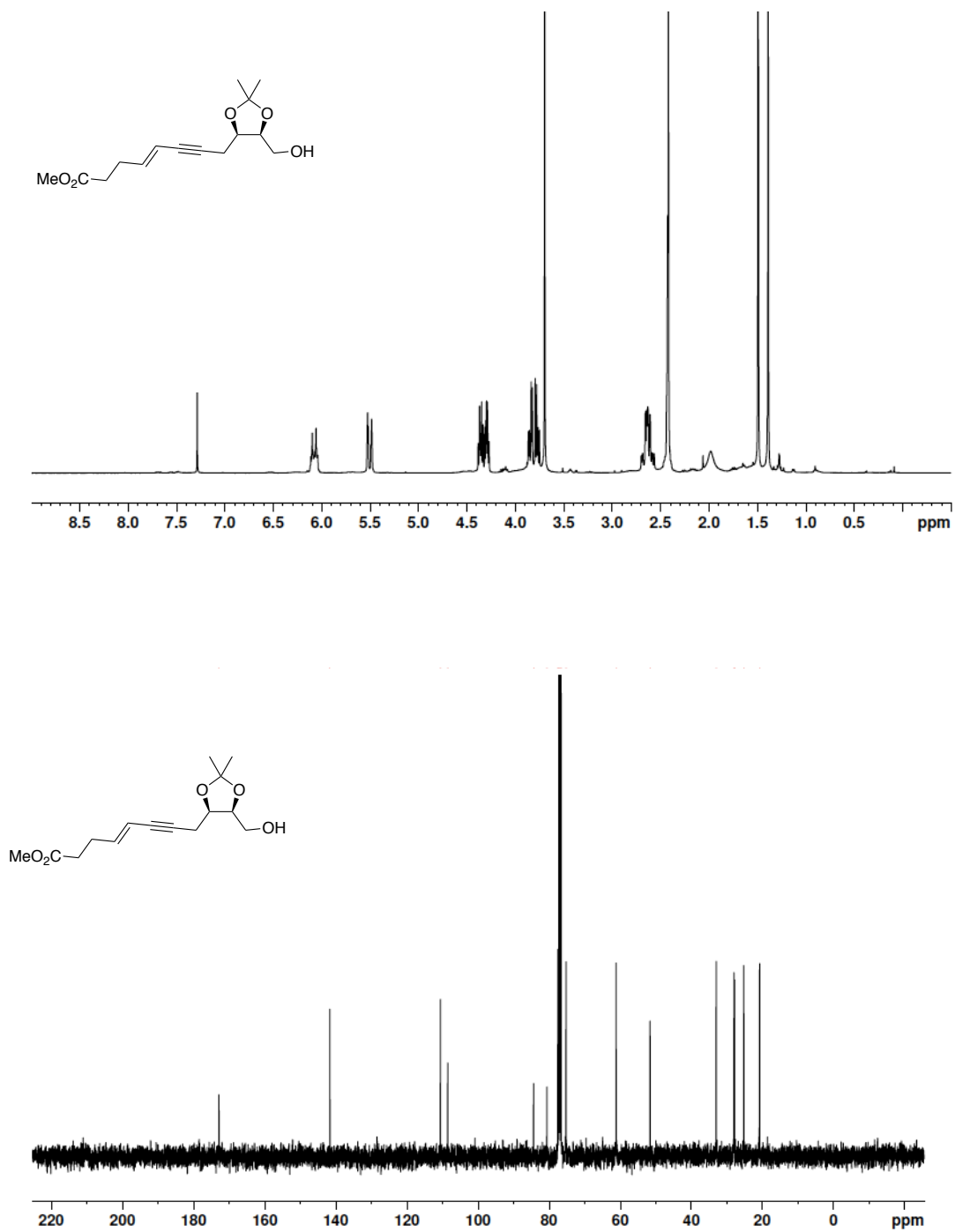


Figure A1.37 400 MHz $^1\text{H-NMR}$ and 100 MHz $^{13}\text{C-NMR}$ spectrum of **1.48** in CDCl_3

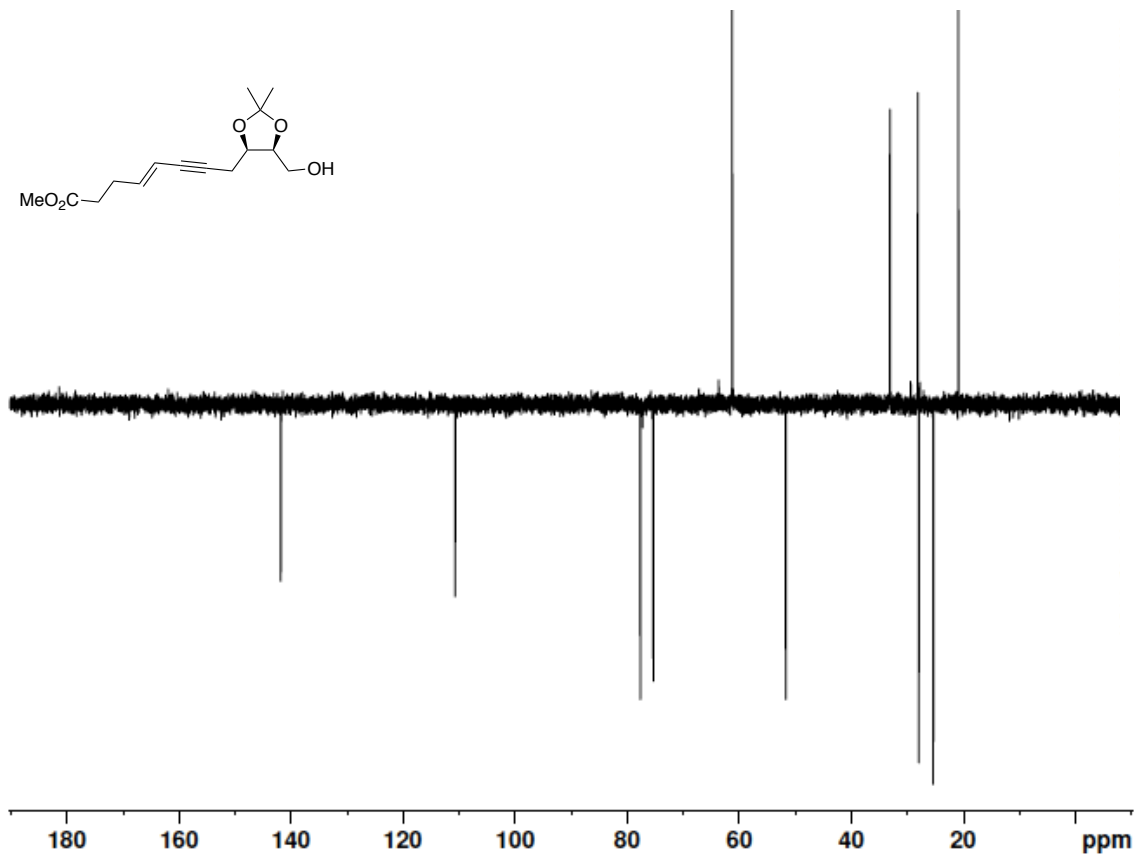


Figure A1.38 100 MHz DEPT 135 NMR spectrum of **1.48** in CDCl_3

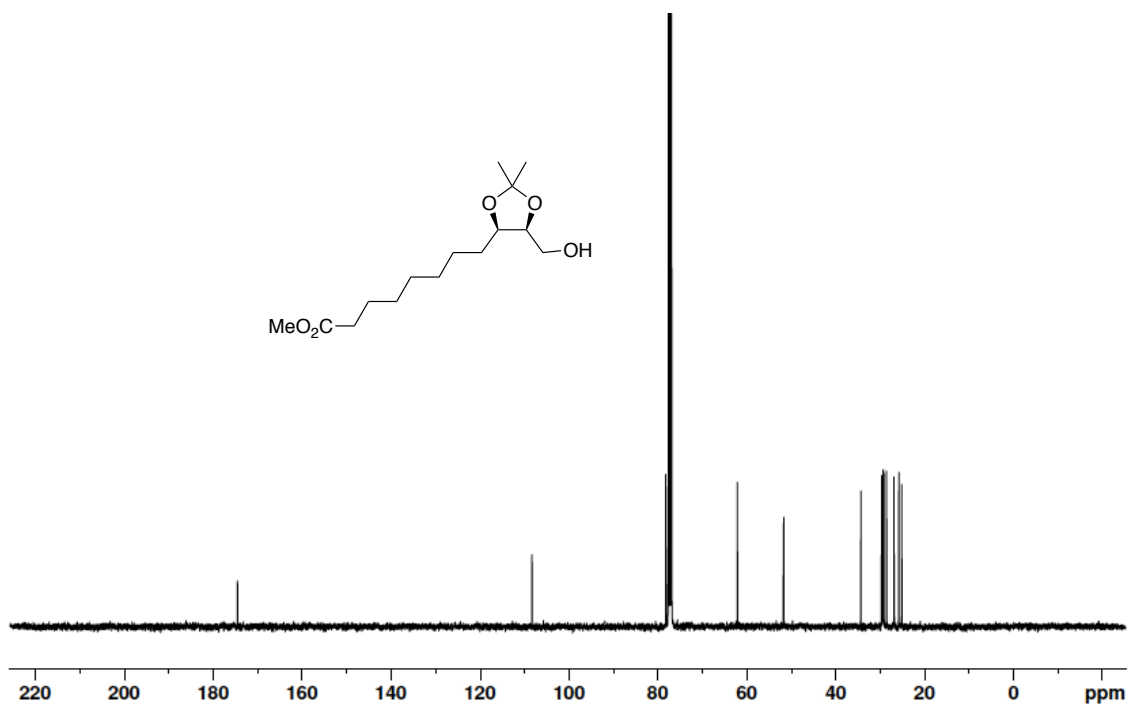
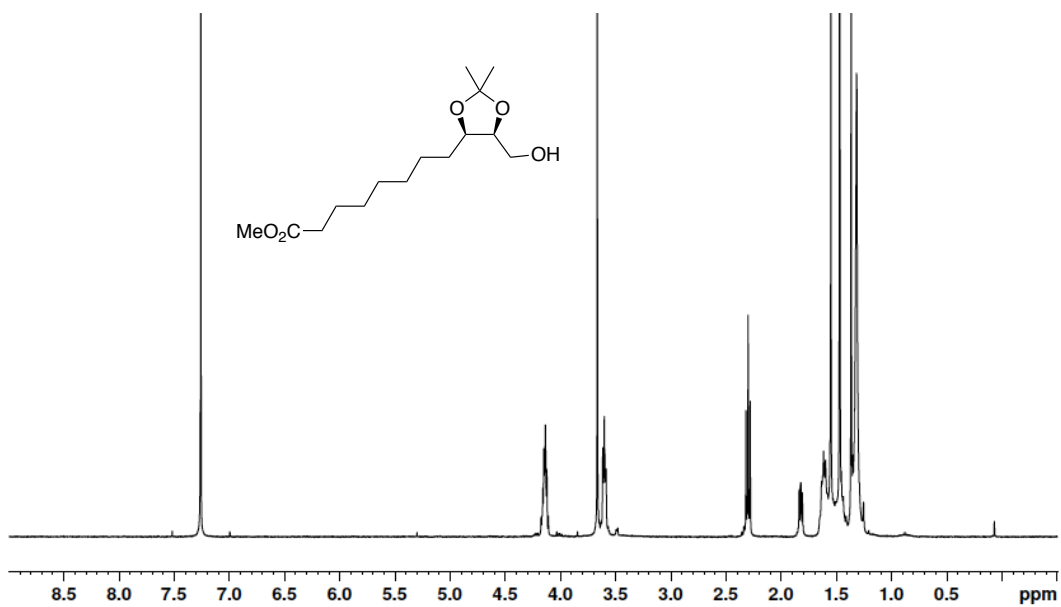


Figure A1.39 400 MHz $^1\text{H-NMR}$ and 100 MHz $^{13}\text{C-NMR}$ spectrum of **1.49** in CDCl_3

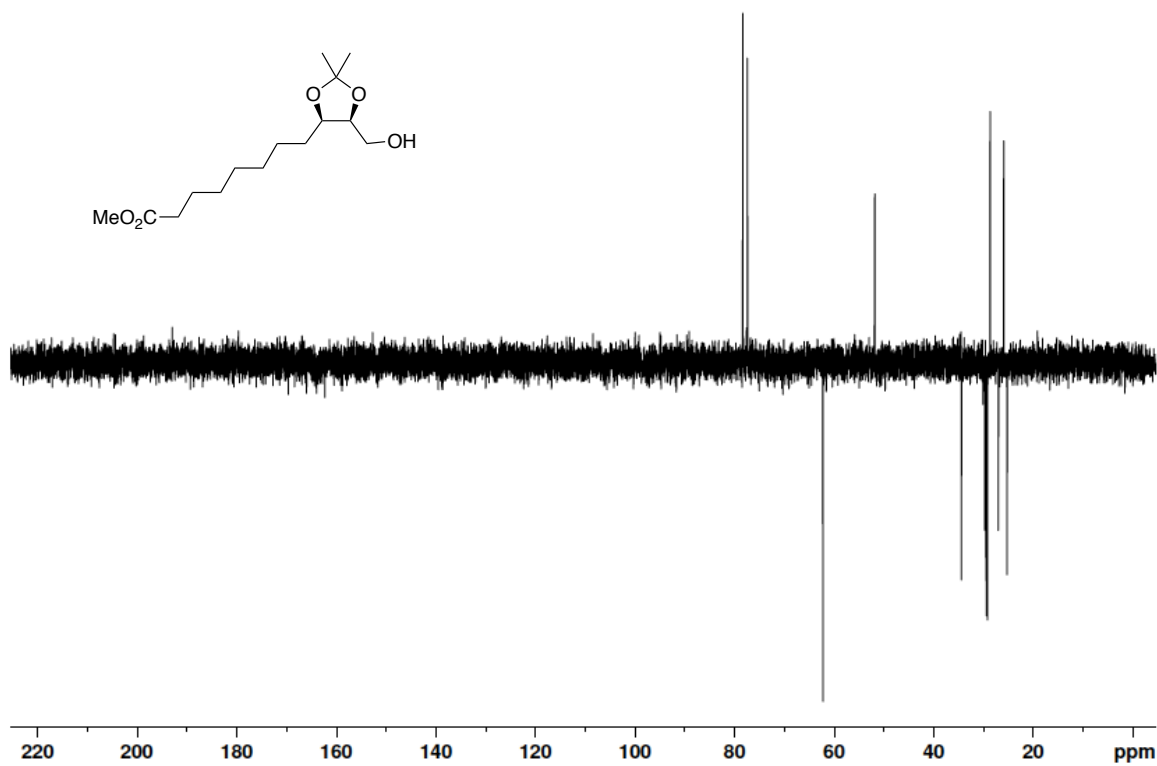


Figure A1.40 100 MHz DEPT 135 NMR spectrum of **1.49** in CDCl₃

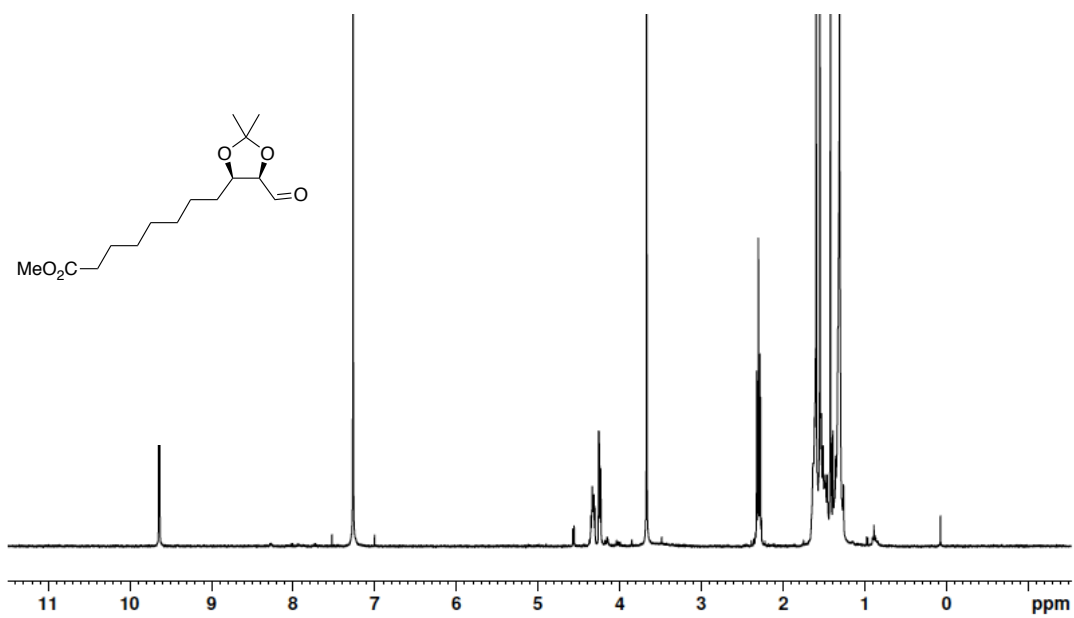


Figure A1.41 400 MHz ¹H-NMR spectrum of **1.50** in CDCl₃

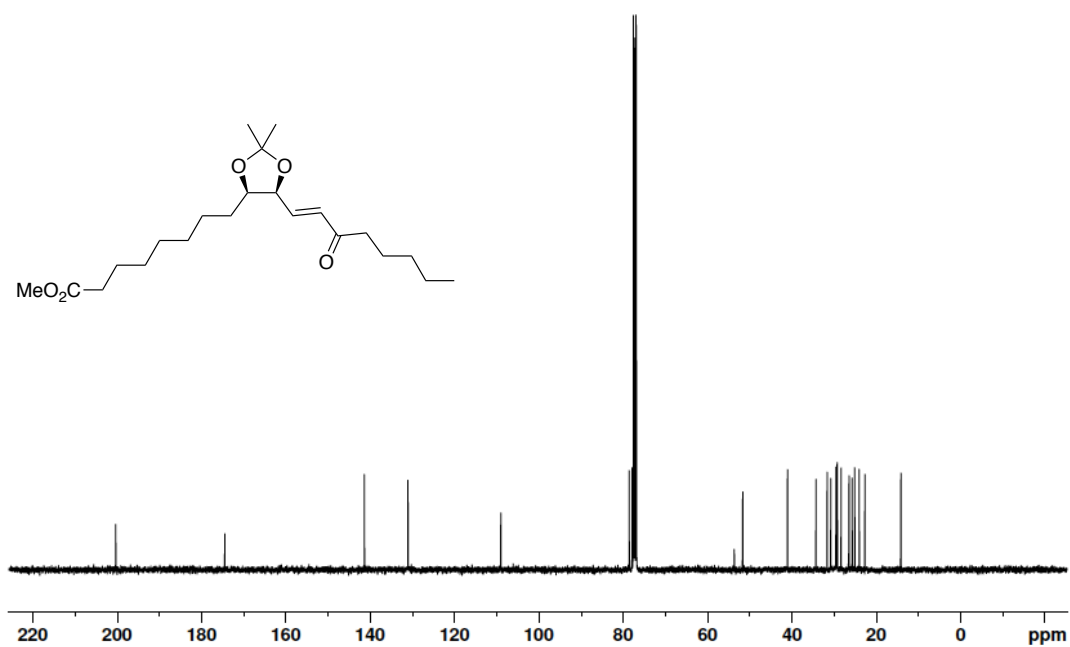
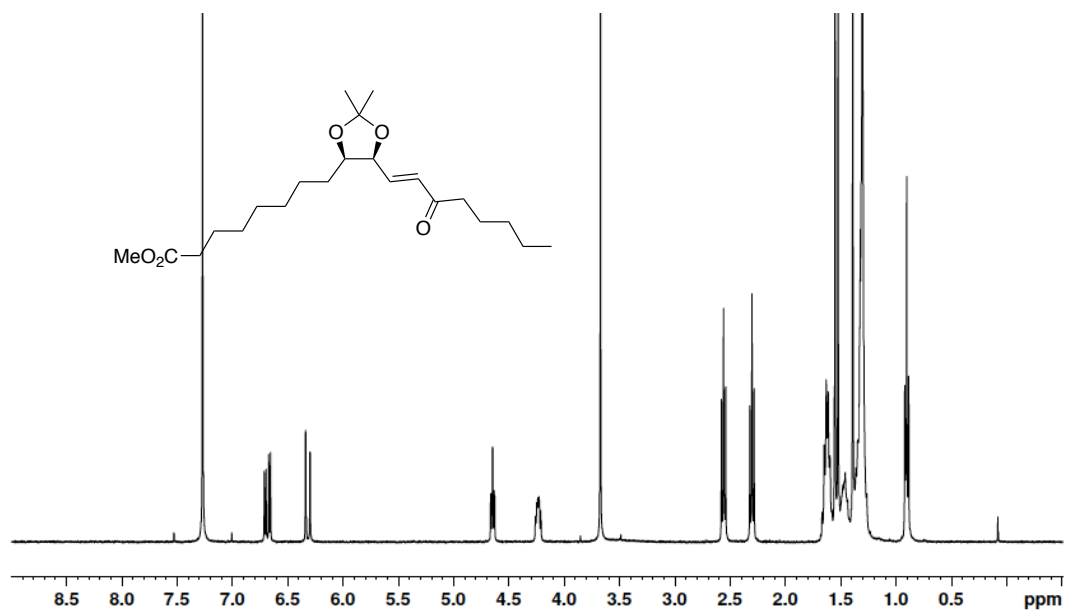


Figure A1.42 400 MHz $^1\text{H-NMR}$ and 100 MHz $^{13}\text{C-NMR}$ spectrum of **1.51** in CDCl_3

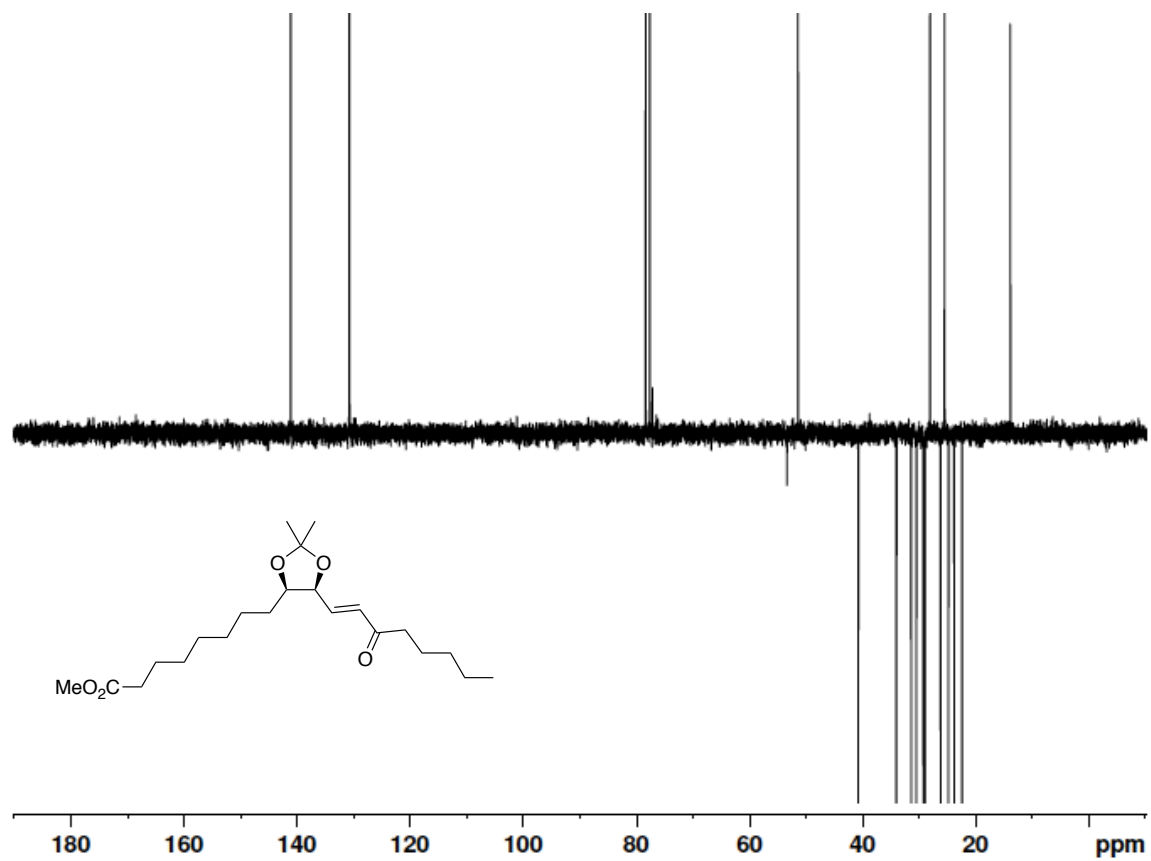


Figure A1.43 100 MHz DEPT 135 NMR spectrum of **1.51** in CDCl₃

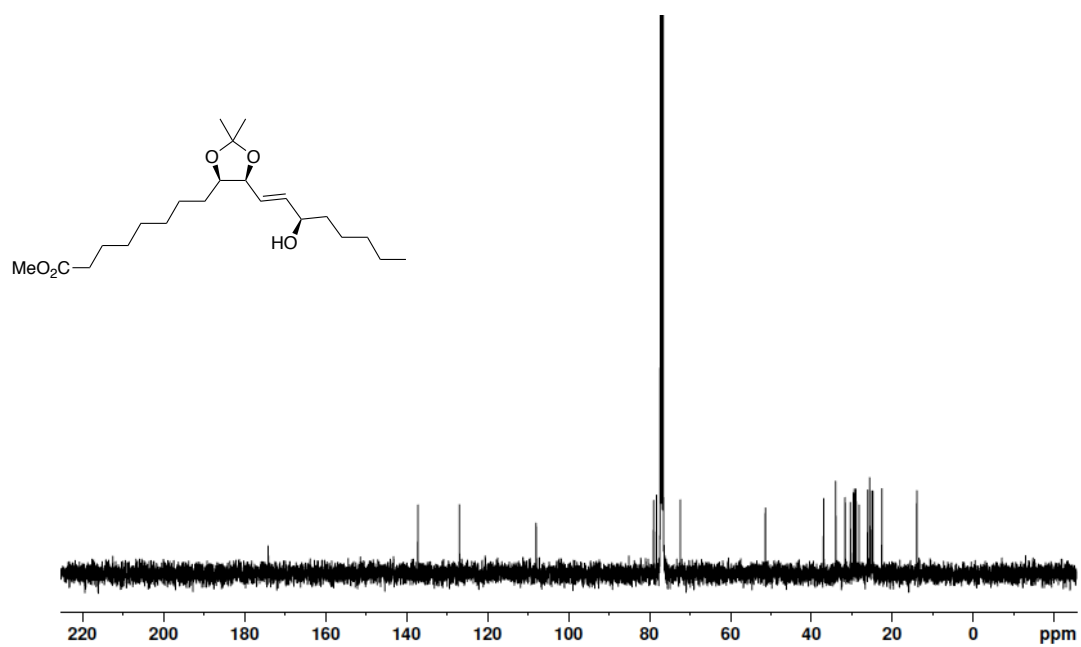
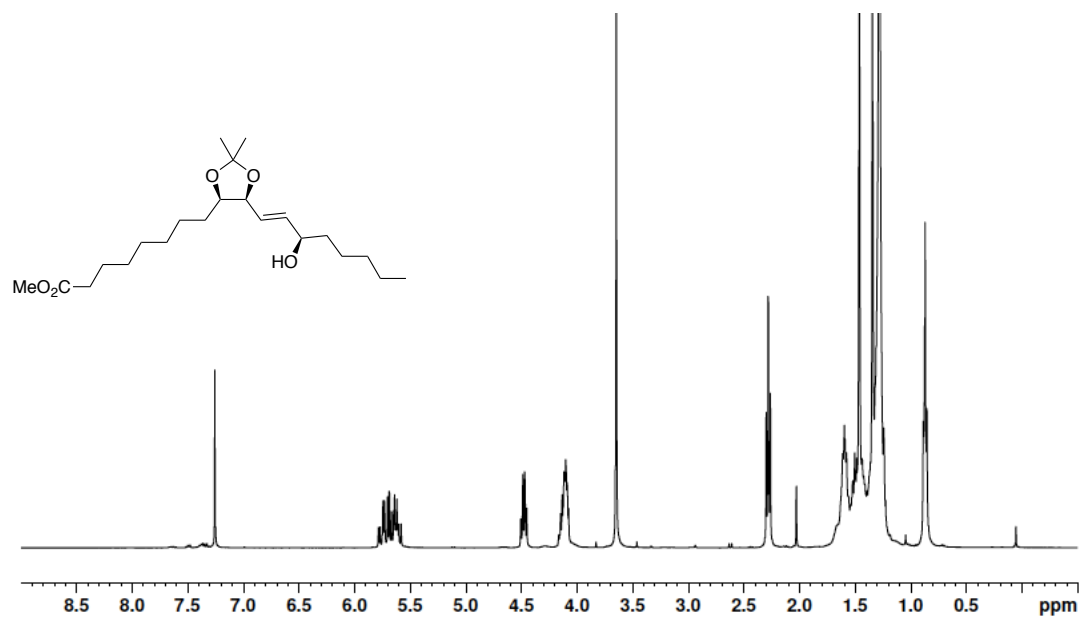


Figure A1.44 400 MHz ¹H-NMR and 100 MHz ¹³C-NMR spectrum of **1.53** in CDCl₃

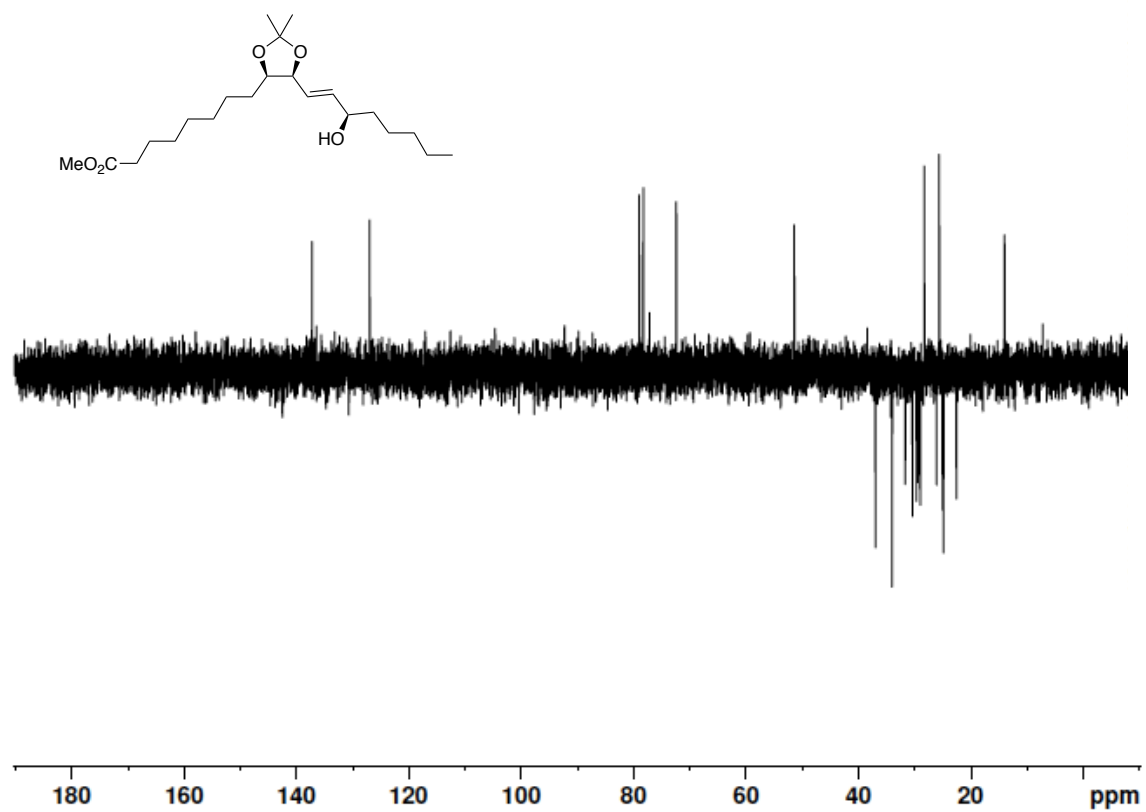


Figure A1.45 100 MHz DEPT 135 NMR spectrum of **1.53** in CDCl₃

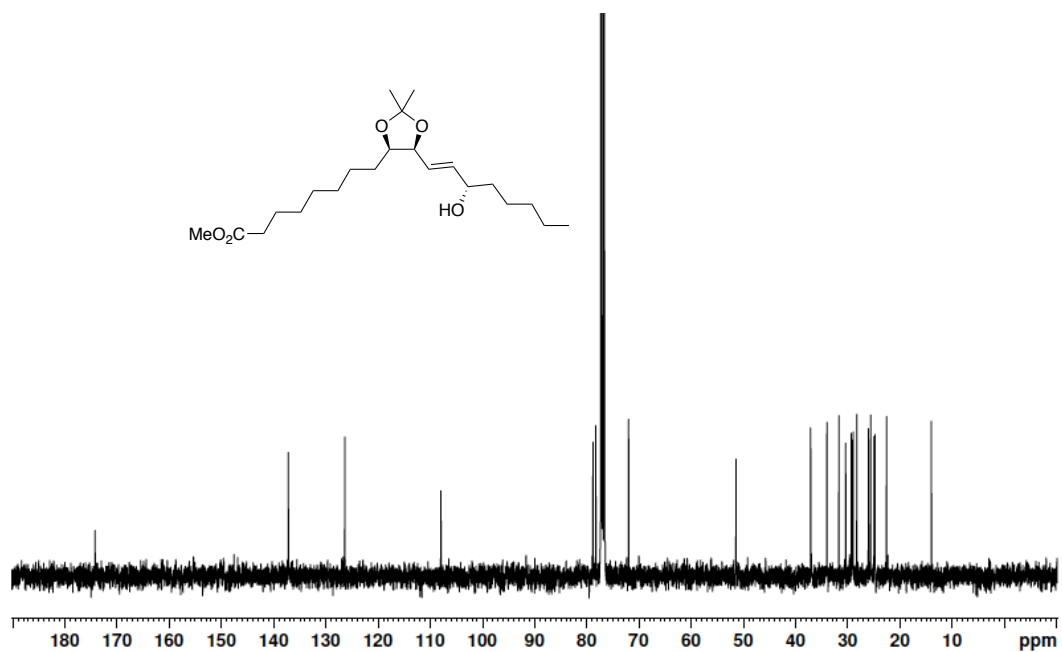
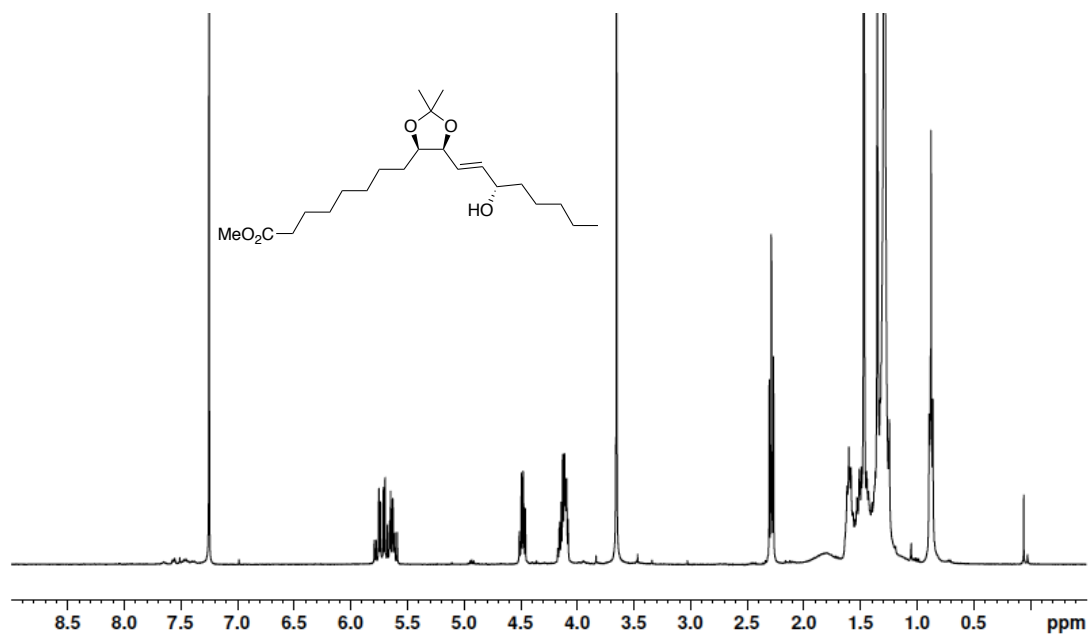


Figure A1.46 400 MHz $^1\text{H-NMR}$ and 100 MHz $^{13}\text{C-NMR}$ spectrum of **1.52** in CDCl_3

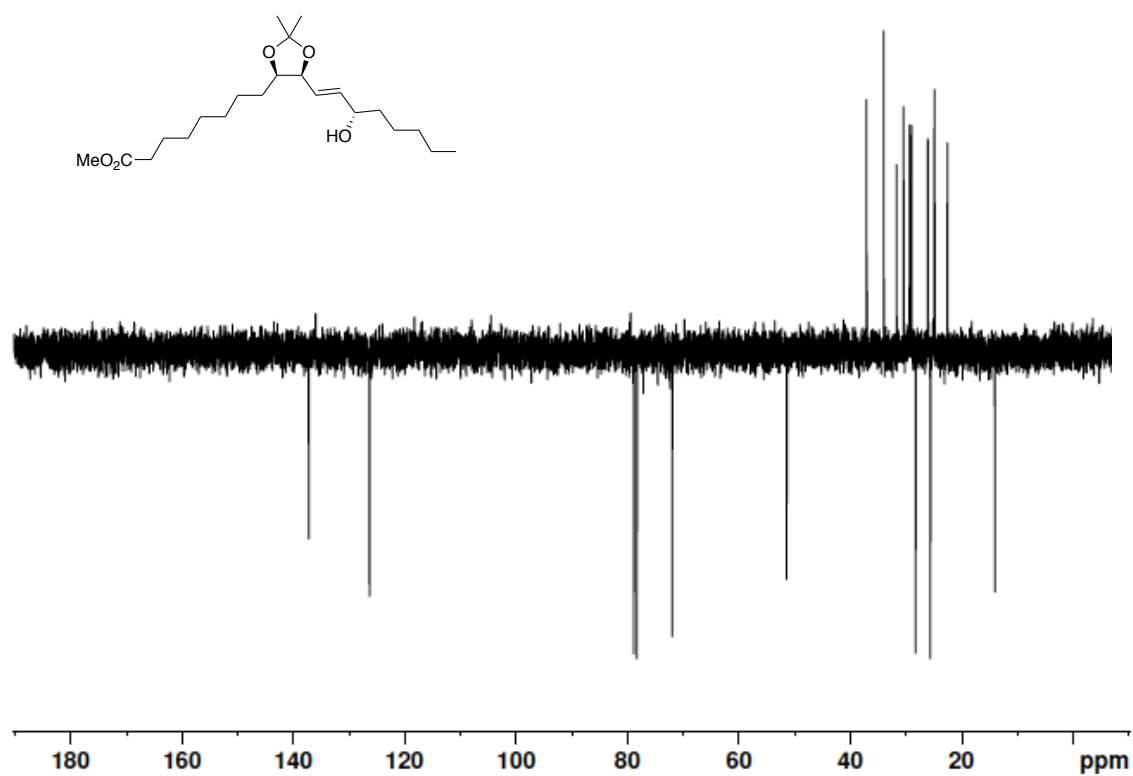


Figure A1.47 100 MHz DEPT 135 NMR spectrum of **1.52** in CDCl₃

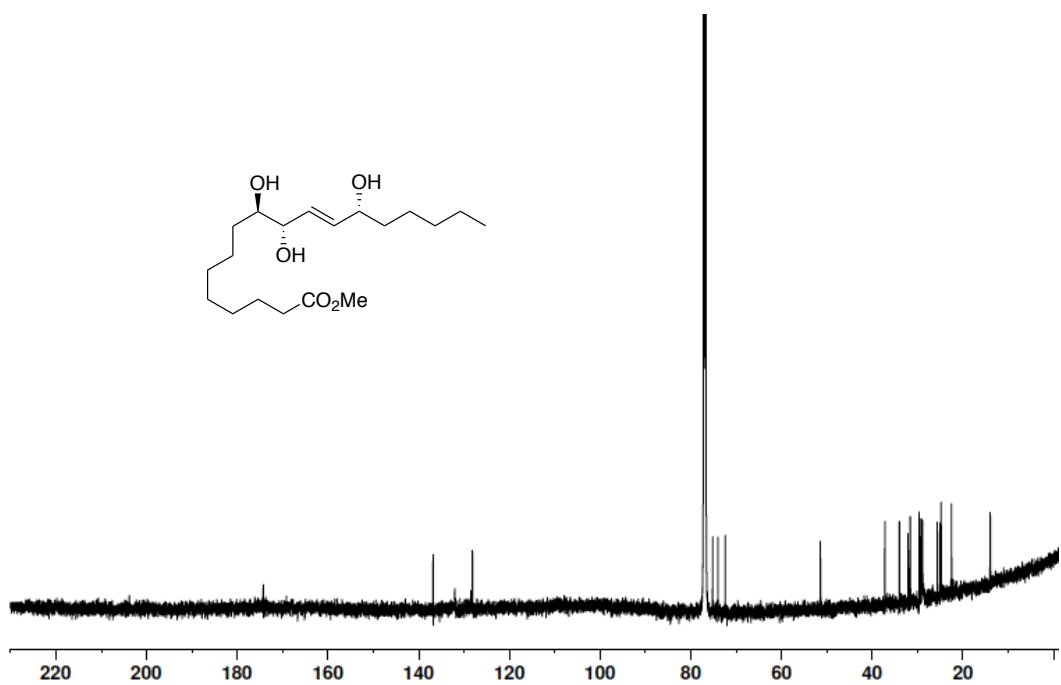
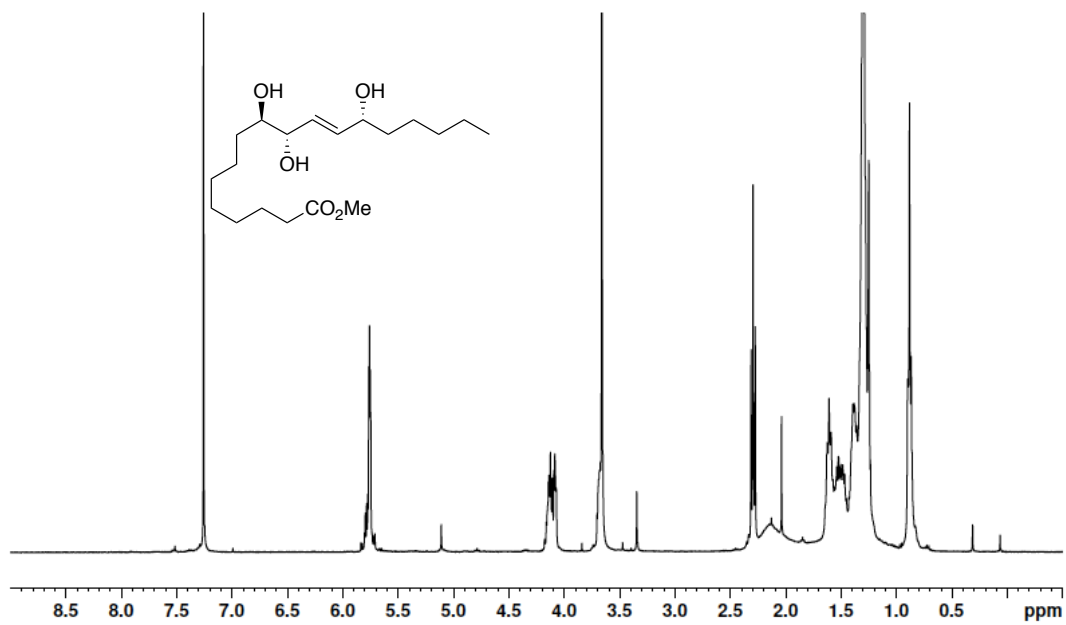


Figure A1.48 400 MHz $^1\text{H-NMR}$ and 100 MHz $^{13}\text{C-NMR}$ spectrum of **1.55** in CDCl_3

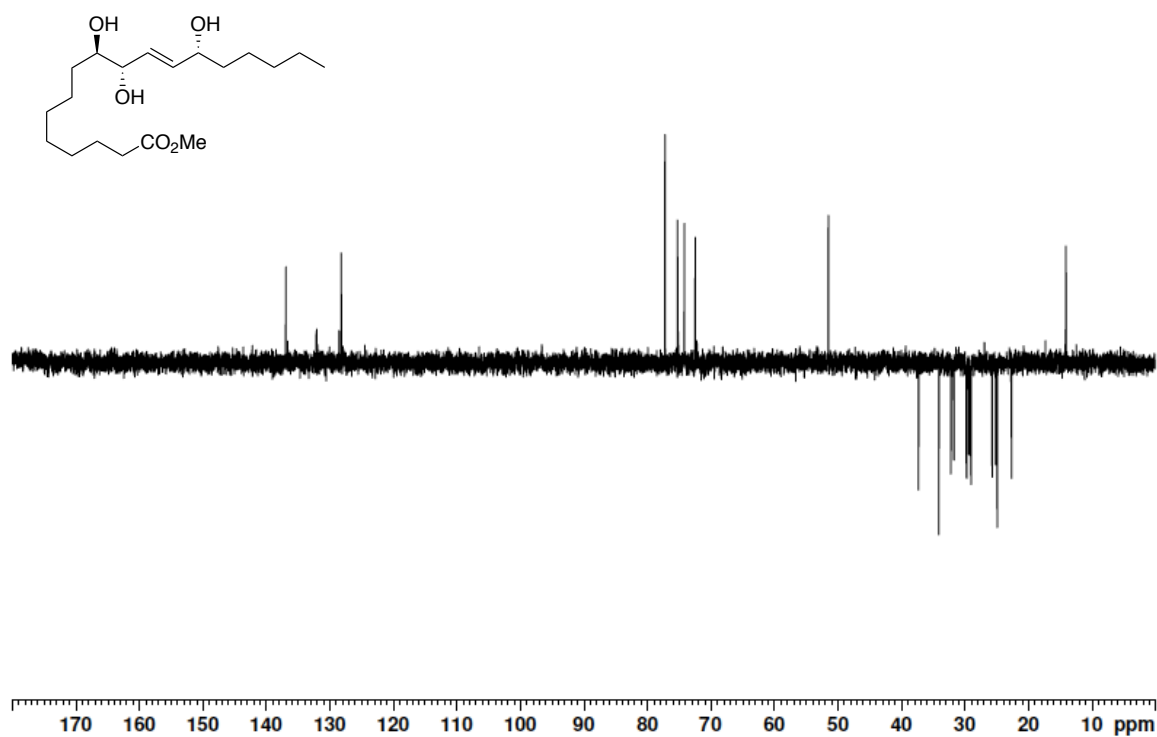


Figure A1.49 100 MHz DEPT 135 NMR spectrum of **1.55** in CDCl_3

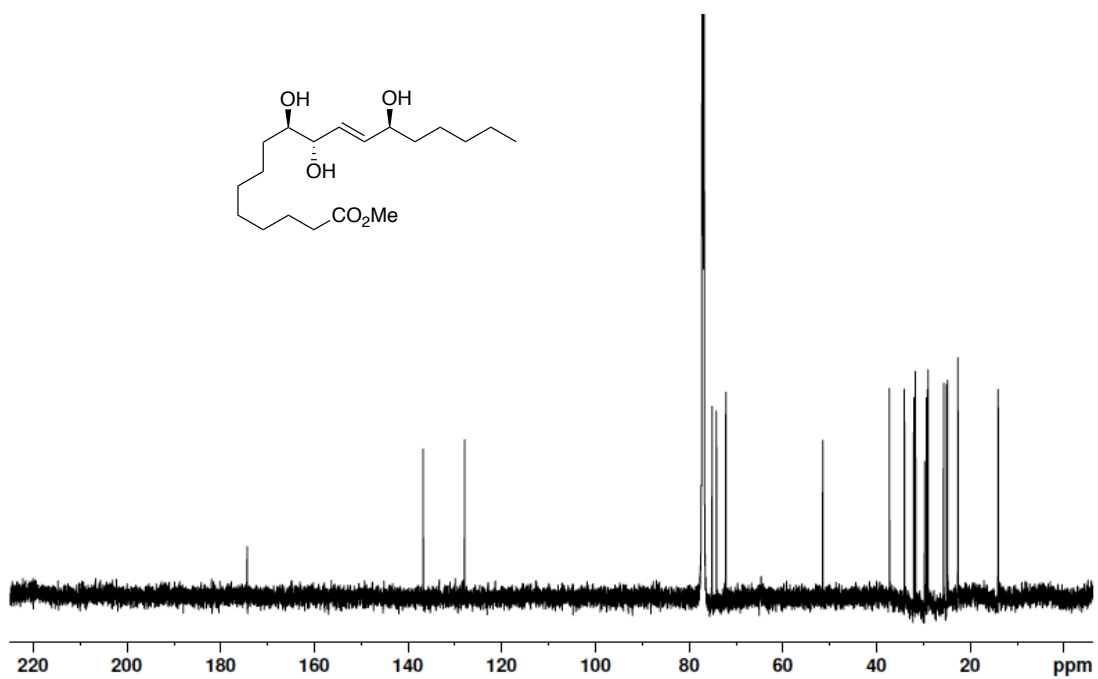
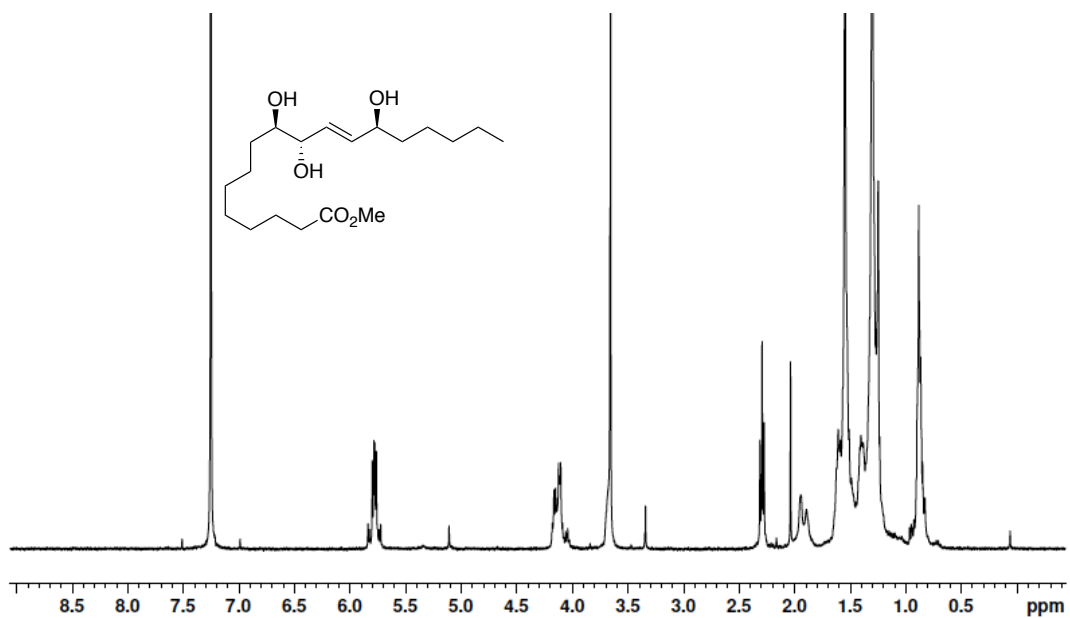


Figure A1.50 400 MHz $^1\text{H-NMR}$ and 100 MHz $^{13}\text{C-NMR}$ spectrum of **1.54** in CDCl_3

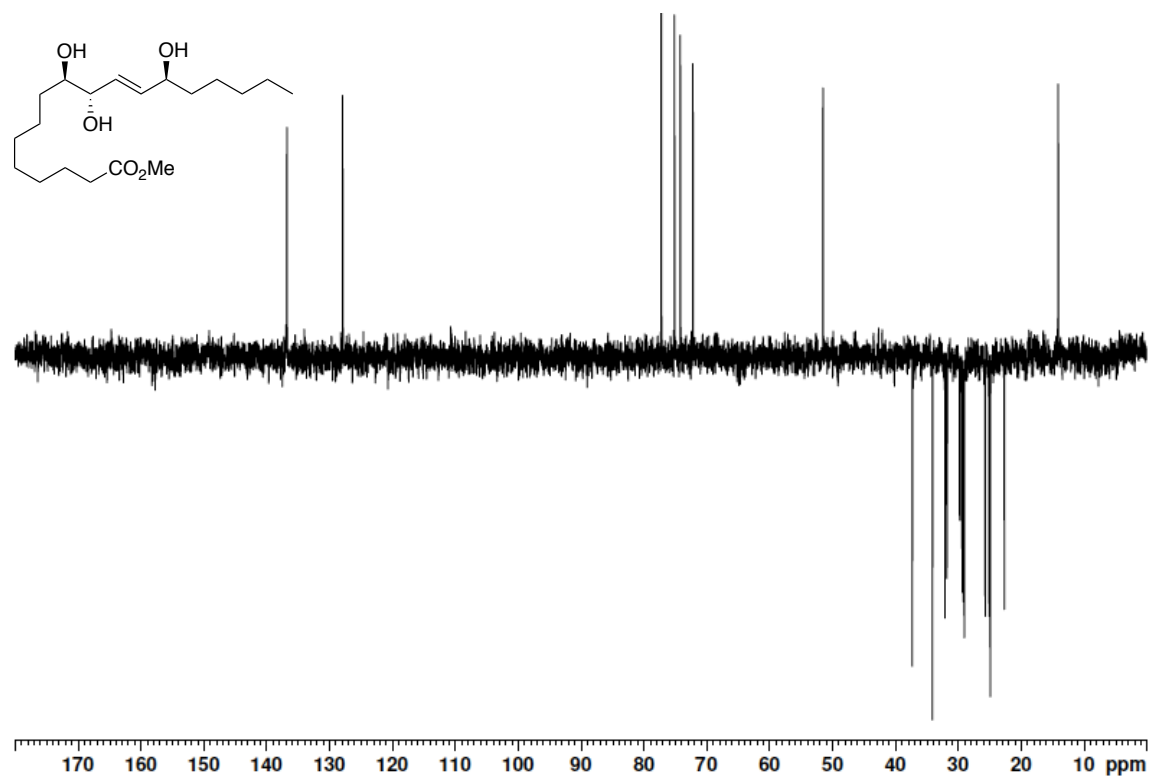


Figure A1.51 100 MHz DEPT 135 NMR spectrum of **1.54** in CDCl₃

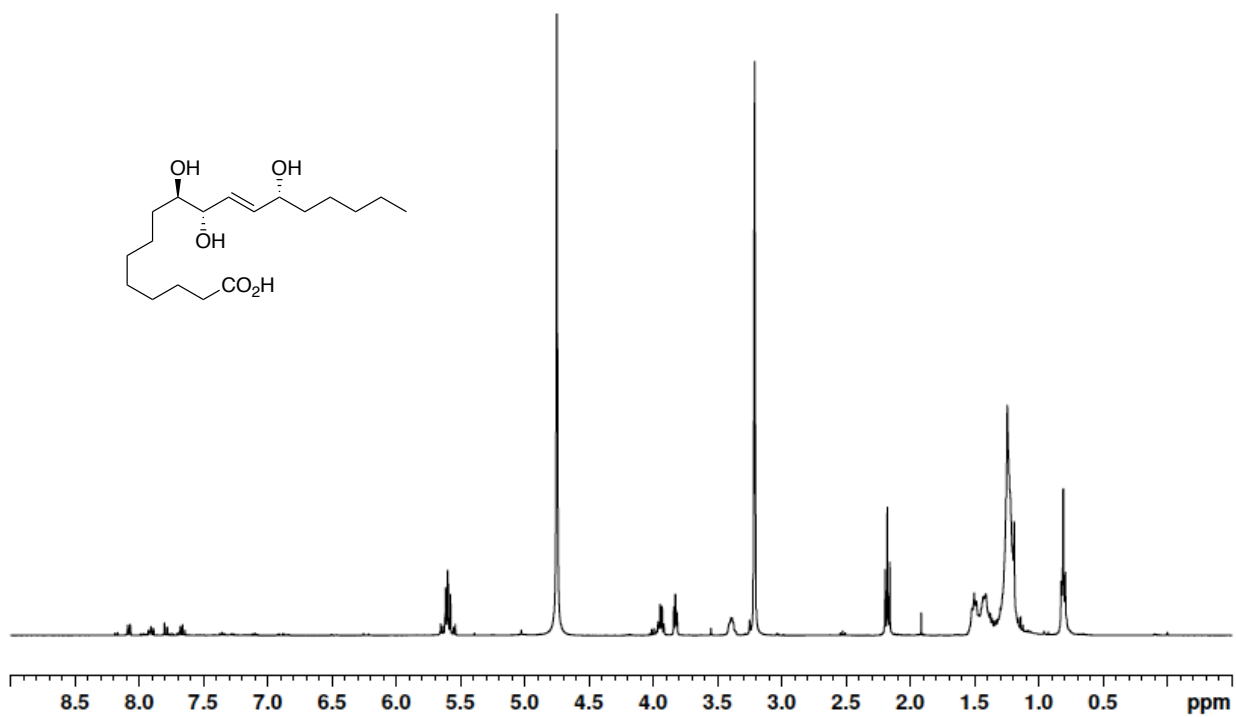


Figure A1.52 400 MHz ¹H-NMR spectrum of **1.2** in MeOD

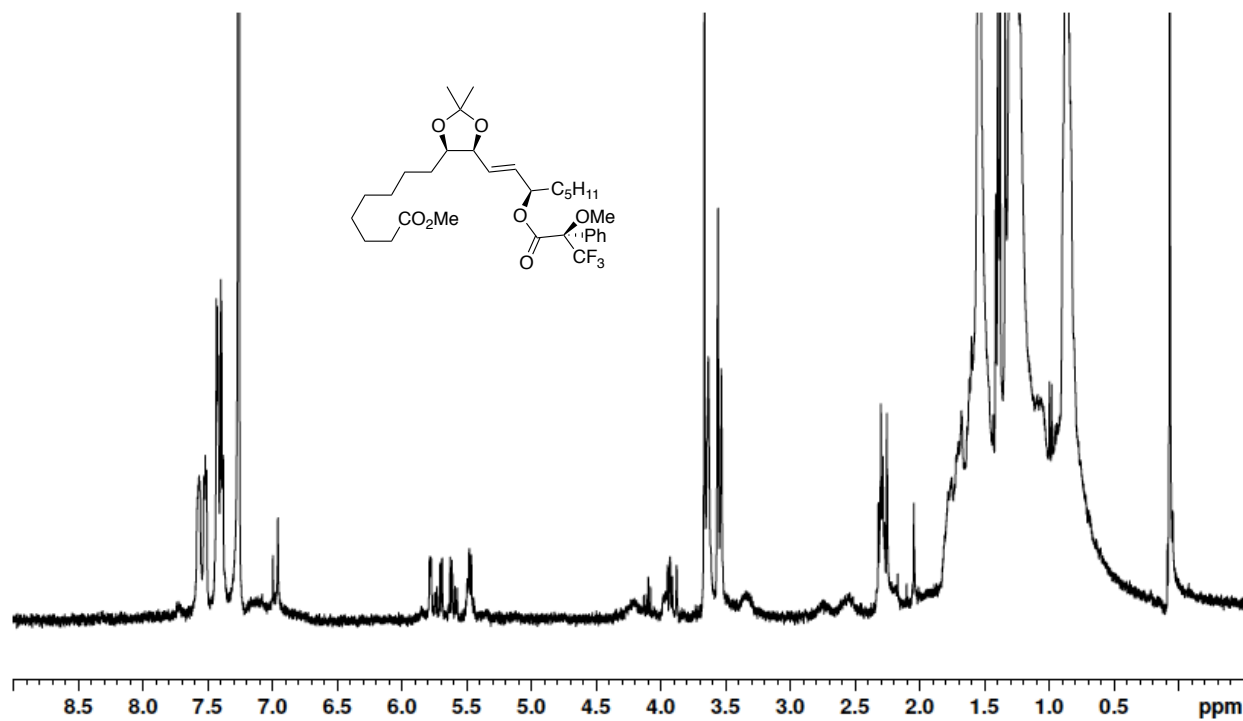
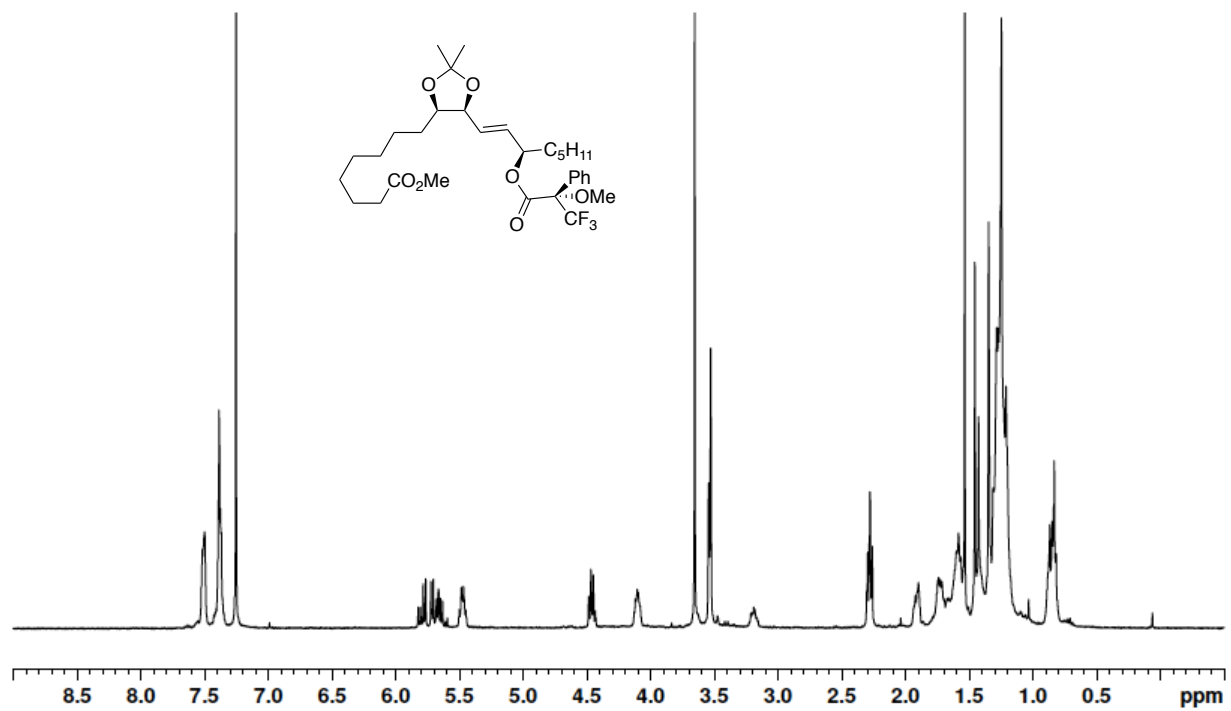


Figure A1.53 400 MHz $^1\text{H-NMR}$ spectrum of **1.58** and **1.59** in CDCl_3

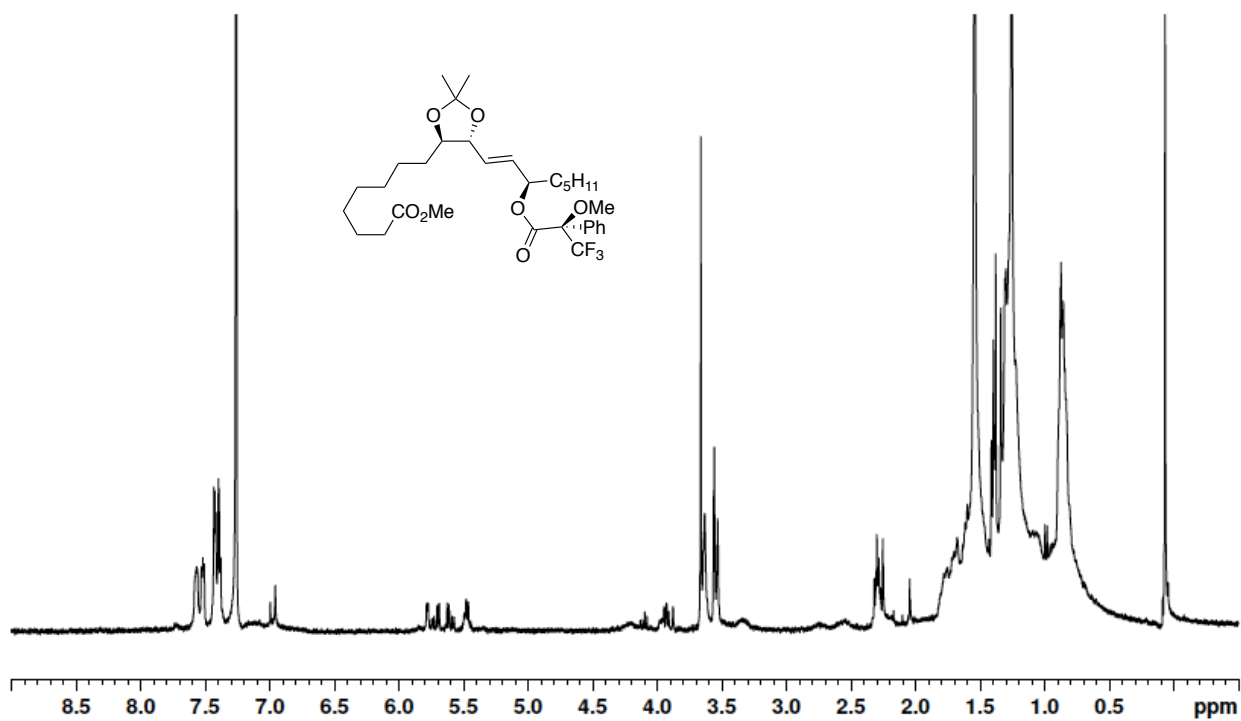
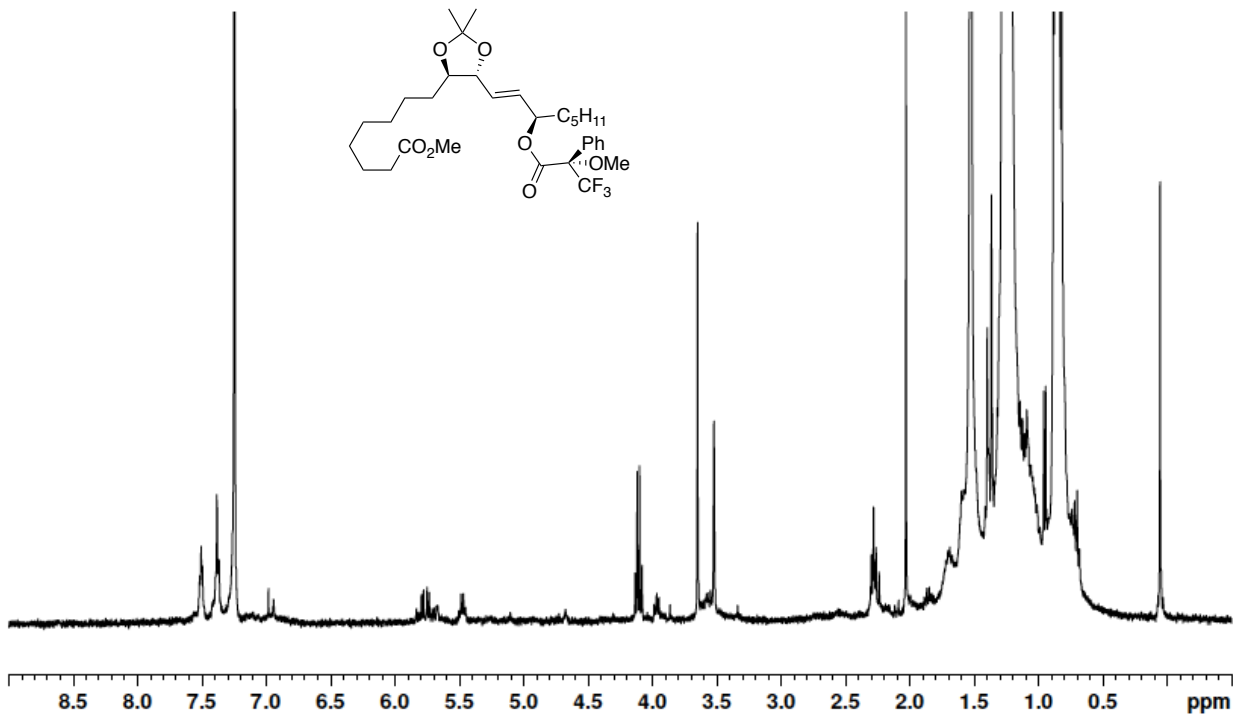


Figure A1.51 400 MHz $^1\text{H-NMR}$ spectrum of 1.62 and 1.63 in CDCl_3

CHAPTER II

DEVELOPMENT OF A LARGE SCALE CONVERGENT APPROACH TO APOPTOLIDINONE C

Apoptolidin: Isolation, Structure, and Biological Activity

In 1997, Seto and co-workers reported the isolation and identification of apoptolidin A, (a reportedly potent producer of apoptosis) from the culture broth of *Nocardioopsis sp.* FU40¹ (Figure 2.1). The aptly named apoptolidin appeared to selectively induce apoptotic activity against E1A induced rat glial cells over untransformed cells.¹

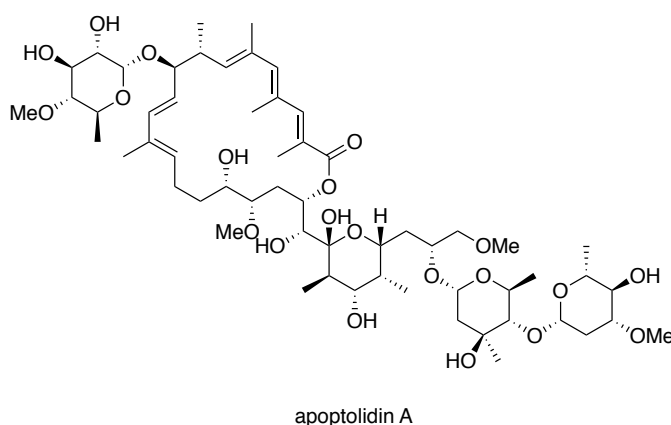


Figure 2.1 Structure of the *Nocardioopsis sp.* FU40 metabolite apoptolidin A

Apoptolidin is a 20-membered macrolactone possessing a fully substituted hemi-ketal pyran, 25 stereocenters, 5 double bonds, a 6-deoxy-4-*O*-methyl-L-glucose appended to the C9 hydroxyl group and a disaccharide consisting of L-olivomycose and D-oleandrose appended to the C27 hydroxyl group², (Figure 2.1). Since its isolation, over ten structurally related apoptolidins have been described.³⁻¹⁰ These compounds differ by the presence or absence of the C6 methyl group (R_1), C16 and C20 hydroxyl groups (R_2 and R_3), and the presence or absence of the C27

disacharride. There is a also variation at the 2' position of the monosacharride appended to C9. Additionally, Apoptolidins A, B, and D are known to isomerize between 20 and 21-membered lactone due to acyl migration from the C19 to the C20 hydroxyl group, generating isoapoptolidins A, B, and D (Figure 2.2).^{2,3} Despite their slight structural differences, most members of this class have comparable bioactivity, with only a few exceptions.

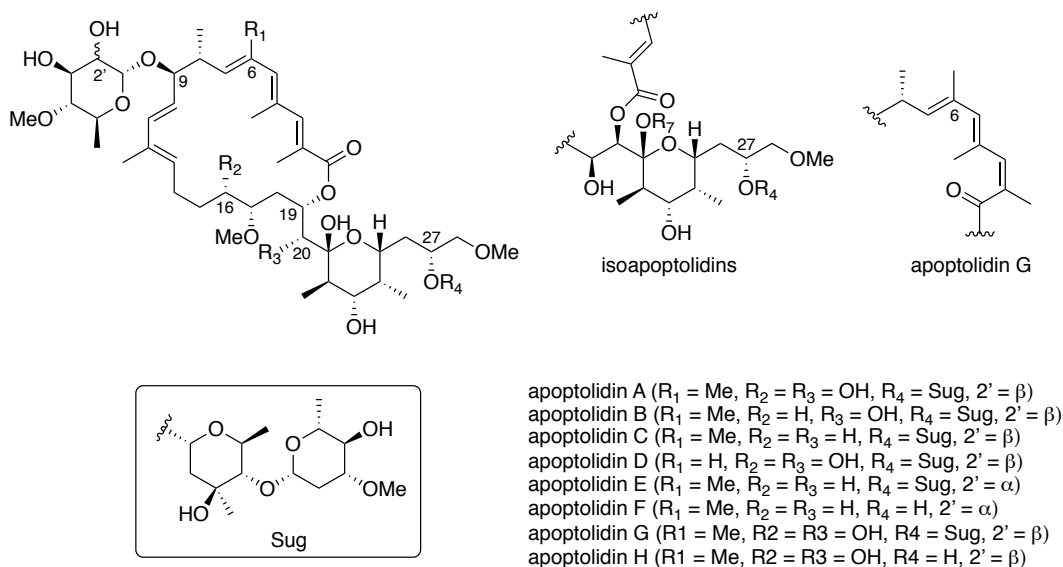


Figure 2.2 Structures of apoptolidin's A-H

Perhaps the most intriguing observation is the dramatically reduced activity of Apoptolidin H and Apoptolidin D disacharride, suggesting the sugar moieties play a crucial role in apoptolidin bioactivity (Figure 2.3).⁷⁻⁸ Further supporting this hypothesis, the fully de-glycosylated (aglycone) apoptolidinone A is completely inactive (Figure 2.3). Despite several elegant syntheses of apoptolidin A and apoptolidinones A, C, and D¹¹⁻¹⁶, little has been done to study the localization of these compounds in cells or their mechanism of action. Furthermore, it is still unknown why dramatic differences in activity are observed when the sugar moieties are removed. While little is known about the apoptolidin mechanism of action, it is not for lack of effort, and a brief history of apoptolidin biological studies will be summarized.

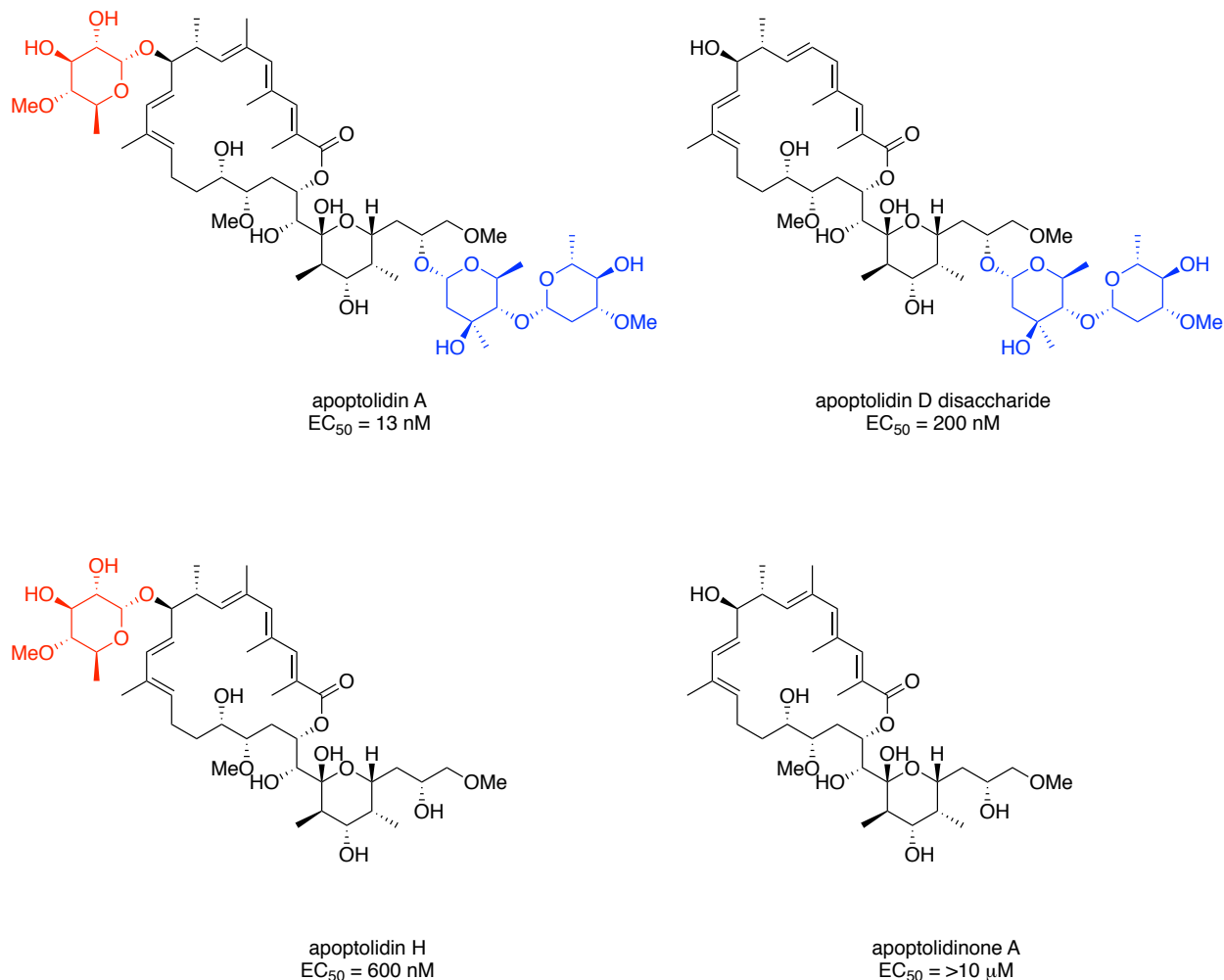


Figure 2.3 EC₅₀ of four apoptolidin glycovariants against H292 cells

Seto and co-workers observed significant DNA-laddering, as well as fragmented nuclei and condensed chromatin when E1A-transformed rat glial cells were treated with apoptolidin.¹ These are hallmark phenotypic signs of the apoptotic pathway. They also observed that apoptolidin displayed diminished cytotoxic activity against untransformed rat glial cells. In 2000, building off of this, Khosla and co-workers reported apoptolidin to be among the top 0.1% most cell-line selective agents screened in the National Cancer Institute (NCI) 60 human cancer cell line panel.¹⁷ They also went on to propose the mitochondrial protein, F₀F₁-ATP synthase (F₀F₁-ATPase), as the target of apoptolidin. There was a high correlation between cell lines that were particularly

sensitive to apoptoludin and cellular expression of genes encoding for the F_0F_1 -ATPase subunits. In addition, apoptoludin was shown to bind F_0F_1 -ATPase *in vitro*.¹⁷

In a later report, Khosla showed that mouse B lymphoma (LYas) cells transfected with the anti-apoptotic protein Bcl-2 were resistant to apoptoludins cytotoxic effects.¹² In contrast, normal LYas cells were surprisingly sensitive to apoptoludin. LYas cells were also co-treated with apoptoludin and known caspase-9 inhibitors, and activity was significantly reduced.^{18,19} These results prompted Khosla and coworkers to conclude apoptoludin works through an apoptotic mechanism.^{18,19}

Building on this, our group, in collaboration with the Bachmann and Marnett groups, reported that Cy3 fluorophore tagged apoptoludin A and apoptoludin H (Figure 2.4) localize in the mitochondria of H292 human lung cancer cells.⁹ Both compounds maintained comparable activity to the natural compounds.

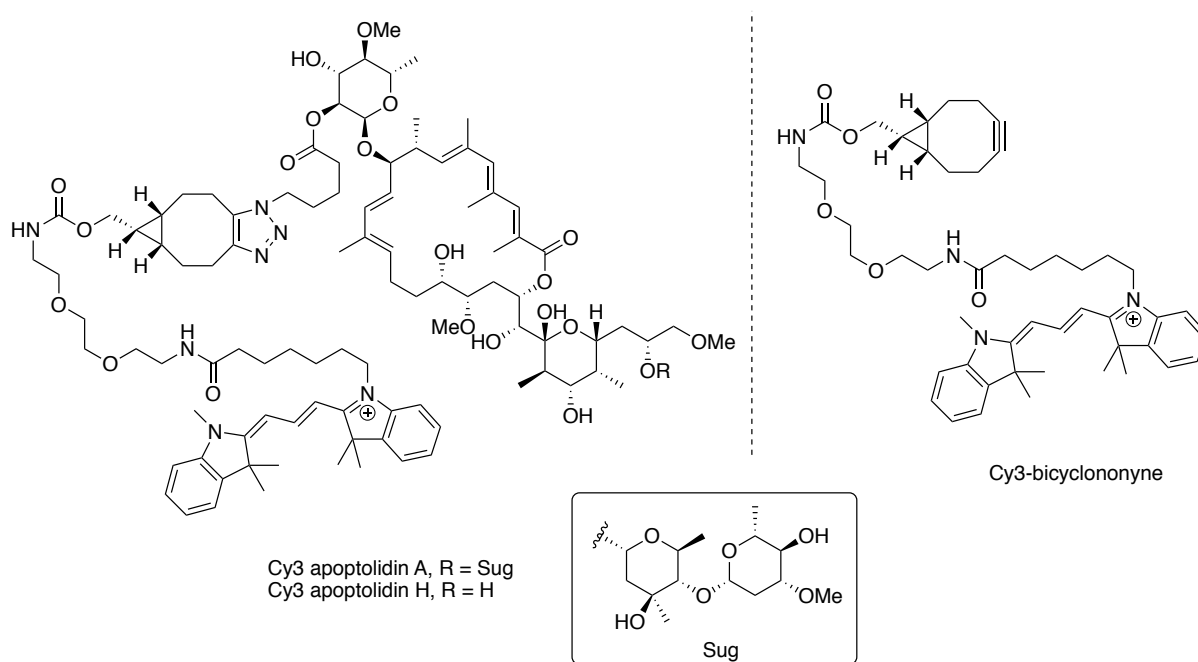


Figure 2.4 Fluorescent Cy3-tagged apoptoludin A and H and Cy3-bicyclononyne

This observation would support the hypothesis of an apoptotic mechanism of action, however, the fluorescent Cy3 dye and linker localized to the mitochondria as well. While the Cy3 dye proved to be non-toxic to cells, and Cy3-tagged apoptolidin A and H were still cytotoxic, it cannot be concluded that apoptolidin localizes to the mitochondria.⁹

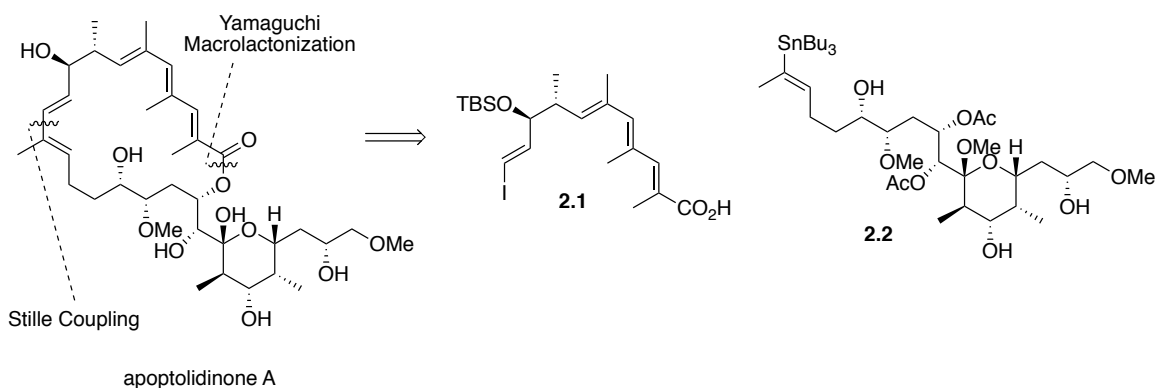
It is important to note the effect of cell confluency and apoptolidin activity. Our group demonstrated that cells at low confluence maintain about a 50% viability in the presence of apoptolidin, whereas high confluence cells are very sensitive to apoptolidin's cytotoxic effect. This observation presents a challenge when comparing historical apoptolidin bioactivities, and must be taken into consideration when designing and implementing experiments in the future. Our reported EC₅₀ values in Figure 2.3 were measured with this understanding, providing accurate and comparable data.

Lastly, in 2016, in a collaboration with the Bachmann and Irish groups, we used cell microscopy imaging, and showed that apoptolidin is selectively taken up by cancer cell lines over healthy cell models.²⁰ These results were quantified by single-cell fluorescent phospho-specific flow cytometry.²⁰ In order to further these results and probe the role of apoptolidin glycosylation state in mechanism of action, we sought to access all four apoptolidin glycovariants (Figure 2.3). Apoptolidin A and H are available through fermentation⁹, while the aglycone is only accessible via total synthesis.^{21,22} Once accessed, the aglycone can be subjected to precursor directed biosynthesis to afford the C27 disaccharide.²³ With all four glycovariants in hand, we can continue to elucidate the role of glycosylation state in apoptolidin bioactivity, but first, a robust, large-scale synthesis of the aglycone is necessary.

Chemical Synthesis of Apoptolidins

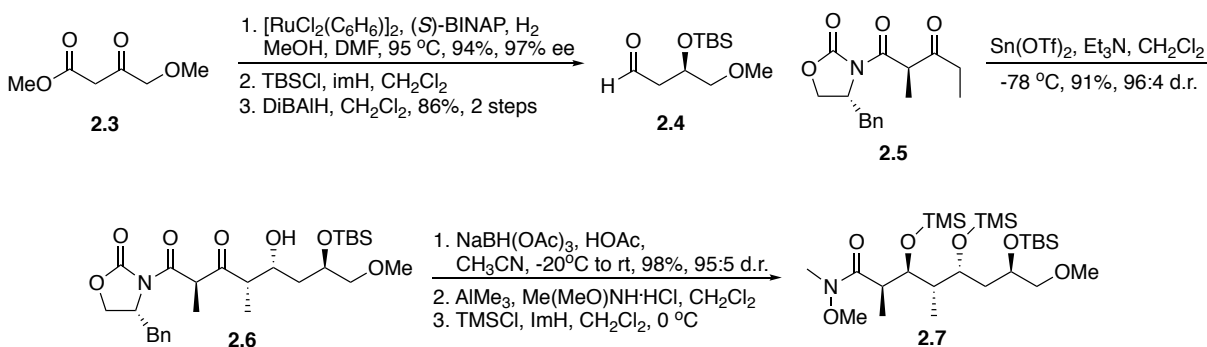
Koert's Synthesis of Apoptolidinone A

The Koert group's strategy to apoptolidinone A focused on two key disconnections; a Stille coupling to form the C11-C12 bond and a Yamaguchi macrolactonization to form the 20-membered lactone (Scheme 2.1).¹¹ The proposed Northern (**2.1**) and Southern (**2.2**) hemispheres were assembled in a relatively succinct 13 and 15 linear steps respectively.



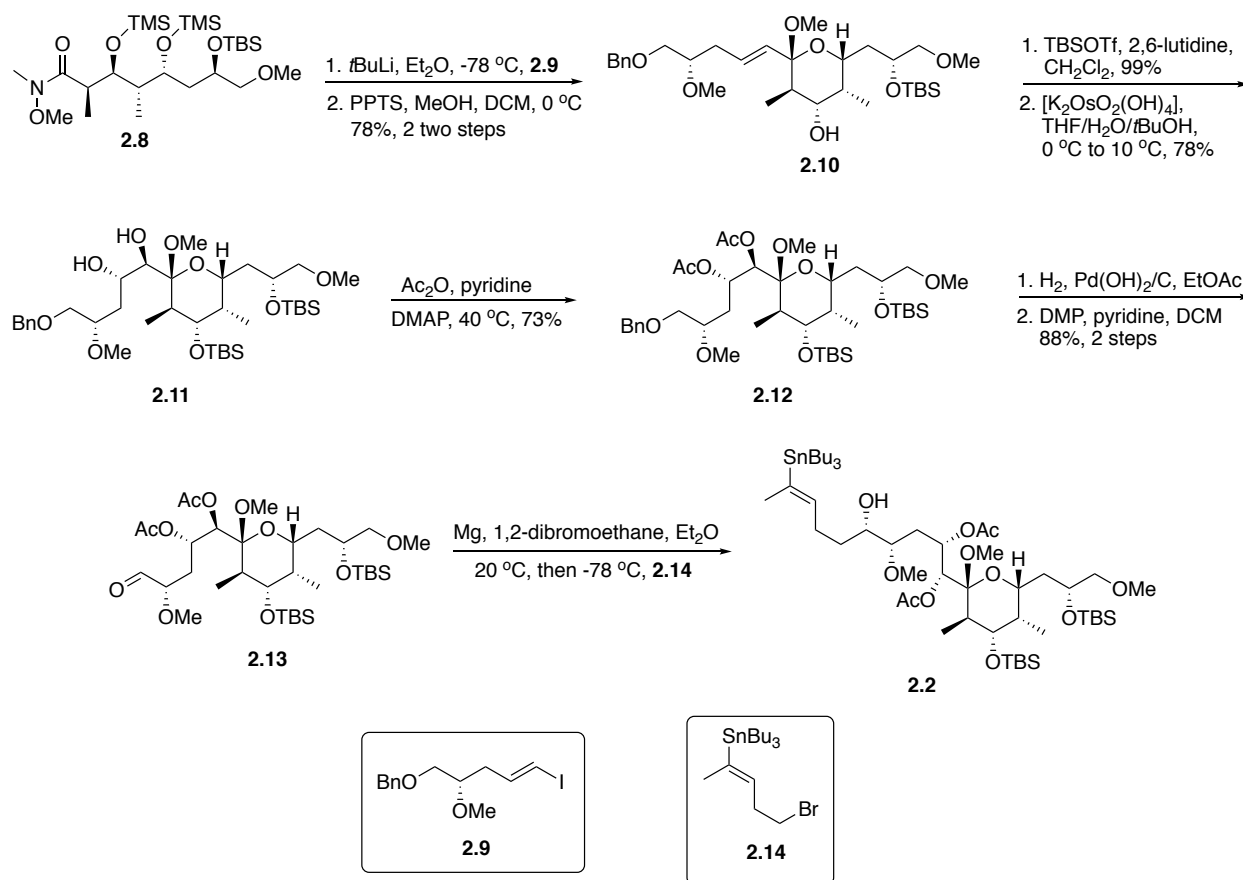
Scheme 2.1 Koert's retrosynthetic strategy toward apoptolidinone A

The synthesis of the southern hemisphere began with Noyori hydrogenation of 4-methoxy-acetoacetate (**2.3**), affording the chiral alcohol in nearly quantitative yield, with excellent enantioselectivity. Resultant silyl-protection and reduction of the methyl ester afforded aldehyde **2.4**. The tin(II) triflate-mediated aldol utilizing the beta-keto imide derived enolate of **2.5** afforded the Evan's *syn* product in 91% yield with excellent diastereoselectivity. Alcohol-directed asymmetric hydride delivery, trans-amidation and silyl-protection afforded **2.7** (Scheme 2.2).



Scheme 2.2 Synthesis of weinreb amide **2.7**

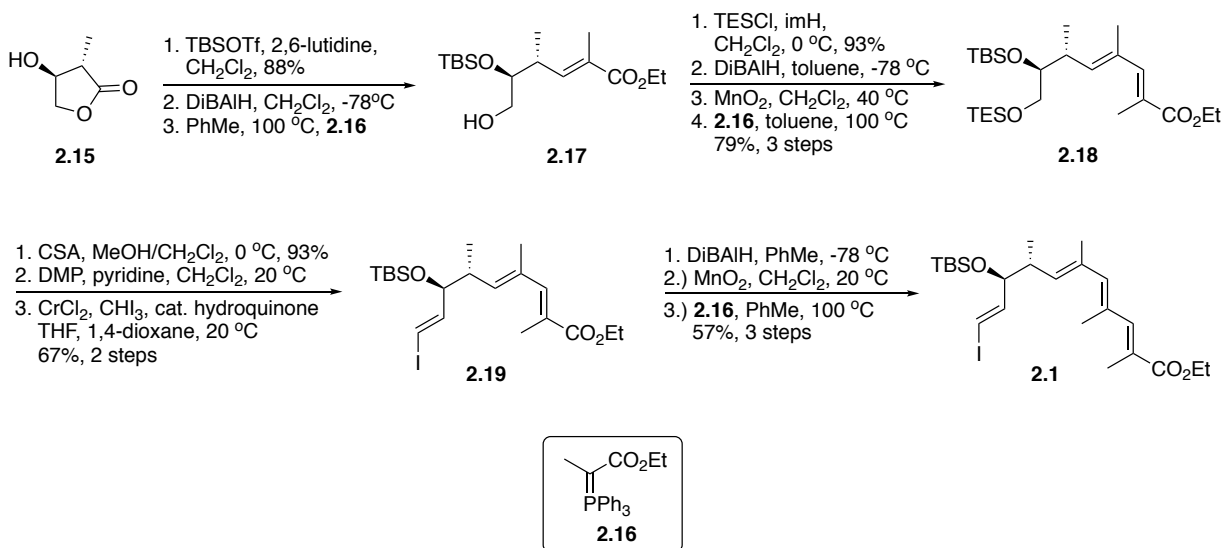
Lithiate addition of **2.9** to weinreb amide **2.8**, followed by a one-pot silyl-deprotection and acetal formation gave pyran **2.10** in 78% yield over the two steps. Protection of the secondary alcohol and substrate-controlled dihydroxylation gave diol **2.11**, again in good yields. Acetylation of diol **2.11** afforded pyran **2.12** (Scheme 2.3).



Scheme 2.3 Koert's synthesis of the Southern hemisphere of apoptolidinone A

Hydrogenation using Pearlman's catalyst and oxidation with Dess-Martin reagent yielded aldehyde **2.13** in 88% over two steps. Grignard addition to the aldehyde gave the desired vinyl stannane **2.2**, completing the synthesis of the southern hemisphere (Scheme 2.3).

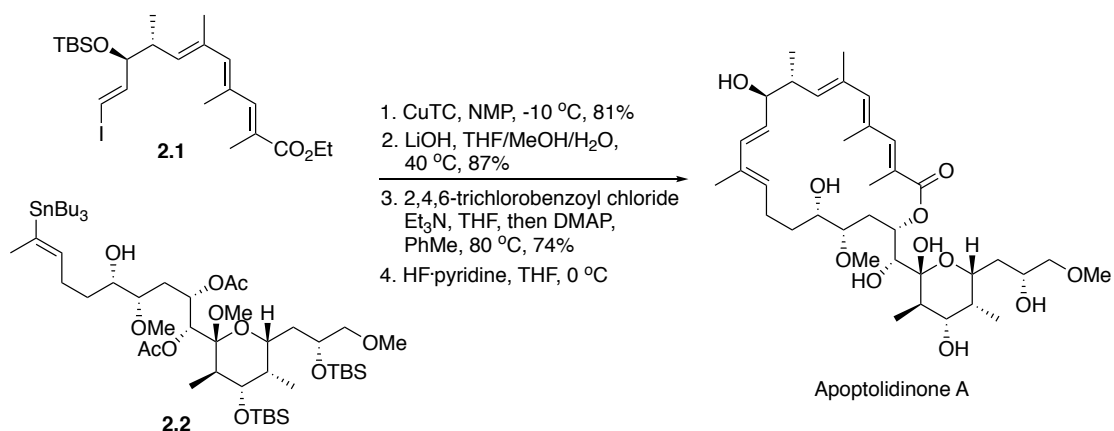
The synthesis of the Northern hemisphere began from β -hydroxy- γ -lactone **2.8**, which can be prepared from (L)-malic acid in 3 steps.¹¹ Protection of the chiral secondary alcohol, reduction of the lactone with DiBALH, and treatment with Wittig reagent **2.16** gives the linear alcohol **2.17** in only three steps. Silyl-protection of the primary alcohol **2.17** followed by reduction of the ester with DiBALH, oxidation with MnO_2 , and treatment with Wittig reagent **2.16** afforded the diene (**2.18**) in good yields. De-protection of the triethylsilyl ether with CSA in MeOH, and subsequent oxidation and Takai olefination afforded the vinyl iodide **2.19** (Scheme 2.4).



Scheme 2.4 Koert's synthesis of the Northern hemisphere

Reduction of the ester moiety with DiBAIH, oxidation with MnO₂, and treatment with wittig reagent **2.16** gave vinyl iodide **2.1** in 57% yield over three steps, and completed the synthesis of the northern hemisphere. It should be noted, that with the trienoate in hand, all reactions with linear intermediates were performed in amber glassware, with the exclusion of daylight to prevent isomerization of the trienoate moiety (Scheme 2.6).

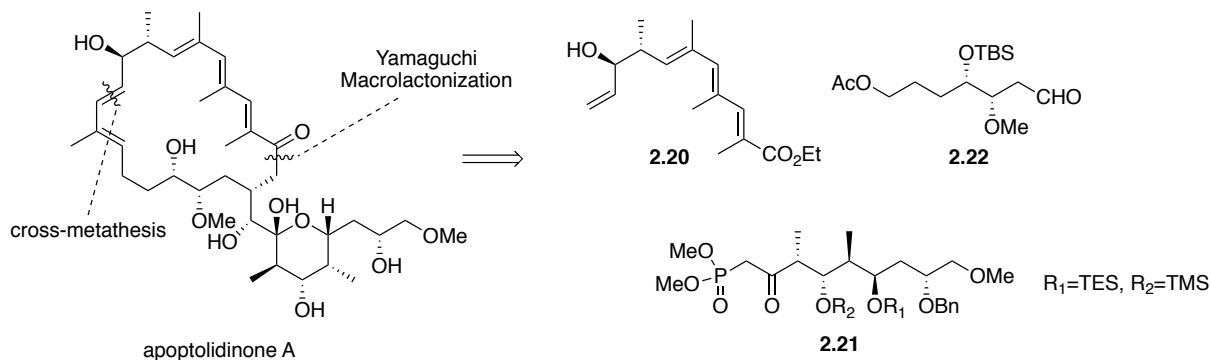
With both the Northern and Southern hemispheres in hand, the Koert group investigated multiple conditions for the Stille coupling of **2.1** and **2.2**. While several Pd⁰-mediated cross-couplings afforded the desired product, yields were below 30% (even with the use of long reaction times and higher temperatures). Surprisingly, the use of Cu(I)-thiophene carboxylate under mild conditions, gave the desired product in 81% yield in only 1 hour. We noted the non-triviality of this bond formation, as it is a common problem in later syntheses as well. With the C11-C12 bond formed, attention turned to the second key disconnection. Hydrolysis of the ester with lithium hydroxide gave the corresponding acid in 87% yield (Scheme 2.5). Yamaguchi macrolactonization was employed to form the 20-membered macrolactone. Global de-protection proceeded in good yields, affording apoptolidinone A in 19 linear steps (Scheme 2.5).¹¹



Scheme 2.5 Completion of apoptolidinone A

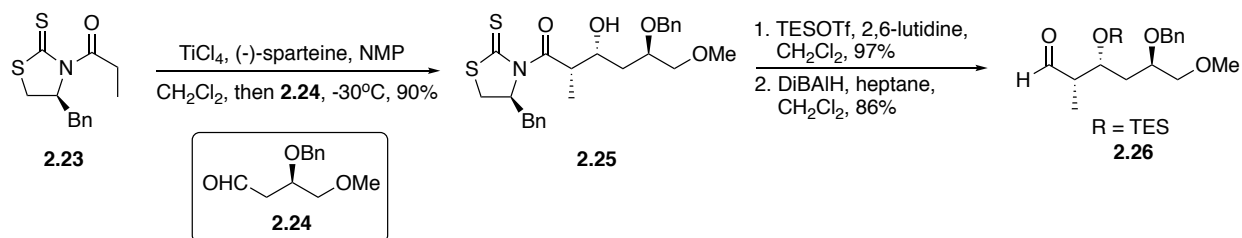
Crimmin's Synthesis of Apoptolidinone A

The Crimmin's approach to apoptolidinone A is unique in that a cross metathesis was used to form the C10-C13 diene, rather than a cross-coupling to form the C11-C12 bond (Scheme 2.36).¹⁵ While in general the approach was not highly convergent, the use of Crimmin's aldol technology proved to be very efficient. These efforts will be briefly highlighted.



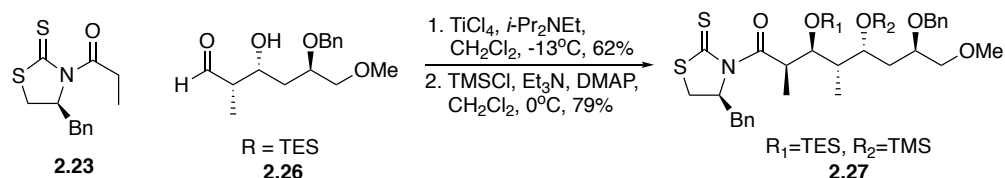
Scheme 2.6 Crimmin's approach to apoptolidinone A

Crimmin's aldol between auxiliary **2.23** and aldehyde **2.24** using 1 equivalent each of titanium(IV) tetrachloride, (-)-sparteine and NMP gave the Evan's *syn* aldol adduct **2.25** in 90% yield. Protection of the resulting alcohol as the triethylsilyl ether and subsequent reduction utilizing DiBAIH gave aldehyde **2.26** (Scheme 2.7).



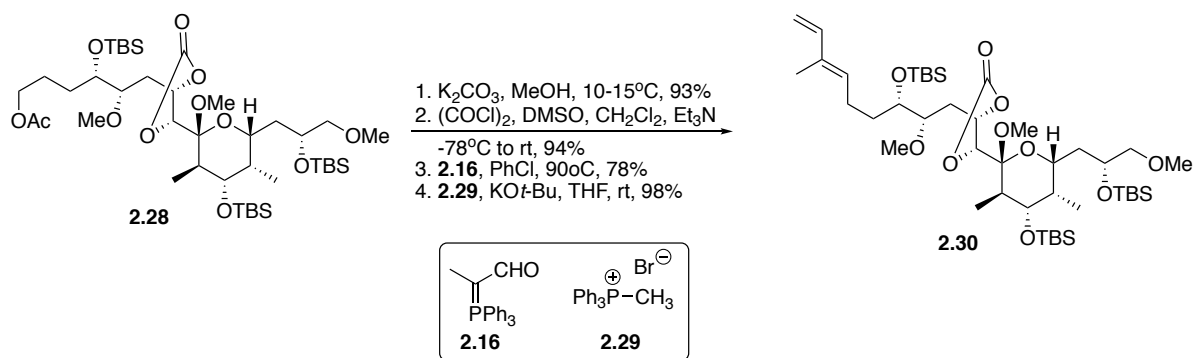
Scheme 2.7 Synthesis of aldehyde **2.26** via Crimmin's aldol technology

Crimmin's aldol between auxiliary **2.23** and aldehyde **2.26** using 1 equivalent of titanium(IV) tetrachloride and excess Hunig's base gave the non-Evan's *syn* aldol adduct **2.27** in 62% yield. The resultant alcohol was protected as the trimethylsilyl ether (Scheme 2.8).



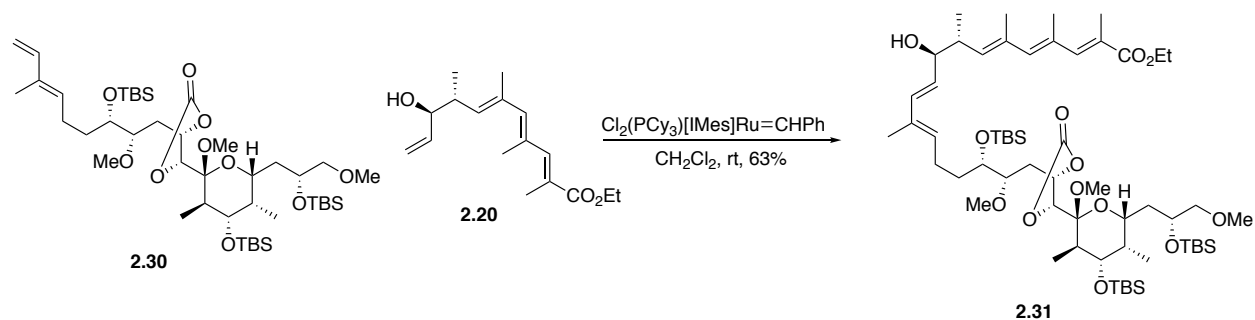
Scheme 2.8 Crimmin's aldol to afford the non-Evan's *syn* adduct **2.27**

After further elaboration of the southern hemisphere, in a reaction sequence that would inspire our future efforts, the primary alcohol moiety was converted to the cross-metathesis precursor **2.30**. Deprotection of the acetate group of **2.28**, followed by Swern oxidation and iterative Wittig reactions utilizing reagent **2.16** and **2.29** afforded diene **2.30** (Scheme 2.9).



Scheme 2.9 Synthesis of cross metathesis precursor diene **2.30**

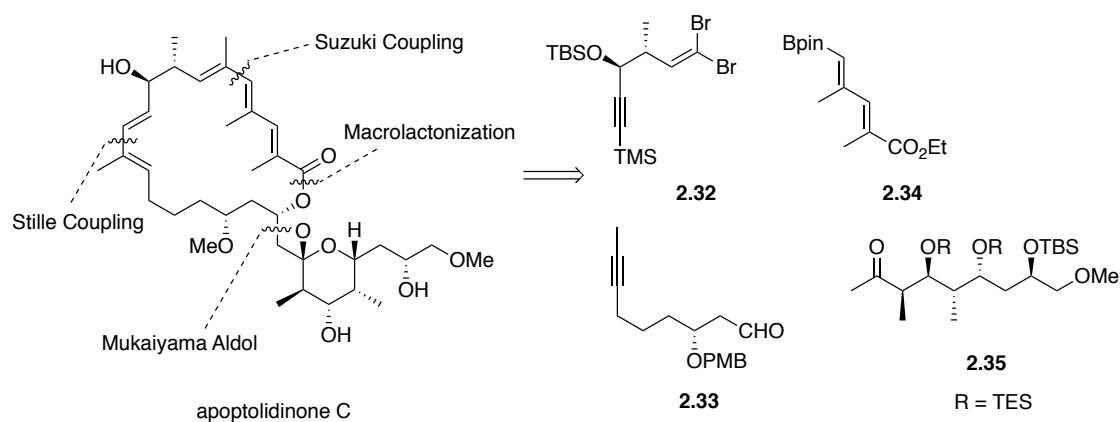
Cross metathesis between the terminal vinyl groups of **2.30** and **2.20** using the Grubbs heterocyclic carbene catalyst provided the *E* isomer, **2.31**, in 63% yield (Scheme 2.10). It is worth noting that two equivalents of **2.20** were required due to competing homodimerization. This undesired product could, however, be isolated and recycled.



Scheme 2.10 Cross metathesis to yield the seco-acid precursor **2.31**

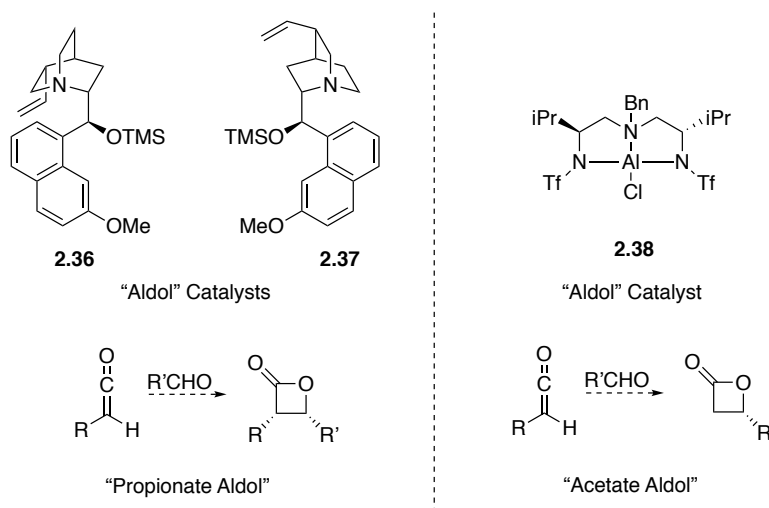
Nelson's Synthesis of Apoptolidinone C

The Nelson group's approach to apoptolidinone C centered on four key disconnections. Cross-couplings were employed to form the C5-C6 bond and C11-C12 bond and Mukaiyama aldol was used to establish the southern hemisphere. Yamaguchi macrolactonization formed the 20-membered macrolactone (Scheme 2.11). While the disconnections were hardly unique, the Nelson group developed a highly convergent synthesis and demonstrated the utility of enantioselective catalytic aldol surrogates to set stereochemistry through reagent control (Scheme 2.12).¹⁶



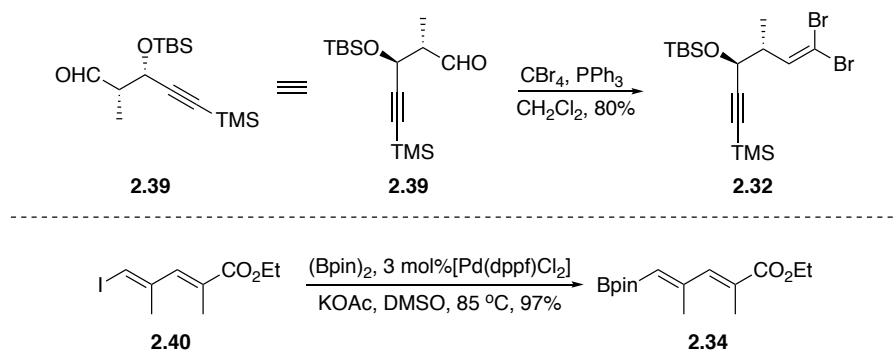
Scheme 2.11 The Nelson group's strategy toward apoptolidinone C

The catalytic asymmetric acyl halide–aldehyde cyclocondensation (AAC) developed in the Nelson group begins via [2+2] cycloaddition of a ketene and aldehyde, in which a chiral Lewis acid (**2.38**) or Lewis base (**2.36**, **2.37**) can influence the facial selectivity of the approach (Scheme 2.12). The resulting β -lactone can be opened via nucleophilic acyl substitution. This methodology was used to install nearly every stereocenter in apoptolidinone C.



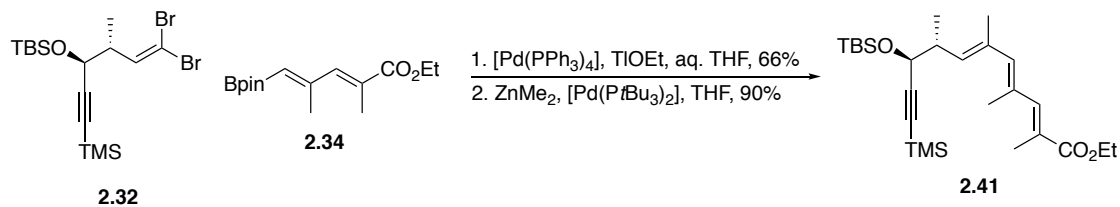
Scheme 2.12 Enantioselective catalysis employed in Nelson's synthesis of apoptolidinone C

We drew inspiration from the Nelson group's approach to the Northern hemisphere and this route will be briefly summarized. Aldehyde **2.39** was treated with carbon tetrabromide and triphenylphosphine to afford the key fragment, dibromide **2.32**, in 80% yield. Likewise, the coupling partner, boronate **2.34** was synthesized from previously reported vinyl iodide **2.40** via Suzuki cross-coupling in an impressive 97% yield (Scheme 2.13).



Scheme 2.13 Synthesis of the key fragments dibromide **2.32** and vinyl boronate **2.34**

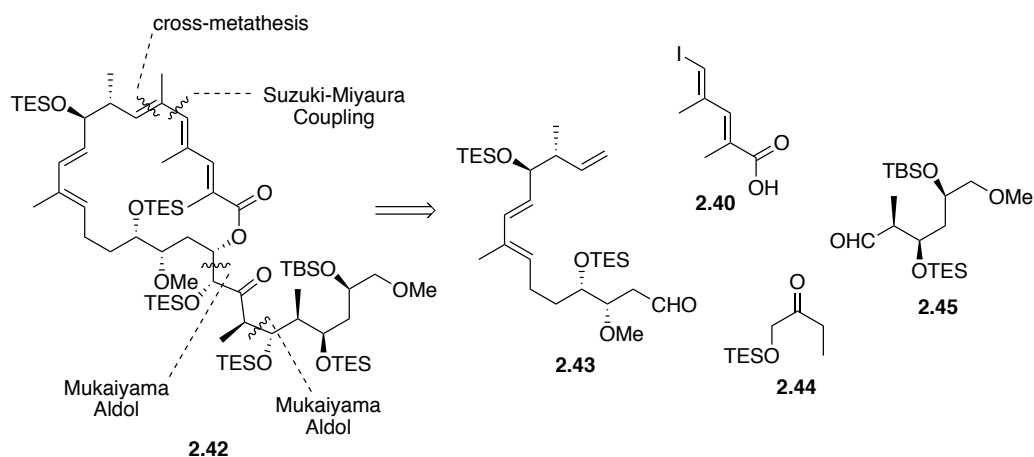
Chemoselective Suzuki cross-coupling afforded the desired trienoate as a single regioisomer in 66% yield. The resulting vinyl bromide was subjected to Negishi conditions to complete the construction of the apoptolidin trienoate moiety and furnish **2.41** in 90% yield (Scheme 2.14).



Scheme 2.14 Synthesis of trienoate **2.41** via iterative cross-couplings

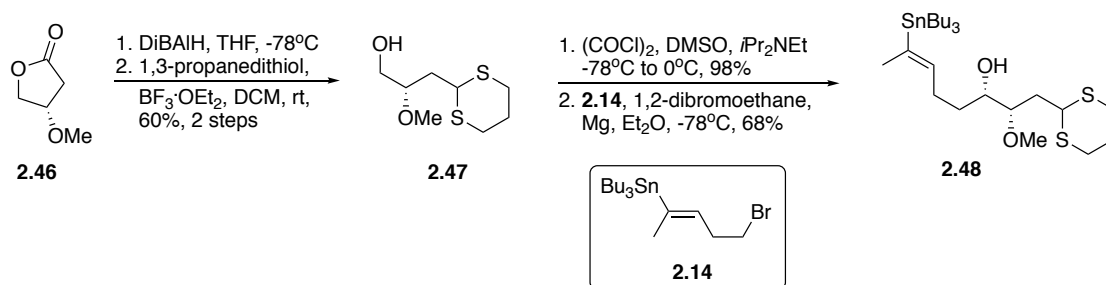
Sulikowski's Synthesis of Apoptolidinone A

Sulikowski's approach to apoptolidinone A was highly convergent, focusing on several key disconnections. Cross-coupling to establish the C11-C12 bond, Yamaguchi esterification, Suzuki-Miyaura coupling was used to form the C5-C6 bond and aldol reactions were used in construction of the southern hemisphere (Scheme 2.15).¹⁴



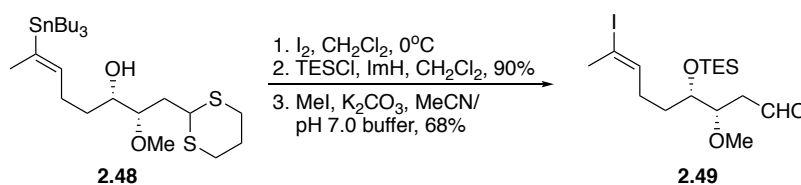
Scheme 2.15 Sulikowski's approach to apoptolidinone A

Compound **2.46** was synthesized from (*S*)-malic acid using a known procedure in four steps. Reduction of the lactone moiety of **2.46** with DiBALH, followed by condensation with 1,3-propanedithiol afforded 1,3-dithiane **2.47** in 60% yield over two steps. The alcohol was oxidized via Swern conditions and Grignard addition of **2.14** to the resulting aldehyde proceeded with chelation-control yielding the **2.48** from lactone **2.46** in only four steps (Scheme 2.16).



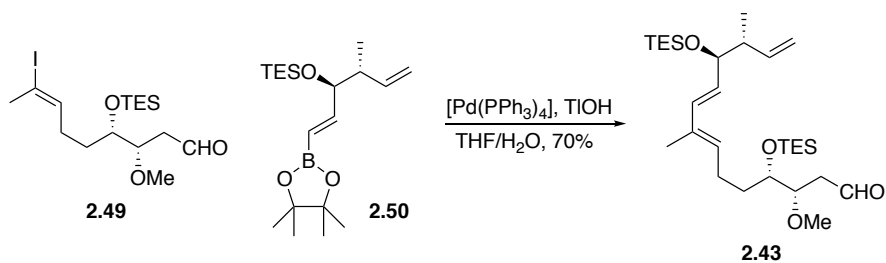
Scheme 2.16 Synthesis of vinyl stannane **2.48**

Vinyl stannane **2.48** was treated with iodine, and the alcohol was protected as the triethylsilyl ether before the dithiane was cleaved using Fetizon-Jurion conditions to unmask the aldehyde moiety, yielding **2.49** (Scheme 2.17).



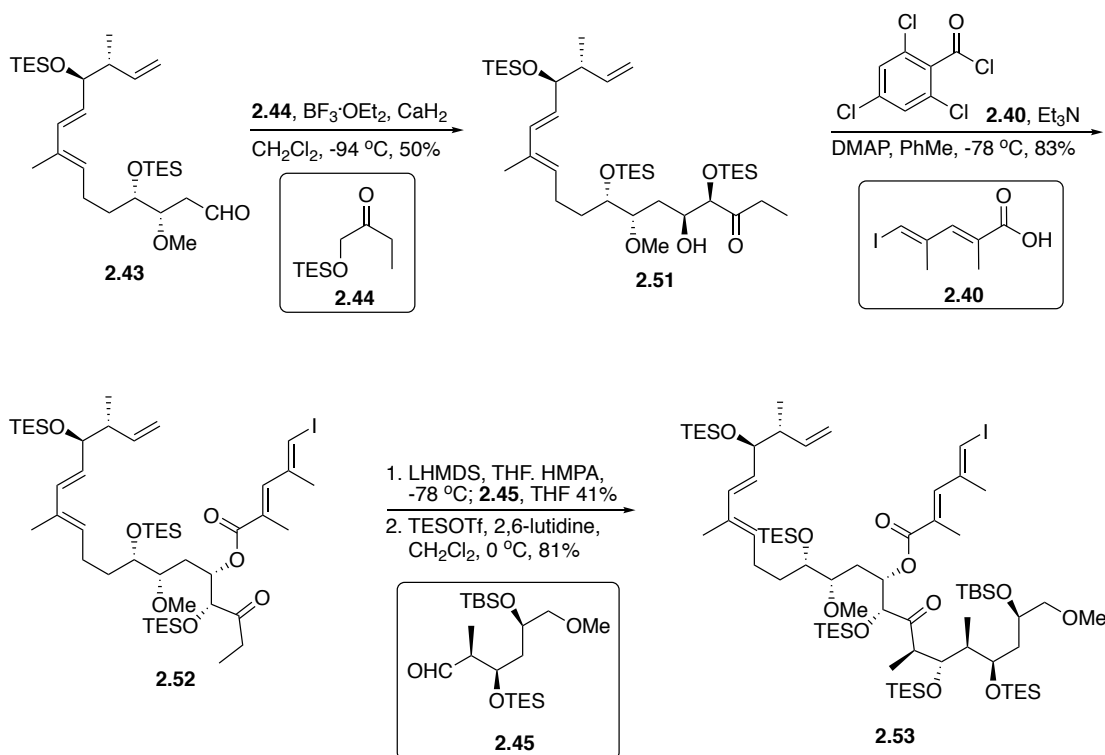
Scheme 2.17 Synthesis of key aldehyde **2.49**

Vinyl boronate **2.50** was prepared via Roush crotylation conditions and subsequent protection of the resultant free hydroxyl as the triethylsilyl ether. Suzuki-Miyaura cross-coupling between vinyl iodide **2.49** and vinyl boronate **2.50** yielded diene **2.43** in 70% yield (Scheme 2.18).



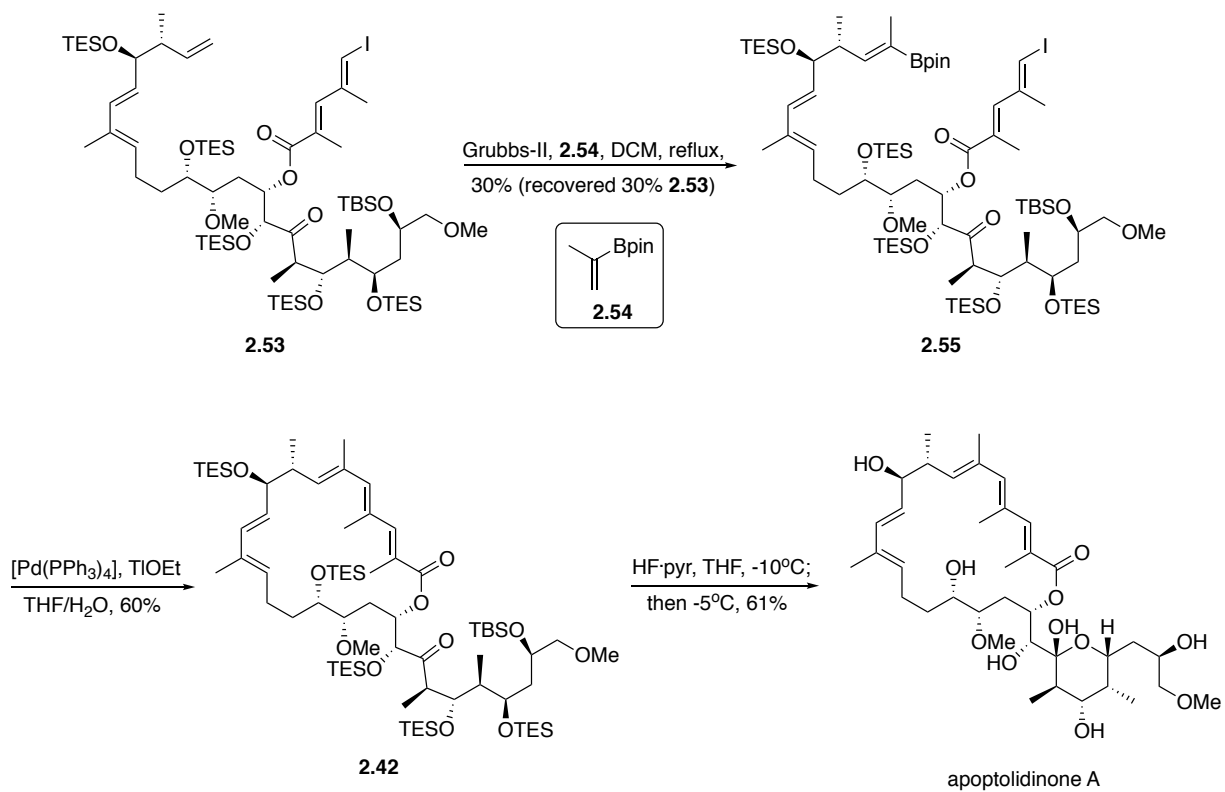
Scheme 2.18 Synthesis of the western hemisphere through Suzuki coupling

Diastereoselective Mukaiyama aldol between aldehyde **2.43** and the enol silane of **2.44** afforded the ketone **2.51** in 50% yield as a 4:1 mixture of diastereomers. Yamaguchi esterification of **2.51** with carboxylic acid **2.40** gave dienoate **2.52** in 83% yield (Scheme 2.19). Aldol addition between the kinetic enolate of **2.52** and aldehyde **2.45** afforded the *syn* aldol product, **2.53**, as a single isomer in 41% yield. The late stage intermediate ketone **2.52** was recovered (30%), and the high convergence of this approach offers some compensation for the relatively low yield of the aldol, although room for improvement remained. The resulting alcohol was protected as the triethylsilyl ether (Scheme 2.19).



Scheme 2.19 Synthesis of late-stage intermediate **2.53** via aldol

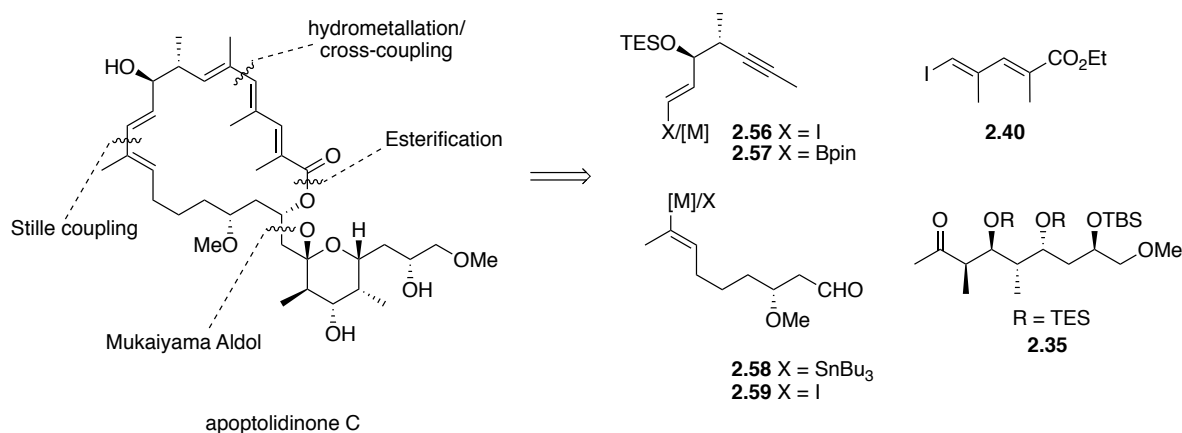
Alkene **2.53** was subjected to cross-metathesis with propenyl boronate (**2.54**) using Grubbs second-generation catalyst to afford vinyl boronate **2.55** in 30% yield as a single regioisomer. Intramolecular Suzuki-Miyaura cross-coupling gave the macrolactone **2.42** in 60% yield (Scheme 2.20). This approach avoids the linear trienoate intermediates, which readily isomerize, and is therefore favorable. Desilylation via treatment with HF·pyr in THF afforded apoptolidinone A in 61% yield.¹⁴ This approach to apoptolidinone A was completed in 14 steps from lactone **2.46**, proving to be the most convergent route (Scheme 2.20). Several late stage steps were fairly low yielding, however the insights gained from this approach have proved very important in our current investigation of large-scale apoptolidinone synthesis, which would be next to impossible without a highly convergent approach.



Scheme 2.20 Completion of the total synthesis of apoptoldinone A

Progress Toward Apoptolidinone C

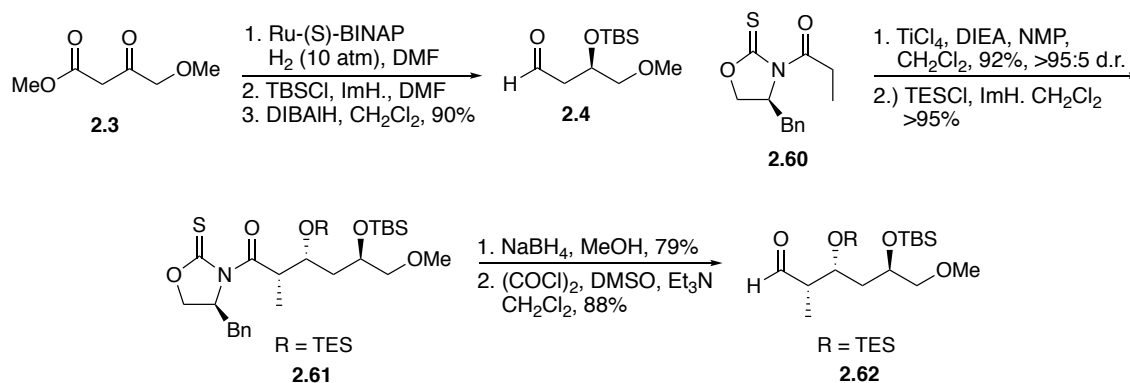
When studying previously completed syntheses of apoptolidin natural products, a few themes emerge. First demonstrated by Sulikowski and then the Nelson group, the Mukaiyama aldol^{14,16} approach to the southern hemisphere is convergent and highly diastereoselective. With the less stereocomplex apoptolidinone C as the target, we could avoid the sequential late stage Mukaiyama aldols required for the synthesis of apoptolidinone A. Instead Mukaiyama aldol between **2.35** and **2.56** or **2.57** would furnish the Southern hemisphere. The use of chiral auxiliaries by Koert¹¹ and Crimmins¹⁵ provides a robust and scalable process for the synthesis of the enantiomerically pure polyketide backbone of the southern hemisphere (**2.35**). The convergent approaches of Sulikowski¹⁴ and Nelson¹⁶ demonstrate the utility of fragments such as **2.40** in cross-couplings to establish the C5-C6 bond. In regards to the C11-C12 bond, much variation exists, in fact, the western portion of the molecule varies considerably from one groups approach to the next. Recognizing this, we sought a synthesis that would allow ready access to multiple potential coupling partners for C11-C12 cross-coupling (**2.56-2.59**).



Scheme 2.21 Our original synthetic strategy to apoptolidinone C

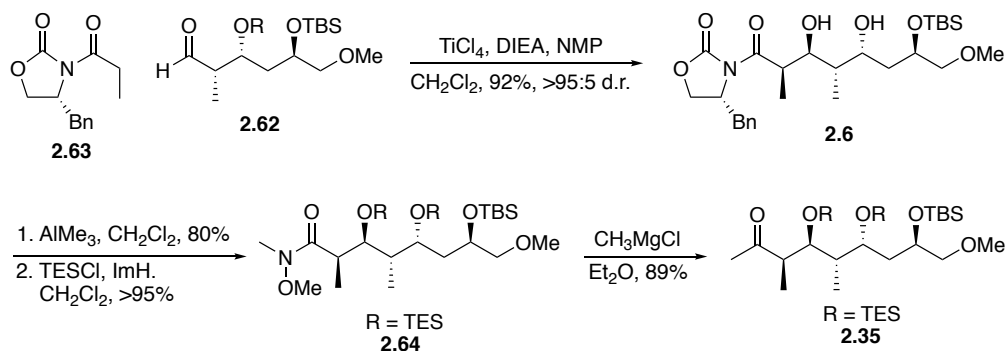
Synthesis of the C20-C28 Fragment

Recognizing the utility of this approach for our purposes, we utilized an aldol between thiozolidinone **2.60** and aldehyde **2.4** using Crimmin's conditions.^{15,27} We were delighted when the transformation produced the aldol adduct consistently in 88-92% yields with >95:5 diastereoselectivity. The auxiliary was reductively cleaved using sodium borohydride in MeOH, and oxidation of the resulting alcohol using Swern conditions afforded the aldehyde, **2.62**, in 88% yield (Scheme 2.24).



Scheme 2.22 Synthesis of aldehyde **2.62**

Aldehyde **2.62** was reacted with oxazolidinone **2.63** under Crimmin's conditions to afford the adduct **2.6** in 92% yield, again with >95:5 diastereoselectivity. Transamidation of the aldol adduct and protection of the free alcohols as TES ethers proceeded smoothly, yielding Weinreb amide **2.64**.¹¹ Treatment of **2.64** with methylmagnesium bromide in ether afforded the key fragment, methyl ketone **2.35** in 89% yield (Scheme 2.25).¹⁶



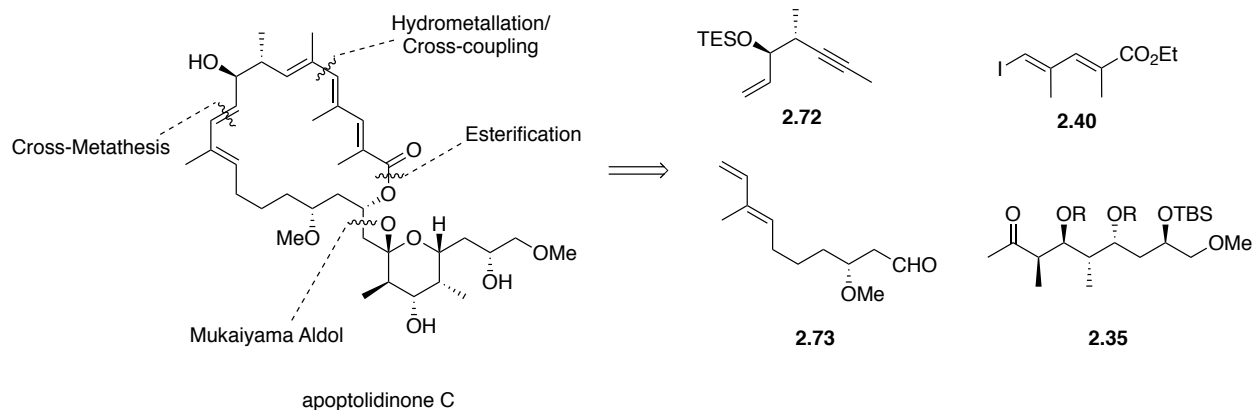
Scheme 2.23 Synthesis of key fragment methyl ketone **2.35**

With our key methyl ketone fragment **2.35** in hand, we turned our attention to the synthesis of **2.56** and **2.57**. Aldol coupling between **2.65** and **2.66** gave disappointing yields, while aldol reaction between **2.65** and **2.67** proceeded in modest yields (Scheme 2.26). Realizing this would serve as a bottleneck in our large scale synthesis, we opted for the high yielding aldol between **2.65** and acrolein (**2.68**), which proceeded in 82% giving good diastereoselectivity (Scheme 2.26).



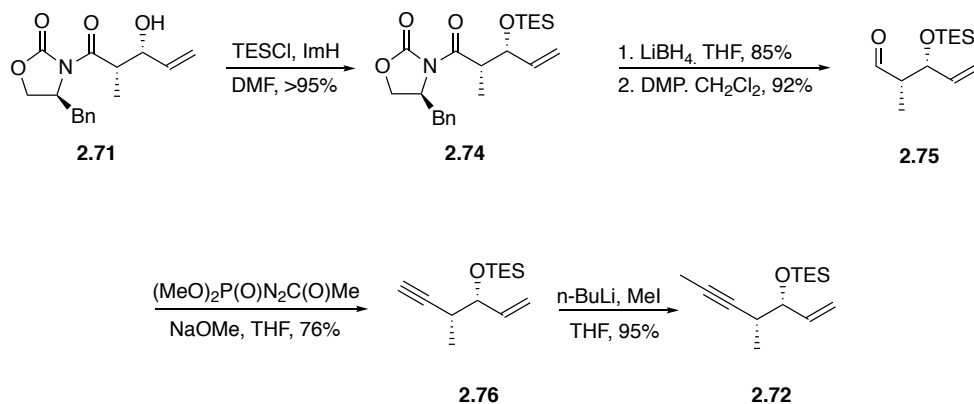
Scheme 2.24 Aldol reactions between auxiliary **2.65** and aldehydes **2.66-2.68**

After investigating aldol couplings to synthesize various cross-coupling partners for the synthesis of the C11-C12 bond, we refined our strategy and considered cross metathesis. This disconnection revealed two new fragments, **2.72** and **2.73**, as targets (Scheme 2.27).



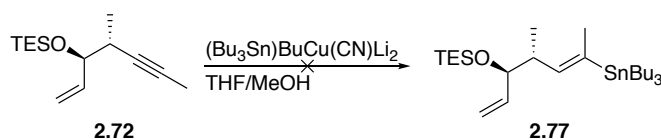
Scheme 2.25 Revised synthetic strategy toward apoptolidinone C

The aldol adduct **2.71** was protected as the TES ether to afford **2.74** in quantitative yield. Reductive cleavage of the auxiliary using lithium borohydride, followed by oxidation of the resulting alcohol with Dess-Martin reagent gave the aldehyde **2.75** in good yields. In a procedure borrowed from Nicolaou, a one carbon homologation via Ohira-Bestmann reagent and subsequent methylation afforded the acetylene (**2.72**) in good yields (Scheme 2.28).^{12,13}



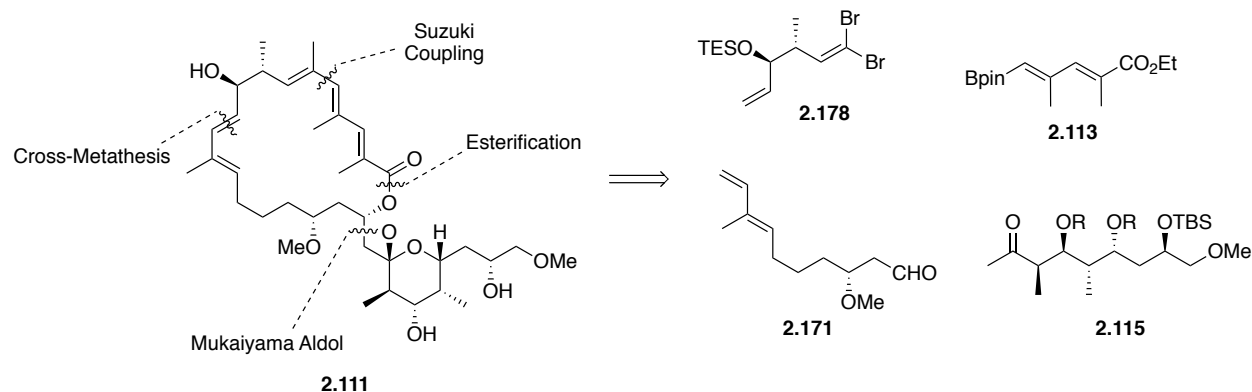
Scheme 2.26 Synthesis of key fragment **2.72** from aldol adduct **2.71**

We then attempted selective hydrometallations of the alkyne moiety of **2.76**, but were unable to effect the desired transformation selectively, or in a manner we deemed scalable and robust (Scheme 2.29).²⁸



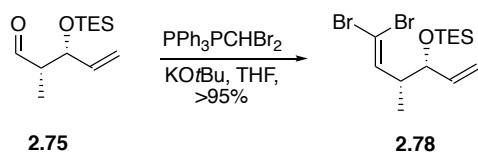
Scheme 2.27 Failed selective hydrostannylation of alkyne **2.77**

Chemistry demonstrated in previous syntheses showed fragment **2.78** could be coupled to fragment **2.34** via Suzuki coupling (Scheme 2.30). Taking advantage of this, we have begun to explore the synthesis of these fragments and investigate cross-couplings.



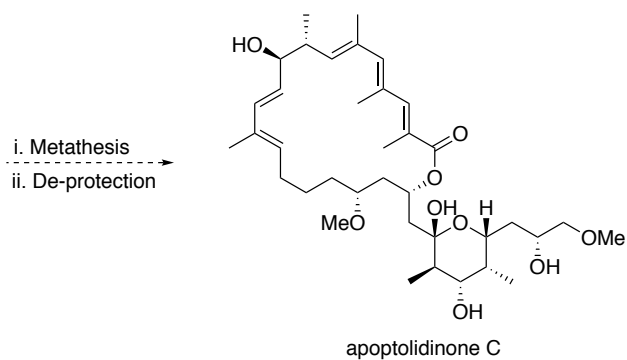
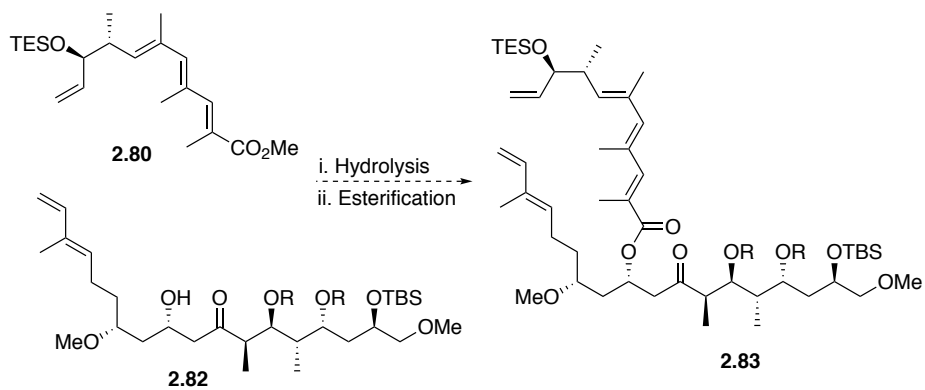
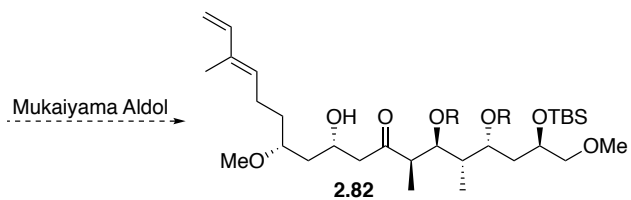
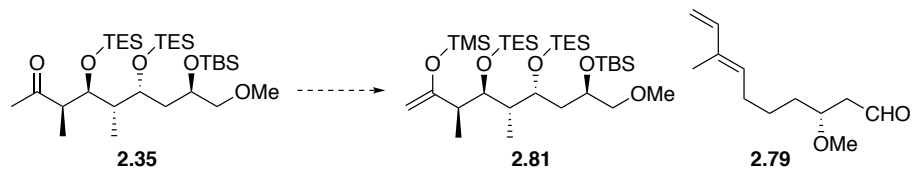
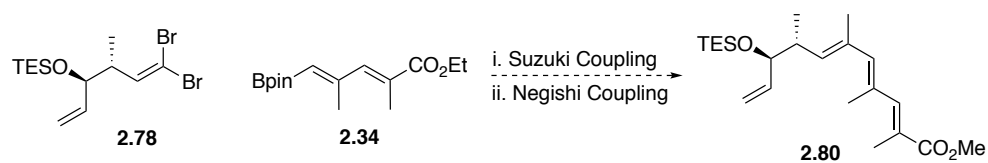
Scheme 2.28 Current strategy toward apoptolidinone C

Wittig like conditions can be used to convert aldehyde **2.75** to the key fragment vinyl bromide **2.178** (Scheme 2.84). Investigation into cross-couplings and unification of our four key fragments is currently underway, and will be facilitated by the scalable and robust routes developed.



Scheme 2.29 Synthesis of key fragment **2.78**

Suzuki coupling between **2.78** and **2.34** followed by Negishi coupling is expected to afford the Northern hemisphere (**2.80**) and Mukaiyama aldol between **2.81** and **2.79** is expected to provide the Southern hemisphere (**2.82**). Esterification is proposed to unify the Northern and Southern hemispheres, and ring closing metathesis is expected to form the macrocycle. Global de-protection will afford apoptolidinone C.



Scheme 2.30 Proposed completion of apoptolidinone C

References

1. Kim, J. W., Adachi, H., Shin-Ya, K., Yoichi, H., Seto, H. Apoptolidin, a New Apoptosis Inducer in Transformed Cells from *Nocardiosis* sp. *J. Antibiot.* **1997**, 50, 628-630.
2. Hayakawa, Y., Kim, J. W., Adachi, H., Shin-ya, K., Fujita, K., Seto, H. Structure of Apoptolidin, a Specific Apoptosis Inducer in Transformed Cells *J. Am. Chem. Soc.* **1998**, 120, 3524-3525.
3. Wender, P. A., Gullledge, A. V., Jankowski, O. D., Seto, H. Isoapoptolidin: Structure and Activity of the Ring-Expanded Isomer of Apoptolidin *Org. Lett.* **2002**, 4, 3819- 3822.
4. Pennington, J. D., Williams, H. J., Salomon, A. R., Sulikowski, G. A. Toward a Stable Apoptolidin Derivative: Identification of Isoapoptolidin and Selective Deglycosylation of Apoptolidin *Org. Lett.* **2002**, 4, 3823-3825.
5. Wender, P. A., Sukopp, M., Longcore, K. Apoptolidins B and C: Isolation, Structure Determination, and Biological Activity *Org. Lett.* **2005**, 7, 3025-3028.
6. Wender, P. A., Longcore, K. E. Isolation, Structure Determination, and Anti-Cancer Activity of Apoptolidin D *Org. Lett.* **2007**, 9, 691-694.
7. Wender, P. A., Longcore, K. E. Apoptolidins E and F, New Glycosylated Macrolactones Isolated from *Nocardiosis* sp *Org. Lett.* **2009**, 23, 5474-5477.
8. Bachmann, B. O., McNeese, R., Melancon, B. J., Ghidu, V. P., Clark, R., Crews, B. C., Deguire, S. M., Marnett, L. J., Sulikowski, G. A. Light-Induced Isomerization of Apoptolidin A leads to Inversion of C2-C3 Double Bond Geometry *Org. Lett.* **2010**, 12, 2944-2947.
9. Deguire, S. M., Earl, D. C., Du, Y., Crews, B. A., Jacobs, A. T., Ustione, A., Daniel, C., Chong, K. M., Marnett, L. J., Piston, D. W., Bachmann, B. O., Sulikowski, G. A. Fluorescent Probes of the Apoptolidins and their Utility in Cellular Localization Studies *Angew. Chem. Int. Ed.* **2015**, 54, 961-964.
10. Sheng, Y., Fotso, S., Serill, J. D., Shahab, S., Santosa, D. W., Ishmael, J. E., Proteau, P. J., Zabriskie, T. M., Mahmud, T. Succinylated Apoptolidins from *Amycolatopsis* sp. ICBB 8242 *Org. Lett.* **2015**, 17, 2526-2529.
11. Schuppan, J., Wehlan, H., Keiper, S., Koert, U. Apoptolidinone A: Synthesis of the Apoptolidin A Aglycone *Chem. Eur. J.* **2006**, 12, 7364-7377.
12. Nicolaou, K. C., Fylaktakidou, K. C., Monenschein, H., Li, Y., Weyershausen, B., Mitchell, H. J., Wei, H.-X., Guntupalli, P., Hepworth, D., Sugita, K. Total Synthesis of Apoptolidin: Construction of Enantiomerically Pure Fragments *J. Am. Chem. Soc.* **2003**, 125, 15433-15442.

13. Nicolaou, K. C., Li, Y., Fylaktakidou, K. C., Mitchell, H. J., Sugita, K. Total Synthesis of Apoptolidin: Part 2. Coupling of Key Building Blocks and Completion of the Synthesis *Angew. Chem. Int. Ed.* **2001**, 40, 3854-3857.
14. Wu, B.; Liu, Q., Sulikowski, G. A. Total Synthesis of Apoptolidinone *Angew. Chem. Int. Ed.* **2004**, 43, 6673-6675.
15. Crimmins, M. T., Christie, H. S., Chaudhary, K., Long, A. Enantioselective Synthesis of Apoptolidinone: Exploiting the Versatility of Thiazolidinethione Chiral Auxiliaries *J. Am. Chem. Soc.* **2005**, 127, 13810-13812.
16. Vargo, T. R., Hale, J. S., Nelson, S. G. Catalytic Asymmetric Aldol Equivalents in the Enantioselective Synthesis of the Apoptolidin C Aglycone *Angew. Chem. Int. Ed.* **2010**, 49, 8678-8681.
17. Salomon, A. R., Voehringer, D. W., Herzenberg, L. A., Khosla, C. Understanding and exploiting the mechanistic basis for selectivity of polyketide inhibitors F₁F₀-ATPase *Proc. Natl. Acad. Sci. U. S. A.* **2000**, 97, 14766-14771.
18. Salomon, A. R., Voehringer, D. W., Herzenberg, L. A., Khosla, C. Apoptolidin, a selective cytotoxic agent, is an inhibitor of F₁F₀-ATPase *Chem. Biol.* **2001**, 8, 71-80.
19. Daniel, P. T., Koert, U., Schuppan, J. Apoptolidin: Induction of Apoptosis by a Natural Product *Angew. Chem. Int. Ed.* **2006**, 45, 872-893.
20. Chong, K. M., Leelatian, N., Deguire, S. M., Brockman, A. A., Earl, D., Ihrie, R. A., Irish, J. M., Bachmann, B. O., Sulikowski, G. A. The use of fluorescently-tagged apoptolidins in cellular uptake and response studies *J. Antibiot.* **2016**, 69, 327-330.
21. Pennington, J. D., Williams, H. J., Salomon, A. R., Sulikowski, G. A. Toward a Stable Apoptolidin Derivative: Identification of Isoapoptolidin and Selective Deglycosylation of Apoptolidin *Org. Lett.* **2002**, 4, 3823-3825.
22. Salomon, A. R., Zhang, Yongbo, Seto, H., Khosla, C. Structure-Activity Relationships within a Family of Selectively Cytotoxic Macrolide Natural Products *Org. Lett.* **2001**, 3, 57-59.
23. Ghidu, V. P., Ntai, I., Wang, J., Jacobs, A. T., Marnett, L. J., Bachmann, B. O., Sulikowski, G. A. Combined Chemical and Biosynthetic Route to Access a New Apoptolidin Congener *Org. Lett.* **2009**, 11, 3032-3034.
24. Jin, B., Liu, Q., Sulikowski, G. A. Development of an end-game strategy towards apoptolidin: a sequential Suzuki coupling approach *Tetrahedron* **2005**, 61, 401-408.
25. Evans, D. A., Clark, J. S., Metternich, R., Novack, V. J., Sheppard, G. S. Diastereoselective Aldol Reactions Using β -Keto Imide Derived Enolates. A Versatile Approach to the Assemblage of Polypropionate Systems *J. Am. Chem. Soc.* **1990**, 112, 866-868.

26. Crimmins, M. T., King, B. W., Tabet, E. A., Chaudhary, K. Asymmetric Aldol Additions: Use of Titanium Tetrachloride and (-)-Sparteine for the Soft Enolization of *N*-Acyl Oxazolidinones, Oxazolidinethiones, and Thiazolidinethiones *J. Org. Chem.* **2001**, 66, 894-902.
27. Aldrich, L. N., Berry, C. B., Bates, B. S., Konkol, L. C., So, M., Lindsley, C. W. Towards the Total Synthesis of Marineosin A: Construction of the Macrocyclic Pyrrole and an Advanced, Functionalized Spiroaminal Model *Eur. J. Org. Chem.* **2013**, 4215-4218.
28. Lipshutz, B. H., Lindsley, C. A Streamlined Route to Highly Conjugated, *All-E* Polyenes Characteristic of Oxo Polyene Macrolide Antibiotics *J. Am. Chem. Soc.* **1997**, 119, 4555-4556.

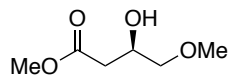
Experimental Procedures

General Procedure: All reactions sensitive to air or moisture were conducted in flame-dried or oven dried glassware under an atmosphere of argon. Reaction temperatures were controlled using a thermocouple thermometer and analog hotplate stirrer. Reactions were conducted at room temperature (rt, approximately 23 °C) unless otherwise noted. Flash column chromatography was conducted using silica gel 230-400 mesh. Analytical thin-layer chromatography (TLC) was performed on E. Merck silica gel 60 F254 plates and visualized using UV, *p*-anisaldehyde stain and potassium permanganate stain. Yields were reported as isolated, spectroscopically pure compounds.

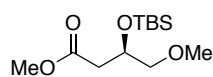
Materials: Solvents were obtained from either an MBraun MB-SPS solvent system or freshly distilled. THF was distilled from sodium/benzophenone. MeOH was dried over magnesium and stored over molecular sieves. CH₂Cl₂ and N-methylpyrrolidinone were dried over CaH₂, distilled, and stored over molecular sieves. Et₃N and diisopropylethylamine were dried over CaH₂, distilled, and stored over KOH pellets. Oxalyl chloride was distilled fresh, prior to use. All starting materials and reagents were used as received unless noted otherwise. The molarity of *n*-butyllithium solutions was determined by titration using diphenylacetic acid as an indicator (average of three determinations).

Instrumentation: ¹H NMR spectra were recorded on Bruker 400, 500, or 600 MHz spectrometers and are reported relative to deuterated solvent signals. Data for ¹H NMR spectra are reported as follows: chemical shift (δ ppm), multiplicity (s = singlet, d = doublet, t = triplet, q = quartet, p = pentet, m = multiplet, br = broad, app = apparent), coupling constants (Hz), and integration. ¹³C NMR spectra were recorded on Bruker 100, 125, or 150 MHz spectrometers and are reported relative to deuterated solvent signals.

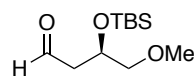
Chemical Synthesis:



S3: To a suspension of $[\text{RuCl}_2(\text{C}_6\text{H}_6)]_2$ (126 mg, 0.25 mmol) in DMF (5.0 mL) at 115 °C was added (*S*)-BINAP (255 mg, 0.41 mmol). The resulting slurry was stirred over 15 min. After cooling to room temperature, the solution was transferred into a hydrogenation apparatus. A solution of methyl **2.3** (9.97 g, 68.2 mmol) in MeOH (30 mL) was transferred into the hydrogenation apparatus. The apparatus was filled with hydrogen (10 bar) and stirred at 95 °C over 72 h. Upon completion, the reaction mixture was cooled to room temperature and concentrated *in vacuo*. The resulting residue was purified by flash column chromatography (1:2 hexanes/ethyl acetate) to yield the product **S3** (8.5 g, 84%) as a yellow oil. ^1H NMR (400 MHz, CDCl_3): δ = 4.13 (m, 1H), 3.71 (s, 3H), 3.42 (m, 2H), 3.40 (s, 3H), 2.95 (d, 1H), 2.54 (d, 2H); ^{13}C NMR (100 MHz, CDCl_3): δ = 171.7, 75.3, 66.2, 58.3, 51.0, 37.7. Identical in all respects to published data

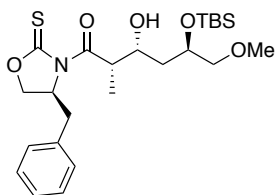


S4: To a solution of Alcohol **S3** (8.15 g, 55.0 mmol) in DMF (80 mL) at 0°C was added imidazole (8.6 g, 127.0 mmol) and TBSCl (21.6 g, 71.5 mmol). The reaction was allowed to stir at room temperature for 18 h. Reaction was quenched with sat. aq. NH_4Cl (150 mL). The aqueous layer was extracted with diethyl ether (3 x 100 ml) and the combined organic extracts were washed with brine, dried (MgSO_4), filtered, and concentrated *in vacuo*. The residue was purified by flash column chromatography (5:1 hexanes/ethyl acetate) to yield the product **S4** (14.2 g, >95%) as a colorless oil. ^1H NMR (400 MHz, CDCl_3): δ = 4.25 (m, 1H), 3.65 (s, 3H), 3.31 (s, 3H), 3.27 (dd, 1H), 2.58 (dd, 1H), 2.44 (dd, 1H) 0.84 (s, 9H), 0.06, 0.03 (2s, 6H); ^{13}C NMR (100 MHz, CDCl_3): δ = 171.7, 76.5, 68.2, 58.8, 51.3, 40.1, 25.6, 17.9, -4.7, -5.3. Identical in all respects to published data

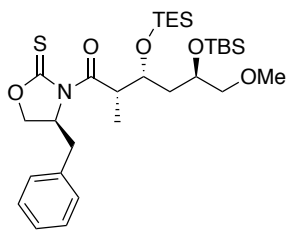


2.4: To a stirred solution of Ester **S4** (9.3 g, 35.5 mmol) in CH_2Cl_2 (250 mL) at -78 °C was added DiBAIH dropwise (42.6 mL, 1.0 M in hexanes) over 2 h. After complete addition, the reaction was allowed to stir at -78 °C for 1 h. The reaction was quenched with MeOH (20 mL), added to a solution of Rochelle's salt (700 mL, 1.0 M), and stirred for 3 h. The layers were separated and the aqueous layer was extracted with CH_2Cl_2 (3 x 100 mL). The combined organic extracts were dried (MgSO_4), filtered, and concentrated *in vacuo*. The residue

was purified by flash column chromatography (10:1 hexanes/ethyl acetate) to yield aldehyde **2.4** (7.26 g, 88%) as a colorless oil. ^1H NMR (400 MHz, CDCl_3): δ = 9.81 (s, 1H), 4.36 (m, 1H), 3.44 (dd, 1H), 3.34 (s, 3H), 3.32 (dd, 1H), 2.56 (m, 2H), 0.88 (s, 9H), 0.10, 0.09 (2s, 6H); ^{13}C NMR (100 MHz, CDCl_3): δ = 201.3, 76.6, 67.1, 59.1, 48.7, 25.6, 17.7, -4.5, -4.9. Identical in all respects to published data

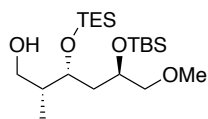


S5: To a solution of acyloxazolidinethione (6.82 g, 27.4 mmol) in CH_2Cl_2 (110 mL) at 0 °C was added TiCl_4 (30.2 mL, 1.0 M in CH_2Cl_2). The yellow slurry was stirred for 15 min at 0 °C. Diisopropylethylamine (4.77 mL, 27.4 mmol) was added slowly and the reaction was stirred for 40 min at 0 °C. N-methylpyrrolidinone (2.64 mL, 27.4 mmol) was added the reaction was stirred an additional 10 min. A solution of aldehyde **2.4** (7.0 g, 30.2 mmol) in CH_2Cl_2 (10 mL) was added dropwise. After complete addition, the reaction was stirred at 0 °C for 1.5 h. The reaction was quenched with sat. aq. NH_4Cl and the aqueous layer was extracted with CH_2Cl_2 (3 x 150 mL). The combined organic extracts were dried (MgSO_4), filtered, and concentrated *in vacuo*. The residue was purified by flash column chromatography (10:1 to 6:1 hexanes/ethyl acetate) to yield the *syn* aldol adduct **S5** (12.2 g, 92%) as a separable >95:5 mixture of diastereomers. ^1H NMR (400 MHz, CDCl_3): δ = 7.37-7.22 (m, 5H), 4.96 (m, 1H), 4.72 (m, 1H), 4.32 (m, 3H), 4.11 (m, 1H), 3.40 (m, 2H), 3.36 (s, 3H), 3.29 (dd, 1H), 2.80 (dd, 1H), 1.80 (m, 1H), 1.68 (m, 1H), 1.33 (d, 3H), 0.90 (s, 9H), 0.12, 0.11 (2s, 6H); ^{13}C NMR (100 MHz, CDCl_3): δ = 185.1, 177.0, 135.1, 129.3, 128.9, 127.3, 70.0, 69.6, 68.6, 65.7, 60.2, 59.0, 53.3, 43.0, 38.3, 37.4, 25.7, 18.0, 15.1, 10.7, -4.66, -5.04. Identical in all respects to published data

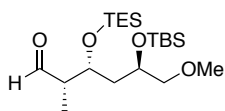


2.61: To a solution of alcohol **S5** (5.2 g, 10.8 mmol) in DMF (18 mL) at 0 °C was added imidazole (2.2 g, 32.4 mmol) followed by TESCl (4.88 g, 32.4 mmol). The reaction was stirred at 0 °C for 3 h and quenched with water (50 mL). The aqueous layer was extracted with diethyl ether (3 x 70 mL). The combined organic extracts were washed with water, dried (MgSO_4), filtered, and concentrated *in vacuo*. The residue was purified by flash column chromatography (20:1 hexanes/ethyl acetate) to yield the product **2.61** (6.4 g, >95%) as a colorless

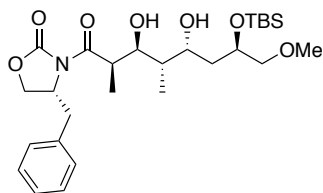
oil. ^1H NMR (400 MHz, CDCl_3): δ = 7.37-7.22 (m, 5H), 4.83 (m, 2H), 4.29 (m, 1H), 4.19 (m, 2H), 3.95 (m, 1H), 3.33 (m, 4H), 2.78 (m, 1H), 1.69 (m, 2H), 1.37 (d, 3H), 0.99 (s, 9H), 0.60 (m, 15H), 0.11, 0.10 (2s, 6H); ^{13}C NMR (100 MHz, CDCl_3): δ = 185.0, 175.9, 135.3, 129.3, 128.8, 127.2, 71.4, 69.0, 68.6, 60.7, 59.0, 43.4, 37.2, 25.8, 22.5, 13.9, 12.3, 6.81, 6.43, -3.94, -4.71. Identical in all respects to published data



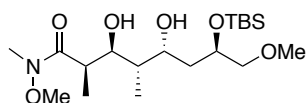
S6: To a solution of **2.61** (7.85 g, 13.2 mmol) in MeOH (100 mL) at 0 °C was added sodium borohydride (2.99 g, 79.0 mmol). The reaction was stirred at 0 °C for 3 h and the volatiles were removed *in vacuo*. The residue was partitioned between water (70 mL) and CH_2Cl_2 (90 mL). The aqueous layer was extracted with CH_2Cl_2 (3 x 100 mL) and the combined organic extracts were washed with brine, dried (MgSO_4), filtered and concentrated *in vacuo*. The residue was purified by flash column chromatography (10:1 hexanes/ethyl acetate) to yield the product **S6** (4.2 g, 79%) as a colorless oil. ^1H NMR (400 MHz, CDCl_3): δ = 4.13 (m, 1H), 3.99 (m, 1H), 3.87 (m, 1H), 3.68 (m, 1H), 3.32 (s, 3H), 3.30 (m, 2H), 2.74 (m, 1H), 2.00 (m, 1H), 1.69 (t, 2H), 0.98 (s, 9H), 0.87 (m, 12H), 0.64 (m, 6H), 0.08, 0.07 (2s, 6H); ^{13}C NMR (100 MHz, CDCl_3): δ = 77.6, 73.1, 69.2, 65.6, 58.5, 40.0, 38.0, 25.7, 18.0, 11.9, 6.68, 6.43, 5.68, 5.00, -3.94, -4.86. Identical in all respects to published data



2.62: To a solution of $(\text{COCl})_2$ (0.043 mL, 0.493 mmol) in CH_2Cl_2 (1.0 mL) at -78 °C was added DMSO (0.070 mL, 0.986 mmol). The mixture was stirred at -78 °C for 15 min before a solution of alcohol **S6** (125 mg, 0.308 mmol) in CH_2Cl_2 (1.0 mL) was added. The mixture was stirred for 15 min before adding triethylamine (0.216 mL, 1.54 mmol). The reaction was allowed to stir at -78 °C for 15 min then at 0 °C for 40 min. The reaction was quenched with water (10 mL) and the aqueous layer was extracted with CH_2Cl_2 (3 x 20 mL). The combined organic extracts were washed with brine, dried (MgSO_4), filtered and concentrated *in vacuo*. The residue was purified by flash column chromatography (20:1 hexanes/ethyl acetate) to afford the aldehyde **2.62** (100 mg, 80%) as a light yellow oil. ^1H NMR (400 MHz, CDCl_3): δ = 9.81 (s, 1H), 4.31 (m, 1H), 3.88 (m, 1H), 3.35 (s, 3H), 3.31 (d, 2H), 2.53 (m, 1H), 1.68 (m, 2H), 1.08 (d, 3H), 0.96 (s, 9H), 0.90 (m, 12H), 0.63 (m, 6H), 0.10 (s, 6H); ^{13}C NMR (100 MHz, CDCl_3): δ = 205.0, 77.5, 69.7, 69.1, 58.7, 52.1, 40.0, 25.8, 18.0, 6.76, 6.49, 5.37, 5.08, -4.00, -4.75. Identical in all respects to published data.

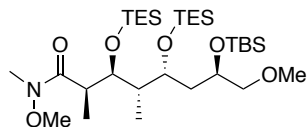


2.6: To a solution of propionyloxazolidinone (1.3 g, 5.64 mmol) in CH_2Cl_2 (25 mL) at 0°C was added TiCl_4 (6.2 mL, 1.0 M in CH_2Cl_2). The yellow slurry was stirred for 15 min. Diisopropylethylamine (0.98 mL, 5.64 mmol) was added and the reaction was stirred for 40 min at 0°C . N-methylpyrrolidinone (0.54 mL, 5.64 mmol) was added and the reaction was stirred for 10 min. A solution of aldehyde **2.62** (2.5 g, 6.2 mmol) in CH_2Cl_2 (5.0 mL) was added dropwise. After complete addition, the reaction was stirred at 0°C for 1.5 h. The reaction was quenched with sat. aq. NH_4Cl (10 mL) and the aqueous layer was extracted with CH_2Cl_2 (3 x 20 mL). The combined organic extracts were washed with water, dried (MgSO_4), filtered, and concentrated *in vacuo*. The residue was purified by flash column chromatography (6:1 \rightarrow 2:3 hexanes/ethyl acetate) to afford the product **2.6** (2.7 g, 92%) as a separable >95:5 mixture of diastereomers. ^1H NMR (400 MHz, CDCl_3): $\delta = 7.33\text{--}7.21$ (m, 5H), 4.69 (m, 1H), 4.19 (m, 2H), 4.11 (m, 2H), 4.09 (m, 2H), 3.39 (m, 2H), 3.33 (s, 3H), 3.29 (dd, 1H), 2.80 (dd, 1H), 1.84 (m, 2H), 1.60 (m, 1H), 1.25 (d, 3H), 0.87 (s, 9H), 0.09, 0.08 (2s, 6H); ^{13}C NMR (100 MHz, CDCl_3): $\delta = 176.9, 152.9, 135.2, 129.3, 128.8, 127.2, 77.3, 73.6, 71.8, 70.7, 66.0, 60.2, 55.4, 40.0, 39.3, 37.62, 36.4, 25.7, 17.9, 11.8, 9.73, -4.68, -5.01$. Identical in all respects to published data



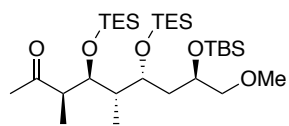
S7: To a solution of Weinreb salt (519 mg, 5.32 mmol) in CH_2Cl_2 (8.0 mL) at -10°C , added AlMe_3 (2.66 mL, 2.0 M in hexanes). The mixture was allowed to stir at room temperature for 1 h. The reaction was cooled to -10°C and a solution of adduct **2.6** (400 mg, 0.76 mmol) in CH_2Cl_2 (8 mL) was added. The reaction was stirred at -10°C over 4 h. The mixture was then transferred via cannula to a solution of aq. Rochelle's salt (60 mL, 1.0 M) and stirred overnight. The two layers were separated and the aqueous layer was extracted with CH_2Cl_2 (3 x 60 mL). The combined organic extracts were washed with brine, dried (MgSO_4), filtered, and concentrated *in vacuo*. The residue was purified by flash column chromatography (4:1 \rightarrow 1:1 hexanes/ethyl acetate) to afford the product **S7** (310 mg, 80%) as a colorless oil. ^1H NMR (400 MHz, CDCl_3): $\delta = 4.37$ (s, 1H), 4.10 (m, 1H), 4.09 (1H), 3.85 (m, 1H), 3.71 (br s, 1H), 3.68 (s, 3H), 3.38 (m, 2H), 3.33 (s, 3H), 3.17 (s, 3H), 3.07 (br m, 1H), 1.81 (m, 2H), 1.50 (m, 1H), 1.17 (d, 3H), 0.87 (s, 9H), 0.09, 0.07 (2s, 6H); ^{13}C NMR (100 MHz, CDCl_3):

$\delta = 178.2, 77.2, 74.3, 69.9, 69.3, 60.8, 58.9, 39.2, 37.4, 32.3, 25.9, 18.0, 11.9, 10.0, -4.56, -5.06$.
Identical in all respects to published data



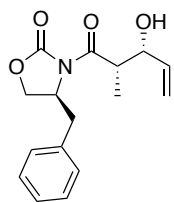
2.64: To a solution of amide **S7** (250 mg, 0.61 mmol) in CH_2Cl_2 (10 mL) stirring at 0°C was added imidazole (332 mg, 4.9 mmol) and TESCO (0.62 mL, 3.7 mmol). The solution was stirred at 0°C for 3 h.

The reaction was quenched with pH = 7 phosphate buffer (10 mL). The two layers were separated and the aqueous layer was extracted with ether (3 x 10 mL). The combined organic extracts were dried (MgSO_4), filtered, and concentrated *in vacuo*. The residue was purified by flash column chromatography (20:1 hexanes/ethyl acetate) to afford the product **2.64** (370 mg, >95%) as a colorless oil. ^1H NMR (400 MHz, CDCl_3): $\delta = 4.14$ (m, 1H), 3.99 (m, 1H), 3.74 (m, 1H), 3.66 (s, 3H), 3.32 (s, 3H), 3.31 (m, 2H), 3.16 (s, 3H), 2.97 (m, 1H), 1.80 (m, 2H), 1.47 (m, 1H), 1.03 (d, 3H), 0.92 (s, 9H), 0.88 (m, 12H), 0.52 (m, 6H), 0.07 (s, 6H). ^{13}C NMR (100 MHz, CDCl_3): $\delta = 176.2, 77.2, 73.71, 69.6, 69.3, 60.4, 58.6, 42.1, 40.3, 38.7, 31.4, 25.7, 22.5, 18.0, 13.9, 9.71, 10., 10.5, -4.48, -4.87$. Identical in all respects to published data

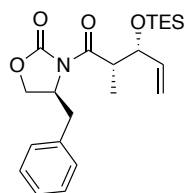


2.35: To a solution of amide **2.64** (250 mg, 0.39 mmol) in THF (0.39 mL) at 0°C , added CH_3MgCl (0.39 mL, 3.0 M in THF) dropwise. The reaction was allowed to stir for 30 min, before quenching with sat. aq. NH_4Cl (10 mL).

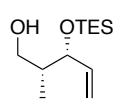
The layers were separated and the aqueous layer was extracted with CH_2Cl_2 (3 x 10 mL). The combined organic extracts were dried (MgSO_4), filtered, and concentrated *in vacuo*. The residue was purified by flash column chromatography (20:1 hexanes/ethyl acetate) to afford the product **2.35** (208 mg, 89%) as a colorless oil. ^1H NMR (400 MHz, CDCl_3): $\delta = 4.26$ (m, 1H), 3.95 (m, 1H), 3.71 (m, 1H), 3.33 (s, 3H), 3.29 (m, 2H), 2.70 (m, 1H), 2.15 (s, 3H), 1.78 (m, 2H), 1.62 (m, 1H), 1.09 (d, 3H), 0.92 (s, 9H), 0.88 (m, 12H), 0.52 (m, 6H), 0.69 (s, 6H); ^{13}C NMR (100 MHz, CDCl_3): $\delta = 210.1, 73.0, 70.1, 69.3, 58.8, 50.2, 42.8, 40.5, 28.5, 25.8, 11.9, 9.72, 9.41, 7.00, 5.91, 5.33, -4.36, -4.75$. Identical in all respects to published data.



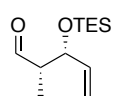
2.71: To a solution of propionylloxazolidinone (3.00 g, 12.84 mmol) in CH₂Cl₂ (53.5 mL) at 0 °C was added TiCl₄ (14.12 mL, 1 M in CH₂Cl₂). The yellow slurry was stirred for 15 min at 0 °C. Diisopropylethylamine (2.23 mL, 12.84 mmol) was added slowly and the reaction was stirred for 40 min at 0 °C. Added N-methylpyrrolidinone (1.24 mL, 12.84 mmol) and stirred for 10 min. A solution of acrolein (792 mg, 14.12 mmol) in CH₂Cl₂ (5 mL) was added dropwise. After complete addition, the reaction was stirred at 0 °C over 1.5 h. The reaction was quenched with sat. aq. NH₄Cl (150 mL) and the aqueous layer was extracted with CH₂Cl₂ (3 x 150 mL). The combined organic extracts were dried (MgSO₄), filtered, and concentrated *in vacuo*. The residue was purified by flash column chromatography (4:1 petroleum ether/ethyl acetate) to yield the *syn* aldol adduct **2.71** (3.26 g, 81%). ¹H NMR (400 MHz, CDCl₃): δ = 7.18-7.32 (m, 5H), 5.84 (m, 1H), 5.37 (d, *J* = 17.24, 1H), 5.23 (d, *J* = 10.6 Hz, 1H), 4.70 (m, 1H), 4.50 (br. s, 1H), 4.19 (m, 2H), 3.87 (m, 1H), 3.26 (d, *J* = 10.4 Hz, 1H), 2.79 (m, 1H), 1.25 (d, *J* = 7.0 Hz, 3H); ¹³C NMR (100 MHz, CDCl₃): δ = 176.4, 153.1, 137.4, 135.0, 129.4, 128.9, 127.3, 116.1, 72.6, 66.2, 55.1, 42.5, 37.7, 11.1. Identical in all respects to published data



2.74: To a solution of alcohol **2.71** (1.34 g, 4.6 mmol) in CH₂Cl₂ (34 mL) at 0 °C was added imidazole (940 mg, 13.8 mmol) and TESCl (2.08 g, 13.8 mmol). The reaction was allowed to warm to room temperature, stirred for 16 h and quenched with water (50 mL). The aqueous layer was extracted with CH₂Cl₂ (3 x 30 mL). The combined organic extracts were washed with water, dried (MgSO₄), filtered, and concentrated *in vacuo*. The residue was purified by flash column chromatography (8:1 hexanes/ethyl acetate) to yield the product **2.74** (1.83 g, >95%) as a colorless oil. ¹H NMR (400 MHz, CDCl₃): δ = 7.15-7.25 (m, 5H), 5.79 (m, 1H), 5.14 (d, *J* = 17.2, 1H), 5.04 (d, *J* = 10.36, 1H), 4.53 (ddd, 1H), 4.24 (t, 1H), 4.06 (m, 2H), 3.95 (m, 1H), 3.18 (d, *J* = 16.48 Hz, 1H), 2.69 (m, 1H), 1.14 (d, 3H), 0.86 (m, 9H), 0.51 (m, 6H); ¹³C NMR (CDCl₃, 100 MHz): δ = 174.7, 153.2, 139.1, 135.3, 129.4, 128.9, 127.2, 115.7, 75.5, 65.9, 55.6, 43.9, 37.8, 29.6, 12.7, 6.7, 4.8.



S8: To a solution of **2.74** (700 mg, 1.74 mmol) in THF (16 mL) stirring at 0 °C was added LiBH₄ (2.0 M in THF, 3.47 mL) dropwise. Let warm to room temperature and stirred for 5 h. The reaction was cooled to 0 °C and quenched by dropwise addition of water. The aqueous layer was extracted with diethyl ether (3 x 10 mL). The combined organic extracts were dried (MgSO₄), filtered, and concentrated *in vacuo*. The residue was purified by flash column chromatography (8:1 hexanes/ethyl acetate) to yield the alcohol **S7** (340 mg, 85%) as a colorless oil. ¹H NMR (400 MHz, CDCl₃): δ = 5.88 (m, 1H), 5.24 (d, *J* = 17.3 Hz, 1H), 5.19 (d, *J* = 10.5 Hz, 1H), 4.24 (t, 1H), 3.65 (m, 1H), 3.49 (m, 1H), 3.02 (br s, 1H), 2.01 (m, 1H), 0.94 (m, 9H), 0.78 (d, 3H), 0.59 (m, 6H); ¹³C NMR (CDCl₃, 100 MHz): δ = 137.4, 116.0, 65.7, 40.6, 12.4, 6.7, 4.7.



2.75: To a solution of the alcohol **S8** (78 mg, 0.339 mmol) in CH₂Cl₂ (6.5 mL) was added Dess-Martin Reagent (215 mg, 0.508 mmol) and NaHCO₃ (24 mg, 0.291 mmol). The reaction was stirred at room temperature for 1 h. The reaction was quenched with sat. aq. Na₂S₂O₃ (8 mL). The layers were separated and the aqueous layer was extracted with CH₂Cl₂ (3 x 10 mL). The combined organic extracts were dried (MgSO₄), filtered, and concentrated *in vacuo*. The residue was purified by flash column chromatography (8:1 hexanes/ethyl acetate) to yield the aldehyde **2.75** (63 mg, 82%) as a colorless oil. ¹H NMR (400 MHz, CDCl₃): δ = 9.76 (d, *J* = 1.3 Hz, 1H), 5.82 (m, 1H), 5.26 (d, 1H), 5.17 (d, 1H), 4.52 (t, 1H), 2.47 (m, 1H), 1.05 (d, *J* = 6.8 Hz, 3H), 0.91 (m, 9H), 0.58 (m, 6H); ¹³C NMR (CDCl₃, 100 MHz): δ = 204.6, 138.3, 115.9, 73.7, 52.5, 8.4, 6.7, 4.8. Identical in all respects to published data

Appendix A2:

Spectra Relevant to Chapter II

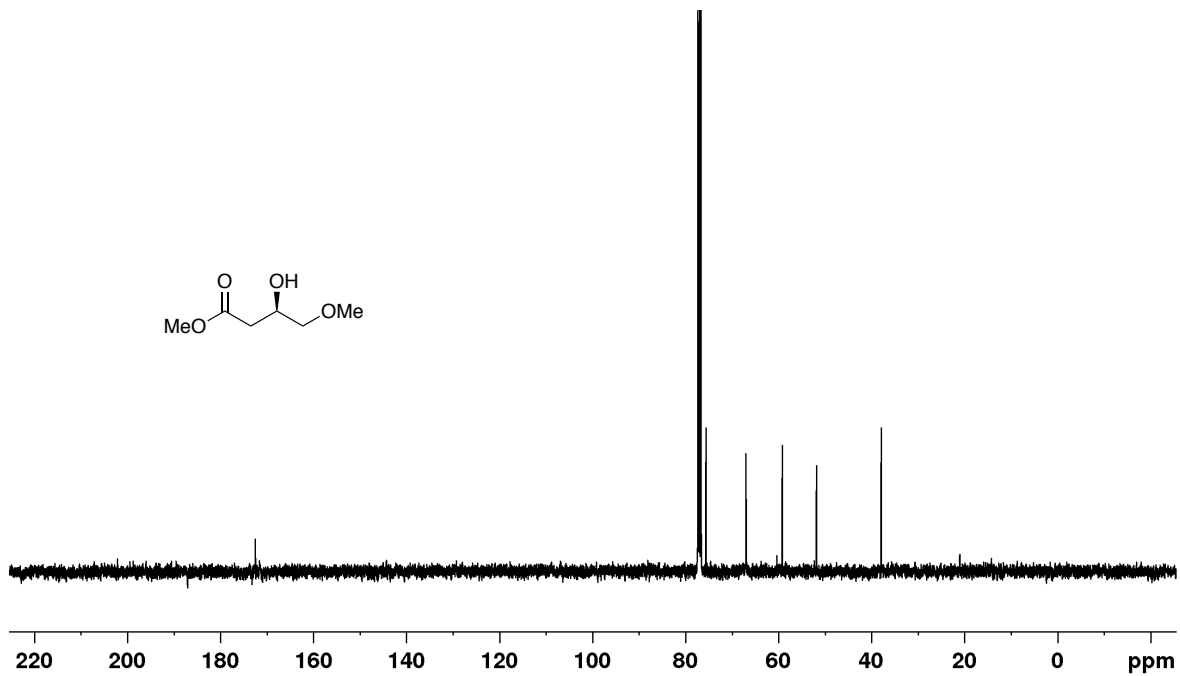
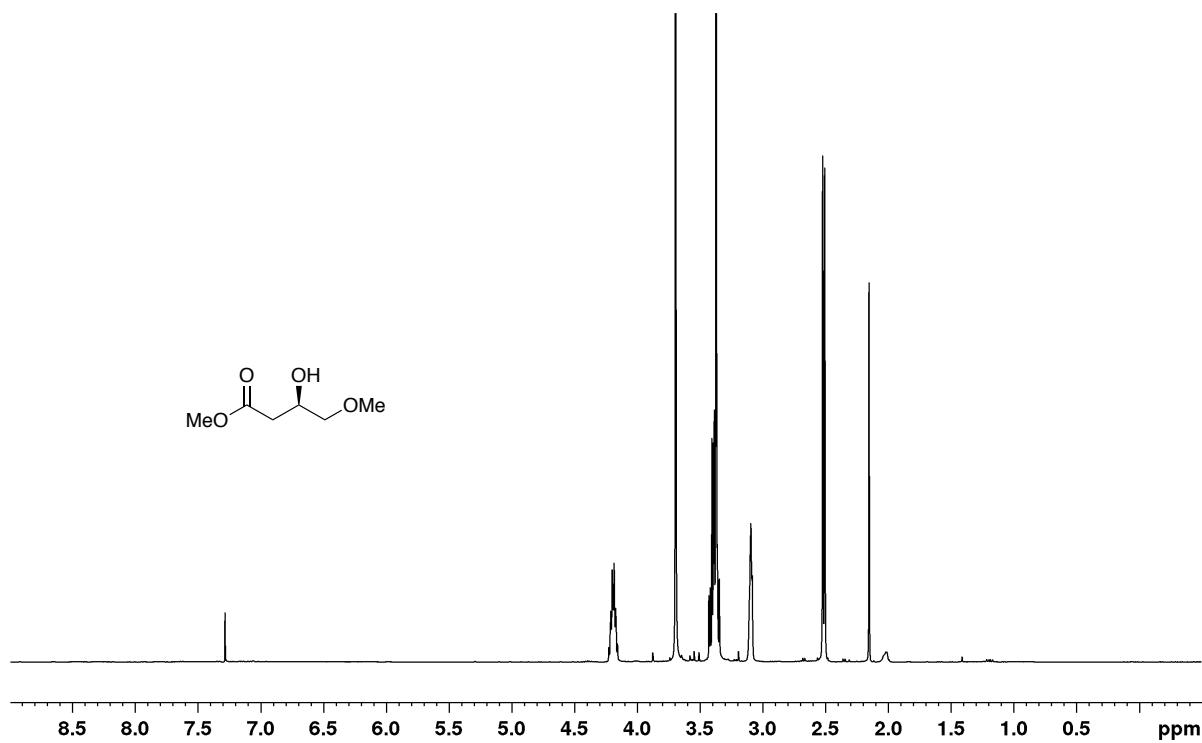


Figure A2.1 400 MHz $^1\text{H-NMR}$ and 100 MHz $^{13}\text{C-NMR}$ spectrum of **S3** in CDCl_3

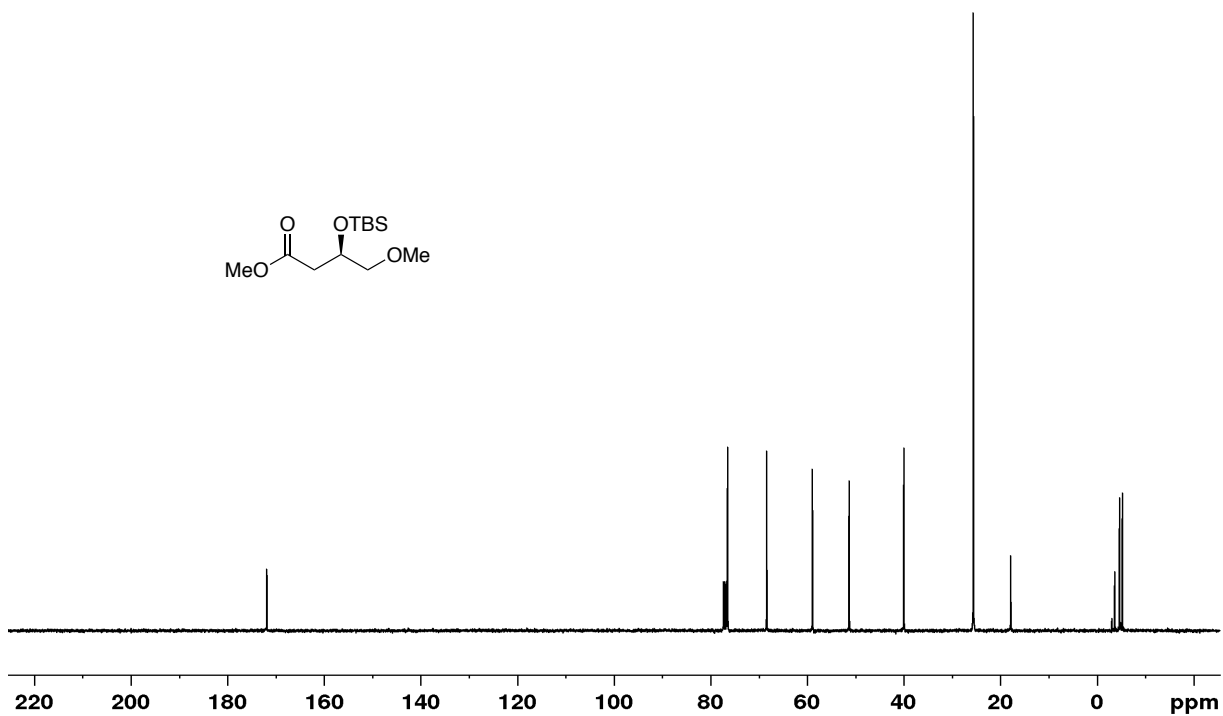
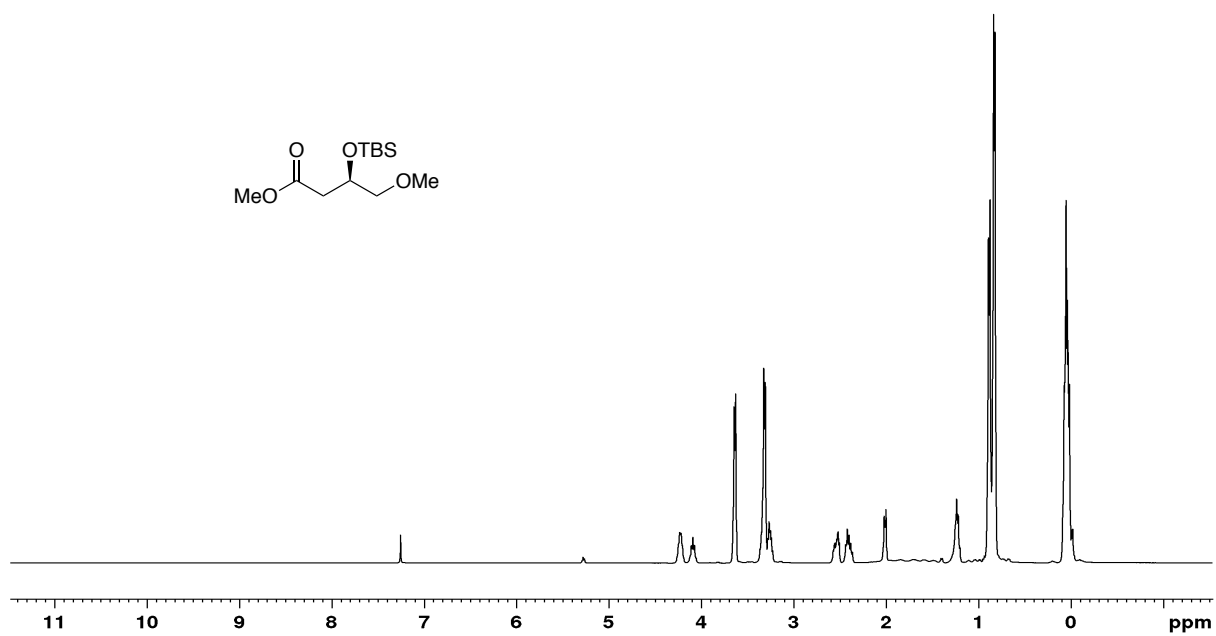


Figure A2.2 400 MHz $^1\text{H-NMR}$ and 100 MHz $^{13}\text{C-NMR}$ spectrum of **S4** in CDCl_3

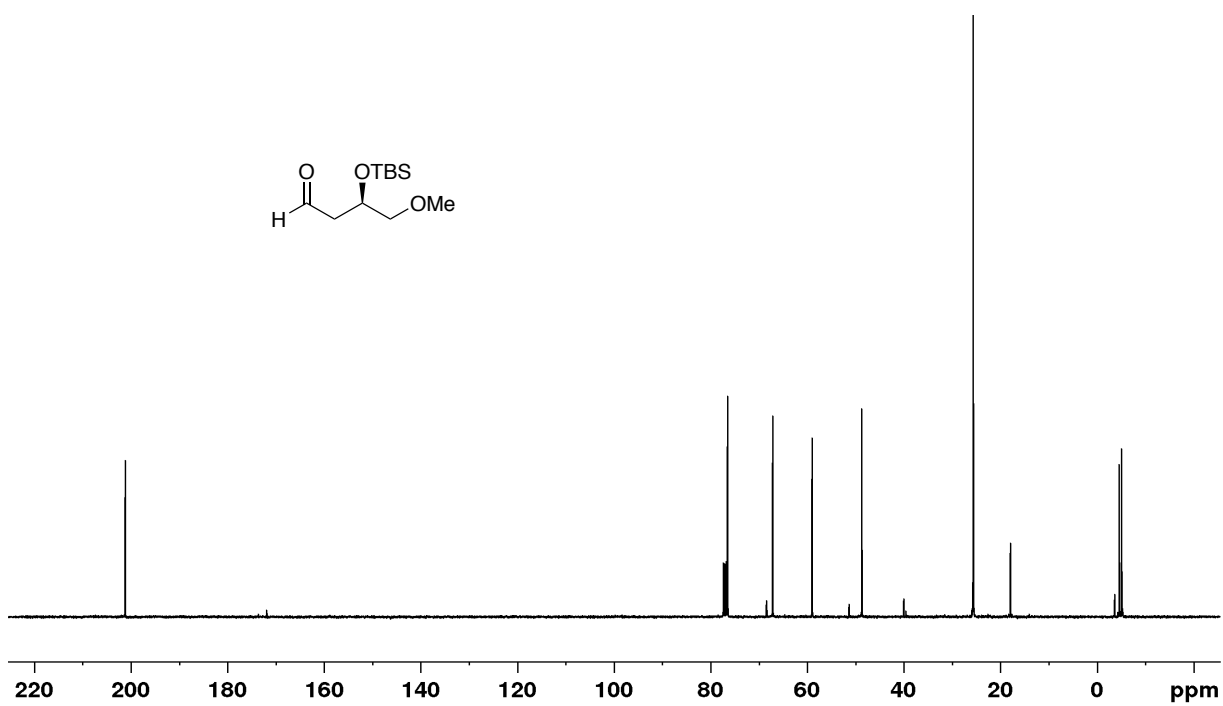
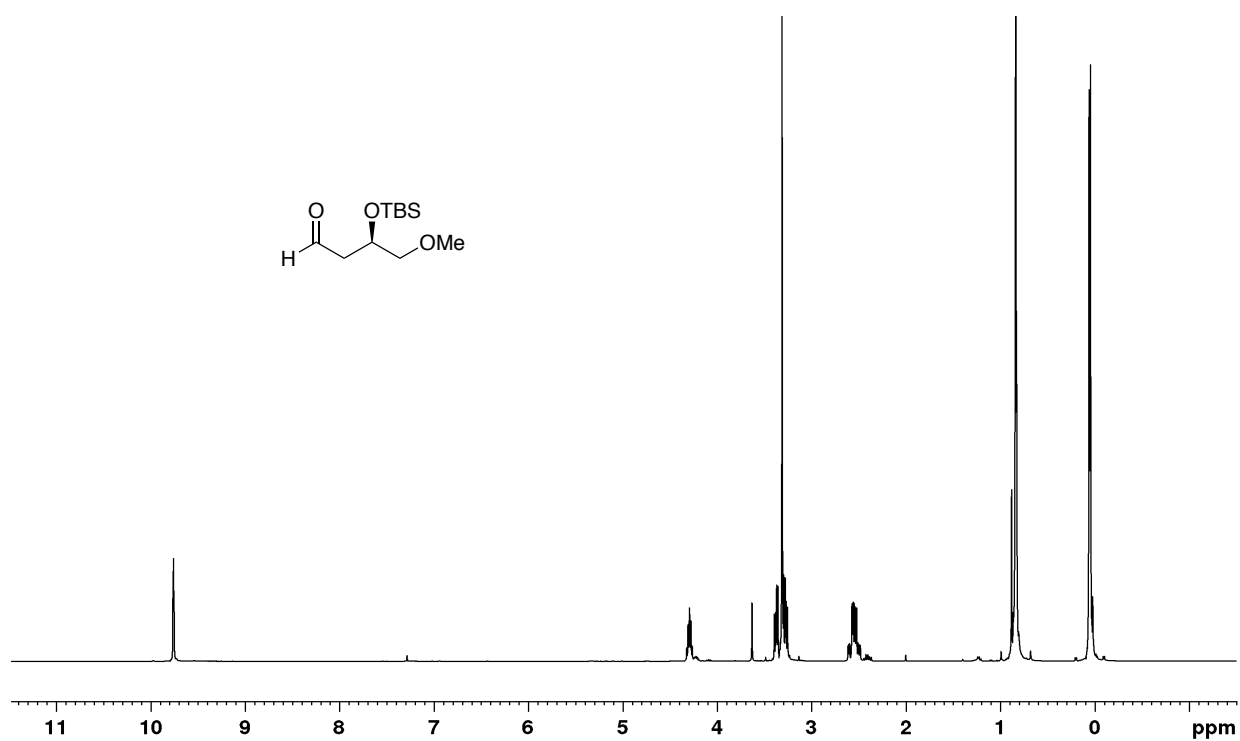


Figure A2.3 400 MHz ^1H -NMR and 100 MHz ^{13}C -NMR spectrum of **2.4** in CDCl_3

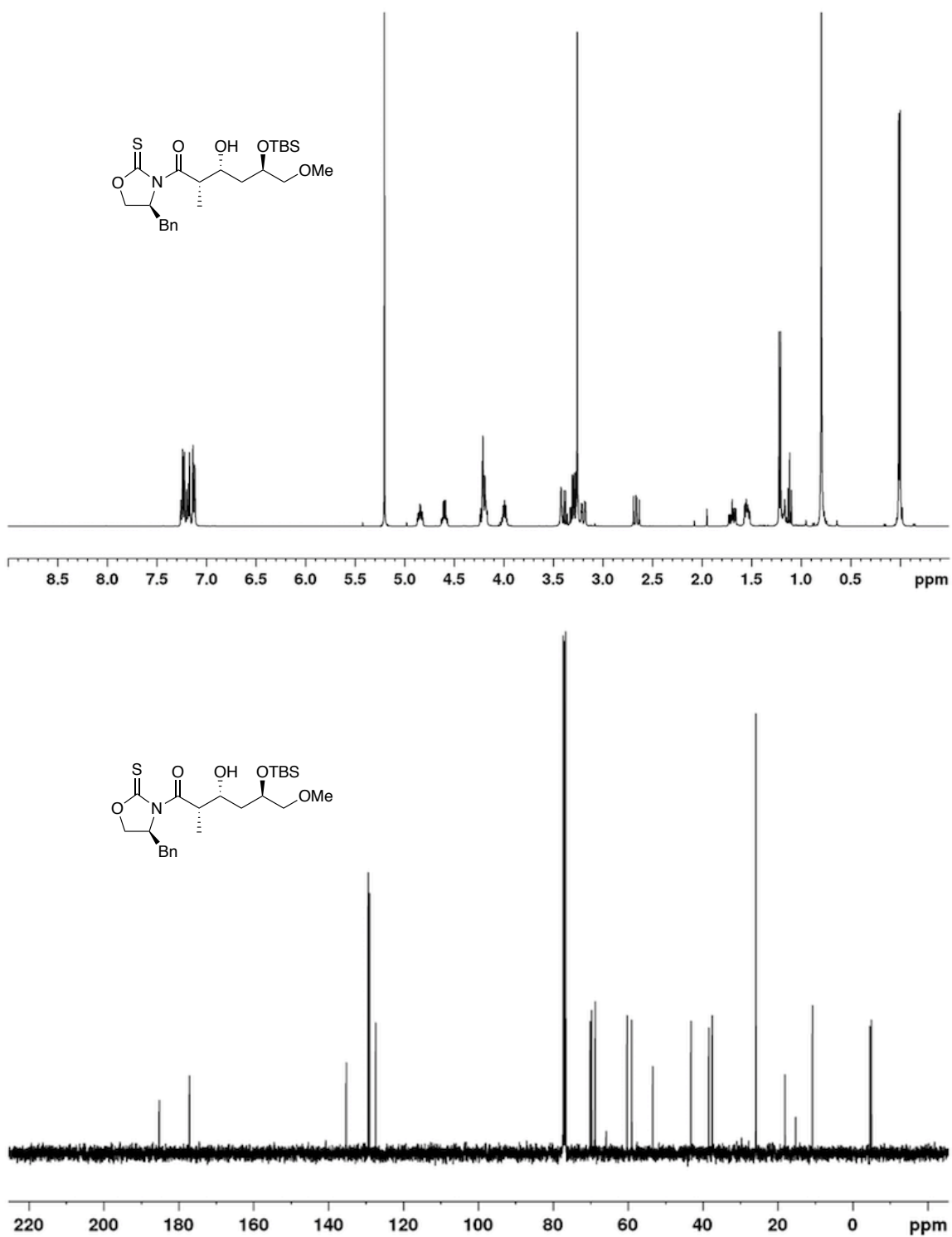


Figure A2.4 400 MHz $^1\text{H-NMR}$ and 100 MHz $^{13}\text{C-NMR}$ spectrum of S5 in CDCl_3

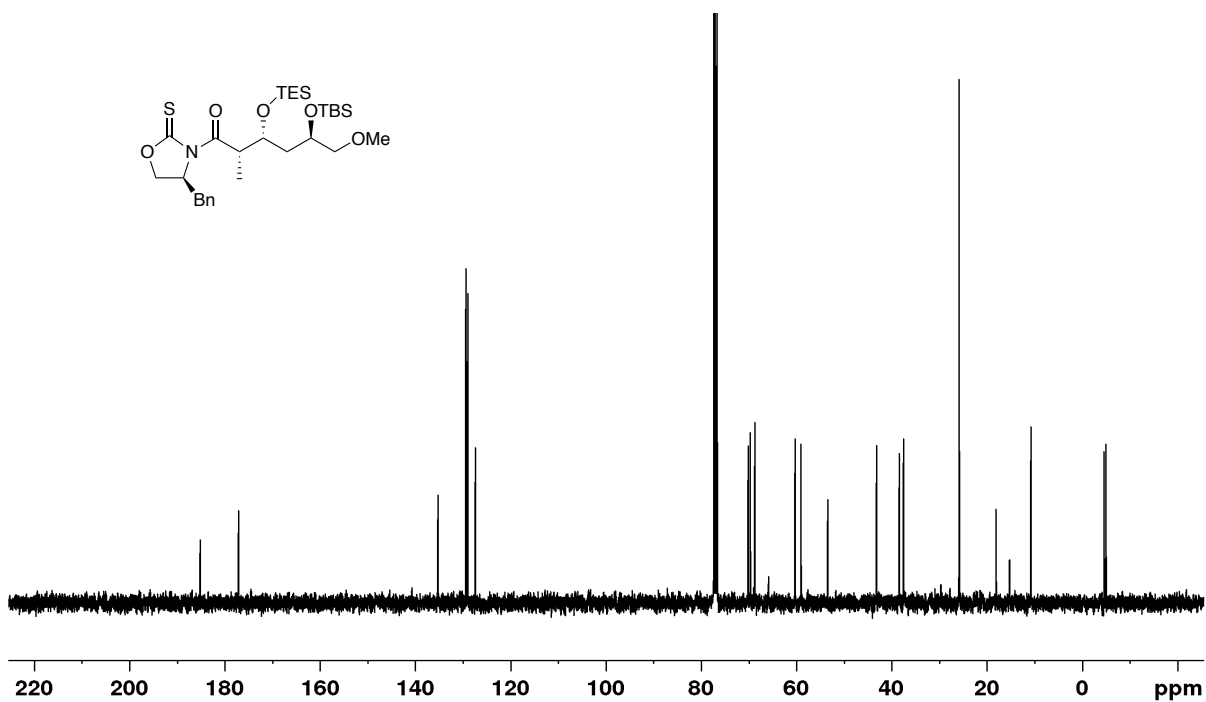
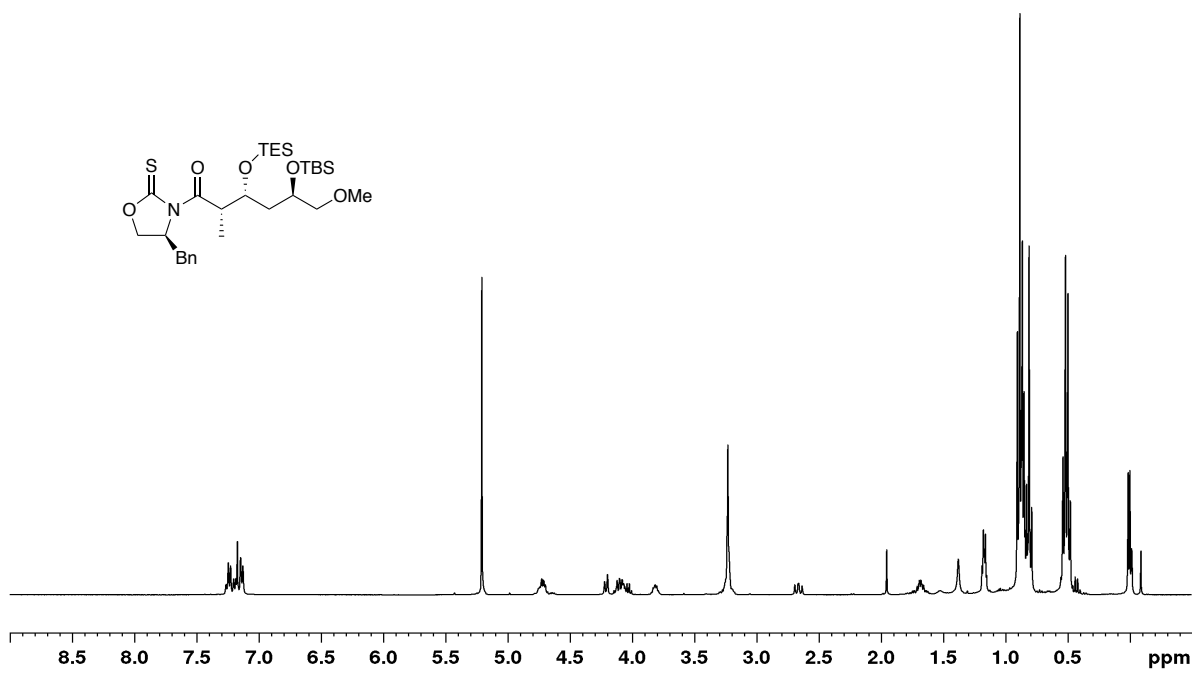


Figure A2.5 400 MHz ^1H -NMR and 100 MHz ^{13}C -NMR spectrum of **2.61** in CDCl_3

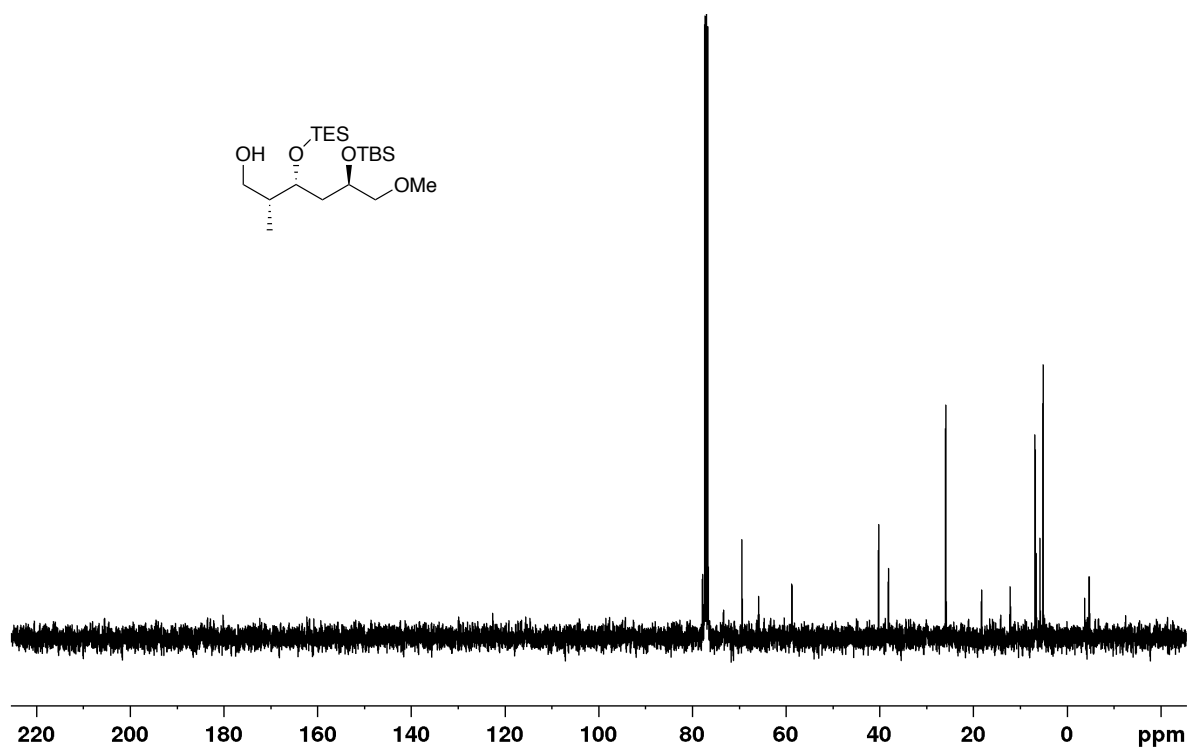
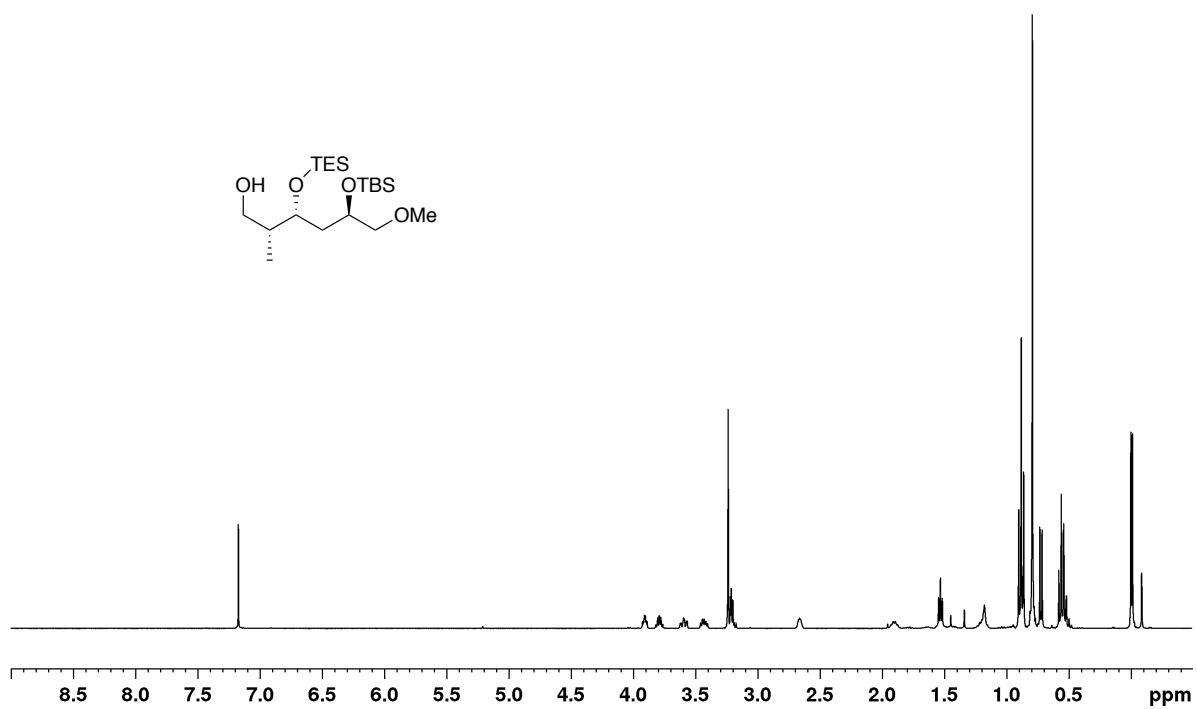


Figure A2.6 400 MHz $^1\text{H-NMR}$ and 100 MHz $^{13}\text{C-NMR}$ spectrum of S6 in CDCl_3

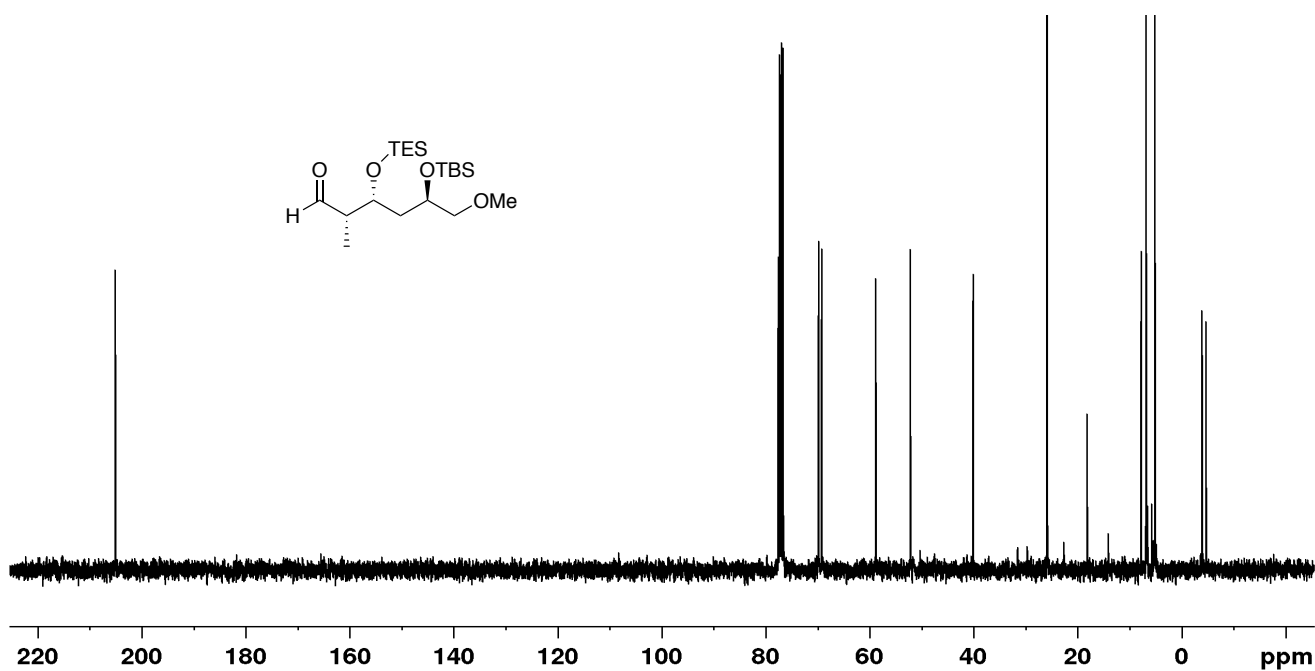
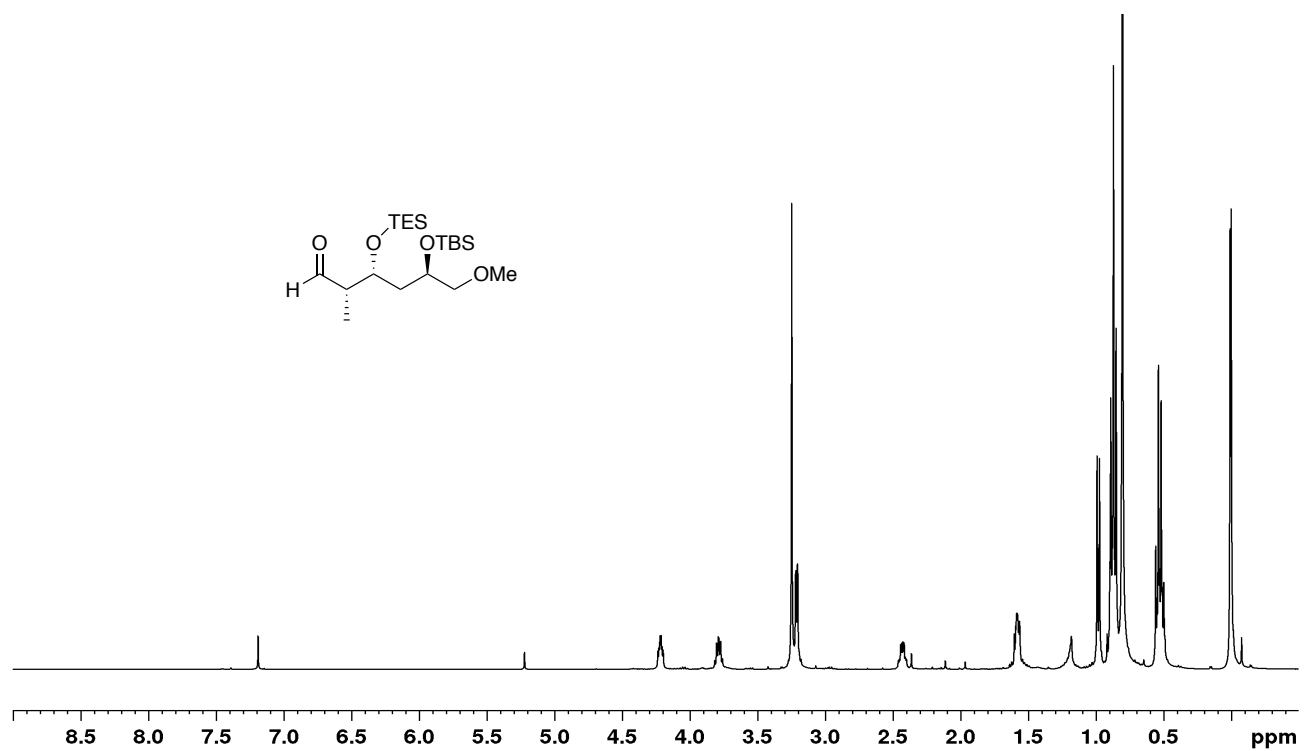


Figure A2.7 400 MHz $^1\text{H-NMR}$ and 100 MHz $^{13}\text{C-NMR}$ spectrum of **2.62** in CDCl_3

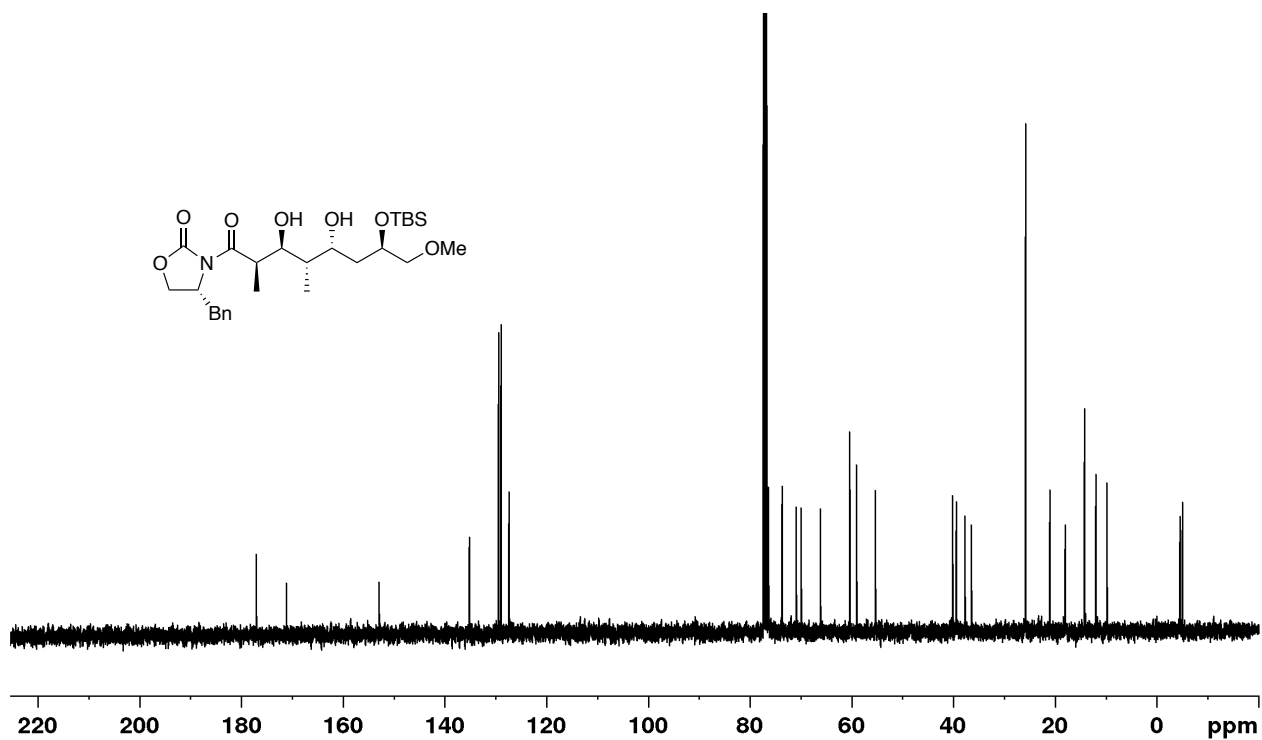
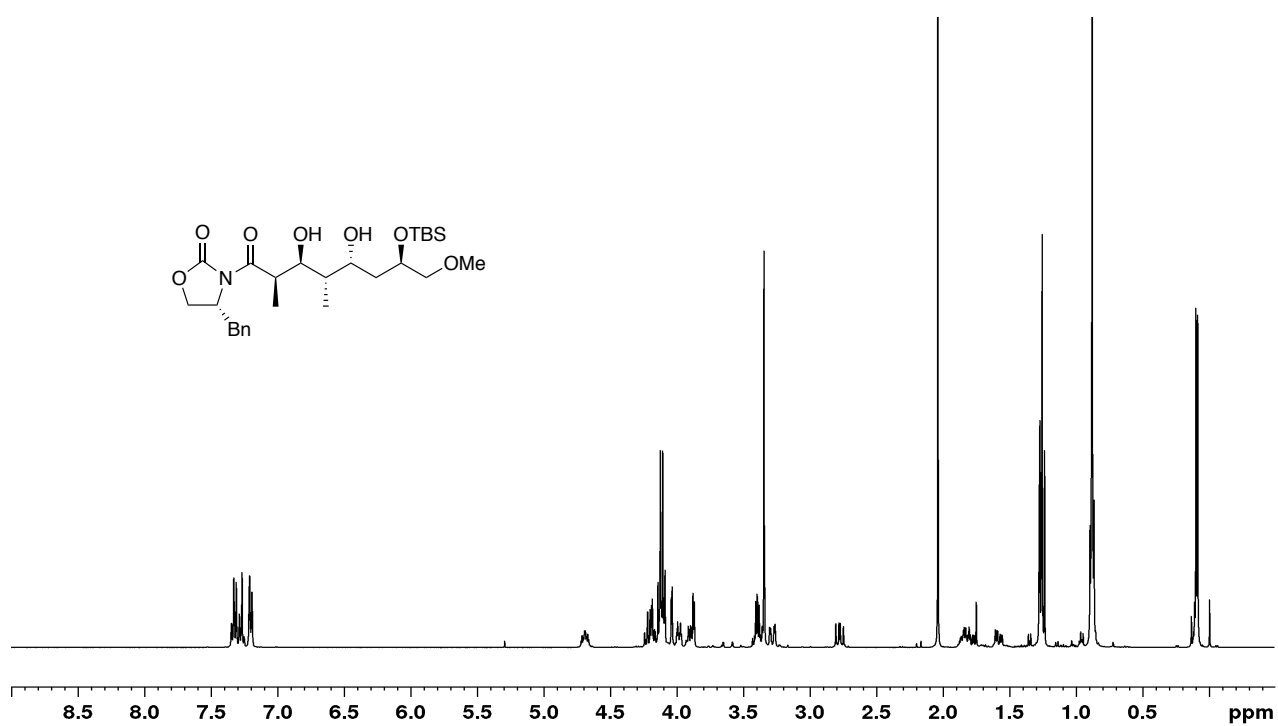


Figure A2.8 400 MHz ^1H -NMR and 100 MHz ^{13}C -NMR spectrum of **2.6** in CDCl_3

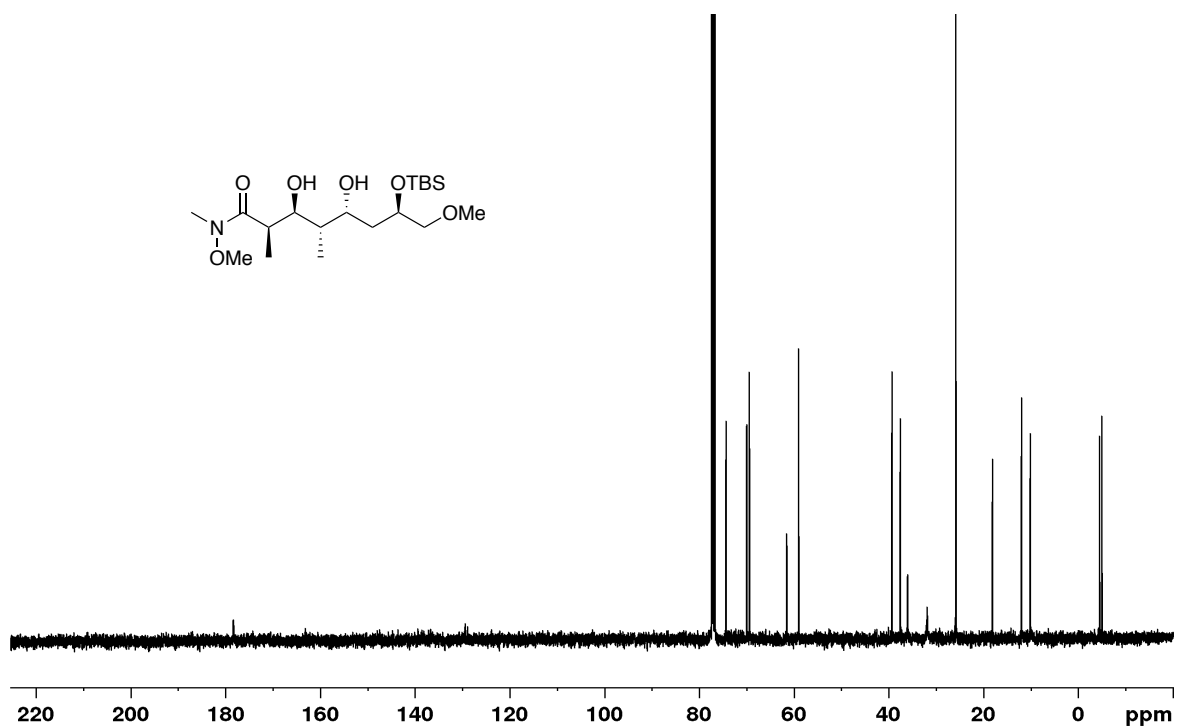
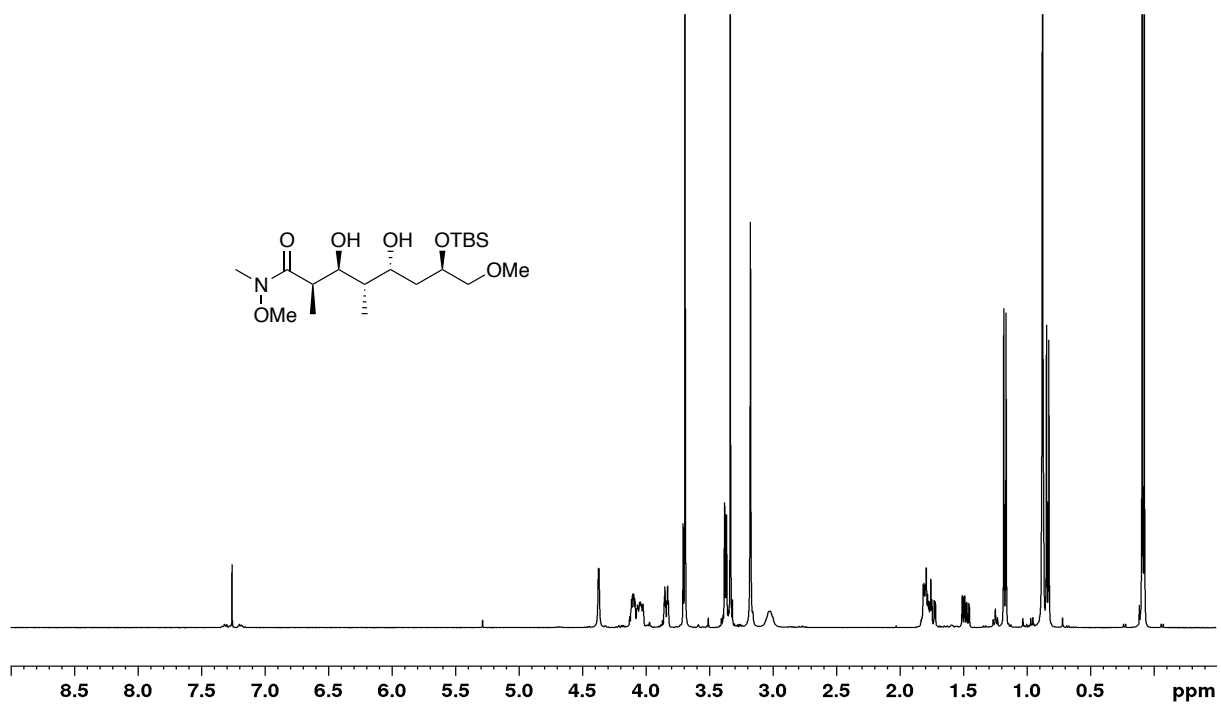


Figure A2.9 400 MHz $^1\text{H-NMR}$ and 100 MHz $^{13}\text{C-NMR}$ spectrum of S7 in CDCl_3

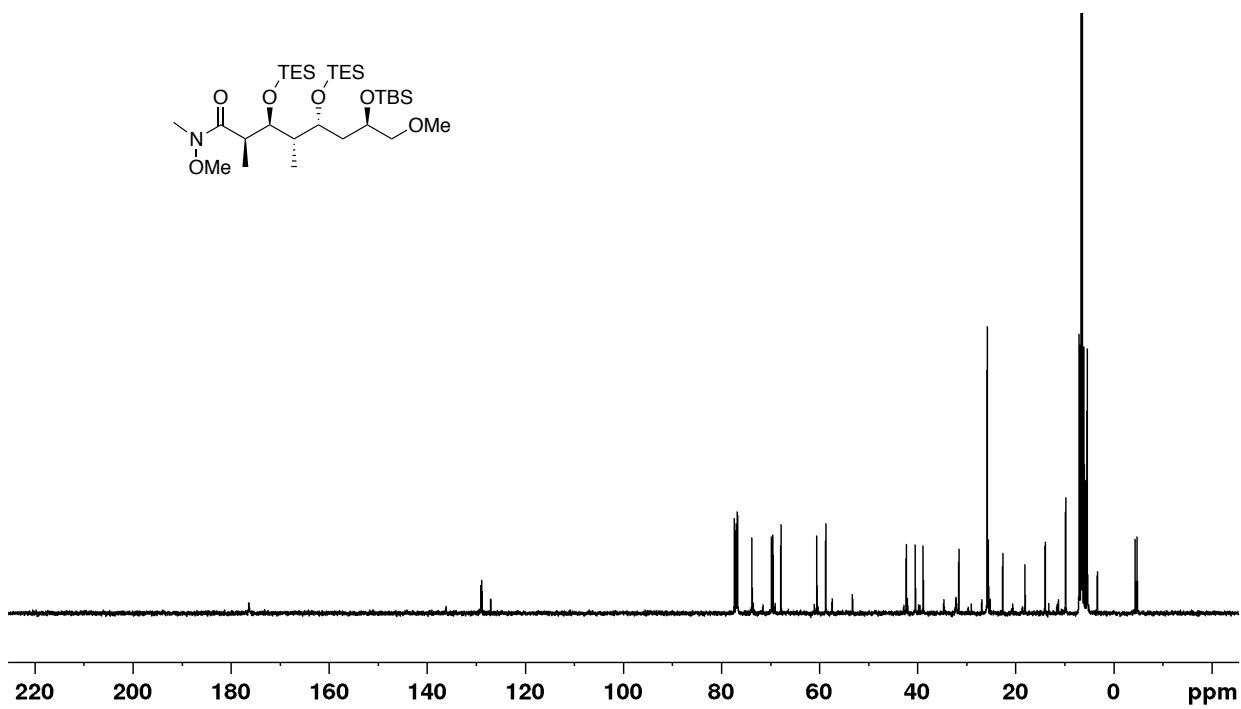
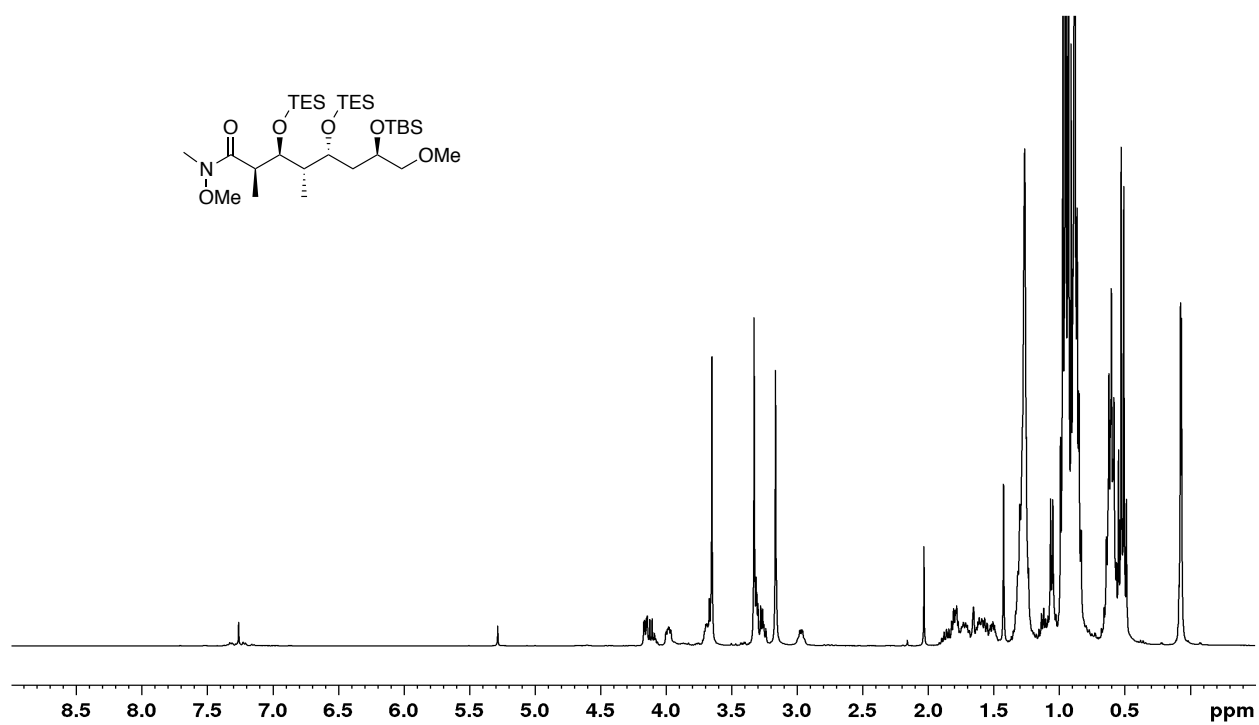


Figure A2.10 400 MHz ¹H-NMR and 100 MHz ¹³C-NMR spectrum of **2.64** in CDCl₃

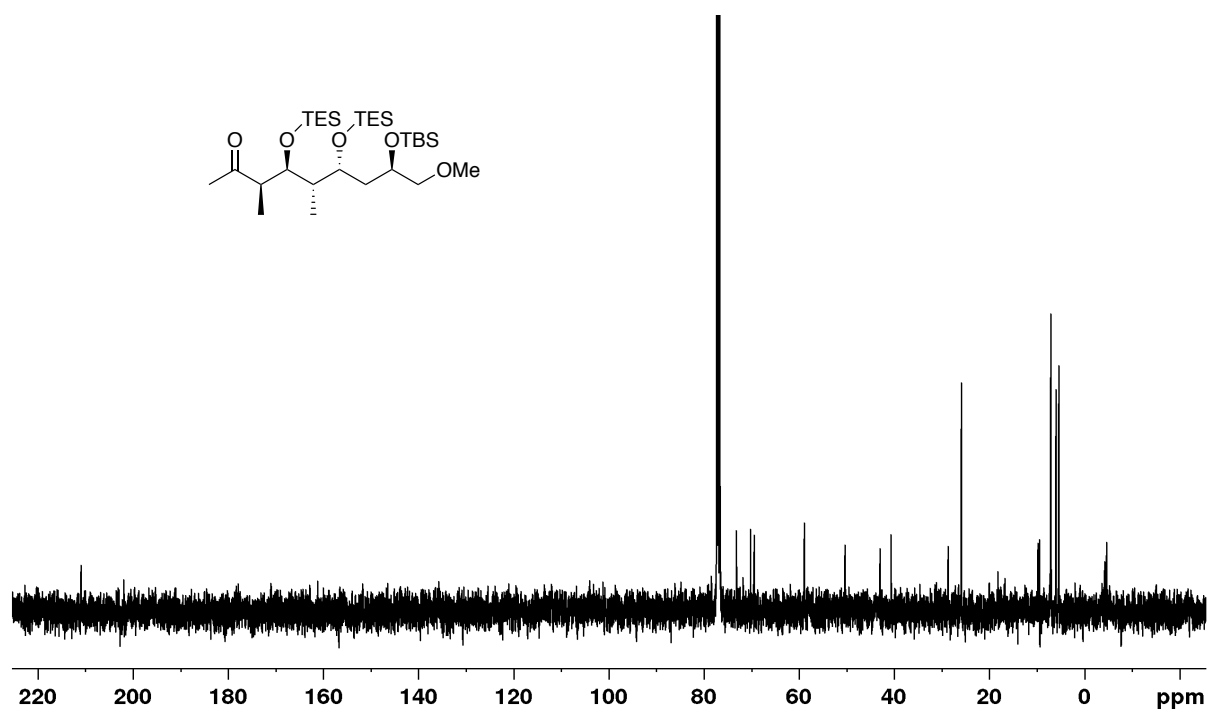
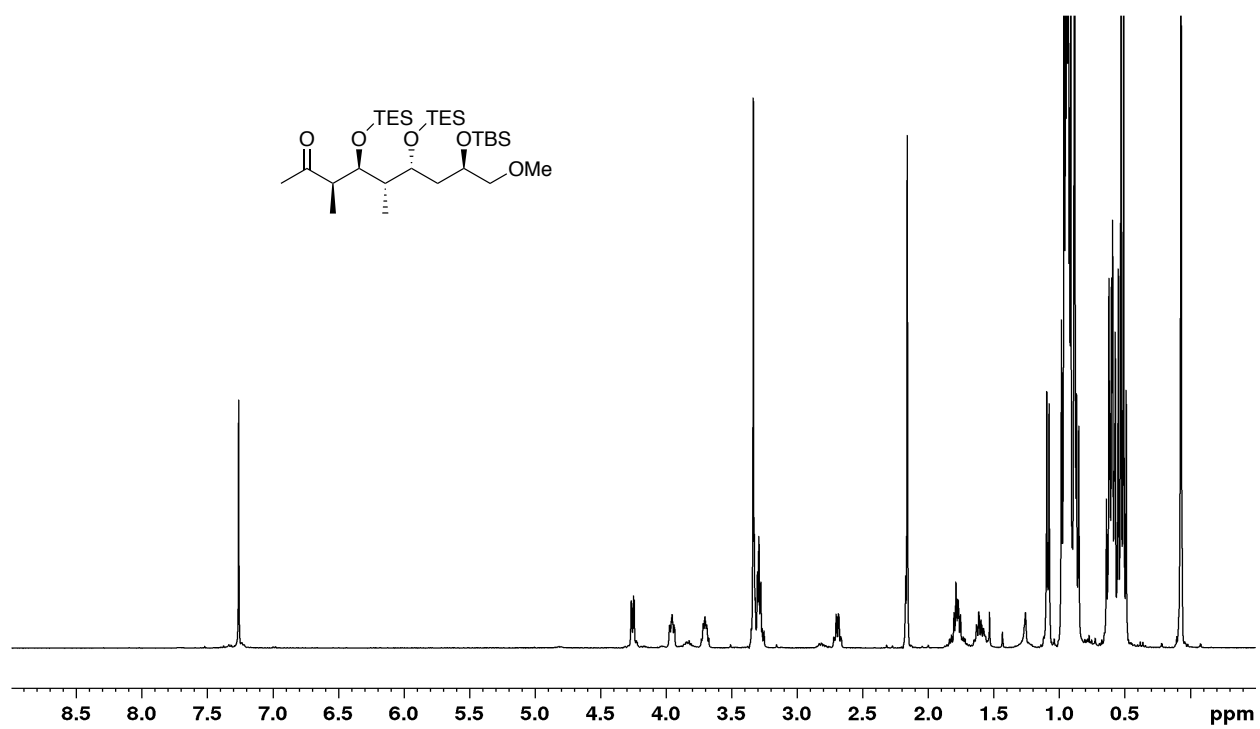


Figure A2.11 400 MHz ¹H-NMR and 100 MHz ¹³C-NMR spectrum of 2.35 in CDCl₃

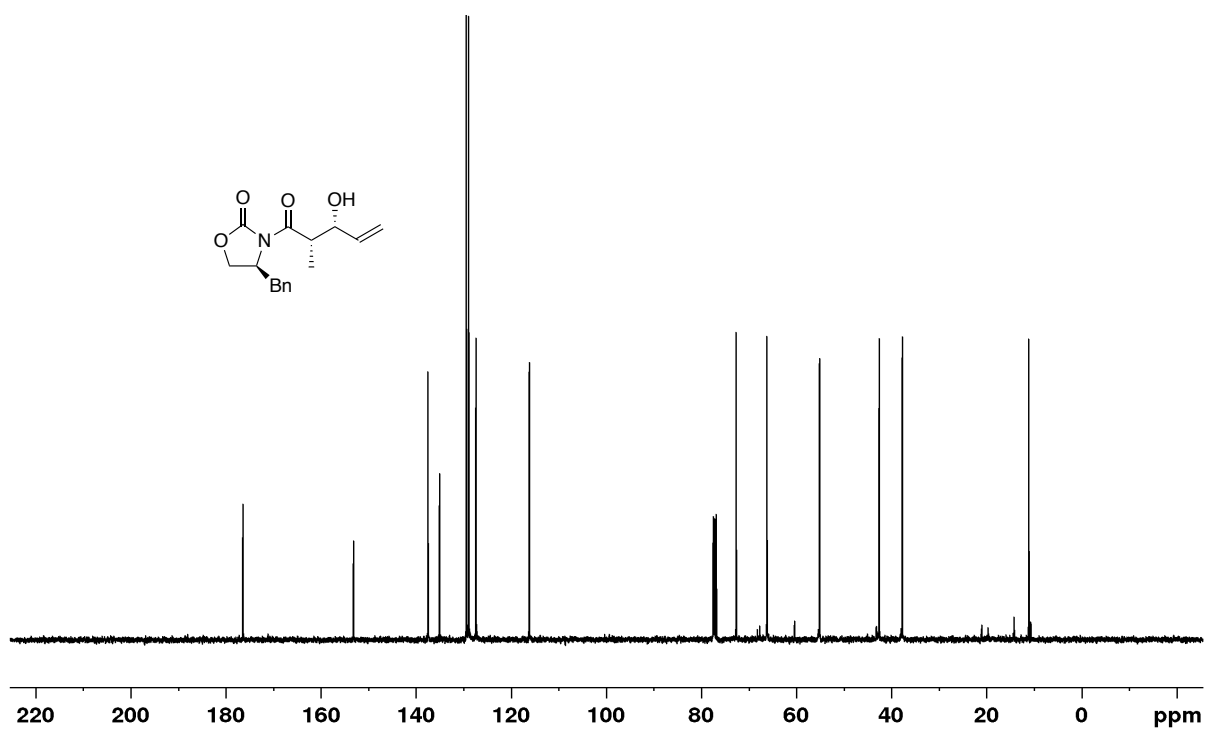
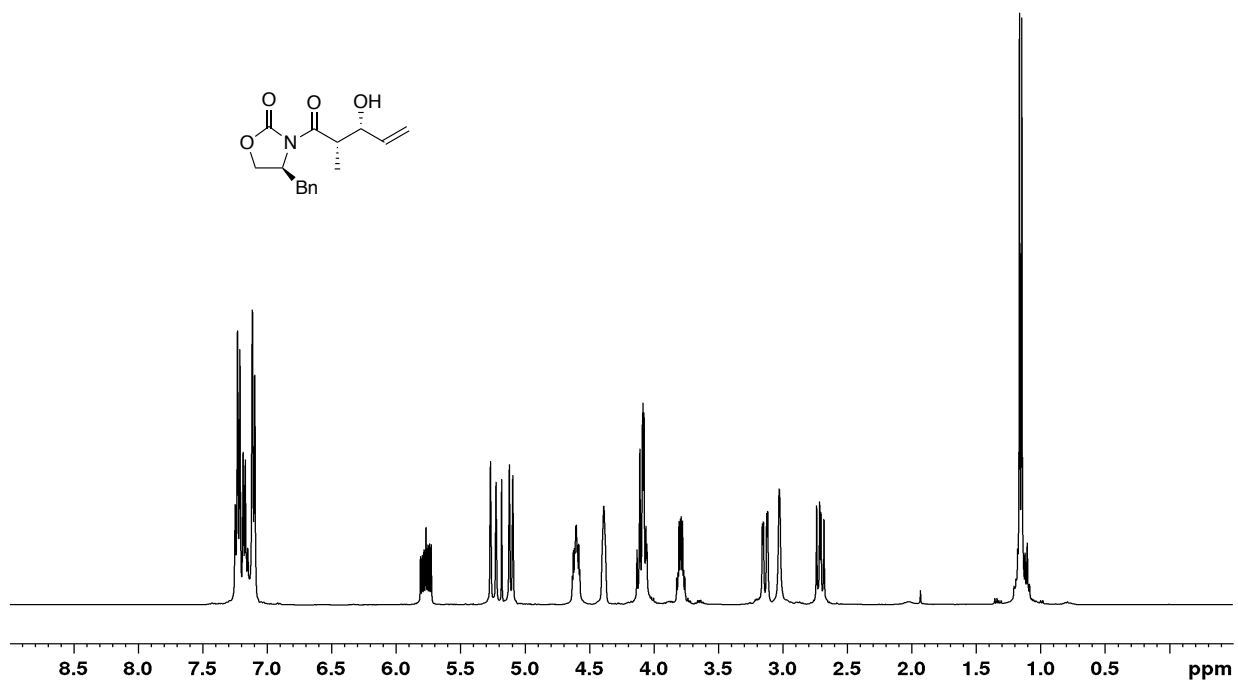


Figure A2.12 400 MHz $^1\text{H-NMR}$ and 100 MHz $^{13}\text{C-NMR}$ spectrum of **2.71** in CDCl_3

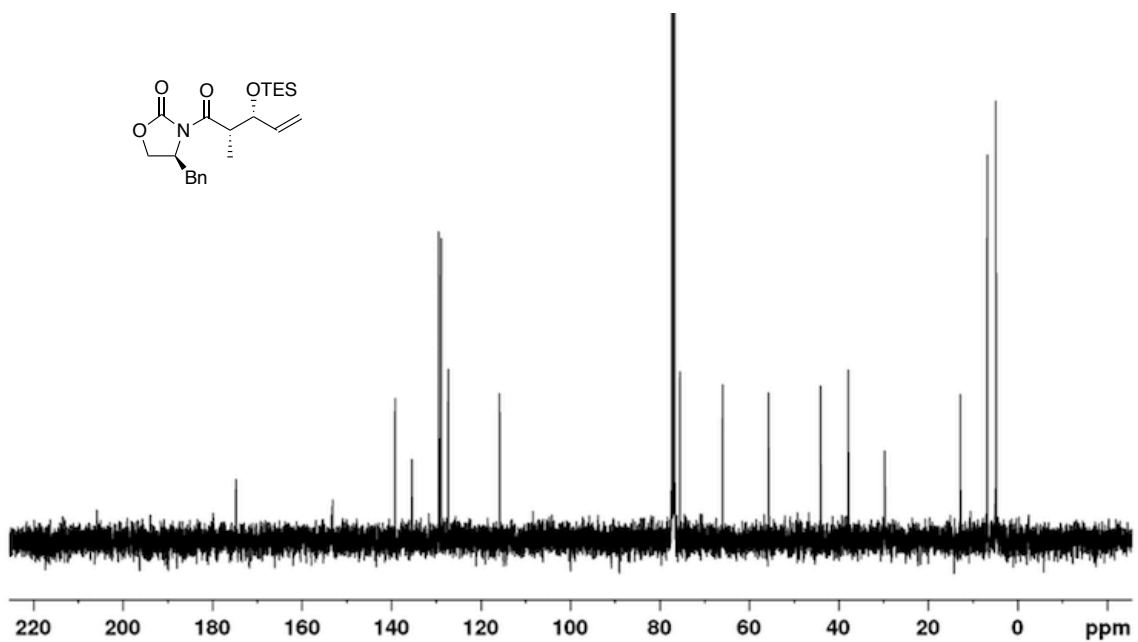
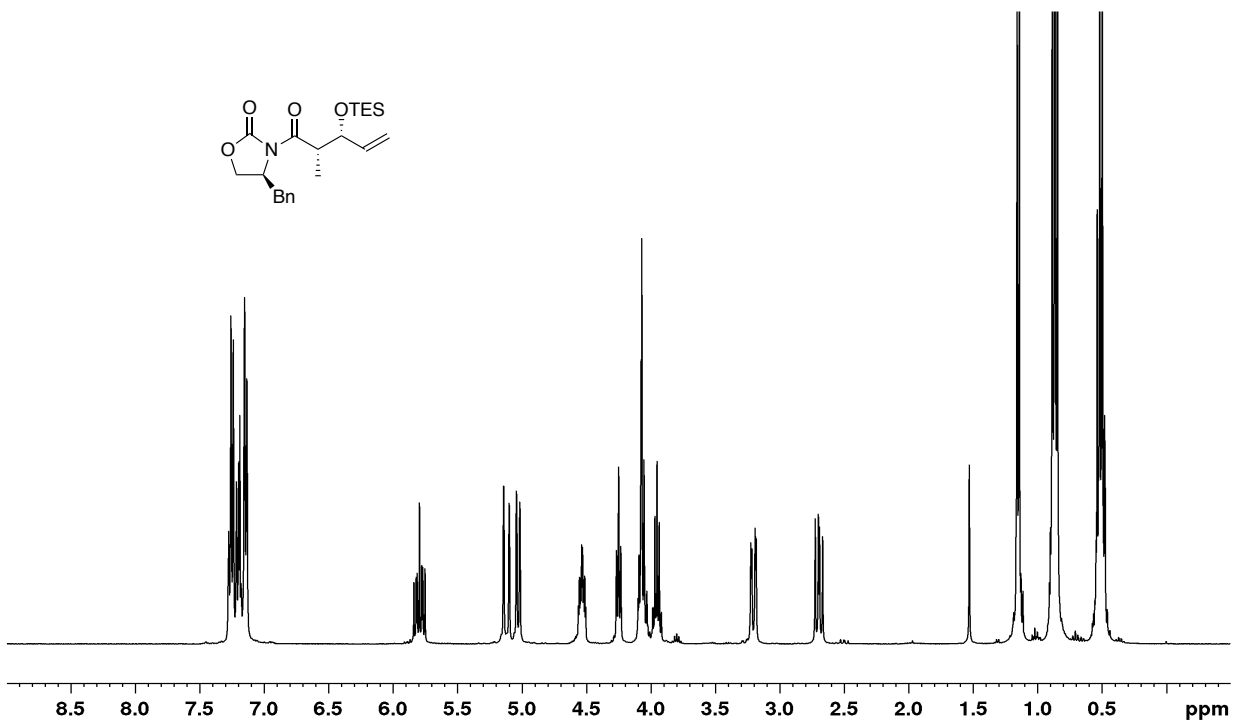


Figure A2.13 400 MHz $^1\text{H-NMR}$ and 100 MHz $^{13}\text{C-NMR}$ spectrum of **2.74** in CDCl_3

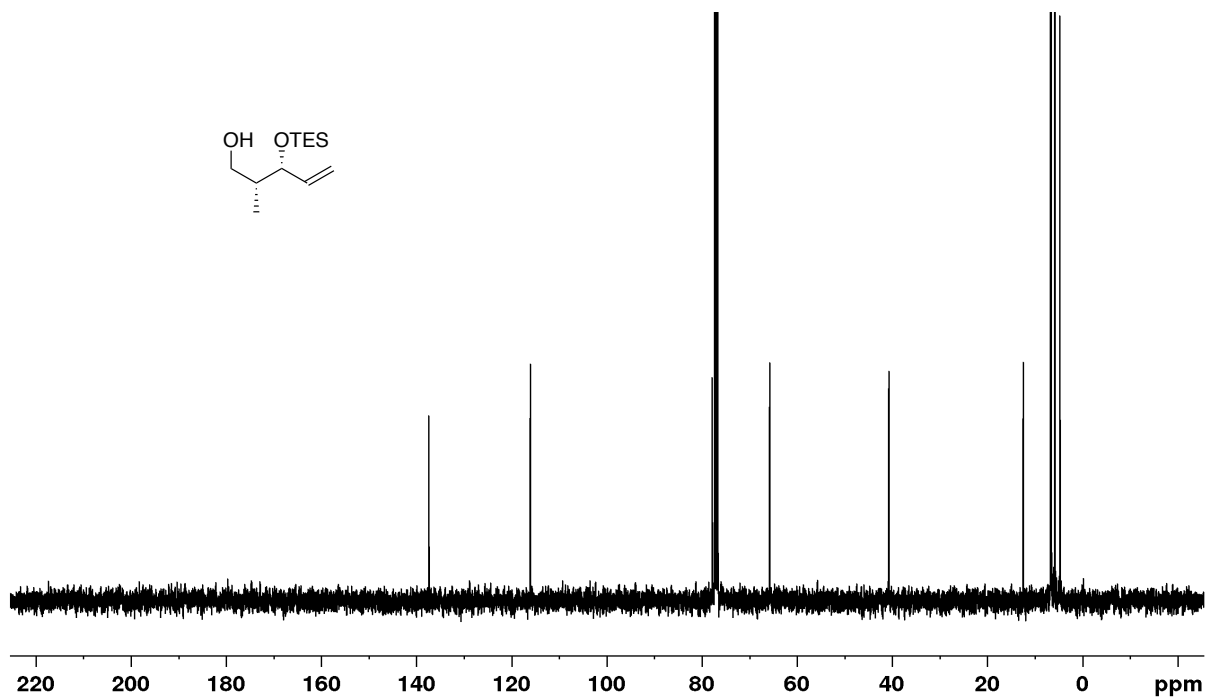
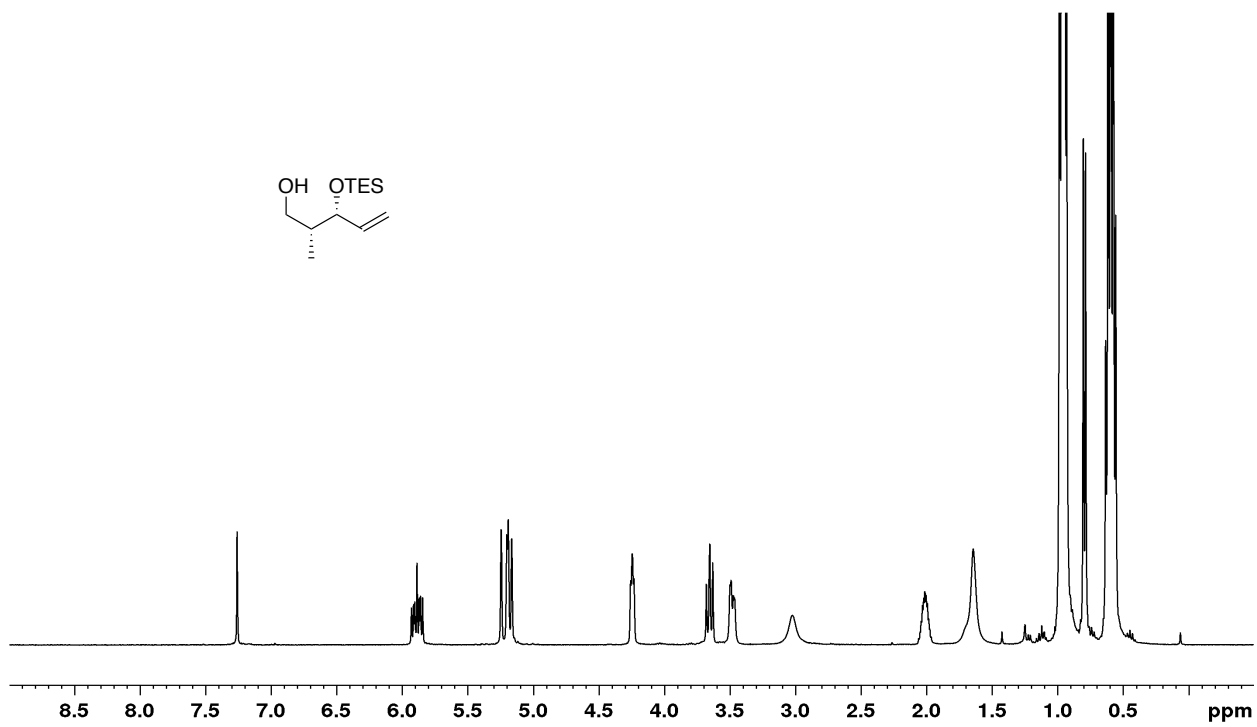


Figure A2.14 400 MHz ^1H -NMR and 100 MHz ^{13}C -NMR spectrum of **S8** in CDCl_3

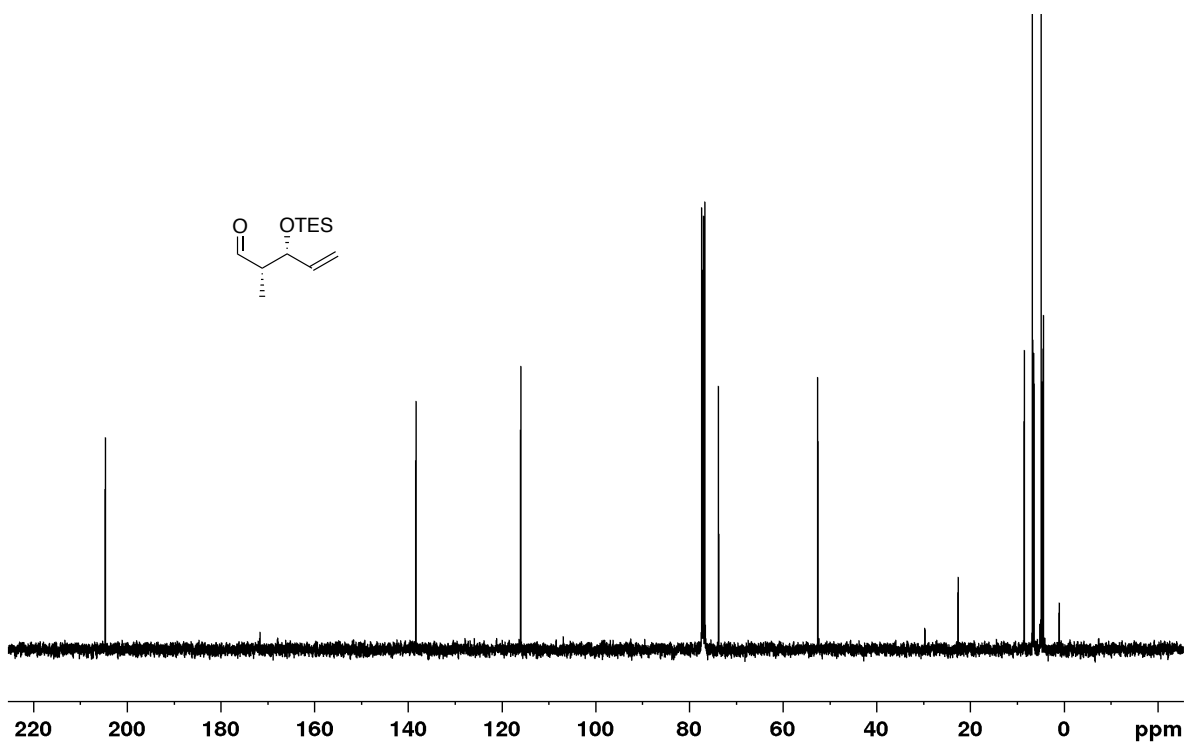
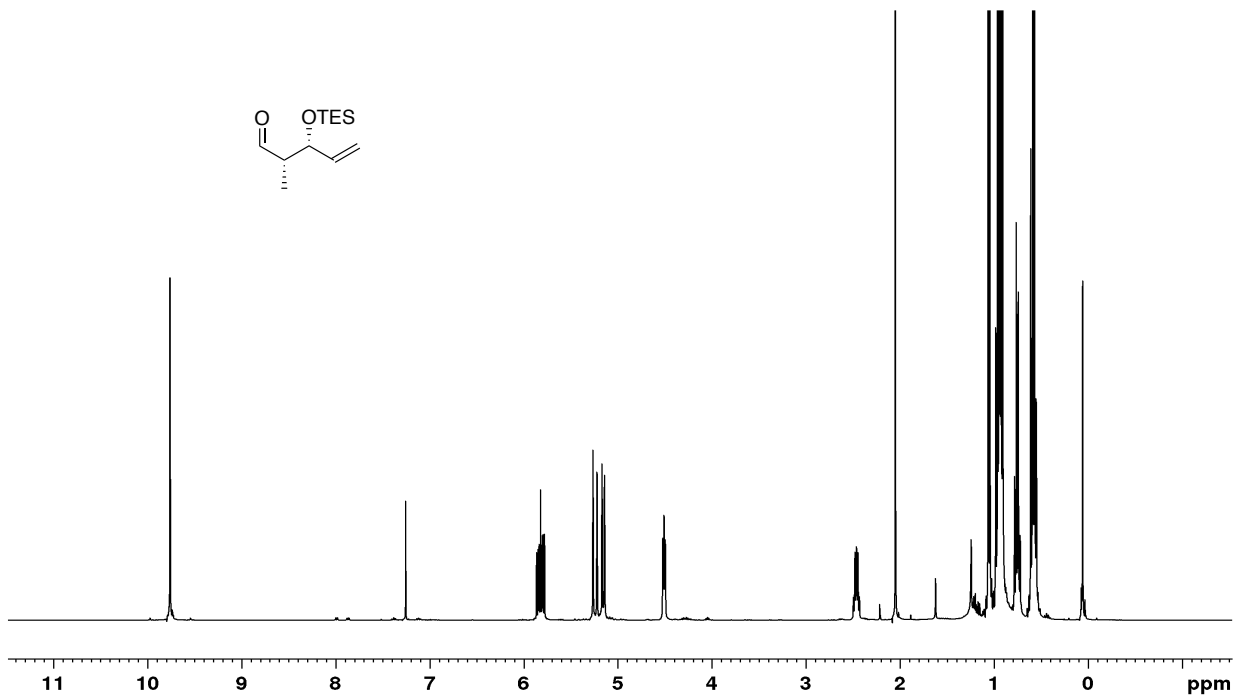


Figure A2.15 400 MHz $^1\text{H-NMR}$ and 100 MHz $^{13}\text{C-NMR}$ spectrum of **2.72** in CDCl_3

Robert Woods Davis- Graduate Research Assistant, Department of Chemistry,
Vanderbilt University, Nashville, TN

Education

2013- M.S. (Chemistry): Villanova University, GPA: 3.6
Thesis: Chemical Ecology of an Amphibian-Bacterial-Fungal System:
Techniques to Identify Secondary Metabolites

2011- B.S. *Magna Cum Laude* (Biology): James Madison University, GPA: 3.7
Thesis: Polycephalic Amphiphiles as Novel Surfactants

Research Experience

2013-present Graduate Research Assistant, Vanderbilt University Department of Chemistry

2012-2013 Graduate Research Assistant, Villanova University, Department of Chemistry and Biochemistry

2010-2011 Undergraduate Research Assistant, James Madison University, Department of Chemistry

Teaching Experience

2015 Teaching Fellow, Vanderbilt University Department of Chemistry

2014 Teaching Assistant, Vanderbilt University Department of Chemistry

2013 Teaching Assistant, Villanova University Department of Chemistry

2010 Teaching Assistant, James Madison University Department of Biology

Publications

5. Yamanashi, H., Boeglin, W. E., Morisseau, C., Davis, R. W., Sulikowski, G. A., Hammock, B. D., Brash, A. R. Catalytic activities of mammalian epoxide hydrolases with *cis* and *trans* fatty acid epoxides relevant to skin barrier function *J. Lip. Res.* in press.

4. Ozakin, S., Davis, R. W., Umile, T. P., Pirinccioglu, N., Kizil, M., Celik, G., Sen, A., Minbiole, K. P. C., Ince, E. The isolation of tetrangomycin from terrestrial *Streptomyces* sp. CAH29: evaluation of antioxidant, anticancer, and anti-MRSA activity *Med. Chem. Res.* **2016**, 25, 2872-2881.

3. Umile, T.P.; McLaughlin, P.J.; Johnson, K.R.; Honarvar, S.; Blackman, A.L; Burzynski, E.A.; Davis, R.W.; Teotonio, T.L.; Hearn, G.W.; Hughey, C.A.; Lagalante, A.F.; Minbiole; K.P.C. Nonlethal Amphibian Skin Swabbing of Cutaneous Natural Products for HPLC Fingerprinting. *Anal. Methods*, **2014**, 6, 3277-3284.

2. The Antibacterial Activity of 4,4'-Bipyridinium Amphiphiles with Conventional, Bicephalic and Gemini Architectures. Grenier, M.C., Davis, R. W., Wilson-Henjum, K. L., LaDow, J. E., Black, J. W., Caran, K. L., Seifert, K., Minbiole. K. P. C. *Bioorganic and Medicinal Chemistry Letters*, **2012**, 4055-4058.

1. LaDow, J. E., Warnock, D. C., Hamill, K. M., Simmons, K. L., Davis, R. W., Schwantes, C. R., Flaherty, D. C., Caran, K. L, Minbiole, K. P. C., Seifert, K. Bicephalic Amphiphile Architecture Affects Antimicrobial Activity. *European Journal of Medicinal Chemistry*, **2011**, 4219-4226.

Honors, Awards, and Societies

- | | |
|--------------|---|
| 2013 | Vanderbilt Institute of Chemical Biology Graduate Fellowship |
| 2011 | Distinguished Graduate in Chemistry, James Madison University |
| 2011-present | Member of the American Chemical Society |
| 2011-2013 | Member of the International Society of Chemical Ecology |

Posters and Presentations

- 2016- Vanderbilt Institute of Chemical Biology Symposium, Nashville, TN.
Poster- *Total synthesis of hemiketals D₂ and E₂ in support of biological studies*

- 2015- Vanderbilt Institute of Chemical Biology Symposium, Nashville, TN.
Poster- *Comprehensive Access to Apoptolidin Derived Chemical Probes to Study Cancer Cell Metabolism*
- 2013- 245th National American Chemical Society meeting, New Orleans, LA.
Presentation- *Chemical ecology of an amphibian-bacterial-fungal ecosystem*
- 2012- 244th National American Chemical Society meeting, Philadelphia, PA.
Poster- *Bioactive natural products from an amphibian-bacterial-fungal ecosystem*
- 2012- Villanova University Sigma Xi Research Symposium, Villanova, PA.
Poster- *Bioactive natural products from an amphibian-bacterial-fungal ecosystem*
- 2012- St. Joseph University Sigma Xi Research Symposium, Lower Merion, PA.
Poster- *Bioactive natural products from an amphibian-bacterial-fungal ecosystem*
- 2011- 9th annual Colonial Academic Alliance (CAA) Undergraduate Research Conference, Hofstra University, Hempstead, NY.
Presentation- *Polycephalic (Multi-Headed) Cationic Amphiphiles As Novel Surfactants*
- 2010- University of Maryland Baltimore County Undergraduate Research Symposium, Baltimore, MD
Poster- *Polycephalic (Multi-Headed) Cationic Amphiphiles As Novel Surfactants.*
- 2010- Virginia Academy of Science - 2010 Annual Meeting, James Madison University, Harrisonburg, VA.
Poster- *Polycephalic (Multi-Headed) Cationic Amphiphiles as Novel Surfactants and Antimicrobial Agents.*